Phytoplankton facing global change: Ecological and physiological perspectives

UNIVERSIDAD DE GRANADA

UNIVERSITÀ POLITECNICA DELLE MARCHE

Departamento de Ecología & Instituto del Agua (UGR)
&
Dipartimento Scienze della vita e dell'Ambiente (UNIVPM)

PhD Programme: Biología Fundamental y de Sistemas

PhD Thesis:

A Thesis submitted by Juan Manuel González Olalla for the degree of Doctor of Philosophy in the University of Granada (Spain) and Polytechnic University of Marche (Italy)

Granada, October 2019

Editor: Universidad de Granada. Tesis Doctorales
Autor: Juan Manuel González Olalla
ISBN: 978-84-1306-418-5
URI: http://hdl.handle.net/10481/58817

The present work has been conducted between the group of Functional Ecology (RNM 367) of the Department of Ecology of University of Granada and Universitary Institute of Water Research (Spain) and the group of Algal and Plant Physiology of the Polytechnic University of Marche (Italy).

This research has been supported by:

- Ministerio de Economía y Competitividad (MINECO) and Fondo Europeo de Desarrollo Regional (FEDER) (CGL2011-23681/BOS and CGL2015-67682-R)
- Junta de Andalucía (Excelencia projects P12-RNM-327)
- The Czech Science Foundation, Grantová Agentura České Republiky (GAČR 16-16343S)

Juan Manuel González Olalla was supported by Ministerio de Educación, Cultura y Deporte through a "Formación de Profesorado Universitario" PhD fellowship (FPU14/00977) and a short-term fellowship by Campus de Excelencia Interacional-University of Granada (CeiBiotic-UGR) (call. 2015 and 2016) and a long-term fellowship by ERASMUS+ Programme of the European Union (call. 2016) in Polytechnic University of Marche.

LIST OF PUBLISHED PAPERS

- **CHAPTER 2 -** Contrasting effect of Saharan dust and UVR on autotrophic picoplankton in nearshore versus offshore waters of Mediterranean Sea. González Olalla, J.M., Medina-Sánchez, J.M., Cabrerizo, M.J., Villar-Argaiz, M., Sánchez-Castillo, P.M. and Carrillo, P. (2017). *Journal of Geophysical Research: Biogeosciences* 122(8): 2085-2103

- **CHAPTER 3 -** Climate-driven shifts in algal-bacterial interaction of high-mountain lakes in two years spanning a decade. González Olalla, J.M., Medina-Sánchez, J.M., Lozano, I.L., Villar-Argaiz, M. and Carrillo, P. (2018). *Scientific Reports* 8: 10278.

- **CHAPTER 5 -** Mixotrophic trade-off under warming and UVR in a marine and a freshwater alga. González Olalla, J.M., Medina-Sánchez, J.M. and Carrillo, P. (2019). *Journal of Phycology* 55(5): 1028-1040

General Index

ABSTRACT

ABSTRACT

The global change induced by human action is the result of the interaction of multiple abiotic factors. Today, a crucial field of research concerns the study of how ecosystems will respond to future environmental conditions, since global-change factors interact synergistically or antagonistically and can aggravate or mitigate the effects of this phenomenon. In this thesis, an analysis is undertaken concerning the alteration of three abiotic factors associated with the current climatic crisis (temperature increase; greater UV radiation-exposure and increase in nutrient concentration) and the impact on phytoplanktonic organisms, located at the base of aquatic trophic webs, from a physiological and ecological perspective. The connection between these two aspects has scarcely been studied, despite that an understanding of physiological responses is necessary to understand ecological dynamics. Furthermore, this thesis focuses on photosynthetic microorganisms that have phagotrophic ability within the same cell (i.e. mixotrophic protists). In recent decades, this metabolic capacity has been discovered to be widespread among phytoplankton groups. Therefore, it becomes critical to determine how mixotrophic cells might respond to global-change factors, regulating their metabolism towards autotrophy or heterotrophy, as well as to examine the implications for the energy and nutrient fluxes. This thesis is designed to help fill these information gaps carrying out experiments and observational studies over different time scales (from hours to years); at different levels of biological organization (from the cell to ecosystems); and with organisms from different environments (natural marine samples, freshwater and laboratory cultures).

The results of these experiments show the effects of global-change factors on marine and freshwater organisms. Our experiments in the Alboran Sea (Chapter 2) have revealed a dual sensitivity to Saharan dust and UVR exposure between

areas located inside and outside of oligotrophic gyres, where autotrophic picoplankton plays an important role in primary production and biogeochemical cycles. The results indicate greater sensitivity in the offshore area (within the gyre) than in the nearshore area (outside the gyre), and reveal how the microbial web of two different communities can respond differently to future conditions of high UVR-incidence and higher nutrient inputs associated with Saharan dust.

Global change factors (higher temperature or UVR exposure) exert a strong influence on the high mountain regions. Furthermore, peaks of the Iberian Peninsula are also exposed to dust inputs from Sahara desert. To test the impact of these factors on freshwater ecosystems, an observational study was conducted on 13 lakes in Sierra Nevada mountains (southern Spain), examining how global change has altered the algae-bacteria interaction over a 10-year period (2005-2015) (Chapter 3). The results showed that the relationship between the two components changed from bacterivory control by algae to a commensalistic relationship, just when the water temperature increased and the N:P sestonic ratio decreased in relation to higher dust inputs. This change in the algae-bacteria relationship could alter the role of mixotrophs in these lakes by acting as a carbon-bypass in the microbial web, reducing the efficiency of biomass transfer to the upper trophic levels.

Based on the effect of nutrients and temperature on the algae-bacteria relationship, an investigation was made concerning how the two factors could modulate the metabolism and structure of a simplified protist community. For this, an experiment was undertaken in which two protists species of Sierra Nevada (*Chromulina* sp. as mixotrophic and *Monoraphidium minutum* as strict autotrophic species) were exposed to different temperature and nutrient conditions (Chapter 4). According to the results, increased temperature stimulated the metabolic rates while the fluctuation intensified this effect, favouring

heterotrophic metabolism according to the Metabolic Theory of Ecology (MTE). However, the nutrient × increased or fluctuating temperature interaction stimulated autotroph more than mixotroph metabolism and abundance. The results show that a higher nutrient concentration limited the effect of rising and fluctuating temperature on protists. This study reveals that a straight application of MTE does not hold at higher nutrient concentrations.

Given the ubiquity of mixotrophic metabolism in aquatic ecosystems, Chapter 5 deals with the mixotrophic balance in the cell and its regulation under stress factors (temperature and UVR). This was studied with two mixotrophic species (*Chromulina* sp. and *Isochrysis galbana*) that occupy different positions along the mixotrophic gradient. The results showed that the Temperature × UVR interaction increased the primary production: bacterivory ratio and displaced the organisms towards autotrophy, regardless of their position on the mixotrophic gradient. This effect can alter the role of mixotrophs in trophic webs and reduce carbon-transfer efficiency and organic matter at the highest levels.

Previous results raise the question of whether the combination of phototrophy and phagotrophy is an advantage for mixotrophs. In Chapter 6, a physiological study of mixotrophy in *I. galbana* is made, analysing the changes in enzymatic activities and composition in the cell driven by phagotrophy. This study revealed that phagotrophy benefits mixotrophic cells by stimulating the activity of β-carboxylase enzymes, boosting the phosphorous-cell quota, and accelerating the cell-division rate, thereby potentially improving cell fitness. On the other hand, conditions that should stimulate phagotrophy and under which mixotrophy could be a distinctive trait (low light and low nutrients) led the cell to a state of high stress, activating mechanisms that dissipate the reducing power. These results indicate that, despite increasing phagotrophy, *I. galbana* is predominantly

phototrophic and that conditions of low nutrients or light that encourage bacterivory do not imply a greater carbon-flux in the aquatic community.

This thesis advances knowledge of the ecological and physiological effects of global change on aquatic ecosystems. The results reflect the need to consider the interaction of multiple abiotic factors that elicit different responses from the phytoplankton community. The results show that phagotrophy is an advantage for mixotrophic cells because it accelerates their growth rate. However, field and laboratory experiments support that the most extreme future environmental conditions will negatively affect mixotrophs and will benefit strict autotrophs. All this improves our predictive capacity concerning the structure and functioning of aquatic ecosystems in their adaptation to global change.

RESUMEN

El cambio global inducido por la actividad humana es el resultado de la interacción de múltiples factores abióticos. Un campo de investigación de interés actual es el estudio de las respuestas de los ecosistemas frente a las futuras condiciones ambientales, ya que los factores de cambio global interactúan sinérgica o antagónicamente y pueden amplificar o mitigar los efectos de dicho fenómeno. En esta Tesis analizamos cómo la alteración de tres factores abióticos asociados a la actual crisis climática (incremento de temperatura; mayor exposición a radiación UV y aumento en la concentración de nutrientes) pueden afectar al fitoplancton, ubicado en la base de las redes tróficas de ecosistemas acuáticos, desde una perspectiva ecológica y fisiológica. La conexión entre ambas disciplinas ha sido escasamente estudiada, a pesar de que la comprensión de las respuestas fisiológicas es necesaria para entender las dinámicas ecológicas. Además, esta Tesis se centra concretamente en aquellos microorganismos fotosintéticos con capacidad fagotrófica dentro de la misma célula (i.e. protistas mixótrofos). En recientes décadas se ha demostrado que esta capacidad metabólica está ampliamente extendida entre los grupos fitoplanctónicos. Por esta razón, es importante saber cómo las células mixotróficas pueden responder a los factores de cambio global, regulando su metabolismo hacia la autotrofia o la heterotrofia, y las implicaciones que puede tener en los flujos de energía y nutrientes. Esta tesis está diseñada para tratar de llenar estos vacíos de información llevando a cabo experimentos y estudios observacionales a lo largo de diferentes escalas temporales (de horas a años), de organización biológica (de la célula a ecosistemas) y con organismos de diferentes ambientes (muestras naturales marinas, de agua dulce y cultivos de laboratorio).

Los resultados de estos experimentos muestran los efectos de los factores de cambio global en organismos marinos y de agua dulce. Nuestro experimento en

mar de Alborán (Capítulo 2) reveló una sensibilidad dual al polvo del Sahara y exposición a UVR entre zonas ubicadas dentro y fuera de giros oceánicos oligotróficos, donde el picoplancton autótrofo desempeña un papel importante en la producción primaria y los ciclos biogeoquímicos. Los resultados mostraron una mayor sensibilidad de la zona de mar abierto (dentro del giro) que la zona de costa (fuera del giro), y pone de manifiesto cómo la red microbiana de dos comunidades diferentes puede exhibir diferentes respuestas ante condiciones futuras de alta incidencia de UVR y polvo del desierto.

Los factores de cambio global, como el incremento de temperatura y UVR, tienen una gran incidencia en las zonas de alta montaña. Además, los picos de la Península Ibérica están expuestos a las entradas de polvo procedente del desierto del Sahara. Para testar el impacto de estos factores sobre ecosistemas acuáticos de agua dulce, un estudio observacional fue realizado a lo largo de 13 lagunas de Sierra Nevada (Sur España), analizando cómo el cambio global ha modificado la relación alga-bacteria a lo largo de un periodo de 10 años (2005-2015) (Capítulo 3). Los resultados mostraron que la relación entre ambos componentes cambió desde un control por bacterivoría por las algas hacia una relación comensalista, coincidiendo con una mayor temperatura del agua y un menor ratio sestónico Nitrógeno:Fósforo relacionado con mayores entradas de polvo. Este cambio en la relación alga-bacteria podría alterar el papel de los mixótrofos en estas lagunas actuando como un by-pass de carbono en la red microbiana, reduciendo la eficiencia de transferencia de biomasa a niveles superiores de la red trófica.

Basado en el efecto de los nutrientes y la temperatura en la relación alga-bacteria, una investigación fue llevada a cabo acerca de cómo podrían ambos factores modular el metabolismo y estructura de los protistas. Para ello, se condujo un experimento donde expusimos dos especies protistas modelo de Sierra Nevada (*Chromulina* sp. como mixótrofa y *Monoraphidium minutum* como autótrofa

estricta) a diferentes condiciones de temperatura y nutrientes (Capítulo 4). Los resultados evidenciaron que el incremento de temperatura estimuló las tasas metabólicas y que la fluctuación potenció este efecto, favoreciendo el metabolismo heterotrófico de acuerdo con la Teoría Metabólica de la Ecología (MTE). Sin embargo, la interacción nutrientes×incremento o fluctuación de temperatura tuvo un efecto estimulador de mayor magnitud en el metabolismo y abundancia de los autótrofos en comparación a los mixótrofos. Los resultados muestran que el incremento en la concentración de nutrientes limitó el efecto de la temperatura y de la fluctuación térmica sobre los protistas. Este estudio revela que una aplicación estricta de la MTE no se cumple en altas concentraciones de nutrientes.

Dada la ubicuidad del metabolismo mixotrófico en los ecosistemas acuáticos, en el Capítulo 5 se estudió el balance mixótrofo en la célula y su regulación frente a factores de estrés (temperatura y UVR). Este fue llevado a cabo con dos especies mixótrofas (*Chromulina* sp. e *Isochrysis galbana*) ubicadas en diferentes posiciones del gradiente mixotrófico. Los resultados mostraron que la interacción Temperatura×UVR incrementó la ratio producción primaria:bacterivoría y desplazó a los organismos hacia la autotrofia, independientemente de su posición en el gradiente mixotrófico. Dicho efecto puede alterar el papel de los mixótrofos en las redes tróficas y disminuir la eficiencia en la transferencia de carbono y materia orgánica hacia los niveles superiores.

Los estudios previos llevan a cuestionar si la combinación de fototrofia y fagotrofia supone una ventaja para los mixótrofos. En el Capítulo 6, un estudio fisiológico de la mixotrofia en *I. galbana* fue realizado, analizando los cambios a nivel enzimático y de composición celular que tienen lugar debido a la fagotrofia. El estudio reveló que la fagotrofia es una ventaja para la célula mixotrófica ya que estimula la actividad de enzimas β-carboxilasas, incrementa el contenido de

fósforo en la célula y acelera la tasa de división, lo que puede mejorar el estado de la célula. Por otro lado, aquellas condiciones que deberían estimular la fagotrofia y donde la mixotrofia puede ser un rasgo distintivo (baja luz y bajos nutrientes) llevaron a la célula a un estado de alto estrés celular, activando mecanismos de disipación de poder reductor. Estos resultados muestran que a pesar de incrementar la fagotrofia, *I. galbana* es predominantemente fototrófica, y que condiciones de escasez de nutrientes o luz que potencian la bacterivoría no implican un mayor flujo de carbono en la comunidad acuática.

Esta tesis representa un avance en el conocimiento de los efectos del cambio global sobre los ecosistemas acuáticos, abordado desde un punto de vista que engrana las ciencias de la ecología y la fisiología. En conjunto, reflejamos la necesidad de considerar la interacción de múltiples factores abióticos que provocan diferentes respuestas de la comunidad fitoplanctónica. Los resultados muestran que la fagotrofia es una ventaja para las células mixotróficas ya que acelera su tasa de crecimiento. Sin embargo, estudios de campo y laboratorio revelan que condiciones ambientales extremas futuras afectarán negativamente a los mixótrofos y beneficiarán a los autótrofos estrictos. Todo ello nos permite mejorar nuestra capacidad predictiva sobre la estructura y funcionamiento de los ecosistemas acuáticos en su adaptación al cambio global.

SOMMARIO

Il cambiamento climatico globale, indotto dall'attività umana, è il risultato dell'interazione di molteplici fattori abiotici che possono interagire tra loro con un'azione sinergica o da antagonisti, amplificandone o mitigandone gli effetti. Per questo, attualemtne, un'area di notevole interesse di studio è sapere come gli ecosistemi risponderanno alle future condizioni ambientali. Sebbene la comprensione delle risposte fisiologiche degli organismi sia necessaria per comprendere le dinamiche ecologiche degli ecosistemi, la connessione tra le due discipline è stata scarsamente studiata. In questa tesi abbiamo analizzato come l'incremento di tre fattori ambientali (temperatura; nutrienti e radiazioni UV) possa influenzare sia dal punto di vista ecologico che fisiologico, il fitoplancton che costituisce la base delle reti trofiche degli ecosistemi acquatici. Inoltre, questa tesi si concentra in particolare sui microrganismi fotosintetici con capacità fagotrofica (i.e. protisti mixotrofici). Negli ultimi decenni è stato dimostrato che questa capacità metabolica è molto diffusa tra i gruppi fitoplanctonici. Per questo è importante comprendere quali sono i fattori che possono spostare il metabolismo delle cellule mixotrofiche verso l'autotrofia o l'eterotrofia e le implicazioni che questo cambiamento può avere sui flussi di energia e sui nutrienti. Questa tesi è progettata per cercare di colmare questo gap informativo, effettuando esperimenti e studi osservazionali su diverse scale temporali (da ore ad anni), a livello di organizzazione biologica (da cellula a ecosistemi) e vengono analizzati organismi di diversi ambienti (campioni marini naturali, acqua dolce e colture da laboratorio).

Nei vortici oligotrofici il picoplancton autotrofico svolge un ruolo importante sia nella produzione primaria che nei cicli biogeochimici. In particolare il nostro esperimento nel Mare di Alboran (Capitolo 2) ha rivelato una differente sensibilità alla polvere sahariana e all'esposizione ai raggi UV tra le aree situate all'interno e

all'esterno dei vortici oligotrofici. I risultati hanno mostrato una maggiore sensibilità ai cambiamenti nell'area di mare aperto (all'interno della virata) rispetto alla zona costiera (all'esterno della virata) e mostrano come due diverse comunità microbiche possano mostrare risposte differenti alle condizioni future di elevata incidenza di UVR e polvere del deserto.

I fattori di cambiamento globale (temperatura più elevata ed esposizione a UVR) esercitano una forte influenza sulle regioni di alta montagna. Inoltre, le cime della penisola iberica sono anche esposte agli input di polvere sahariana. Per testare l'impatto di questi fattori sugli ecosistemi di acqua dolce, uno studio osservazionale su 13 lagune nella Sierra Nevada (Spagna meridionale) é stato condotto analizzando come il cambiamento climatico globale abbia modificato le relazioni alghe-batteri durante un periodo di 10 anni (2005-2015) (Capitolo 3). I risultati hanno mostrato che in corrispondenza del'incremento della temperatura dell'acqua e della diminuzione del rapporto sestonico di azoto:fosforo, dovuto da un maggiori input di polvere, la relazione tra alghe e batteri è cambiata da un controllo batterivoro delle alghe a una relazione commensalistica. In questi laghi i mixotrofi fungono da bypass del carbonio all'interno del tessuto microbico e il cambiamento nella relazione tra alghe e batteri potrebbe alterare il ruolo dei mixotrofi stessi, riducendo di fatto l'efficienza del trasferimento di biomassa ai livelli superiori.

Sono ancora poco conosciuti gli effetti dell’interazione tra i cambiamenti nella concentrazione di nutrienti e della temperatura sul metabolismo e la struttura dei protisti. Per questo, è stato condotto un esperimento in cui abbiamo esposto due specie modello di protisti della Sierra Nevada (*Chromulina* sp. come mixotrofio e *Monoraphidium minutum* come autotrofio rigoroso) a diverse condizioni di temperatura e nutrienti (Capitolo 4). I risultati hanno mostrato che l'aumento della temperatura stimola i tassi metabolici ma sue fluttuazioni migliorano

ulteriormente questo effetto, favorendo il metabolismo eterotrofico e questo è concorde con la Metabolic Theory of Ecology (MTE). Tuttavia, l'interazione tra incremento di nutrienti × l'incremento o fluttuazione della temperatura ha avuto un maggiore effetto stimolante sul metabolismo e sull'abbondanza di autotrofi rispetto ai mixotrofi. I risultati mostrano che una maggiore concentrazione di nutrienti ha limitato l'effetto della fluttuazione e/o dell'incremento della temperatura sui protisti. Questo studio mostra che con una maggiore concentrazione di nutrienti, gli effetti descritti dalla MTE non sono rigorosamente applicati.

Data l'ubiquità del metabolismo mixotrofico negli ecosistemi acquatici, nel Capitolo 5 abbiamo studiato l'equilibrio mixotrofico nella cellula e la sua regolazione contro i fattori di stress (temperatura e UVR). Ciò è stato effettuato con due specie mixotrofiche, *Chromulina* sp. e *Isochrysis galbana*, situate in diverse posizioni del gradiente mixotrofico. I risultati hanno mostrato che l'interazione Temperatura × UVR incrementa il rapporto produzione primaria:attività batterivora e indipendentemente dal grado di mixotrofia mostrato, sposta il metabolismo degli organismi verso l'autotrofia. Questo effetto può alterare il ruolo dei mixotrofi nelle catene trofiche e quindi ridurre l'efficienza di trasferimento del carbonio e della materia organica ai livelli più alti.

I risultati precedenti sollevano la questione se la combinazione di fototrofia e fagotrofia sia un vantaggio per i mixotrofi. Nel Capitolo 6, uno studio di mixotrofia analizzando fisiologia, cinetica enzimatica e cambiamenti nella composizione organica in organismi fagotrofici (*I. galbana*) é condotto. Il studio ha rivelato che la fagotrofia è un vantaggio per le cellule mixotrofiche poichè stimola l'attività degli enzimi β-carbossilasi, aumenta la quota di cellulare di fosforo e accelera il tasso di divisione e quindi può migliorare la fitness della cellula stessa. Tuttavia, le condizioni che dovrebbero stimolare la fagotrofia, dove

la mixotrofia può essere una caratteristica distintiva (scarsa luminosità e bassi nutrienti) hanno portato la cellula a uno stato di elevato stress cellulare e hanno attivato meccanismi di dissipazione del potere riducente. Questi risultati mostrano che, le sole condizioni di carenza di nutrienti o di luce che favoriscono la predazione di batteri, non dovrebbero comportare un maggior flusso di carbonio all'interno della comunità acquatica, in quanto, nonostante l'aumento dell'attività fagotrofica, *I. galbana* rimane prevalentemente fototrofica.

Questa tesi rappresenta un progresso nella conoscenza degli effetti del cambiamento climatico globale sugli ecosistemi acquatici, affrontando il problema sia da un punto di vista 'ecologico che fisiologico. I risultati mostrano che la fagotrofia è un vantaggio per le cellule mixotrofiche perché accelera il loro tasso di crescita. Tuttavia, esperimenti sul campo e in laboratorio supportano il fatto che le condizioni ambientali future più estreme influenzeranno negativamente i mixotrofi e andranno a beneficio di autotrofi rigorosi. Tutto ciò ci consente di migliorare la nostra capacità predittiva sulla struttura e sul funzionamento degli ecosistemi acquatici nel loro adattamento al cambiamento globale.

CHAPTER 1

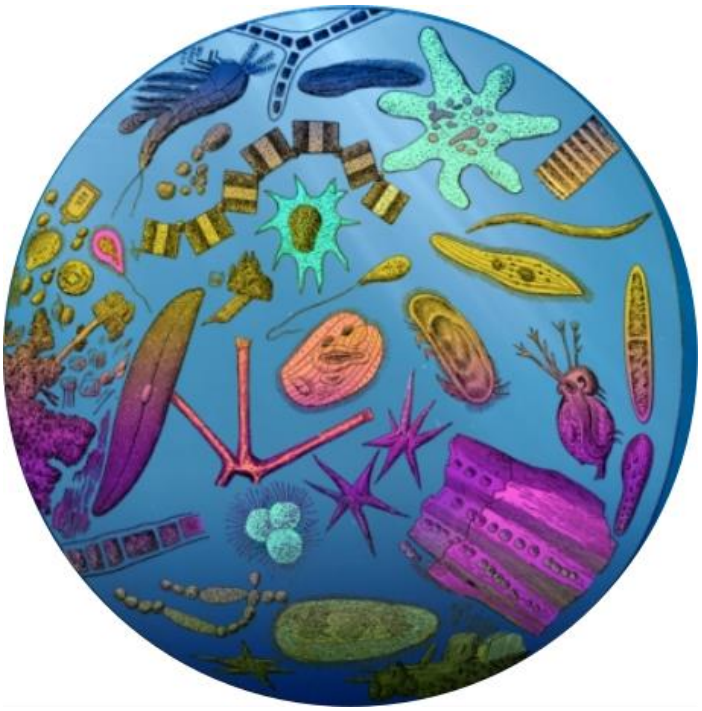

Reference: MIT News

CHAPTER 1 – Introduction Thesis

The context of global change: Factors interacting in aquatic ecosystems

Global change, induced by human actions, includes alterations in climate and in nutrient fluxes resulting from the interaction of multiple abiotic environmental factors (Schulhof *et al.*, 2019). This set of abiotic factors, commonly referred to as drivers or stressors, include high temperatures, increased CO_2, greater nutrient concentrations (eutrophication), and intensified visible/UV irradiance (Boyd *et al.*, 2019). The action of global-change drivers can disturb the natural environments across different scales, i.e. influencing individual species (Wenger *et al.*, 2016) which in turn alter community composition and trophic webs (Schulhof *et al.*, 2019) and, ultimately, ecosystem function and stability (Ives & Carpenter, 2007). Therefore, new studies are needed to predict the responses to stressors in a changing world.

To date, most studies concerning global change and its impact on organisms and ecosystems have focused only on single stressors. However, this approach ignores the many possible combinations of interacting stressors, and their synergistic or antagonistic effects (Woodward *et al.*, 2010; Wake, 2019). The complexity of natural systems requires the assessment of interactions among multiple abiotic stressors acting at different temporal rates and on local [e.g. increased ultraviolet radiation (UVR)], regional (e.g. atmospheric dust) and global (warming) scales (Carrillo *et al.*, 2008; Durán *et al.*, 2016). All together, these stressors can exert a cumulative impact (Fig. 1), intensifying the pressures on ecosystems and altering species distribution, richness, and composition (Smale & Wernberg, 2013; Boucek & Rehage, 2014). This cumulative impact make species, communities, and ecosystems increasingly vulnerable to global

change (Dudgeon *et al.*, 2006; Koehn *et al.*, 2011). The result involves the possibility of non-additive responses that could mitigate or intensify the effects of global change (Giller *et al.*, 2004; Feuchtmayr *et al.*, 2009; Woodward *et al.*, 2010).

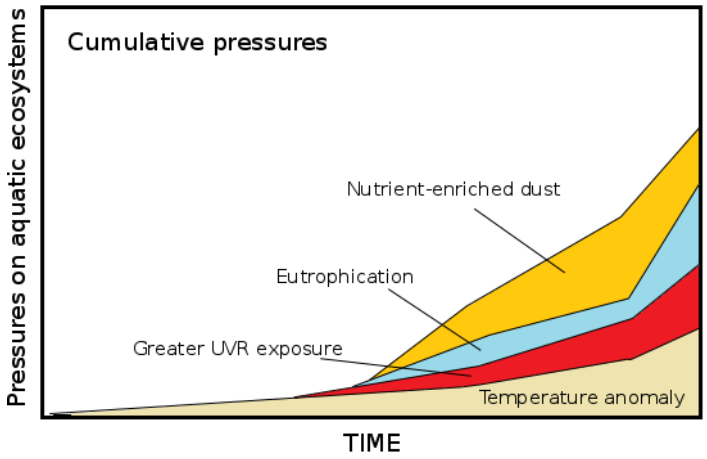

Figure 1. Hypothetical time lines for the emergence of cumulative pressures in the aquatic ecosystems. Modified from Duarte (2013), *In: The Conversation, http://theconversation.com/auditing-the-seven-plagues-of-coastal-ecosystems-13637.*

Aquatic ecosystems constitute key elements in global change given that they are the main sinks of carbon (C) on earth (Mendonça *et al.*, 2017) and, more specifically, given that their microbial food web is involved in the control of the energy storage and flux (Schramski *et al.*, 2015), regulation of nutrient cycles, trophic interaction, and gas exchanges in the water-atmosphere interface (Mostajir *et al.*, 2015).

Phytoplankton is an essential component in these ecosystems (Field *et al.*, 1998; Falkowski *et al.*, 2004), where processes such as primary production, respiration, and grazing affect the biogeochemical cycles (Roy *et al.*, 2013). The extent of the impact of phytoplanktonic activity on ecosystems depends on the spatial/temporal abundance and structure variation (Ward *et al.*, 2014).

Knowledge concerning the structure of phytoplanktonic community has notably transformed in recent decades (Flynn *et al.*, 2019). Contrary to the longstanding paradigm, based on the dichotomy of strict autotrophs and heterotrophs, today the two groups of organisms are known to constitute two ends of a gradient where cells able to combine autotrophy and heterotrophy (i.e. mixotrophs) predominate (Mitra *et al.*, 2014). Figure 2 shows a global distribution of protists, including the organisms considered to be primary producers (strict autotrophs and mixotrophs) and heterotrophic flagellates in some marine and freshwater areas.

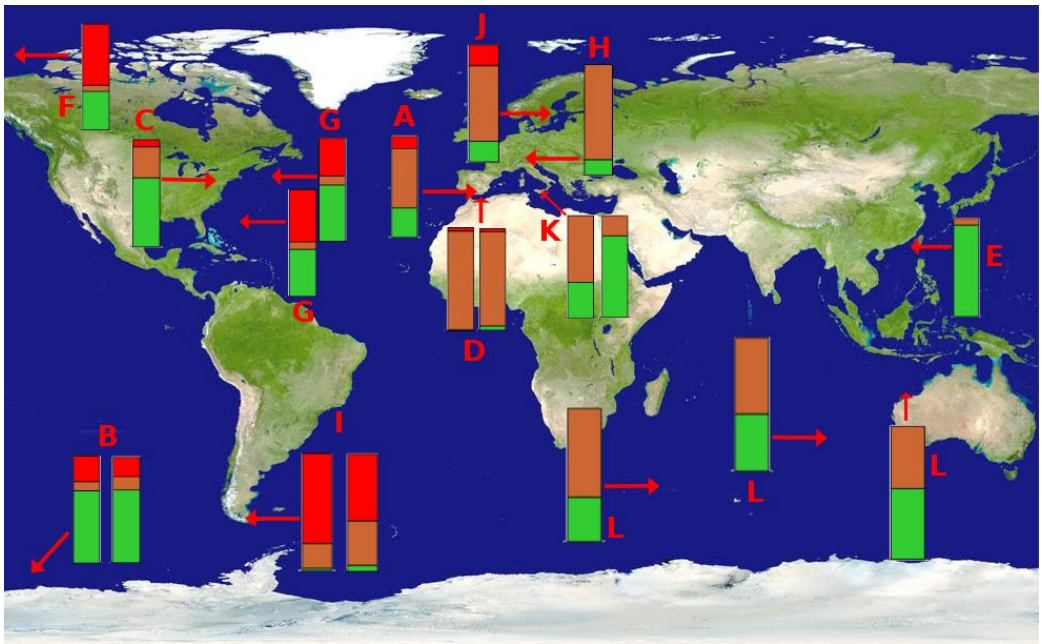

Figure 2. Global distribution of phytoplankton and heterotrophic flagellates in freshwater and marine areas. The columns are represented as percentage of abundance/biomass for strict autotrophs (green), mixotrophs (brown) and heterotrophs (red). References: A (González-Olalla et al., 2018), B (Gast et al., 2018), C (Princiotta & Sanders, 2017), D (González-Olalla et al., 2017), E (Wang et al., 2009), F (Sanders & Gast, 2012), G (Sanders et al., 2000), H (Callieri *et al.*, 2003), *I* (Saad *et al.*, 2013), *J* (Jansson *et al.*, 1996), *K* (Naselli-Flores & Barone, 2018), *L (Schlüter et al., 2011).*

Mixotrophic protists are ubiquitous (Fig. 2) and often abundant in marine and freshwater ecosystems ranging from low to high latitudes and elevations along different trophic states (from eutrophic to oligotrophic waters) (see Sanders *et al.*, 2000; Medina-Sánchez *et al.*, 2004; Unrein *et al.*, 2007; Moorthi *et al.*, 2009; Hartmann *et al.*, 2012; Hansen & Anderson, 2019). Several studies have reported that the competitive ability of these organisms increases in oligotrophic ecosystems (Modenutti, 2014), such as high-mountain lakes (Callieri *et al.*, 2003; Carrillo *et al.*, 2017) or oligotrophic marine areas (Hartmann *et al.*, 2012; Unrein *et al.*, 2014); whereas strict autotrophs and heterotrophs are more abundant in eutrophic waters or regions not limited by prey (Leles *et al.*, 2018).
Nevertheless, a critical gap in information persists concerning how and why the different protists groups are distributed, their abundance, and how they can modulate trophic-web dynamics and biogeochemical cycles (Leles *et al.*, 2018). Thus, it is necessary to identify the drivers and mechanisms (Stanca & Parsons, 2017) that can potentially affect these groups (Harding *et al.*, 2015; Bussi *et al.*, 2016).

With respect to the factors determining the abundance and distribution of protist organisms, this thesis focuses on the single and interactive effects of three such factors of special interest for their local as well as global impact: high temperatures, greater nutrient inputs, and intensified UVR exposure.
Temperature is a global factor with the capacity to regulate metabolic rates. This is the mainstay of the Metabolic Theory of Ecology (MTE; Brown *et al.*, 2004), which provides a common response spanning levels from individuals to ecosystems and affecting the trophic-web structure as well as its productivity (Müren *et al.*, 2005; O'Connor *et al.*, 2009). Several studies have revealed that rising temperatures affect the heterotrophic more strongly than autotrophic metabolism (Allen, 2005; Rose & Caron, 2007; Wilken *et al.*, 2013). This in

turn can affect the ratio of primary production: respiration and can shift the ecosystem balance from net autotrophy to heterotrophy (Yvon-Durocher *et al.*, 2010). Temperature affects not only organisms but also the physical conditions of water, altering stratification patterns and thereby leading to a greater exposure of cells to solar radiation, including UVR (Häder *et al.*, 2014; see Fig. 3). Although the effects of UVR on phytoplankton vary with the taxonomic group, habitat, and developmental stage (Bancroft *et al.*, 2007), some of these effects have negative consequences for cells, including inhibition of DNA synthesis and the reduction of primary production and growth, particularly due to UV-B (Buma *et al.*, 2003; Villafañe *et al.*, 2003). The algal response to UVR exposure and temperature is species-specific and, furthermore, this particular sensitivity depends on nutrient availability (mainly N and P; see Korbee- Peinado *et al.*, 2004; Medina-Sánchez *et al.*, 2006).

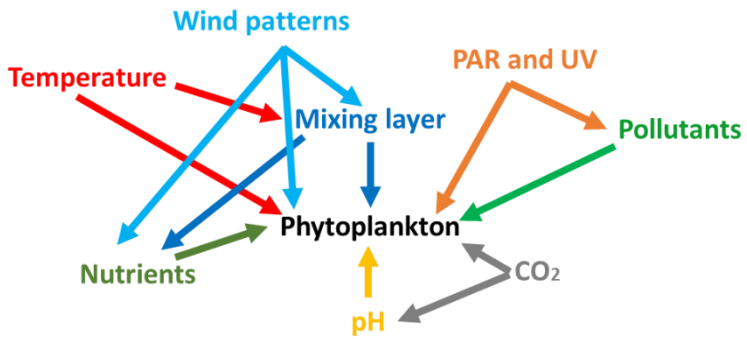

Figure 3. Interaction of factors affecting phytoplankton (from Häder & Gao, 2015)

In this regard, the increase of nutrient-enriched dust inputs from the Sahara desert (Villar-Argaiz *et al.*, submitted) can determine the organism's response (Chien *et al.*, 2016; Zhang *et al.*, 2018). In fact, dust from Sahara desert (Bozlaker *et al.*, 2013) constitutes a major portion of the global aerosol (Monks

et al., 2009) that affects the earth's radiative balance (Mahowald *et al.*, 2014; Weinzierl *et al.*, 2017) and supplies aquatic systems with micronutrients such as Fe and P (Zhang *et al.*, 2015). In a future scenario where land becomes drier worldwide due to higher temperatures, dust inputs from deserts to the atmosphere are expected to increase following the trend described by Villar-Argaiz *et al.*, (submitted) from 1980 (see Fig. 4). Greater dust inputs can exert opposite effects on phytoplankton, such as stimulation (Jickells & Moore, 2015) or inhibition (Knippertz & Stuut, 2014) of primary production, while the interaction with other environmental factors can affect biogeochemical processes (Jickells & Moore, 2015; Reche *et al.*, 2018).

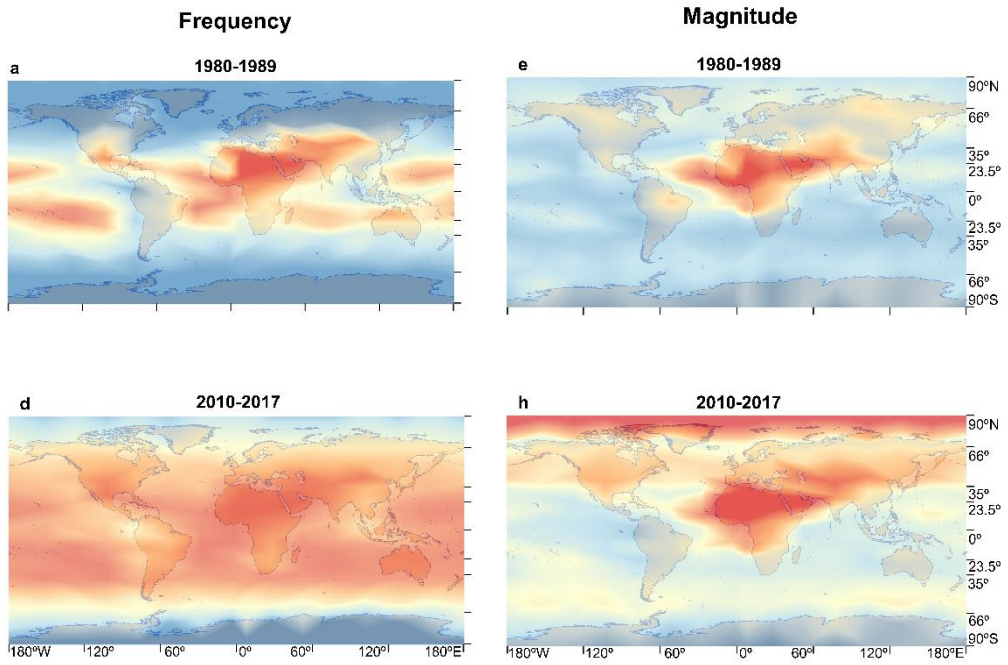

Figure 4. Frequency (left) and magnitude (right) of aerosol index events higher than 0.5, obtained from satellite observations for the periods from 1980 to 1989 (top graphs) and from 2010 to 2017 (bottom graphs) (from Villar-Argaiz *et al.*, submitted).

The study of global change from different organization levels and temporal gradients

The connection between organizational levels in plankton ecology has been scarcely studied, despite the fact that biological dynamics exert an effect across scales (Prairie *et al.*, 2012). For example, the action of environmental factors can benefit the physiological activity of certain cells, selecting particular species in a specific niche, and the changes in physiological activity allow species to adapt to new environments (Allen & Polimene, 2011). Likewise, the global-change effect on the biochemical activity of unicellular microorganisms plays a fundamental role in the biosphere due to its involvement in the biogeochemical cycles of the elements (Canfield *et al.*, 2005; see Fig. 5). Therefore, a thorough study of the physiological mechanisms that operate within the cell (photosynthesis, respiration, antioxidant response, etc.) is necessary in order to understand ecological dynamics (e.g. Armstrong, 2006).

The necessity of associating responses at different organizational levels (Woodward *et al.*, 2010) has led to a novel discipline (Matantseva & Skarlato, 2013) which seeks to interconnect classical ecology and cell physiology. The present thesis follows this line, using different methods to explore how the warming, nutrient inputs, and UVR-exposure affect the phytoplankton, from cellular activity (quantum photosyntetic yield, enzymatic activities; cell respiration, etc.) to cell distribution and interaction with other microorganisms. For example, the evaluation of physiological state of phytoplankton cells using Fast Repetition Rate fluorometry, or measuring primary production or respiration helps to diagnose the stress of phytoplankton caused by high temperatures, nutrient limitation or light inhibition (Greene *et al.*, 1994). This response can be connected with phytoplankton abundance and composition, as demonstrated in Chapters 2 and 3.

In addition, the effect of the interacting factors may vary depending on the time of experimentation or observation, since organisms can acclimate to new environmental conditions over the short term, or adapt over the long term (Hennon *et al.*, 2014). Studies over different temporal gradients can help detect the impacts of global change on organisms and ecosystems and determine how ecological processes respond to change. In this thesis, the long-term studies use observational approaches (Chapter 3), which identify the temporal development of phytoplankton, as well as their relationship with other organisms.

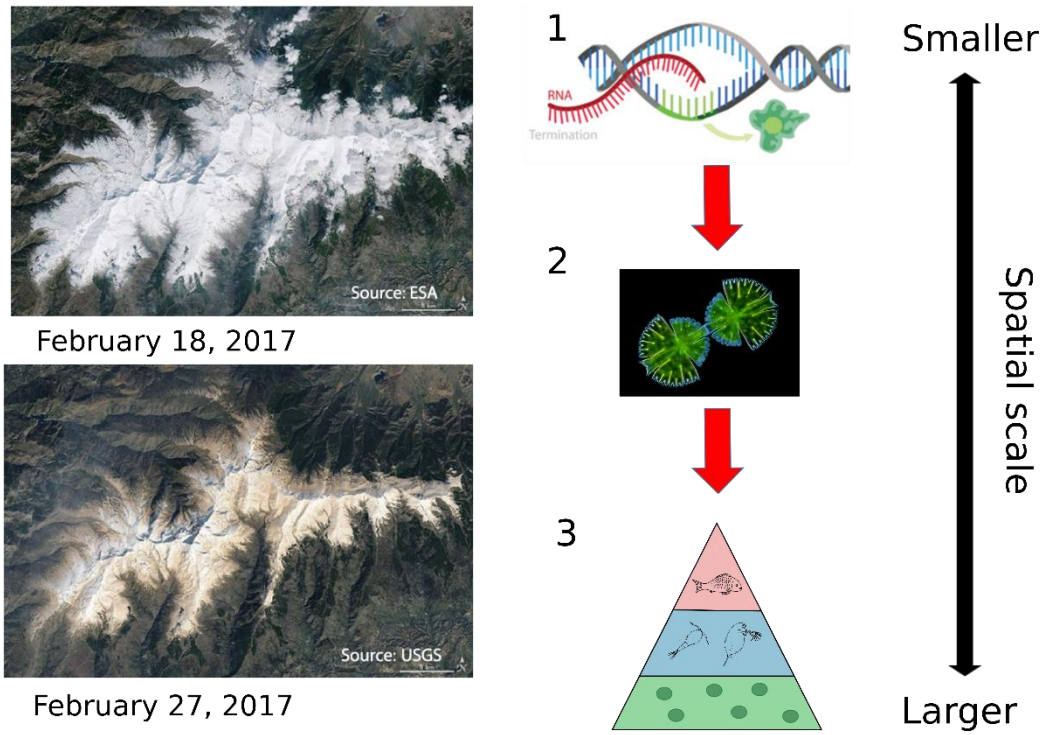

Figure 5. Schematic diagram showing how different levels of organization in the plankton can interact across scales affected by a global process. This example shows how the P-enriched Saharan dust inputs to high-mountain lakes of Sierra Nevada (S Spain; photos on the left side from González-Olalla *et al.*, 2018) *can increase RNA synthesis (1), necessary to sustain a higher growth rate of phytoplankton (2; in the image, Micrasterias rotate undergoing cell division; Dr. Wim van Egmond) and that can affect the trophic dynamics (3).*

The long-term observational study will be carried out in high-mountain lakes, areas recognized as sentinels of global change (Williamson *et al.*, 2008) because of their inherent sensitivity to environmental stressors (Battarbee *et al.*, 2002; Catalan *et al.*, 2013) and because these areas undergo the fastest rates of warming on the planet (Hassan *et al.*, 2005).

On the contrary, the experimental approaches in this thesis (Chapter 4, 5, and 6) are related to short-term studies (from hours to days), enabling inquiry into the relationship between a driver (or drivers) and the ecological and physiological response of the organisms (Riebesell & Gattuso, 2015). A fuller understanding of the responses and physiological tolerances of organisms to environmental factors and their interaction will also improve the ability of researchers to identify the most vulnerable metabolism, species, and trophic interactions (Nicotra *et al.*, 2015).

Regulation of mixotrophy by global-change drivers

Given the increasingly acknowledged importance that mixotrophy (or mixoplankton; see Fig. 6) plays in trophic webs (Stoecker *et al.*, 2017), and the lack of studies showing how this metabolism can be affected by the interaction of global-change factors, this thesis focuses on mixotrophy.

Table 1. Comparison between number of articles related to mixotrophy and phytoplankton over the period 1980-2019, according to Web of Science catalogue.

	Years 1980-1999	**Years 2000-2009**	**Years 2010-2019**
Mixotrophy	79	192	527
Phytoplankton	13,521	18,934	27,118

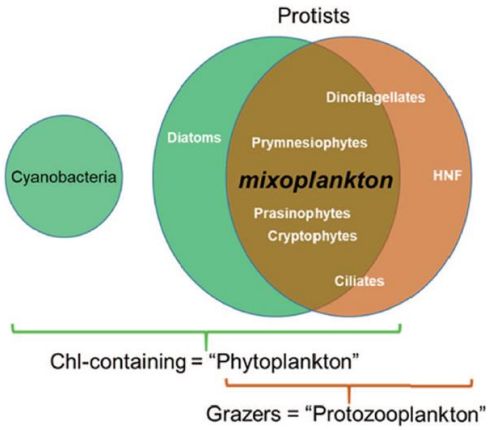

Figure 6. Overlaps in the trophic capacity of different microplankton, with organisms containing Chl-a such as phytoplankton and grazers such as protozooplankton. Mixoplankton organisms combine both characteristics. From Flynn *et al.* (2019).

The study of mixotrophic metabolism and its role in the trophic web is a relatively new field of study in Ecology (see Table 1). The first article referring to mixotrophy was published in 1982, related to the bacterium *Aquaspirillum autotrophicum*, and in 1988, the first manuscript referring to a mixotrophic microalgae ("Phagotrophic Phototrophs - The Ecological Significance of Mixotrophy") was published (Boraas *et al.*, 1988).

It has been proposed that mixotrophy can reinforce the biological carbon pump and the transfer or organic matter to upper levels of the trophic web (Ward & Follows, 2016; Stoecker *et al.*, 2017), and the consequences for communities and ecosystem functioning are still scarcely understood. Furthermore, it is important to determine which conditions favour the mixotrophy because mixotrophs are likely to vary their strategy across environmental gradients (Berge *et al.*, 2017; Chakraborty *et al.*, 2017). Previous studies have demonstrated that the success of this strategy is determined by light availability (Medina-Sánchez *et al.*, 2004), nutrient concentration, and prey (Modenutti,

2014; Liu *et al.*, 2016), and also the competition with strict autotrophs and heterotrophs for the resources (Tittel *et al.*, 2003). In this regard, culture-based ecophysiology will help refine the characterization of mixotrophic strategies and associated trade-offs (Edwards, 2019).

Thesis structure and objectives

Throughout this doctoral thesis, evaluations are made concerning how the interactive effects of global change factors can affect aspects ranging from the structure and functioning of ecosystems to their impact on metabolism and physiology of organisms. Studies on interactive effects articulate how these factors interact with each other, identifying their causal relationship with community and organisms, and determining their relative importance.

Thus, in the first part of the thesis, from an observational and experimental approach, an evaluation is made of how global-change factors affect the phytoplankton community in marine and freshwater aquatic ecosystems. The objectives of this first part are:

1. To understand how the UVR × Dust interaction affects phytoplankton metabolism in two areas with contrasting trophic status of western Mediterranean Sea (Chapter 2: Contrasting effect of Saharan dust and UVR on autotrophic picoplankton in nearshore versus offshore waters of Mediterranean Sea).

2. To evaluate how global change has altered phytoplankton metabolism and the algae-bacteria relationship along trophic gradients in aquatic ecosystems from the southern Iberian Peninsula (Chapter 3: Climate-driven shifts in algae-bacteria interaction of high-mountain lakes in two years spanning a decade).

Finally, the last chapters of this thesis focus on mixotrophic protists due to their increasingly recognized role in trophic webs. The objectives about mixotrophy are:

3. To assess how the nutrient enrichment can alter the protist's response to high temperatures in a simplified assemblage formed by a strict autotroph and a mixotroph (Chapter 4: Testing the Metabolic Theory of Ecology on protists under fluctuating temperature and nutrient enrichment).

4. To evaluate the metabolic and stoichiometric response of mixotrophic species under the interaction of stress factors (Chapter 5: Mixotrophic trade-off under warming and UVR in a marine and a freshwater alga).

5. To analyse, from a physiological perspective, how phagotrophy in mixotrophic organisms may provide an advantage over strict autotrophy (Chapter 6: Regulation of phagotrophy in the mixotrophic haptophyte *Isochrysis galbana*).

Finally, Chapter 7 summarizes the main findings of this thesis while Chapter 8 provides the conclusions.

References

Allen, A. P., Gilloly, J. F. & Brown, J. H. (2005). Linking the global carbon cycle to individual metabolism. *Funct. Ecol.* 19(2): 202–213.

Allen, J. I. & Polimene, L. (2011). Linking physiology to ecology: Towards a new generation of plankton models. *J. Plankton Res.* 33: 898–997

Armstrong, R. A. (2006). Optimality-based modeling of nitrogen allocation and photoacclimation in photosynthesis. *Deep-Sea Res. Part II-Top. Stud. Oceanogr.* 53: 513–531

Bancroft, B. A, Baker, N. J. & Blaustein, A. R. (2007). Effects of UVB radiation on marine and freshwater organisms: A synthesis through meta-analysis. *Ecol. Lett.* 10: 332–345

Battarbee, R. W., Grytnes, J., Thompson, R., Appleby, P. G., Catalan, J., Korhola, A., Heegaard, E. & Lami, A. (2002). Comparing palaeolimnological and instrumental evidence of climate change for remote mountain lakes over the last. *J. Paleolimn.* 28(1): 161–179.

Berge, T., Chakraborty, S., Hansen, P. J. & Andersen, K. H. (2017). Modeling succession of key resource-harvesting traits of mixotrophic plankton. *ISME J.* 11: 212–223

Boraas, M. E., Estep, K. W., Johnson, P. W. & Sieburth, J. M. N. (1988). Phagotrophic Phototrophs: The Ecological Significance of Mixotrophy,. *J. Protozool.* 35: 249–252

Boucek, R. E. & Rehage, J. S. (2014). Climate extremes drive changes in functional community structure. *Glob. Change Biol.* 20: 1821–1831

Boyd, P. W., Collins, S., Dupont, S., Fabricius, K., Gattuso, J. P., Havenhand, J., Hutchins, D. A., McGraw, C. M., Riebesell, U., Vichi, M. *et al.* (2019). *SCOR WG149 Handbook to support the SCOR Best Practice Guide for 'Multiple Drivers' Marine Research*. University of Tasmania.

Bozlaker, A., Prospero, J. M., Fraser, M. P. & Chellam, S. (2013). Quantifying the contribution of long-range saharan dust transport on particulate matter concentrations in Houston, Texas, using detailed elemental analysis. *Environ. Sci. Technol.* 47: 10179–10187

Brown, J.H., Gilooly, J.F., Allen, A.P., Savage, V.M. & West, G.B. (2004). Toward a metabolich theory of ecology. *Ecology* 85: 1771–1789.

Buma, A. G. J., Boelen, P. & Jeffrey, W. H. (2003). UVR-induced DNA damage in aquatic organisms. In: Helbling EW, Zagarese HE, eds. UV Effects in Aquatic Organisms and Ecosystems. Comprehensive Series in Photochemistry and Photobiology. Cambridge: Cambridge Royal Society of Chemistry. 291–327

Bussi, G., Whitehead, P. G., Bowes, M. J., Read, D. S., Prudhomme, C. & Dadson, S. J. (2016). Impacts of climate change, land-use change and phosphorus reduction on phytoplankton in the River Thames (UK). *Sci. Total Environ.* 572: 1507–1519

Callieri, C., Bertoni, R. & Corno, G. (2002). Dynamics of bacteria and mixotrophic flagellates in an Alpine lake in relation to Daphnia population development Dynamics of bacteria and mixotrophic flagellates in an Alpine lake in relation to Daphnia population development. *J. Limnol.* 61(2): 177-182

Canfield, D. E., Kristensen, E. & Thamdrup, B. (2005). *Aquat. Geomicrobiol.* (DE Canfield, E Kristensen, and B Thamdrup, Eds.). Elsevier Academic Press. pp. 599

Carrillo, P., Delgado-Molina, J. A., Medina-Sánchez, J. M., Bullejos, F. G. & Villar-Argaiz, M. (2008). Phosphorus inputs unmask negative effects of ultraviolet radiation on algae in a high mountain lake. *Glob. Change Biol.* 14: 423–439

Carrillo, P., Medina-Sánchez, J.M., Villar-Argaiz, M., Bullejos, F.J., Durán, C.,

Bastidas-Navarro, M., Souza, M.S., Balseiro, E.G. & Modenutti, B.E. (2017). Vulnerability of mixotrophic algae to nutrient pulses and UVR in an oligotrophic Southern and Northern Hemisphere lake. *Sci. Rep.* 7: 1–11.

Catalan, J., Pla-Rabés, S., Wolfe, A. P., Smol, J. P., Rühland, K. M., Anderson, N. J., Kopáček, J., Stuchlík, E., Schmidt, R., Koinig, K. A. *et al.* (2013). Global change revealed by palaeolimnological records from remote lakes: A review. *J. Paleolimn.* 49: 513–535

Chakraborty, S., Nielsen, L. T., Andersen, K. H. (2017). Trophic strategies of unicellular plankton. *Am. Nat.* 189: E77–E90

Chien, C.-T., Mackey, K. R. M., Dutkiewicz, S., Mahowald, N. M., Prospero, J. M. & Paytan, A. (2016). Effects of African dust deposition on phytoplankton in the western tropical Atlantic Ocean off Barbados. *Glob. Biogeochem. Cycles.* 30(5): 716-734

Duarte, C. M. (2013). Auditing the Seven Plagues of Coastal Ecosystems. *The Conversation*.

Dudgeon, D., Arthington, A. H., Gessner, M. O., Kawabata, Z. I., Knowler, D. J., Lévêque, C., Naiman, R. J., Prieur-Richard, A. H., Soto, D., Stiassny, M. L. J. *et al.* (2006). Freshwater biodiversity: Importance, threats, status and conservation challenges. *Biological Reviews of the Cambridge Philosophical Society.* 81: 163–182

Durán, C., Medina-Sánchez, J.M., Herrera, G. & Carrillo, P. (2016). Changes in the phytoplankton-bacteria coupling triggered by joint action of UVR, nutrients, and warming in Mediterranean high-mountain lakes. *Limnol. Oceanogr.* 61: 413–429.

Edwards, K. F. (2019). Mixotrophy in nanoflagellates across environmental gradients in the ocean. *Proc. Nat. Acad. Sci.* 116: 6211–6220

Falkowski, P. G., Katz, M. E., Knoll, A. H., Quigg, A., Raven, J. A., Schofield, O. & Taylor, F. J. R. (2004). The evolution of modern eukaryotic phytoplankton. *Science.* 305: 354–360

Feuchtmayr, H., Moran, R., Hatton, K., Connor, L., Heyes, T., Moss, B., Harvey, I. & Atkinson, D. (2009). Global warming and eutrophication: Effects on water chemistry and autotrophic communities in experimental hypertrophic shallow lake mesocosms. *J. Appl. Ecol.* 46: 713–723

Field, C. B., Behrenfeld, M. J., Randerson, J. T. & Falkowski, P. (1998). Primary production of the biosphere: Integrating terrestrial and oceanic components. *Science.* 281: 237–240

Flynn, K. J., Mitra, A., Anestis, K., Anschütz, A. A., Calbet, A., Ferreira, G. D., Gypens, N., Hansen, P. J., John, U., Martin, J. L. *et al.* (2019). Mixotrophic protists and a new paradigm for marine ecology: where does plankton research go now? *J. Plankton Res.* 00: 1–17

Gast, R. J., Fay, S. A. & Sanders, R. W. (2018). Mixotrophic activity and diversity of Antarctic marine protists in austral summer. *Front. Mar. Sci.* 5: 1–12

Giller, P. S., Hillebrand, H., Berninger, U. G., Gessner, M. O., Hawkins, S., Inchausti, P., Inglis, C., Leslie, H., Malmqvist, B., Monaghan, MT. *et al.* (2004). Biodiversity effects on ecosystem functioning: Emerging issues and their experimental test in aquatic environments. *Oikos.* 104: 423–436

González-Olalla, J. M., Medina-Sánchez, J. M., Cabrerizo, M. J., Villar-Argáiz, M., Sánchez-Castillo, P. M. & Carrillo, P. (2017). Contrasting effect of Saharan dust and UVR on autotrophic picoplankton in nearshore versus offshore waters of Mediterranean Sea. *Journal of Geophysical Research: Biogeosciences.* 122: 2085–2103

González-Olalla, J. M., Medina-Sánchez, J. M., Lozano, I. L., Villar-Argaiz, M. & Carrillo, P. (2018). Climate-driven shifts in algal-bacterial interaction of high-mountain lakes in two years spanning a decade. *Sci. Rep.* 8: 1–12

Greene, R. M., Kolber, Z. S., Swift, D. G., Tindale, N. W. & Falkowski, P. G. (1994). Physiological limitation of phytoplankton photosynthesis in the eastern equatorial Pacific determined from variability in the quantum yield of fluorescence. *Limnol. Oceanogr.* 39: 1061–1074

Häder, D. P. & Gao, K. (2015). Interactions of anthropogenic stress factors on marine phytoplankton. *Front. Environ. Sci.* 3: 1–14

Häder, D. P., Villafañe, V. E. & Helbling, E. W. (2014). Productivity of aquatic primary producers under global climate change. *Photochem. Photobiol. Sci.* 13: 1370–1392

Hansen, P. J. & Anderson, R. (2019). *Mixotrophy Among Freshwater and Marine Protists*. Encyclopledia of Microbiology, 4e. Elsevier Ltd.

Harding, L. W., Adolf, J. E., Mallonee, M. E., Miller, W. D., Gallegos, C. L., Perry, E. S., Johnson, J. M., Sellner, K. G. & Paerl, H. W. (2015). Climate effects on phytoplankton floral composition in Chesapeake Bay. *Estuar. Coast. Shelf Sci.* 162: 53–68

Hartmann, M., Grob, C., Tarran, G. A., Martin, A. P., Burkill, P. H., Scanlan, D. J. & Zubkov, M. V. (2012). Mixotrophic basis of Atlantic oligotrophic ecosystems. *Proc. Nat. Acad. Sci.* 109: 5756–5760

Hassan, R., Scholes, R. & Ash, N. (2005). *Millenium Ecosystem Assessment, Ecosystems and Human Well-being: Current State and Trends, vol. 1*. Washington DC: Island Press.

Hennon, G. M. M., Quay, P., Morales, R. L., Swanson, L. M. & Virginia Armbrust, E. (2014). Acclimation conditions modify physiological response of the diatom Thalassiosira pseudonana to elevated CO2 concentrations in a nitrate-limited chemostat. *J. Phycol.* 50: 243–253

Ives, A. R. & Carpenter, S. R. (2007). Stability and diversity of ecosystems. *Science.* 317: 58–62

Jansson, M., Blomqvist, P., Jonsson, A. & BergstrÖm, A. (1996). Nutrient limitation of bacterioplankton, autotrophic and mixotophic phytoplankton, and heterotrophic nanoflagellates in Lake Örträsket. Limnol. Oceanogr. 41: 1552–1559

Jickells T, Moore CM. 2015. The Importance of Atmospheric Deposition for Ocean Productivity. *Annu. Rev. Ecol. Evol. Syst.* 46: 481–501

Knippertz, P. & Stuut, J. B. W. (2014). Mineral dust: A key player in the earth system. *Mineral Dust: A Key Player in the Earth System*. 1–509

Koehn, J. D., Hobday, A. J., Pratchett, M. S. & Gillanders, B. M. (2011). Climate change and Australian marine and freshwater environments, fishes and fisheries: Synthesis and options for adaptation. *Mar. Freshw. Res.* 62: 1148–1164

Korbee- Peinado, N., Abdala Díaz, R. T., Figueroa, F. L. & Helbling, E. W. (2004). Ammonium and UV radiation stimulate the accumulation of mycosporine-like amino acids in Porphyra columbina (Rhodophyta) from Patagonia, Argentina. *J. Phycol.* 40: 248–259

Leles, S. G., Polimene, L., Bruggeman, J., Blackford, J. & Ciavatta, S. (2018). Modelling mixotrophic functional diversity and implications for ecosystem function. 00: 1–16

Liu, Z., Campbell, V., Heidelberg, K. B. & Caron, D. A. (2016). Gene expression characterizes different nutritional strategies among three mixotrophic protists. *FEMS Microbiol. Ecol.* 92: 1–11

Mahowald, N., Albani, S., Kok, J. F., Engelstaeder, S., Scanza, R., Ward, D. S. & Flanner, M. G. (2014). The size distribution of desert dust aerosols and its impact on the Earth system. *Aeolian Res.* 15: 53–71

Matantseva, O. V. & Skarlato, S. O. (2013). Mixotrophy in Microorganisms: Ecological and Cytophysiological Aspects. 49

Medina-Sánchez, J.M., Villar-Argaiz, M., & Carrillo P. (2004). Neither with nor without you: A complex algal control on bacterioplankton in a high mountain lake. *Limnol. Oceanogr.* 49: 1722–1733.

Medina-Sánchez, J. M., Villar-Argaiz, M. & Carrillo, P. (2006). Solar radiation – nutrient interaction enhances the resource and predation algal control on bacterioplankton : A short-term experimental study. *Limnol. Oceanogr.* 51: 913–924

Mendonça, R., Müller, R. A., Clow, D., Verpoorter, C., Raymond, P., Tranvik, L. J. & Sobek, S. (2017). Organic carbon burial in global lakes and reservoirs. *Nat. Commun.* 8: 1694

Mitra, A., Flynn, K. J., Burkholder, J. M., Berge, T., Calbet, A., Raven, J. A., Granéli, E., Glibert, P. M., Hansen, P. J., Stoecker, D. K. *et al.* (2014). The role of mixotrophic protists in the biological carbon pump. *Biogeosciences.* 11: 995–1005

Modenutti, B. (2014). Mixotrophy in Argentina freshwaters. *Adv. Limnol.* 65: 359–374

Monks, P. S., Granier, C., Fuzzi, S., Stohl, A., Williams, M. L., Akimoto, H., Amann, M., Baklanov, A., Baltensperger, U., Bey, I. *et al.* (2009). Atmospheric composition change - global and regional air quality. *Atmos. Environ.* 43: 5268–5350

Moorthi, S., Caron, D. A., Gast, R. J. & Sanders, R. W. (2009). Mixotrophy : a widespread and important ecological strategy for planktonic and sea-ice nanoflagellates in the Ross Sea , Antarctica. 54: 269–277

Mostajir, B., Amblard, C., Buffan-Dubau, E., De Wit, R., Lensi, R., Sime-Ngando, T. (2015). Microbial food webs in aquatic and terrestrial ecosystems. In: Bertrand JC, Caumette P, Lebaron P, Matheron R, Normand P, Sime-Ngando T, eds. Environmental Microbiology: Fundamentals and Applications. Dordrecht, The Netherlands: Springer Netherlands. 485–509

Müren, U., Berglund, J., Samuelsson, K. & Andersson, A. (2005). Potential effects of elevated sea-water temperature on pelagic food webs. *Hydrobiologia.* 545: 153–166

Naselli-Flores, L. & Barone, R. (2018). Mixotrophic phytoplankton dynamics in a shallow Mediterranean water body: how to make a virtue out of necessity. *Hydrobiologia.* 831: 33–41

Nicotra, A. B., Beever, E. A., Robertson, A. L., Hofmann, G. E. & O'Leary, J. (2015). Assessing the components of adaptive capacity to improve conservation and management efforts under global change. *Conserv. Biol.* 29: 1268–1278

O'Connor, M. I., Piehler, M. F., Leech, D. M., Anton, A. & Bruno, J. F. (2009). Warming and resource availability shift food web structure and metabolism. *PLoS. Biol.* 7

Prairie, J. C., Sutherland, K. R., Nickols, K. J. & Kaltenberg, A. M. (2012). Biophysical interactions in the plankton: A cross-scale review. *Limnol. Oceanogr.: Fluids and Environments.* 2: 121–145

Princiotta, S. D. V. & Sanders, R. W. (2017). Heterotrophic and mixotrophic nanoflagellates in a mesotrophic lake: Abundance and grazing impacts across season and depth. *Limnol. Oceanogr.* 62: 632–644

Reche I, D'Orta G, Mladenov N, Winget DM, Suttle CA. 2018. Deposition rates of viruses and bacteria above the atmospheric boundary layer. *ISME J.* 12: 1154–1162

Riebesell, U. & Gattuso, J. P. (2015). Lessons learned from ocean acidification research. *Nat. Clim. Chang.* 5: 12–14

Rose, J.M. & Caron, D.A. (2007). Does low temperature constrain the growth rates of

heterotrophic protists? Evidence and implications for algal blooms in cold waters. *Limnol. Oceanogr.* 52: 886–895.

Roy, S., Sathyendranath, S., Bouman, H. & Platt, T. (2013). The global distribution of phytoplankton size spectrum and size classes from their light-absorption spectra derived from satellite data. *Remote Sen. Environ.* 139: 185–197.

Saad, J. F., Schiaffino, M. R., Vinocur, A., O'Farrell, I., Tell, G. & Izaguirre, I. (2013). Microbial planktonic communities of freshwater environments from Tierra del Fuego: Dominant trophic strategies in lakes with contrasting features. *J. Plankton Res.* 35: 1220–1233

Sanders, R. W., Berninger, U. G., Lim, E. L., Kemp, P. F. & Caron, DA. (2000). Heterotrophic and mixotrophic nanoplankton predation on picoplankton in the Sargasso Sea and on Georges Bank. *Mar. Ecol.-Prog. Ser.* 192: 103–118

Sanders, R. W. & Gast, R. J. (2012). Bacterivory by phototrophic picoplankton and nanoplankton in Arctic waters. *FEMS Microbiol. Ecol.* 82: 242–253

Schlüter, L., Henriksen, P., Nielsen, T. G. & Jakobsen, H. H. (2011). Phytoplankton composition and biomass across the southern Indian Ocean. *Deep-Sea Res. Part I-Oceanogr. Res. Pap.* 58: 546–556

Schramski, J. R., Dell, A. I., Grady, J. M., Sibly, R. M. & Brown, J. H. (2015). Metabolic theory predicts whole-ecosystem properties. Proc. Natl. Acad. Sci. U.S.A. 112: 2617–2622

Schulhof, M. A., Shurin, J. B., Declerck, S. A. J. & Van de Waal, D. B. (2019). Phytoplankton growth and stoichiometric responses to warming, nutrient addition and grazing depend on lake productivity and cell size. *Glob. Change Biol.* 25: 2751–2762

Smale, D. A. & Wernberg, T. (2013). Extreme climatic event drives range contraction of a habitat-forming species. *Proc. R. Soc. B-Biol. Sci.* 280

Stanca, E. & Parsons, M. L. (2017). Phytoplankton diversity along spatial and temporal gradients in the Florida Keys. *J. Plankton Res.* 39: 531–549

Stoecker, D. K., Hansen, P. J., Caron, D. A. & Mitra, A. (2017). Mixotrophy in the Marine Plankton. *Annu. Rev. Mar. Sci.* 9: 311–335

Tittel, J., Bissinger, V., Zippel, B., Gaedke, U., Bell, E., Lorke, A. & Kamjunke, N. (2003). Mixotrophs combine resource use to outcompete specialists: Implications for aquatic food webs. *Proc. Nat. Acad. Sci.* 100: 12776–12781

Unrein, F., Gasol, J.M., Not, F., Forn, I. & Massana, R. (2013). Mixotrophic haptophytes are key bacterial grazers in oligotrophic coastal waters. *ISME J.* 8: 164–176.

Unrein, F., Massana, R., Alonso-sa, L. & Gasol, J. M. (2007). Significant year-round

effect of small mixotrophic flagellates on bacterioplankton in an oligotrophic coastal system. 52: 456–469

Villafañe, V. E., Sundbäck, K., Figueroa, F. L. & Helbling, E. W. (2003). Photosynthesis in the aquatic environment as affected by UVR. In: Helbling EW, Zagarese HE, eds. UV Effects in Aquatic Organisms and Ecosystems. London: Royal Society of Chemistry. 357–397

Villar-Argaiz, M., González-Olalla, J. M., Medina-Sánchez, J. M., Cabrerizo, M. J., Carrillo, P. & Biddanda, B. A. (2019). Remote sensing evidence for a dustier world in the 21st century. *Submitted to Nature Communications*

Wake, B. (2019). Experimenting with multistressors. *Nat. Clim. Chang.* 9: 357

Wang, Z., Zhao, J., Zhang, Y. & Cao, Y. (2009). Phytoplankton community structure and environmental parameters in aquaculture areas of Daya Bay, South China Sea. *J. Environ. Sci.* 21: 1268–1275

Ward, B. A., Dutkiewicz, S. & Follows, M. J. (2014). Modelling spatial and temporal patterns in size-structured marine plankton communities: Top-down and bottom-up controls. *J. Plankton Res.* 36: 31–47

Ward, B. A. & Follows, M. J. (2016). Marine mixotrophy increases trophic transfer efficiency, mean organism size, and vertical carbon flux. *Proc. Nat. Acad. Sci.* 113: 2958–2963

Weinzierl, B., Ansmann, A., Prospero, J. M., Althausen, D., Benker, N., Chouza, F., Dollner, M., Farrell, D., Fomba, W. K., Freudenthaler, J. *et al.* (2017). The Saharan Aerosol Long-Range Transport and Aerosol–Cloud-Interaction Experiment: overview and selected highlights. *Bull. Amer. Meteorol. Soc.* 98: 1–25

Wenger, A. S., Whinney, J., Taylor, B. & Kroon, F. (2016). The impact of individual and combined abiotic factors on daily otolith growth in a coral reef fish. *Sci. Rep.* 6: 1–10

Wilken, S., Huisman, J., Naus-Wiezer, S. & Van Donk, E. (2013). Mixotrophic organisms become more heterotrophic with rising temperature. *Ecol. Lett.* 16: 225–233.

Williamson, C. E., Dodds, W., Kratz., T. K. & Palmer, M. A. (2008). Lakes and streams as sentinels of environmental change in terrestrial and atmospheric processes. *Front. Ecol. Environ.* 6: 247–254

Woodward, G., Perkins, D. M., Brown, L. E. (2010). Climate change and freshwater ecosystems: Impacts across multiple levels of organization. *Philosophical Transactions of the Royal Society B: Biological Sciences.* 365: 2093–2106

Yvon-durocher, G., Jones, J.I., Trimmer, M., Woodward, G. & Montoya, J.M. (2010). Warming alters the metabolic balance of ecosystems. *Philos. Trans. R. Soc. B-Biol. Sci.* 365: 2117–2126.

Zhang, C., Gao, H., Yao, X., Shi, Z., Shi, J., Yu, Y., Meng, L. & Guo, X. (2018). Phytoplankton growth response to Asian dust addition in the northwest Pacific Ocean versus the Yellow Sea. *Biogeosciences.* 15: 749-765

Zhang, Y., Mahowald, N., Scanza, R. A., Journet, E., Desboeufs, K., Albani, S., Kok, J. F., Zhuang, G., Chen, Y., Cohen, D. D. *et al.* (2015). Modeling the global emission, transport and deposition of trace elements associated with mineral dust. *Biogeosciences.* 12: 5771–5792

CHAPTER 2

Sunset aboard the oceanographic ship Fco. De Paula Navarro in the middle of the Western Mediterranean Sea

CHAPTER 2 - Contrasting effect of Saharan dust and UVR on autotrophic picoplankton in nearshore versus offshore waters of Mediterranean Sea

J. M. González-Olalla, J. M. Medina-Sánchez, M. J. Cabrerizo, M. Villar-Argáiz, P. M. Sánchez-Castillo, and P. Carrillo

Published in Journal of Geophysical Research: Biogeosciences; 122 (8): 2085-2103; 2017; https://doi.org/10.1002/2017JG003834

Abstract

Autotrophic picoplankton (APP) is responsible for the vast majority of primary production in oligotrophic marine areas, such as the Alboran Sea. The increase in atmospheric dust deposition (e.g., from Sahara Desert) associated with global warming, together with the high UV radiation (UVR) on these ecosystems, may generate effects on APP hitherto unknown. We performed an observational study across the Alboran Sea to establish which factors control the abundance and distribution of APP, and we made a microcosm experiment in two distinct areas, nearshore and offshore, to predict the joint UVR × dust impact on APP at midterm scales. Our observational study showed that temperature (T) was the main factor explaining the APP distribution whereas total dissolved nitrogen positively correlated with APP abundance.

Our experimental study revealed that Saharan dust inputs reduced or inverted the UVR damage on the photosynthetic quantum yield (Φ_{PSII}) and picoplanktonic primary production (PP_P) in the nearshore area but accentuated it in the offshore. This contrasting effect is partially explained by the nonphotochemical quenching, acting as a photorepair mechanism. Picoeukaryotes reflected the observed effects on the physiological and metabolic variables, and Synechococcus was the only picoprokaryotic group that showed a positive response under UVR × dust conditions. Our study highlights a dual sensitivity of nearshore versus offshore

picoplankton to dust inputs and UVR fluxes, just at the time in which these two global-change factors show their highest intensities and may recreate a potential future response of the microbial food web under global-change conditions.

1. Introduction

Alboran Sea (south-western Mediterranean region) displays two quasi-permanent anticyclonic gyres determined mainly by the Atlantic current, topography, the Earth's rotational effect, and the predominant west winds (García-Górriz & Carr, 2001). Traditionally, these subtropical gyres are considered oligotrophic areas where autotrophic picoplankton (APP) (Prochlorococcus, Synechococcus, and picoeukaryotes) accounts for the major part of the phytoplankton biomass and primary production (PP) (Agawin *et al*., 2000; Alvain *et al*., 2005; Grossman *et al*., 2010; Buitenhuis *et al*., 2013). The small size and higher surface:volume ratio of APP give them a competitive advantage against nanoplankton growing at low nutrient concentrations (Agustí & Llabrés, 2007). Also, due to their smaller size, APP inhabiting low-resource environments are more efficient than larger-sized cells in photon absorption because of reduced chromophore self-shading (Raven, 1998). Nevertheless, its size may also pose a disadvantage under high levels of photosynthetically active radiation (PAR) or ultraviolet radiation (UVR), as APP possesses a low capacity for screening out damaging radiation probably due to a lower ability to distribute the intracellular UVR absorbed (Wu *et al*., 2016) and its inefficient photorepair mechanisms (Raven, 1998).

The Mediterranean region is an area particularly sensitive to global change (e.g., Belkin, 2009). In fact, the increase in severe droughts and positive anomalies in the North Atlantic Oscillation index (Mukhopadhyay & Kreycik, 2008), together with its position on the boundary between two climatic regimes (Giorgi & Lionello, 2008) and bordering the largest desert area in the world, leads to

frequent inputs of mineral-dust particles, prevalently during the summer (Bullejos *et al*., 2010; Gallisai *et al*., 2014). Recent evidence from dust-addition experiments (Lekunberri *et al*., 2010; Marañón *et al*., 2010) have indicated that dust inputs provide multiple nutrients to marine ecosystems (Mackey *et al*., 2015). Of special interest are the dust-derived phosphorus (P) effects on P-limited oligotrophic ecosystems, such as the Mediterranean Sea (Tanhua *et al*., 2013). Hence, dust deposition may alter phytoplankton physiology (e.g., Photosystem II functioning (Φ_{PSII}) (Strzepek & Harrison, 2004; Behrenfeld *et al*., 2009)), community structure (Finkel *et al*., 2010), marine productivity, and carbon sequestration (Jickells *et al*., 2005; Jickells & Moore, 2015; Cabrerizo *et al*., 2016). Although dust deposition increases macronutrients (e.g., P; Prospero & Lamb, 2003) as well as micronutrients (e.g., iron and calcium (Pulido-Villena *et al*., 2006; Shao *et al*., 2011)), and thus improves phytoplankton growth, it is not clear whether the excessive concentration of trace metals (e.g., copper) and contaminants contained in dust may also harm the metabolism and physiology of marine planktonic communities (Paytan *et al*., 2009), counterbalancing the positive effect of nutrients.

In the current global-change scenario, higher dust inputs together with many other anthropogenic stressors can simultaneously interact. In fact, global warming is expected to increase UVR exposure as result of a shallower upper mixed layer (UML) due to greater stratification of the water column (Barbieri *et al*., 2002; Häder *et al*., 2011; Carrillo *et al*., 2015a). In addition, the oligotrophic nature of waters and the high-incident fluxes of UVR in the Mediterranean region favor the deep penetration of radiation into the water column (Tedetti & Sempéré, 2006; Carrillo *et al*., 2015b). The contribution of UV-B (280–315 nm) and, to a lesser extent, UV-A (315–400 nm) to photoinhibition on primary producers is notable in the uppermost layer (Figueroa *et al*., 1997a, 1997b; Gang *et al*., 2011). Previous

studies have shown that UVR has a negative impact on several targets and processes (e.g., DNA synthesis, photosynthesis, and nutrient uptake) (Hessen *et al*., 1997; Buma *et al*., 2001; Day & Neale, 2002), including biomass, species composition, and growth rates of phytoplankton (Buma *et al*., 2003; Leu *et al*., 2007). However, beneficial UVR effects have also been reported (e.g., increased DNA photorepair (Helbling & Zagarese, 2003)). Therefore, the interaction between high UVR and increased dust aerosol deposition could create a new balance between damage and repair on the phytoplankton community, which is unknown.

Due to global warming, a greater extension of the subtropical oligotrophic gyres is expected to lead to a more important role of APP in global biogeochemical cycles (Morán *et al*., 2010). In this context, we analyze the distribution pattern of APP in Alboran Sea region and its relation with the main abiotic factors of global change with the aim of experimentally determining the nature and direction of interactive effects of Saharan dust and UVR on APP communities of nearshore (outside of the Western Anticyclonic Gyre) and offshore (inside the Western Anticyclonic Gyre) areas at short-term (hours) and midterm (days) scales. These areas were chosen for the potential differences in trophic and optical characteristics between them determined by the geostrophic currents in the region. The Western Anticyclonic Gyre may provide cold nutrient-rich water near the southern coast of Spain (Sarhan *et al*., 2000; García-Górriz & Carr, 2001), exerting a greater fertilizing effect on the photic layer and stimulating primary productivity (Packard *et al*., 1988), compared to offshore area. However, the existence, intensity, and shape of this gyre and the supply of nutrients are also controlled by horizontal circulation and seasonal stratification (García-Górriz & Carr, 2001). These masswater dynamics may bring about two areas with different optical characteristics, with the area of the nearshore usually presenting greater

opacity, due to, among other things, the runoff water and wave action (Romero *et al*., 2011), which in turn determine lesser exposure of phytoplankton to harmful levels of UVR than in Open Sea habitats (Erga *et al*., 2005; Tedetti & Sempéré, 2006). Thus, phytoplankton from the coastal area could be more sensitive to UVR under a shallower UML (Häder *et al*., 2014). Therefore, our working hypothesis is that APP community will be more UVR-damaged in the nearshore area than in the offshore area, because the cells in the latter area would be adapted to high UVR. The dust inputs, mainly through the macronutrient supply, will attenuate the harmful UVR effect, and the magnitude of this effect will be greater in the nearshore areas than in the offshore. To test this hypothesis, we performed an experiment lasting 5 days, evaluating the short-term (24 h) and midterm responses (5 days) of APP to manipulation of the radiation quality and dust supply. In this way, we evaluated the individual and interactive effects of both factors on the Φ_{PSII} yield, non-photochemical quenching (NPQ), picoplanktonic primary production (PP_P), and changes in the taxonomical composition of APP communities.

2. Material and Methods

a. Study area for observational and experimental study

The observational and experimental studies were conducted aboard the B/O Francisco de Paula Navarro (Spanish Institute of Oceanography) during the MICROSENS survey (17–21 June 2014). The cruise sailed from Malaga on 17 June and arrived at Almeria on 21 June. A total of 14 stations distributed along the Alboran Sea were sampled. For the observational study, seawater samples from each station were collected using 10 L-Niskin bottles, at depths of 3 and 15 m, because the UML depth in Alboran Sea tends to oscillate between 14 (±5) and 30 (±15) m (Báez *et al*., 2013; Houpert *et al*., 2015) during the same stage as our

sampling period. Samples from each station were used for the observational study (see details below).

Our experimental study was conducted with samples taken from stations 1 (nearshore, 36°37'N, 4°24'W) and 3 (offshore, 35°59´N, 4°19´W), starting the experiment on 17 June and carrying out biological, chemical, and physical measurements every day until 21 June. The seawater samples (from surface to 15 m depth) were filtered through a 200 μm pore size mesh to remove mesozooplankton and mixed in two acid-cleaned 150 L-PVC tanks. Zooplankton was removed to improve the replicability of the microcosm since its presence can generate unequal effects on the phytoplankton community. Then, prefiltered 15 L seawater from each area was dispensed into 20 L low-density polyethylene (LPDE) (Plasticos Andalucía, Spain) microcosms which were placed floating inside two black-walled tanks with running water to maintain the in situ temperature. LPDE transmits ~90% of PAR, 75% of UV-A, and 60% of UV-B. Microcosms were manually shaken every hour to prevent organisms from settling so that they would receive homogeneous irradiance. The samples were taken using a syringe connected to an acid-washed silicone tube inserted in each microcosm to avoid their being tampered with.

For an assessment of the combined impact of UVR and Saharan dust in each area, a 2 × 2 full factorial experimental design was implemented with (a) two light treatments, +UVR (>280 nm) versus _UVR (>400 nm) and (b) two dust treatments (dust and no-dust additions). Each treatment was applied in triplicate. For the –UVR treatment, the tank was covered with a sheet of Ultraphan Opak Difegra 395 filter, which screens out UVR < 390 nm and transmits ~90% of the PAR. For the +UVR treatments, the tank was covered with LDPE (Plásticos Andalucía, Spain) to ensure that the intensity of PAR received was identical in

both tanks. Also, half of microcosms for each area were amended with 4.1 mg L^{-1} (61.5 g m_2) of Saharan dust collected in situ from soil in the Moroccan region of Merzouga (Tafilalet, Morocco; 31°06´00´´N, 3°59´24´´W). The dust added was obtained from soil fractioning by means of a similar procedure as in Guieu *et al*. (2010)), in order to reproduce fine, long-range transported desert dust particles. Thus, the soil was sieved with a nested column with wire mesh cloth of 100 mm and 1 mm pore size, and dust was collected on a pan underneath the nest of sieves. The particles collected were then winnowed next to a tilted glass, and the particles that adhered to the glass were gently collected with a fine brush. With this method, the size of the collected sample ranged between 1 and 10 μm (LeitzFluovert FS, Leica, Wetzlar, Germany), this being within the range of the mean particle size of the Saharan Desert dust recorded in high-deposition events in the Mediterranean region (Guieu *et al*., 2010). To avoid any contamination with metals, we previously cleaned the plastic material and glass in contact with the soil using a 0.2 M HCl acid bath and Milli-Q® water.

Previously to the experimental dust addition, P-release experiments at the laboratory showed that 4.1 mg L^{-1} of dust released 0.97 ± 0.17 μM P. We calculated this concentration from the dust weight versus P concentration correlation (r2: 0.979; p-value: 0.029). Thus, adding 61.5 mg of Saharan dust to each microcosm (15 L) resulted in an experimental increase of 0.97 μM of P, mimicking a heavy but still realistic Saharan dust deposition, characteristic for the western Mediterranean region (sea and lakes) (Morales-Baquero *et al*., 2006; Lekunberri *et al*., 2010) and dust concentrations ranging 10–64 g m^{-2} (Romero *et al*., 2011; Ridame *et al*., 2014) during intense intrusion events of atmospheric aerosols over this area.

b. Physical parameters

b.1 Radiation measurements

A multichannel radiometer (Biospherical Instruments Inc., CA, USA), located on the deck of oceanographic ship, continuously registered measurements of the incident radiation at wavelengths representative of the different regions of the solar spectrum (305, 320, and 380 nm and full PAR (400–700 nm)) from the sunrise to sunset during the experimental period (17–21 June 2014). Vertical profiles of radiation attenuation with depth (at the same wavelengths as air measurements) and temperature of water column were determined at noon using a submersible radiometer (Biospherical Instruments Inc., CA, USA). Diffuse attenuation coefficients for downward radiation (k_d) in the upper layers (0 to 10 m) were determined from the slope of the linear regression of the natural logarithm of downwelling irradiance versus depth for each wavelength.

The mean irradiance (Im ((λ)) for the different regions of the solar spectrum (305, 320, and 380 nm and PAR) within the surface upper layers for each area was calculated as in following equation:

$$Im\ (\lambda) = \frac{\mathrm{I}_0(\lambda)[1 - \exp(-k_d(\lambda)\mathrm{z})]}{k_d(\lambda)\mathrm{z}}$$

where I_0((λ) is the mean incident surface irradiance, k_d(λ) is the mean attenuation coefficient for different region of the solar spectrum (305, 320, 380 nm and PAR), and z is the depth of the UML, 2 m in offshore and 6 m in the nearshore.

c. Chemical parameters

Samples for chemical determination of total dissolved N (TDN) and total dissolved P (TDP) were collected daily at each station early in the morning from each microcosm in 300 mL PET bottles and frozen at −20°C until analyzed. Water samples for determining the TDN and TDP were filtered at low pressure (<100

mmHg) using glass-fiber filters (Whatman GF/F, 25 mm diameter). The TDP and TDN concentrations were determined in 25 mL aliquots after digestion with a mixture of potassium persulphate and boric acid at 120°C for 30 min following the spectrophotometric method by Koroleff (1977) with a limit detection of 0.2 µM for N and 0.03 µM for P. To determine sestonic carbon (C), N, and P, volumes of 3 L for C-N or 1.5 L for P were filtered through precombusted (1 h at 550°C) glass-fiber filters (Whatman GF/F, 25 mm diameter). Filters for P, N, and C were immediately frozen at −20°C. In the laboratory, C and N analyses were performed using a Perkin-Elmer 2400 elemental analyzer with a limit detection of 1–3600 µg and 1–6000 µg for C and N, respectively. Determination of sestonic P followed the same method described for TP. Blanks were performed in all procedures. The sestonic N:P ratio was calculated on a molar basis.

For dissolved organic carbon (DOC) determination, samples from each microcosm were filtered through precombusted (2 h at 500°C) glass-fiber filters (Whatman GF/F, 25 mm diameter) and acidified with HCl 1 N (2%). The measurements were made in a total organic carbon analyzer (TOC-VCSH/CSN Shimadzu) with a detection limit of 50 ppb.

d. Biological parameters

d.1 Chlorophyll a Concentrations and UV-Absorbing Compounds

The Chlorophyll *a* (Chl *a*) concentration was determined by fluorometric technique using the equations of Jeffrey and Humphrey (1975). The samples were filtered onto glass-fiber filters (Whatman GF/F, 25 mm diameter) and the photosynthetic pigments were extracted in 5 mL of absolute methanol for 24 h at 4°C in darkness to remove all the chlorophyll from the filters. The extracts were measured using a fluorometer (Perkin-Elmer model LS 55, Boston, MA, USA). Previously, a calibration curve was made with pure spinach-chlorophyll extract

(Sigma Aldrich, USA) to transform fluorescence values into Chl a concentration. In addition, the same sample was used to determine UV-absorbing compounds (UV-ACs) by scanning between 250 and 750 nm using a Perkin Elmer UV/VIS spectrophotometer Lambda 45. The resulting scans were processed using a baseline correction, taking in account the whole area under the peak at 337 nm, as well as its height. Owing to the similarities between the two values, the peak height at 337 nm was used as previously described in Helbling *et al*. (1996).

d.2 Chlorophyll Fluorescence

Subsamples of 3 mL were taken from each microcosm every 2.5 h over diel cycles to measure in vivo Chl a fluorescence using a portable pulse-modulation fluorometer (Water-ED PAM, Walz, Germany). Because the time between sampling and fluorescence measurements was on the order of a few seconds, the intrinsic photochemical efficiency of PSII (Photosystem II, ΦPSII) in the light was determined (Maxwell & Johnson, 2000) as next equation:

$$\Phi_{PSII} = \frac{\Delta F}{F'm} = \frac{F'm - F't}{F'm}$$

where F′m is the instantaneous maximum fluorescence induced by a saturating light pulse (~5300 µmol photons m^{-2} s^{-1} in 0.8 s) and F′t is the current steady state fluorescence of light-adapted cells induced by an actinic light ~419 W m^{-2} in light-adapted cells. Each subsample was measured 6 times immediately after sampling, with each measurement lasting 10 s; hence, the total measurement time for each sample was 1 min.

d.3 Integral Yield

The Φ_{PSII} integral was calculated from Φ_{PSII} diel cycles (in triplicate for each treatment) following equation:

$$A = \int_{b}^{a} f(x)dx$$

where a and b are the initial and final times of measurement for each experimental day, respectively, and f(x) is the curve describing the yield over time for each treatment. The integral of the curve was calculated utilizing the software MATLAB® r2015a (Mathworks, Natick, Massachusetts, USA) and represents the balance between photoinhibition and repair of PSII throughout the diel cycle.

d.4 Nonphotochemical Quenching (NPQ)

The nonphotochemical quenching of Chl *a* fluorescence was used as a proxy of the dissipation of the excess energy as heat and was determined directly using the PAM fluorometer as next equation:

$$NPQ = \frac{Fm - F'm}{F'm}$$

where Fm is the maximal fluorescence of dark-adapted sample and F′m is the instantaneous maximum fluorescence induced by a saturating light pulse (~5300 µmol photons m^{-2} s^{-1} in 0.8 s). The software stored the Fm value that was then used with each sample to calculate the NPQ. This is the most important short-term photoprotective mechanism activated by saturating radiation intensities. Because no significant differences were found between NPQ values calculated in this way and those determined from Fm measured after an acclimation period in darkness and F′m measured during the exposure to radiation, we used the data provided directly by the instrument. For calculating the UVR effect, we used NPQ values registered at noon (T2 in Web repository file—

http://hdl.handle.net/10481/46928), corresponding with the moment of maxima inhibition and highest nonphotochemical quenching.

d.5 Primary Production

PP was measured by assessing the ^{14}C incorporation by phytoplankton cells (Steemann Nielsen, 1952). Briefly, two sets (one for each marine area) of 16 FEP narrow-mouth Teflon bottles (35 mL, Nalgene; three clear and one dark bottle per treatment) were filled with water from microcosms, inoculated with 5 μCi of labeled sodium bicarbonate (DHI Water and Environment, Germany), and incubated during 4 h centered at noon in tanks under the same conditions as with the microcosms. Then, the content of each bottle was fractionated through to a serial filtration procedure to determine the microplanktonic primary production (PPM) (cells retained in 3 μm glass-fiber filters, Whatman GF/D, 25 mm diameter) and subsequently the picoplanktonic primary production (PPP) (cells retained in 0.7 μm Whatman GF/F, 25 mm diameter). To minimize cell breakage, we performed the filtrations at low pressure (<100 mm Hg). Filters were put into 20 mL scintillation vials, acidified with 100 μL of 1 N HCl (2%), and kept open for 24 h in an aeration hood following the recommendations of Lignell (1992) to remove DI^{14}C. Finally, 16 mL of scintillation cocktail (Ecoscint A) were added to the vials and counted using a scintillation counter (Beckman LS 6000TA) equipped with autocalibration. Total primary production (TPP) was calculated as the sum of micro (PP_M) and autotrophic picoplanktonic fraction (PP_P).

d.6 Abundance, Biomass, Taxonomical Composition, and Net Growth Rates of Autotrophic Picoplankton

Seawater samples from each microcosm were fixed with glutaraldehyde (1% final concentration) and immediately frozen in liquid nitrogen (Vaulot *et al*., 1989). We took 5 mL subsamples to quantify cell abundance of autotrophic picoplankton

(Prochlorococcus, Synechococcus, and picoeukaryotes) using a Becton Dickinson FACScan flow cytometer (more details in Mercado *et al*. (2006)). Biovolume for these three groups, calculated following Ribés *et al*. (1999) for samples collected in the north-western Mediterranean Sea, were assumed to be 0.18, 0.44, and 1.68 μm^3 for Prochlorococcus, Synechococcus, and picoeukaryotes, respectively.

The net growth rates (NGR) for each experimental period was calculated according to following equation:

$$NGR = \frac{\ln N_t - \ln N_0}{t}$$

where N_t is the cell abundance (cell mL^{-1}) on each experimental day, N_0 is the cell abundance (cell mL^{-1}) at the initial time, and t is the time interval between each consecutive experimental day and the initial time. We considered that net growth rate is a good indicator of UVR effect even though some studies have shown that this rate could be influenced by predation effects (Christaki *et al*., 2001).

e. Calculations and Statistical Analysis

For the observational study, forward stepwise multiple-regression analyses were carried out to assess the relative influence of potential factors (DOC, temperature, k_{305}, k_{320}, k_{380}, k_{PAR}, TDN, TDP, pH, salinity, conductivity, and TNP:TDP ratio) controlling the distribution of Synechococcus, Prochlorococcus, picoeukaryotes, and total APP. Linearity and multiorthogonality among independent variables were verified by previous correlation analysis, whereas the normal distribution of residues was checked by Kolmogorov-Smirnov tests. Maps throughout this article were created using ArcGIS® software by Esri (Release 10.4.1. Redlands), and calculations of regional abundance from station points were interpolated using an inverse distance-weighted technique.

T-test analyses were used to determine the differences between marine areas for TDP, TDN, sestonic C, N, and P, DOC, and Chl *a* at initial conditions of the experiment.

The effect size of UVR for each dust treatment and area on Φ_{PSII} integral, NPQ, PPP, and NGR of Prochlorococcus, Synechococcus, and picoeukaryotes was calculated as follows in the next equation:

$$\text{Effect size of UVR (\%)} = \frac{X_{-UVR} - X_{+UVR}}{X_{-UVR}} \times 100$$

where X is the variable response considered in samples under the −UVR and +UVR treatments. Error propagation was used to calculate the variance of the UVR effect size (as a percentage). The influence of dust over time on the effect size of UVR on Φ_{PSII}-integral, NPQ, PP_P, and NGR was tested using a one-way repeated measures analysis of variance (one-way RM-ANOVA) for each area. A two-way repeated measures analysis of variance (two-way RM-ANOVA) was used to test the effect of UVR, dust addition, and their interaction over time on Φ_{PSII}-integral, NPQ, PP_P, and Prochlorococcus, Synechococcus, and picoeukaryotes NGR. The sphericity (by Mauchly's test) and homoscedasticity (by Levene's test) assumptions were verified, and when significant interactive effects were found, differences among and within treatments were assessed by Fisher's least significant differences (LSDs) post-hoc test.

For each response variable, the direction and magnitude of the interactive effect dust × UVR were calculated comparing the values of nonadditive treatment ($+UVR_{Dust}$) with their expected additive value based on the sum of the terms of the individual effects (e.g., (−UVR) + ((+UVR) ─ (−UVR)) + (($-UVR_{Dust}$) ─

(−UVR))) following Piggott *et al*. [2015] (in their Fig. 2). All tests were performed using Statistica v. 7.0 (Stat Soft, 2007) software.

3. Remote Sensing

The remote-sensing data for the Alboran Sea area were gathered from 1980 to 2015 for the spring-summer (March–September) period. Daily data of the area-average aerosol index (AI) and surface UVR fluxes on this region were downloaded from Giovanni v. 4. 18 3 (Acker & Leptoukh, 2007). The atmospheric dust deposition and UVR fluxes during this season of the year were assessed because both are maximums during this period (see Morales-Baquero *et al*., 2006; Li *et al*., 2015). AI data were taken from the Total Ozone Mapping Spectrometer (TOMS) Nimbus 7 (21 March 1979 to 5 May 1993), TOMS Earth Probe (22 July 1996 to 21 September 2005), and Ozone Monitoring Instrument (21 March 2006 to 21 September 2015) satellites (data from 1993 to 1996 are not available), while surface UVR-flux data came from the Modern-Era Retrospective analysis for Research and Applications, Version 2, model. Yearly data were used to calculate the mean area average AI and UVR fluxes over the spring-summer period as a measure of the atmospheric dust-deposition intensity and the incidence of UVR fluxes on surface waters.

4. Results

a. Dust Deposition and UVR Trends in Alboran Sea

The surface UVR fluxes and, particularly, the AI, exhibited a notable interannual variation (Fig. 7). There was a remarkable increase in the AI average intensity, as a measure of the amount of atmospheric aerosol reaching the Alboran Sea throughout the period of 1980–2014, with values ranging between 0.25 (e.g., 1980) and 1.33 (e.g., 2002).

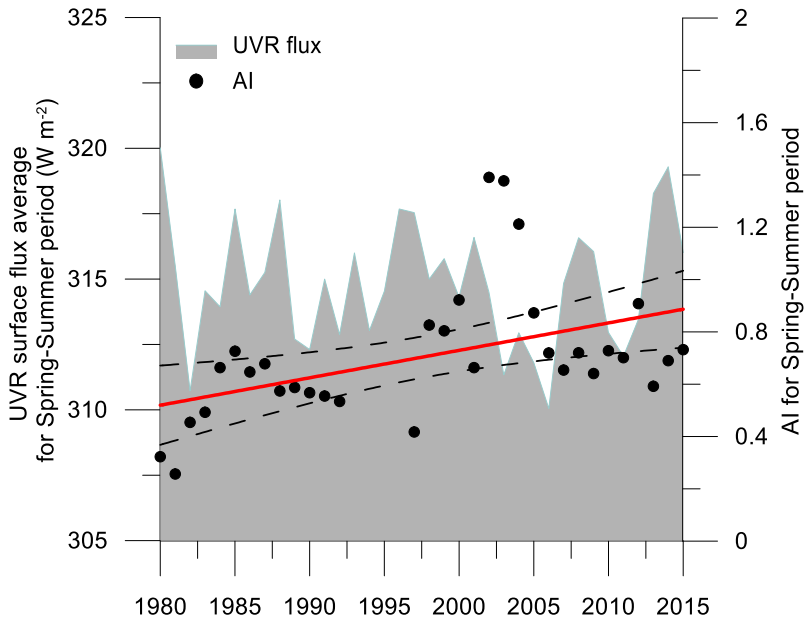

Figure 7. UVR-flux and aerosol index (AI) trend during the 1980–2015 period. The black points represent the area average of AI for the spring-summer period of each year. Linear trend for AI during the studied period is represented through the red line with a positive slope (y: 0.01, x: -20.24) (p-value = 0.046). The grey shaded area shows the surface UVR-flux (in W m^{-2}) from 1980 to 2015.

b. Observational study

Synechococcus, in absolute terms, showed higher abundance values than did the other two picoplanktonic groups throughout the Alboran Sea region (Table S1 in the supplementary information). *Prochlorococcus* exhibited the highest abundance values in the central region located between both Gyres, while picoeukaryote organisms increased their presence in the western region of the Alboran Sea, coinciding with the lowest picoprokaryotic abundance (Fig. 8). The multiple-regression analysis (Table 2) shows that although total APP abundance positively correlated with TDN concentration, temperature was the main abiotic factor explaining the distribution of each APP group in the Alboran Sea. Thus, temperature positively correlated with *Synechococcus* but negatively with *Prochlorococcus* and picoeukaryotes (Table 2). Accordingly, *Synechococcus* abundance was greater in the warmer eastern region, while *Prochlorococcus* and

picoeukaryotes were more abundant in the colder regions (Fig. 8). In addition, greater *Prochlorococcus* abundances were associated with high TDN values, whereas picoeukaryote abundances were also higher at low values of salinity (Table 2).

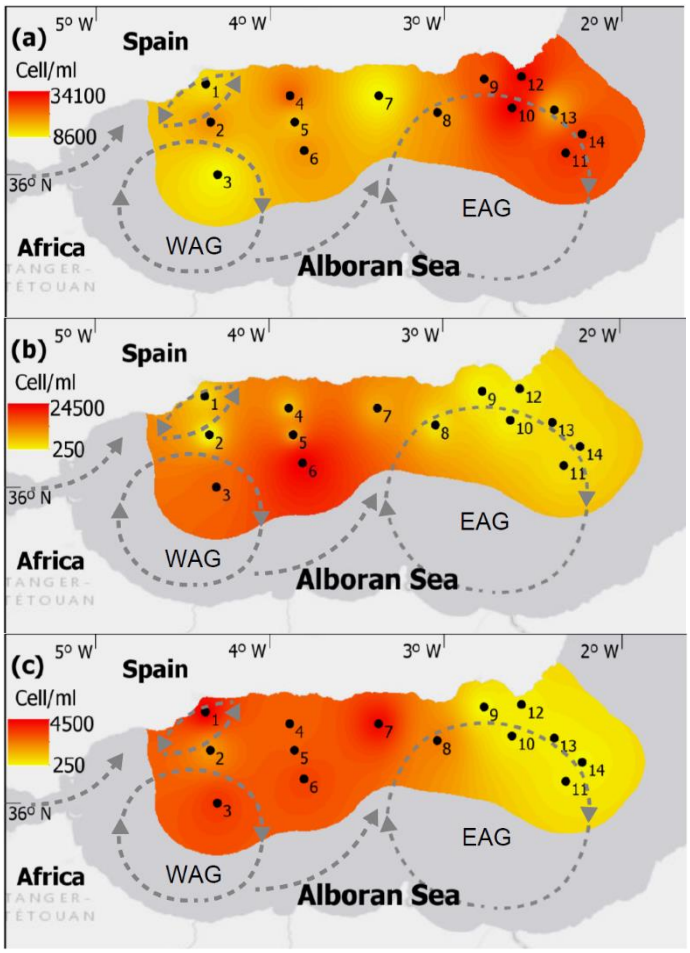

Figure 8. Distribution pattern of (a) Synechococcus, (b) Prochlorococcus, and (c) picoeukaryote abundances (cells mL^{-1}) throughout the Alboran Sea region. The abundance value for each group and for each station has an area of influence of 20 km. The dotted grey lines represent the Western Anticyclonic Gyre (WAG) and Eastern Anticyclonic Gyre (EAG) and the coastal currents. Note that gyres are represented in relative magnitude and shape. Source: Esri, HERE, DeLorme, MapmyIndia, © OpenStreetMap contributors, and the GIS user community.

Table 2. Results of multiple forward stepwise regression analysis for Synechococcus, Prochlorococcus, Picoeukaryotes and total autotrophic picoplankton abundances of the 14 stations analyzed.

Dependent variable	Independent variable	Beta	Multiple R^2	R^2 exchange	*p*
Synechococcus abundance	Temperature	0.628	0.49	0.49	0.02
Prochlorococcus abundance	TDN	0.805	0.43	0.43	0.03
	Temperature	-0.743	0.74	0.30	0.02
Picoeukaryotes abundance	Temperature	-0.423	0.76	0.76	<0.001
	Salinity	-0.594	0.87	0.11	0.03
Total APP	TDN	0.759	0.58	0.58	<0.01

c. Experimental Conditions

Penetration of solar radiation into the upper layers of the water column, the daily surface irradiance received by microcosms during the experiments, and vertical profiles of temperature in both areas are shown in Figure 9. The k_d coefficients for each region of the spectrum were low in both areas (<0.5 m^{-1}), indicating high water transparency (Figs. 9a and 9b), although the Im (λ) values for the different region of solar spectrum were higher in offshore (Station 3) than nearshore (Station 1) (Table 3). Surface UVR and PAR irradiance reaching the microcosms varied among days (Fig. 9c) due to the alternation of cloudy days (19 and 20 June) and sunny days (17, 18, and 21 June). The mean daily irradiance values during the experimental period were 220.2 W m^{-2} for PAR and 0.40, 0.15, and 0.02 W m^{-2} nm^{-1} for the 380, 320, and 305 nm wavelengths, respectively. Surface *T* was higher in the nearshore water column (~17.1°C) than in the offshore (~16.4°C) (Fig. 9d). TDP, Chl *a*, and PP_P values were significantly higher in the offshore than in nearshore area (Table 3). These low levels of nutrients in nearshore could indicate that during the sampling period the input of nutrient-rich waters from the sea bottom could be reduced or suppressed. Remarkably, the TDN:TDP ratio was high (920 and 175 for nearshore and offshore, respectively)

which also matched the high sestonic N:P ratio (566 and 243 for nearshore and offshore, respectively) found, indicating a severe limitation by P compared to previous data obtained in the same region for the sestonic (Mercado *et al*., 2005) and TDN:TDP ratio (Ribera D'Alcalà *et al*., 2003). The TDP concentration in the dust-addition treatments declined progressively over the experiment from ~1 μM to concentrations close to 0.4–0.5 μM (Figs. S1a and S1b in the supplementary information).

Table 3. Values of physical, chemical, and biological conditions at the initial of the experiment in Offshore and Nearshore in Alboran Sea. Values of mean irradiances (Im (λ)) for different regions of the solar spectrum (305, 320, 380 nm and photosynthetically active radiation (PAR, 400-700 nm)) are shown. Mean (±SD) concentrations of total dissolved phosphorous (TDP) and nitrogen (TDN), dissolved organic carbon (DOC), Chlorophyll a (Chl a), sestonic N, P, algal biomass (C), sestonic N:P ratio, picoplanktonic primary production (PP_P) and PP_P:Chl a ratio. Numbers in bold indicate p-values < 0.05.

Variable	**Offshore**	**Nearshore**	***p***
Im_{305} (W m^{-2})	0.019	0.013	
Im_{320} (W m^{-2})	0.185	0.138	
Im_{380} (W m^{-2})	0.689	0.574	
Im_{PAR} (W m^{-2})	536.3	394.4	
TDP (μmol P L^{-1})	0.54 ± 0.012	0.10 ± 0.005	**<0.001**
TDN (μmol N L^{-1})	95 ± 26	92 ± 10	0.86
TDN:TDP ratio	175 ± 52	920 ± 146	**<0.01**
DOC (μmol C L^{-1})	213 ± 31	321 ± 89	0.12
Chl *a* (μg L^{-1})	1.80 ± 0.25	0.80 ± 0.09	**<0.01**
Sestonic N (μmol N L^{-1})	4.38 ± 0.47	8.49 ± 0.45	**<0.001**
Sestonic P (μmol P L^{-1})	0.02 ± 0	0.01 ± 0	**<0.001**
Sestonic N:P ratio	243 ± 30	566 ± 32	**<0.01**
Algal biomass (μg C L^{-1})	120 ± 4	55.7 ± 0.2	**<0.001**
PP_P (μg C L^{-1} h^{-1})	6.26 ± 1.17	1.33 ± 0.41	**<0.01**
PP_P :Chl *a*	3.29 ± 0.01	1.77 ± 0.01	**<0.001**

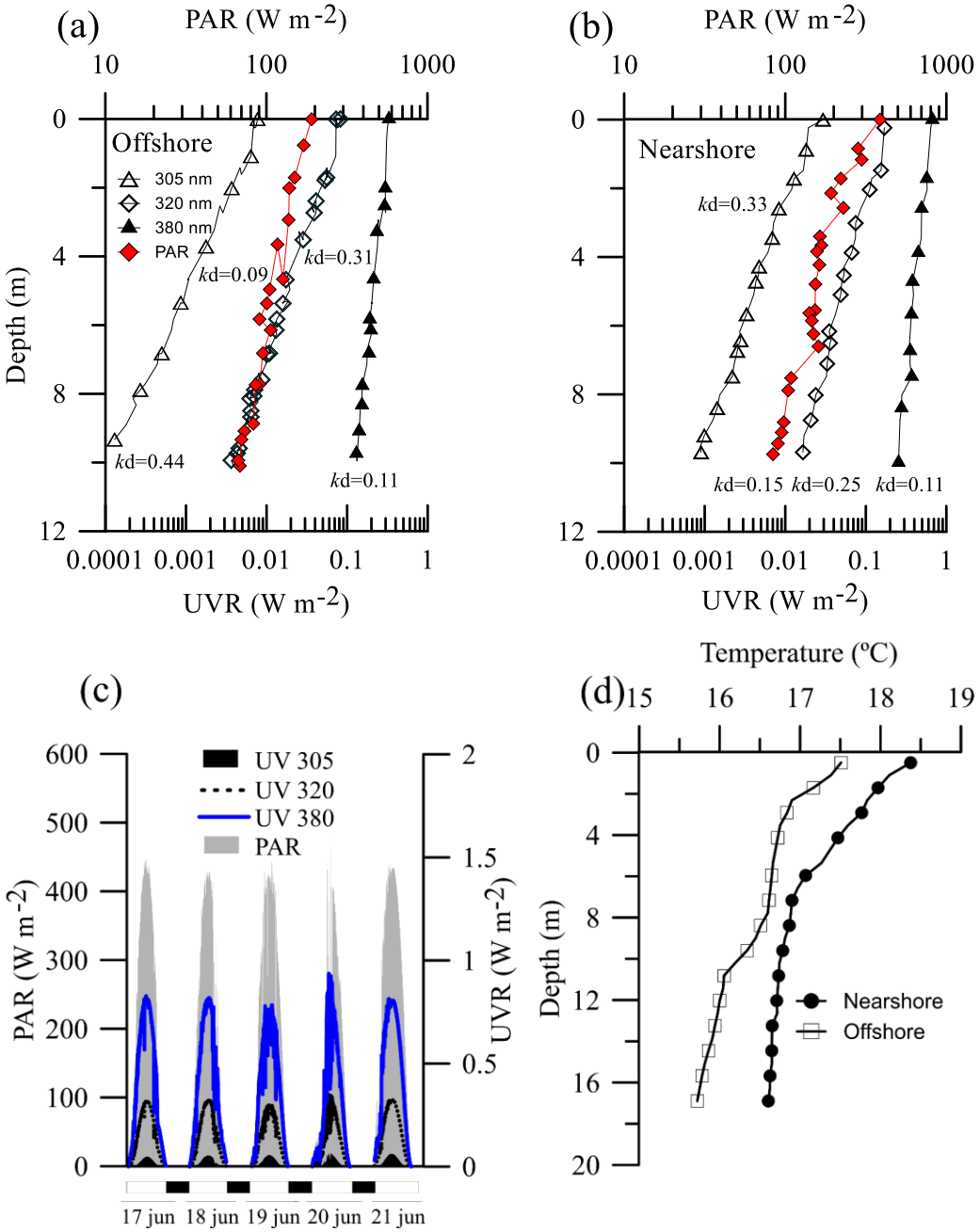

Figure 9. Vertical profiles of radiation and diffuse attenuation coefficients (kd) into the water column of (a) offshore and (b) nearshore for 305, 320, and 380 nm and PAR are shown. (c) Surface solar radiation for PAR and 305, 320, and 380 of wavelength for UVR over microcosms in the Alboran region during the exposure time (17–21 June 2014) and (d) vertical profiles of temperature into the water column are also shown.

d. Joint Effects of Dust and UVR in Offshore

From diel cycles of Φ_{PSII} (Figs. S2a and S3a), we calculated the UVR effect on the Φ_{PSII} integral, as shown in Figure 10a. The Φ_{PSII} diel cycles exhibited a clearly U-shaped, with lowest Φ_{PSII} at noon and the highest values at the beginning of exposure and at night, after the radiation stress had been removed.

For offshore area, under no-dust conditions, UVR exerted a significant stimulatory effect (except for day 2) on the Φ_{PSII} integral (Fig. 10a) with the highest stimulation (i.e., negative values) on day 3 (−118 ± 9.5%) and at the end of the experiment (−88 ± 33% on day 5). Under the dust treatments the opposite pattern was found, as UVR significantly inhibited the Φ_{PSII}integral throughout the experiment (except the first day, −16 ± 1.4%). Hence, a significant dust × time effect was found (Table 4) and the dust × UVR effect shifted from positive antagonism over the short term (i.e., dust diminished UVR damage; Table 5) to negative synergism (i.e., dust accentuated UVR damage; Table 5), with the lowest Φ_{PSII} integral at the end of the experiment.

Because the biological meaning of the NPQ variable coping with UVR stress was opposite to that of the other variables analyzed in our experiment, a positive value of the UVR effect on NPQ means low stress by UVR, as opposed to the other variables, where a positive value signifies an inhibitory UVR effect (see Fig. 10). Over the short term, NPQ values were low under UVR, and therefore, UVR stimulated the NPQ variable (+100 ± 0.75%; Fig. 10b) regardless of dust addition. However, at the end of the experiment (day 5) a dual response was found: under no-dust conditions UVR exerted a stronger inhibitory effect on NPQ, increasing its value (−47.5%), whereas under dust addition the stimulatory effect of UVR significantly decreased (+29.5 ± 7.3) (Fig. 10b).

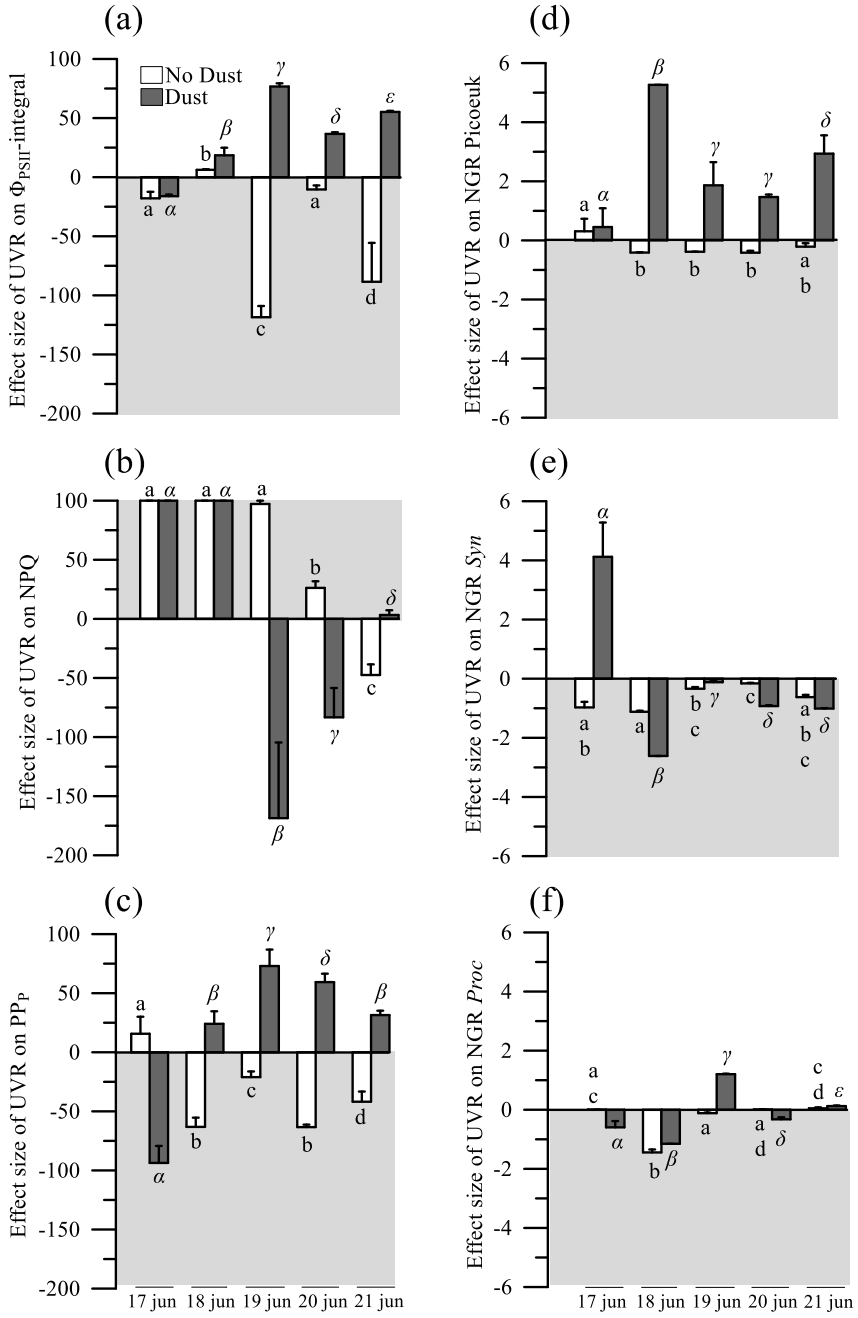

Figure 10. Effect size of UVR on (a) photosynthetic quantum yield (ΦPSII integral), (b) nonphotochemical quenching (NPQ), (c) picoplanktonic primary production (PPP), and net growth rate (NGR) for (d) picoeukaryotes (Picoeuk), (e) Synechococcus (Syn), and (f) Prochlorococcus (Proc) from offshore. The shaded area represents stimulatory effect. Each bar represents the mean values of three replicates, while the vertical lines indicate the standard deviation. The italic letters indicate differences among no-dust treatment, whereas the Greek letters indicate differences among dust treatment by LSD post-hoc test over the experiment.

TPP values ranged from 3.5 to 12 mg C m^{-3} h^{-1} for different treatments over the experiment. Because more than 90% of TPP was due to APP fraction (Fig. S2b), we focused the analysis on this fraction. In the offshore (Fig. 10c), UVR exerted a significant impact on PP_P over the incubation period, shifting from inhibitory to stimulatory effect under the no-dust treatment (from +15.7 to −41.8 values) and from stimulatory to inhibitory effect under the dust treatment (from −93.6 to +31.5 values). Thus, the dust × UVR effect changed from positive synergistic at short term to negative synergistic effect at the end of the experiment (Table 5), showing a response pattern similar to that of Φ_{PSII} integral at day 5.

Biovolumes of the different APP organisms in the offshore area varied from 250 μm^3 $mL^{-1}$for *Prochlorococcus* to 3000 μm^3 mL^{-1} for *Synechococcus* and 6000 μm^3 mL^{-1} for picoeukaryotes at the beginning of the experiment; contrarily, the biovolume fell for picoeukaryotes and *Synechococcus* but rose for *Prochlorococcus* over the experiment (Figs. S2c–S2e).

For picoeukaryotes, the NGR was not significantly affected by UVR over the short term regardless of the dust treatment (Fig. 10d). However, toward the end of the experiment, UVR exerted a significant stimulatory effect under no-dust conditions, but inhibitory under dust addition. Hence, dust × UVR changed from positive antagonism to negative synergism (Table 5). This response pattern is similar to that observed for the Φ_{PSII} integral and PP_P (Table 5). However, the NGR response of *Synechococcus* was different (Fig. 10e) because under no-dust conditions, UVR exerted a stimulatory effect throughout the experiment. Nevertheless, dust addition altered the UVR effect over time (Table 4) from inhibitory (negative synergism) over short term to stimulatory (positive synergism) toward the end of the experiment (Table 5). The NGR of *Prochlorococcus* showed no clear response under no-dust conditions (Fig. 10f). However, as in the case of picoeukaryotes, dust addition significantly shifted the

initial stimulatory (positively synergistic) UVR effect to inhibitory (negatively synergistic) toward the end of the experiment (Table 5).

d. Joint Effects of Dust and UVR in the Nearshore Area

For the nearshore area, under no-dust conditions, UVR exerted a clear inhibitory effect on the Φ_{PSII} integral (except for day 2; Fig. 11a). However, dust addition gradually transformed the inhibitory effect to a stimulatory one over experimental time (−20.1 ± 5.9% on day 5) (significant dust × time; Table 4). Hence, dust × UVR effect ranged from negative synergism (i.e., dust accentuated the inhibitory UVR effect) over the short term to negative antagonism (i.e., dust reversed the inhibitory UVR effect) toward the end of the experiment (see Table 5).

The UVR effect on NPQ is shown in Figure 11b. Under the no-dust conditions, UVR raised NPQ values, exerting a significant inhibitory effect (−44.9 ± 10.8%). This UVR effect was attenuated over the experiment. Dust addition spurred the initial inhibitory UVR effect on NPQ (−99 ± 9.3%), although the effect significantly weakened toward the end of the experiment (16.4 ± 6.7%) (Table 4), which matched the inverse pattern observed in the Φ_{PSII} integral.

TPP values increased from 1 at the beginning of the experiment to 11 mg C m^{-3} h^{-1}on the 21 June. As for the offshore, the APP fraction (<3 μm) in nearshore also represented about 90% of the TPP (Fig. S3b). Under no-dust conditions, UVR inhibited PP_P (16.5 ± 6.1%) over the short term but stimulated it (−89.7 ± 15.7%) at the end of the experiment (Fig. 11c). By contrast, under the dust addition, UVR stimulated PP_P over the short term (−75.4 ± 16.7%) but inhibited it over the experiment (−24.9 ± 27.2% on day 5), hence prompting a change in the interaction between the two factors from negative to positive antagonism (Table 5).

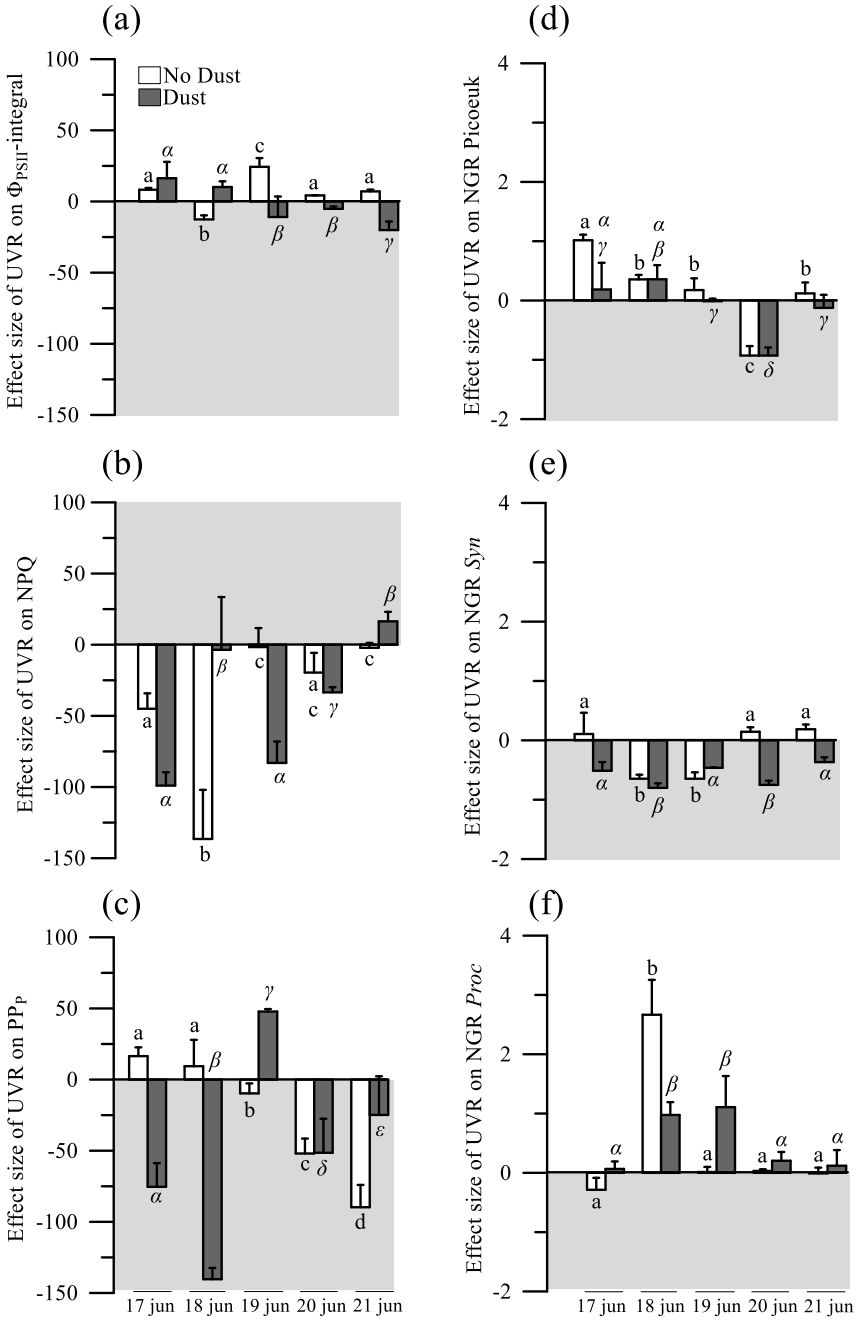

Figure 11. Effect size of UVR on (a) photosynthetic quantum yield (ΦPSII-integral), (b) nonphotochemical quenching (NPQ), (c) picoplanktonic primary production (PPP), and net growth rate (NGR) for (d) picoeukaryotes (Picoeuk), (e) Synechococcus (Syn), and (f) Prochlorococcus (Proc) from nearshore. The shaded area represents stimulatory effect. Each bar represents the mean values of three replicates, while the vertical lines indicate the standard deviation. The italic letters indicate differences among no-dust treatment, whereas the Greek letters indicate differences among dust treatment by LSD post-hoc test over the experiment.

APP biovolumes are represented in Figures S3c–S3e. At initial conditions, biovolumes for picoeukaryotes (7500 μm^3 mL^{-1}) and *Synechococcus* (5300 μm^3 mL^{-1}) were higher than in the offshore, whereas the *Prochlorococcus* biovolume was lower (100 μm^3 mL^{-1}) than in the offshore. Nevertheless, as in the offshore, biovolumes showed a generalized decline for picoeukaryotes and *Synechococcus* but a surge for *Prochlorococcus* over the experiment.

APP showed different responses to UVR depending on the APP group. Thus, an inhibitory UVR effect on NGR of picoeukaryotes declined over the experimental time, being more accentuated under no-dust conditions (Fig. 11d). By contrast, the NGR of *Synechococcus*was stimulated by UVR at short term (-0.65 ± 0.07 on day 2) but inhibited significantly at the end of the experiment (0.18 ± 0.08) under no-dust conditions (Fig. 11e). However, under dust addition, UVR significantly stimulated the NGR of *Synechococcus* over the experiment, generating an antagonistic dust × UVR effect (Table 5). *Prochlorococcus* failed to show a clear response, except for a significant UVR-inhibition on intermediate days (day 2, under no-dust addition; days 2 and 3 under dust addition; Fig. 11f).

5. Discussion

Our observational results indicate that temperature was the common regulating factor of distribution for each APP group in early summer, and that nutrients, mainly TDN, determined the total abundance of APP throughout the Alboran Sea. Although picoeukaryotes and *Prochlorococcus* showed a greater preference for colder western water, *Synechococcus* was the most dominant group in the region (except at stations 1, 3, and 7, dominated by picoeukaryotes). This was probably because the P-limited conditions of Alboran Sea, and their lower demand of P, favored them with respect to picoeukaryotes (Stawiarski, 2014). A global

picoplankton distribution pattern determined by temperature, and, in agreement with our results, has been mentioned by Buitenhuis *et al*. (2012). In addition, the total APP abundance was slightly higher in the warmer eastern region of Alboran Sea, coinciding with the highest TDN. These results agree with those found by Amorim *et al*. (2016) in this area and by Moore *et al*. (2008) in the oligotrophic subtropical North Atlantic Ocean, showing APP development with increasing N sources.

The predicted rising of water temperature funneled by global climate change will promote the stratification of the water column, causing thinner UML and exposing phytoplankton to higher levels of visible and UVR (Peralta-Ferriz & Woodgate, 2015). Additionally, as a consequence of the stronger stratification, the nutrient supply to surface waters from deep mixing will become increasingly low, causing other nutrient sources such as atmospheric dust to acquire a more relevant role as a modulator of the phytoplankton dynamics. Therefore, our experimental approach can be considered representative of these expected conditions of global warming because the water column was already relatively stratified, possibly explaining the low nutrient concentration found in the UML. Moreover, the experimental exposure of the samples to UVR under a relatively thin layer of water simulated the expected shallower UML (i.e., representing the worst scenario of radiation exposure), predicted under global warming. Given the enormous importance of APP on microbial food web structure and functioning of the Alboran Sea, our experimental approach fills a gap of knowledge on how the interaction of these two main factors of global change affects physiology, metabolism, and taxonomical composition of APP. The experimental design allowed us to infer that the response patterns observed in the picoplanktonic community of each region were due to the effects of the two factors

experimentally assayed (UVR and dust), since the conditions to which the microcosms were exposed were identical for all experimental units.

According to our hypothesis, UVR under ambient (no-dust) conditions exerted a stronger inhibitory effect on most of variables measured in nearshore than in offshore over both short-term and midterm (day 5) temporal scales. Moreover, it was remarkable that in offshore, UVR stimulated photosynthetic variables (Φ_{PSII} integral and PP_P) throughout the experiment, indicating a great photoacclimation of picoplanktonic communities to high UVR exposure. This finding could be explained by the differential previous light history of communities, implying different acclimations between the two areas studied. In fact, the picoplanktonic community in the offshore was subjected to higher mean irradiances of UVR and PAR owing to a shallower UML (2 m) than in the nearshore (6 m), which could favor a higher photoacclimation in the former area when the picoplankton was exposed to our experimental conditions. Additionally, this greater acclimation of the offshore picoplankton could be supported by the higher PP_P:Chl *a* ratio (≈2-fold) found (Thomas *et al*., 1992) (see Table 3), as well as by the lower NPQ values found, which may be related to the absence of a chronic damage in the photosynthetic apparatus (Krause & Weis, 1991; Cruz & Serôdio, 2008). Nevertheless, based on our results, we cannot rule out a stimulatory UV-A effect on photosynthesis, as reported by Barbieri *et al*. (2002) & Gao *et al*. (2007). Moreover, the contrasting sensitivity to UVR of both communities in their photosynthetic, metabolic, and structural variables may also be the consequence of their previous nutritional state (Winder, 2009; Romero *et al*., 2011; Helbling *et al*., 2013) basically, a noticeably higher P limitation in the nearshore, because we found no difference in DOC concentrations between the two areas to explain their different UVR sensitivity (Figs. S4a and S4b).

Table 4. Results of the one-way RM-ANOVA of Dust addition on effect size of UVR on photosynthetic quantum yield (ΦPSII-integral), non photochemical quenching (NPQ), picoplanktonic primary production (PP_P) and net growth rate (NGR) for Picoeukaryotes (Picoeuk), Synechococcus (Syn) and Prochlorococcus (Proc) from Offshore and Nearshore area. Significant p-values are typed in bold. df represents the degree of freedom and F the F-test.

	Offshore												
Effect		Φ_{PSII}-integral		NPQ		PP_P		NGR Picoeuk		NGR *Syn*		NGR *Proc*	
	df	F	*p*	F	*p*	F	*p*	F	*p*	F	*p*	F	*p*
Dust	1	340.5	**<0.001**	26.7	**<0.01**	55.6	**<0.01**	294.7	**<0.001**	0.6	**<0.05**	3.6	**<0.01**
Dust×Time	4	87.8	**<0.001**	73.6	**<0.001**	617.5	**<0.001**	73.5	**<0.001**	9.8	**<0.001**	9.3	**<0.001**
	Nearshore												
Effect		Φ_{PSII}-integral		NPQ		PP_P		NGR Picoeuk		NGR *Syn*		NGR *Proc*	
	df	F	*p*	F	*p*	F	*p*	F	*p*	F	*p*	F	*p*
Dust	1	8.5	0.14	0.00	0.97	4.5	0.10	7.81	0.07	79.6	**<0.01**	0.01	0.95
Dust×Time	4	12.8	**<0.001**	36.7	**<0.001**	185.9	**<0.001**	14.2	**<0.01**	32.5	**<0.001**	44.3	**<0.001**

Notably, and partially contrary to our hypothesis, the addition of Saharan dust had a contrasting effect on the photosynthetic activity and C incorporation of the picoplanktonic communities from nearshore versus offshore. In nearshore, the harmful UVR effect was inverted to stimulatory by dust addition at the end of the experiment. This stimulation was promoted from the subcellular level (Φ_{PSII} integral), through metabolism (PP_P), to the community level, as the responses (NGR) of picoeukaryotes and *Synechococcus* sp. Moreover, in the absence of significant UV-AC concentration over the experiment (data not shown) to cope with the UVR damage (Sinha & Häder, 2008), the increase in the Φ_{PSII} integral and the photoacclimation of the communities together with a progressively declining NPQ activity demonstrate a lesser need to dissipate the excess of energy absorbed by PSII, hence supporting the idea of an improved physiological state under UVR after dust addition. Curiously, a similar positive effect of UVR and nutrient enrichment (P, mimicking similar dust inputs as in our study) on PSII and PP_P from the nearshore waters of Alboran Sea has recently been reported by Sobrino *et al*. (2014) and Carrillo *et al*. (2015a), respectively.

By contrast, the negative synergistic dust × UVR effect reported for most of the variables in the offshore suggests a simultaneous constraint exerted after dust addition on the Φ_{PSII}, PP_p, and growth of picoeukaryotes and *Prochlorococcus*, because UVR without dust treatments led to the highest stimulation of all processes (see Table 5). The NPQ photoprotective mechanism also showed a different pattern in the offshore. Thus, the increasing stimulatory UVR effect on NPQ under dust addition over the experiment makes a higher degree of stress evident. This unmasking of a harmful UVR effect on PP and productivity after nutrient enrichment has been widely reported in oligotrophic freshwater (Carrillo *et al*., 2008; Korbee *et al*., 2012; Durán *et al*., 2016) as well as in coastal ecosystems (Carrillo *et al*., 2015a). Furthermore, this negative synergistic effect

on APP could be related to higher rates of DNA synthesis due to stimulated growth induced by the addition of dust rich in limiting nutrients. This can exacerbate the damage of UVR on DNA, increasing the effects of UVR on cell division after addition of dust (Karentz *et al*., 1991).

Our findings also showed general UVR damage on APP biovolume (Figs. S2c–S2e and S3c–S3e) over the short term, in agreement with other authors (Llabrés & Agustí, 2006), even after dust addition in both areas. However, at the end of the experiment, *Prochlorococcus* was the only fraction that showed a slightly positive development. This finding may be explained by a higher ability of *Prochlorococcus* to grow under P-limitation conditions, which may be accentuated by the supply of nitrogen contained in the dust (Chien *et al*., 2016).

According to the picoeukaryote predominance in total APP biovolume of these two stations, it is not surprising that the physiological state of the community was driven fundamentally by them. Thus, picoeukaryote NGR showed a pattern similar to that of the physiological variables, growing in the nearshore (positive synergism) and exhibiting more severe damage and inhibition in the offshore (negative synergism) at the end of the experiment. However, although the influence of *Synechococcus* on physiological variables was not notable, probably due to its lower abundance at the beginning of the experiment, it was the only group that showed a consistent positive response under UVR × dust conditions in the two areas studied. It is probable that *Synechococcus* can gain a greater advantage, not only at low P conditions (observational study) but also under the UVR × dust interaction, as have been already demonstrated by Mackey *et al*. (2009), who reported greater positive changes in C biomass of *Synechococcus* after nutrient enrichment at high light intensities.

Table 5. Short- and mid-term effects of UVR, Dust and magnitude and direction of the UVR×Dust interaction (non-additive) over the experiment for Offshore and Nearshore on photosynthetic quantum yield (ΦPSII-integral), non photochemical quenching (NPQ), picoplanktonic primary production (PP_P) and net growth rate (NGR) for Picoeukaryotes (Picoeuk), Synechococcus (Syn) and Prochlorococcus (Proc). Classification of the UVR×Dust interaction, following Piggott et al., 2015, is positive synergistic (+S), negative synergistic (-S), positive antagonistic (+A), and negative antagonistic (-A). Additive effect and Non-Additive effect are abbreviated as Add and Non-Add, respectively, and the interaction and the biological meaning as Int. and B.M.

		SHORT-TERM EFFECT							MID-TERM EFFECT						
		Control	**UVR**	**Dust**	**Add**	**Non-Add**	**Int.**	**B.M.**	**Control**	**UVR**	**Dust**	**Add**	**Non-Add**	**Int.**	**B.M**
Offshore	Φ_{PSII}-integral	3.01	3.68	3.22	3.89	3.75	**+A**	Stimulation	1.76	3.31	3.27	4.82	1.47	**-S**	Inhibition
	NPQ	0.006	0	0.001	0	0	**-S**	Stimulation	29.26	43.16	26.4	40.26	25.51	**-S**	Stimulation
	PPp	8.17	6.89	5.79	4.51	11.21	**+S**	Stimulation	7.17	10.17	10.14	13.14	6.94	**-S**	Inhibition
	NGR Picoeuk	-0.38	-0.5	-0.29	-0.41	-0.43	**+A**	Inhibition	-0.35	-0.28	-0.15	-0.08	-0.57	**-S**	Inhibition
	NGR *Syn*	-0.21	-0.006	-0.12	0.084	-0.60	**-S**	Inhibition	-0.55	-0.21	-0.46	-0.12	0.005	**+S**	Stimulation
	NGR *Proc*	-1.513	-1.510	-1.66	-1.657	-0.67	**+S**	Stimulation	0.22	0.21	0.199	0.189	0.17	**-S**	Inhibition
Nearshore	Φ_{PSII}-integral	3.29	3.02	2.42	2.15	2.12	**-S**	Inhibition	2.98	2.63	2.63	2.28	2.76	**-A**	Stimulation
	NPQ	0.898	1.30	0.596	0.998	1.19	**+A**	Inhibition	41.01	41.89	30.83	31.71	25.77	**-S**	Stimulation
	PPp	4.80	4.01	1.51	0.72	2.64	**-A**	Stimulation	4.86	9.21	8.02	12.37	10.01	**+A**	Stimulation
	NGR Picoeuk	-0.45	-0.92	-1.66	-2.13	-1.97	**-A**	Inhibition	-0.31	-0.35	-0.32	-0.36	-0.28	**+S**	Stimulation
	NGR *Syn*	-0.16	-0.18	-1.24	-1.26	-0.61	**-A**	Stimulation	-0.36	-0.42	-0.63	-0.69	-0.40	**-A**	Stimulation
	NGR *Proc*	-1.08	-0.77	-1.14	-0.83	-1.21	**-S**	Inhibition	0.35	0.36	0.29	0.30	0.26	**-S**	Inhibition

6. Conclusions

The most striking results of our study were that the joint action of UVR and dust constrained the photosynthesis (Φ_{PSII}-integral and PP_p) and growth rates of the main picoplanktonic groups over time in the offshore. These results call into question the absence of response (Ridame *et al*., 2014) or the widely reported positive dust effect on productivity in open deep-sea areas (i.e., Mediterranean Sea and North and South Atlantic Ocean) through experimental (Pulido-Villena *et al*., 2008; Marañón *et al*., 2010; Giovagnetti *et al*., 2013) and observational studies (Gallisai *et al*., 2014) when the UVR effects are not directly considered. On the other hand, during our observational study, we found that *Synechococcus* represented a high proportion of picoplanktonic community, and our experimental study confirmed that these organisms possess a greater acclimation capacity to new environmental conditions. Therefore, interactions between dust inputs and UVR not only could unravel a contrasting sensitivity of nearshore and offshore picoplanktonic communities from oligotrophic ecosystems but could also suggest that the interaction between these two global-change factors under anticipated future conditions in the Mediterranean region may alter the microbial web structure and functioning of these areas by favoring the greater APP growth, especially of picoprokaryotes. This study underscores the need to know whether the responses of similar organisms can be observed in other oceanic regions conditioned by the presence of gyres that determine different physico-chemical conditions for nearshore and offshore.

References

Acker, J. G. & Leptoukh, G. (2007). Online analysis enhances use of NASA Earth science data. *Eos Trans. AGU*. 88: 2

Agawin, N. S. R., Duarte, C. & Agustí, S. (2000). Nutrient and temperature control of the contribution of picoplankton to phytoplankton biomass and production. *Limnol. Oceanogr.* 45: 591–600

Agustí, S. & Llabrés, M. (2007). Solar radiation-induced mortality of marine pico-phytoplankton in the oligotrophic ocean. *Photochem. Photobiol*. 83: 793–801

Alvain, S., Moulin, C., Dandonneau, Y. & Bréon, F. M. (2005). Remote sensing of phytoplankton groups in case 1 waters from global SeaWiFS imagery. *Deep Sea Res.* Part I. 52: 1989–2004

Amorim, A. L., León, P., Mercado, J. M., Cortés, D., Gómez, F., Putzeys, S., Salles, S. & Yebra, L. (2016). Controls of picophytoplankton abundance and composition in a highly dynamic marine system, the Northern Alboran Sea (Western Mediterranean). *J. Sea Res.* 112: 13–22

Báez, J. C., Gimeno, L., Gómez-Gesteira, M., Ferri-Yáñez, F. & Real, R. (2013). Combined effects of the Arctic Oscillation and the North Atlantic Oscillation on sea surface temperature in the Alborán Sea. *PLoS One.* 8(4): e62201

Barbieri, E. S., Villafañe, V. E. & Helbling, E. W. (2002). Experimental assessment of UV effects upon temperate marine phytoplankton when exposed to variable radiation regimes. *Limnol. Oceanogr.* 47: 1648–1655

Behrenfeld, M. J., *et al*. (2009). Satellite-detected fluorescence reveals global physiology of ocean phytoplankton. *Biogeosciences.* 6: 779–794

Belkin, I. M. (2009). Rapid warming of large marine ecosystems. *Prog. Oceanogr.* 81: 207–213

Buitenhuis, E. T., *et al*. (2012). Picophytoplankton biomass distribution in the global ocean. *Earth Syst. Sci. Data.* 4: 37–46

Buitenhuis, E. T., *et al*. (2013). MAREDAT: Towards a world atlas of MARine EcosystemDATa. *Earth Syst. Sci. Data.* 5: 227–239

Bullejos, F. J., Carrillo, P., Villar-Argaiz, M. & Medina-Sánchez, J. M. (2010). Roles of phosphorus and ultraviolet radiation in the strength of phytoplankton-zooplankton coupling in a Mediterranean high mountain lake. *Limnol. Oceanogr.* 55: 2549–2562

Buma, A. G. J., Helbling, E. W., De Boer, M. K. & Villafañe, V. E. (2001). Patterns of DNA damage and photoinhibition in temperate South- Atlantic picophytoplankton exposed to solar ultraviolet radiation. *J. Photochem. Photobiol. B.* 62: 9–18

Buma, A. G. J., Boelen, P. & Jeffrey, W. H. (2003). UVR-induced DNA damage in aquatic organisms, in UV Effects in Aquatic Organisms and Ecosystems, edited by E. W. Helbling and H. E. Zagarese, pp. 291–327, The Royal Society of Chemistry, Cambridge, U. K.

Cabrerizo, M. J., Medina-Sánchez, J. M., González-Olalla, J. M., Villar-Argáiz, M. & Carrillo, P. (2016). Saharan dust inputs and high UVR levels jointly alter the metabolic balance of marine oligotrophic ecosystems. *Sci. Rep.* 6: 35892

Carrillo, P., Delgado-Molina, J. A., Medina-Sánchez, J. M., Bullejos, F. J. & Villar-Argáiz, M. (2008). Phosphorus inputs unmask negative effects of ultraviolet radiation on algae in a high mountain lake. *Global Change Biol.* 14: 423–439

Carrillo, P., Medina-Sánchez, J. M., Durán, C., Herrera, G., Villafañe, V. E. & Helbling, E. W. (2015a). Synergistic effects of UVR and simulated stratification on commensalistic phytoplankton-bacteria relationship in two optically contrasting oligotrophic Mediterranean lakes. *Biogeosciences.* 12: 697–712

Carrillo, P., Medina-Sánchez, J. M., Herrera, G., Durán, C., Segovia, M., Cortés, D., Salles, S., Korbee, N., Figueroa, F. L. & Mercado, J. M. (2015b), Interactive effect of UVR and phosphorus on the coastal phytoplankton community of the Western Mediterranean Sea: Unravelling ecophysiological mechanisms. *PLoS One.* 10(11): e0142987

Chien, C. T., Mackey, K. R. M., Dutkiewicz, S., Mahowald, N. M., Prospero, J. M. & Paytan, A. (2016). Effects of African dust deposition on phytoplankton in the western tropical Atlantic Ocean off Barbados. *Global Biogeochem. Cycles.* 30: 716–734

Christaki, U., Giannakourou, A., Van Wambeke, F. & Grégori, G. (2001). Nanoflagellate predation on auto- and heterotrophic picoplankton in the oligotrophic Mediterranean Sea. *J. Plankton Res.* 23: 1297–1310

Cruz, S., & Serôdio, J. (2008). Relationship of rapid light curves of variable fluorescence to photoacclimation and non-photochemical quenching in a benthic diatom. *Aquat. Bot.* 88: 256–264

Day, T. A.& Neale, P. J. (2002). Effects of UV-B radiation on terrestrial and aquatic primary producers. *Annu. Rev. Ecol. Syst.* 33: 371–396

Durán, C., Medina-Sánchez, J. M., Herrera, G. & Carrillo, P. (2016). Changes in the phytoplankton-bacteria coupling triggered by joint action of UVR, nutrients, and warming in Mediterranean high-mountain lakes. *Limnol. Oceanogr.* 61: 413–429

Erga, S. R., Aursland, K., Frette, Ø., Hamre, B., Lotsberg, J. K., Stamnes, J. J., Aure, J., Rey, F. & Stamnes, K. (2005). UV transmission in Norwegian marine waters: Controlling factors and possible effects on primary production and vertical distribution of phytoplankton. *Mar. Ecol. Prog. Ser.* 305: 79–100

Figueroa, F. L., Blanco, J. M., Jiménez-Gómez, F. & Rodríguez, J. (1997a). Effects of ultraviolet radiation on carbon fixation in Antarctic nanophytoflagellates. *Photochem. Photobiol.* 66: 185–189

Figueroa, F. L., Mercado, J., Jiménez, C., Salles, S., Aguilera, J., Sánchez-Saavedra, M. P., Lebert, M., Häder, D., Montero, O. & Lubián, L. (1997b), Relationship between bio-optical characteristics and photoinhibition of phytoplankton. *Aquat. Bot.* 59: 237–251

Finkel, Z. V., Beardall, J., Flynn, K. J., Quigg, A., Alwyn, T., Rees, V. & Raven, J. A. (2010). Phytoplankton in a changing world: Cell size and elemental stoichiometry. *J. Plankton Res.* 32: 119–137

Gallisai, R., Peters, F., Volpe, G., Basart, S. & Baldasano, J. M. (2014). Saharan dust deposition may affect phytoplankton growth in the Mediterranean Sea at ecological time scales. *PLoS One.* 9(10): e110762

Gang, L., Gao, K. & Gao, G. (2011). Differential impacts of solar UV radiation on photosynthetic carbon fixation from the coastal to offshore surface waters in the South China Sea. *Photochem. Photobiol.* 87: 329–334

Gao, K., Li, G., Helbling, E. W. & Villafañe, V. E. (2007). Variability of UVR effects on photosynthesis of summer phytoplankton assemblages from a tropical coastal area of the South China Sea. *Photochem. Photobiol.* 83: 802–809

García-Górriz, E. & Carr, M. E. (2001). Physical control of phytoplankton distributions in the Alboran Sea: A numerical and satellite approach. *J. Geophys. Res.* 106 (C8): 16795–16805

Giorgi, F. & Lionello, P. (2008). Climate change projections for the Mediterranean region. *Global Planet. Change.* 63: 90–104

Giovagnetti, V., Brunet, C., Conversano, F., Tramontano, F., Obernosterer, I., Ridame, C. & Guieu, C. (2013). Assessing the role of dust deposition on phytoplankton ecophysiology and succession in a low-nutrient low-chlorophyll ecosystem: A mesocosm experiment in the Mediterranean Sea. *Biogeosciences.* 10: 2973–2991

Grossman, A. R., Mackey, K. R. M. & Bailey, S. (2010). A perspective on photosynthesis in the oligotrophic oceans: Hypotheses concerning alternate routes of electron flow. *J. Phycol.* 46: 629–634

Guieu, C., *et al*. (2010). Large clean mesocosms and simulated dust deposition: A new methodology to investigate responses of marine oligotrophic ecosystems to atmospheric inputs. *Biogeosciences.* 7: 2765–2784

Häder, D. P., Helbling, E. W., Williamson, C. E. & Worrest, R. C. (2011). Effects of UV radiation on aquatic ecosystems and interactions with climate change. *Photochem. Photobiol. Sci.* 10: 242–260

Häder, D. P., Villafañe, V. E. & Helbling, E. W. (2014). Productivity of aquatic primary producers under global climate change. *Photochem. Photobiol. Sci.* 13: 1370–1392

Helbling, E. W. & Zagarese, H. E. (2003). UV Effects in Aquatic Organisms and Ecosystems. From the series Comprehensive Series in Photochemical & Photobiological Sciences. The Royal Society of Chemistry, Cambridge, U. K. pp 598

Helbling, E. W., Chalkerb, B. E., Dunlapb, C., Holm-Hansen, O. & Villafañe, V. E. (1996). Photoacclimation of Antarctic marine diatoms to solar ultraviolet radiation. *J. Exp. Mar. Biol. Ecol.* 204: 85–101

Helbling, E. W., Carrillo, P., Medina-Sánchez, J. M., Durán, C., Herrera, G., Villar-Argaiz, M. & Villafañe, V. E. (2013). Interactive effects of vertical mixing, nutrients and ultraviolet radiation: In situ photosynthetic responses of phytoplankton from high mountain lakes in southern Europe. *Biogeosciences.* 10: 1037–1050

Hessen, D., De Lange, H. & Van Donk, E. (1997). UV-induced changes in phytoplankton cells and its effects on grazers. *Freshwater Biol.* 38: 513–524

Houpert, L., Testor, P., Durrieu de Madrona, X., Somot, S., Ortenzio, F. D., Estournel, C. & Lavigne, H. (2015). Seasonal cycle of the mixed layer, the seasonal thermocline

and the upper-ocean heat storage rate in the Mediterranean Sea derived from observations. *Prog. Oceanogr*. 132: 333–352

Jeffrey, S. W., and G. F. Humphrey (1975), New spectrophotometric equations for determining chlorophylls a, b, c 1 and c 2 in higher plants, algae and natural phytoplankton, Biochem. Physiol. Pflanz. 167: 191–194.

Jickells, T. D. & Moore, C. M. (2015). The importance of atmospheric deposition for ocean productivity. *Annu. Rev. Ecol. Syst.* 46: 481–501

Jickells, T. D., *et al*. (2005). Global iron connections between desert dust, ocean biogeochemistry, and climate. *Science.* 308: 67–71

Karentz, D., Cleaver, J. & Mitchell, D. L. (1991). Cell survival characteristics and molecular responses of Antarctic phytoplankton to ultraviolet-B radiation. *J. Phycol.* 27: 326–341

Korbee, N., Carrillo, P., Mata, M. T., Rosillo, S., Medina-Sánchez, J. M. & Figueroa, F. (2012). Effects of ultraviolet radiation and nutrients on the structure–function of phytoplankton in a high mountain lake. *Photochem. Photobiol. Sci.* 11: 1087–1098

Koroleff, F. (1977). Simultaneous persulphate oxidation of phosphorus and nitrogen compounds in water, in Report on the Baltic Intercalibration Workshop, edited by K. Grasshoff, pp. 52–53. Compiler, Kiel, Germany.

Krause, G. H. & Weis, E. (1991). Chlorophyll fluorescence and photosynthesis: The basics, Annu. *Rev. Plant Physiol. Plant Mol. Biol.* 42: 313–349

Lekunberri, I., Lefort, T., Romero, E., Vazquez-Dominguez, E., Romera-Castillo, C., Marrasé, C., Peters, F., Weinbauer,M. & Gasol, J. M. (2010). Effects of a dust deposition event on coastal marine microbial abundance and activity, bacterial community structure and ecosystem function. *J. Plankton Res.* 32: 381–396

Leu, E., Falk-Petersen, S. & Hessen, D. (2007). Ultraviolet radiation negatively affects growth but not food quality of arctic diatoms. *Limnol. Oceanogr*. 52: 787–797

Li, T., Pan, D., Bai, Y., Li, G., He, X., Chen, C.-T. A., Gao, K., Liu, D. & Lei, H. (2015). Satellite remote sensing of ultraviolet irradiance onthe ocean surface. *Acta Oceanolog. Sin.* 34(6): 101–112

Lignell, R. (1992). Problems in filtration fractionation of 14C primary productivity samples. *Limnol. Oceanogr.* 37: 172–178

Llabrés, M. & Agustí, S. (2006). Picophytoplankton cell death induced by UV radiation: Evidence for oceanic Atlantic communities. *Limnol. Oceanogr.* 51: 21–29

Mackey, K. R. M., Rivlin, T., Grossman, A. R., Post, A. F. & Paytan, A. (2009). Picophytoplankton responses to changing nutrient and light regimes during a bloom. *Mar. Biol.* 156: 1531–1546

Mackey, K. R. M., Chien, C. T., Post, A. F., Saito, M.A. & Paytan, A. (2015). Rapid and gradual modes of aerosol trace metal dissolution in seawater. *Front. Microbiol.* 5(794): 1–11

Marañón, E., *et al*. (2010). Degree of oligotrophy controls the response of microbial plankton to Saharan dust. *Limnol. Oceanogr*. 55: 2339–2352

Maxwell, K. & Johnson, G. N. (2000). Chlorophyll fluorescence—A practical guide. *J. Exp. Bot.* 51: 659–668

Mercado, J. M., Ramírez, T., Cortés, D., Sebastián, M. & Vargas-Núñez, M. (2005). Seasonal and inter-annual variability of the phytoplankton communities in an upwelling area of the Alborán Sea (SW Mediterranean Sea). *Sci. Mar.* 69: 451–465

Mercado, J. M., Ramírez, T., Cortés, D., Sebastián, M., Reul, A. & Bautista, B. (2006). Diurnal changes in the bio-optical properties of the phytoplankton in the Alboran Sea (Mediterranean Sea). *Estuarine Coastal Shelf Sci*. 69: 459–470

Moore, C. M., Mills, M. M., Langlois, R., Milne, A., Achterberg, E. P., La Roche, J. & Geider, R. J. (2008). Relative influence of nitrogen and phosphorus availability on phytoplankton physiology and productivity in the oligotrophic sub-tropical North Atlantic Ocean. *Limnol. Oceanogr.* 53(1): 291–305

Morales-Baquero, R., Pulido-Villena, E. & Reche, I. (2006). Atmospheric inputs of phosphorus and nitrogen to the southwest Mediterranean region: Biogeochemical responses of high mountain lakes. *Limnol. Oceanogr.* 51: 830–837

Morán, X. A. G., López-Urrutia, A., Calvo-Díaz, A. & Li, W. K. W. (2010). Increasing importance of small phytoplankton in a warmer ocean. *Global Change Biol*. 16: 1137–1144

Mukhopadhyay, S. & Kreycik, P. (2008). Dust generation and drought patterns in Africa from helium-4 in a modern Cape Verde coral. *Geophys. Res. Lett.* 35: L20820

Packard, T. T., *et al.* (1988). Formation of the Alboran oxygen minimum zone. *Deep Sea Res., Part A.* 35: 1111–1118

Paytan, A., Mackey, K. R. M., Chen, Y., Lima, I. D., Doney, S. C., Mahowald, N., Labiosa, R. & Post, A. F. (2009). Toxicity of atmospheric aerosols on marine phytoplankton. *Proc. Natl. Acad. Sci. U.S.A.* 106: 4601–4605

Peralta-Ferriz, C. & Woodgate, R. A. (2015). Seasonal and interannual variability of pan-Arctic surface mixed layer properties from 1979 to 2012 from hydrographic data, and the dominance of stratification for multiyear mixed layer depth shoaling. *Prog. Oceanogr.* 134: 19–53

Piggott, J. J., Townsend, C. R. & Matthaei, C. D. (2015). Reconceptualizing synergism and antagonism among multiple stressors. *Ecol. Evol.* 5: 1538–1547

Prospero, J. M. & Lamb, P. J. (2003). African droughts and dust transport to the Caribbean: Climate change implications. *Science.* 302: 1024–1027

Pulido-Villena, E., Reche, I. & Morales-Baquero, R. (2006). Significance of atmospheric inputs of calcium over the southwestern Mediterranean region: High mountain lakes as tools for detection. *Global Biogeochem. Cycles.* 20: GB2012

Pulido-Villena, E., Wagener, T. & Guieu, C. (2008). Bacterial response to dust pulses in the western Mediterranean: Implications for carbon cycling in the oligotrophic ocean. *Global Biogeochem. Cycles.* 22: GB1020

Raven, J. A. (1998). The twelfth Tansley Lecture. Small is beautiful: The picophytoplankton. *Funct. Ecol.* 12: 503–513

Ribera D'Alcalà, M., Civitarese, G., Conversano, F. & Lavezza, R. (2003). Nutrient ratios and fluxes hint at overlooked processes in the Mediterranean Sea. *J. Geophys. Res.* 108(C9). 8106

Ribés, M., Coma, R. & Gili, J. M. (1999). Seasonal variation of particulate organic carbon, dissolved organic carbon and the contribution of microbial communities to the live particulate organic carbon in a shallow near bottom ecosystem in the Northwestern Mediterranean Sea. *J. Plankton Res.* 21: 1077–1100

Ridame, C., Dekaezemacker, J., Guieu, C., Bonnet, S., L´Helguen, S. & Malien, F. (2014). Contrasted saharan dust events in LNLC environments: Impact on nutrient dynamics and primary production. *Biogeosciences.* 11: 4783–4800

Romero, E., Peters, F., Marrasé,C., Guadayol, O., Gasol, J. M. & Weinbauer, M (2011). Coastal Mediterranean plankton stimulation dynamics through a dust storm event: An experimental simulation. *Estuarine Coastal Shelf Sci.* 93: 27–39

Sarhan, T., García Lafuente, J., Vargas, M., Vargas, J. M. & Plaza, F. (2000). Upwelling mechanisms in the northwestern Alboran Sea. *J. Mar. Syst.* 23: 317–331

Shao, Y., Wyrwoll, K. H., Chappell, A., Huang, J., Lin, Z., McTainsh, G. H., Mikami, M., Tanaka, T. Y., Wang, X. & Yoon, S. (2011). Dust cycle: An emerging core theme in Earth system science. *Aeolian Res.* 2: 181–204

Sinha, R. P. & Häder, D. P. (2008). UV-protectants in cyanobacteria. *Plant Sci.* 174: 278–289

Sobrino, C., Segovia, M., Neale, P., Mercado-Carmona, J. M., García-Gómez, C., Kulk, G., Lorenzo, M. R., Camarena, T., Van de Poll, W. & Spilling, K. (2014). Effect of CO2, nutrients and light on coastal plankton IV: Physiological responses. *Aquat. Biol.* 22: 77–93

Stawiarski, B. (2014). Light and temperature induced variability of the elemental composition of picophytoplankton and their minimum requirements based on nutrient limitation experiments, doctoral thesis, The physiological response of picophytoplankton to light, temperature and nutrients, including climate change model simulations.

Steemann Nielsen, E. (1952). The use of radio-active carbon (C14) for measuring organic production in the sea, J. Cons. *Cons. Int. Explor. Mer.* 18: 117–140

Strzepek, R. F. & Harrison, P. J. (2004). Photosynthetic architecture differs in coastal and oceanic diatoms. *Nature.* 43: 689–692

Tanhua, T., Hainbucher, D., Schroeder, K., Cardin, V., Alvarez, M. & Civitarese, G. (2013). The Mediterranean Sea system: A review and an introduction to the special issue. *Ocean Sci.* 9: 789–803

Tedetti, M. & Sempéré, R. (2006). Penetration of ultraviolet radiation in the marine environment. A review. *Photochem. Photobiol.* 82: 389–397

Thomas, D. N., Baumann, M. E. M. & Gleitz, M. (1992). Efficiency of carbon assimilation and photoacclimation in a small unicellular Chaetoceros species from the Weddell Sea (Antarctica): Influence of temperature and irradiance. *J. Exp. Mar. Biol. Ecol.* 157: 195–209

Vaulot, D., Courties, C. & Partensky, F. (1989). A simple method to preserve oceanic phytoplankton for flow cytometric analyses. *Cytom. (N.Y.).* 10: 629–635

Winder, M. (2009). Photosynthetic picoplankton dynamics in Lake Tahoe: Temporal and spatial niche partitioning among prokaryotic and eukaryotic cells. *J. Plankton Res.* 31: 1307–1320

Wu, Y., Li, Z., Du, W. & Gao, K. (2016). Physiological response of marine centric diatoms to ultraviolet radiation, with special reference to cell size. *J. Photochem. Photobiol. B.* 153: 1–6

Supplementary Information

The data represented here were obtained during our observational and experimental study. These data are essential to be able to adequately represent the graphs and final tables that appear in the main manuscript. The description of the processing of these data is shown in the section of material and methods of the manuscript.

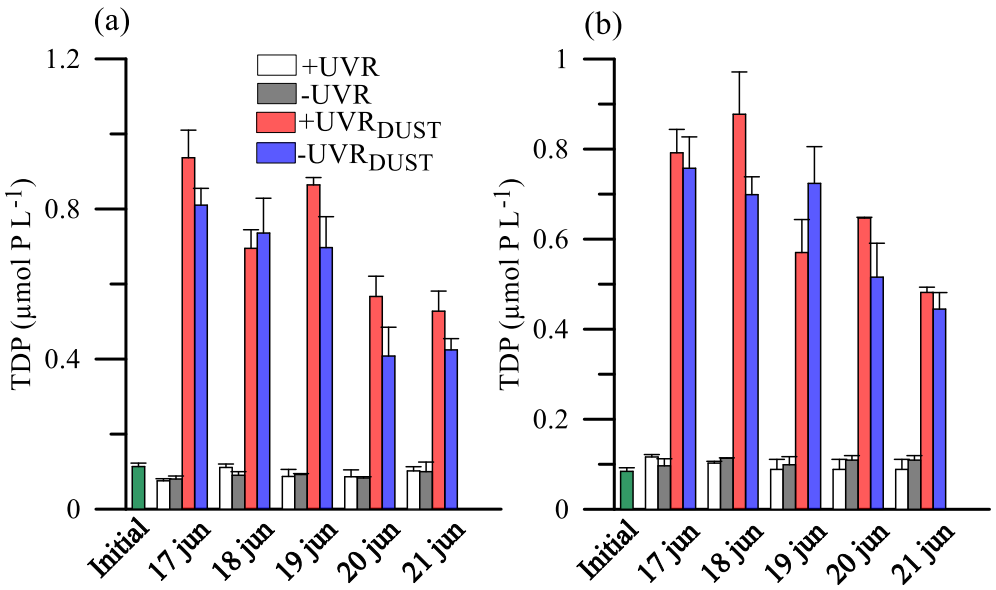

Figure S1. Total Dissolved Phosphorous (TDP) in the microcosms over the experiment for Offshore (a) and Nearshore (b) area. Each bar represents the mean of three replicates while the vertical lines indicate the standard deviation. Green bar shows initial concentration.

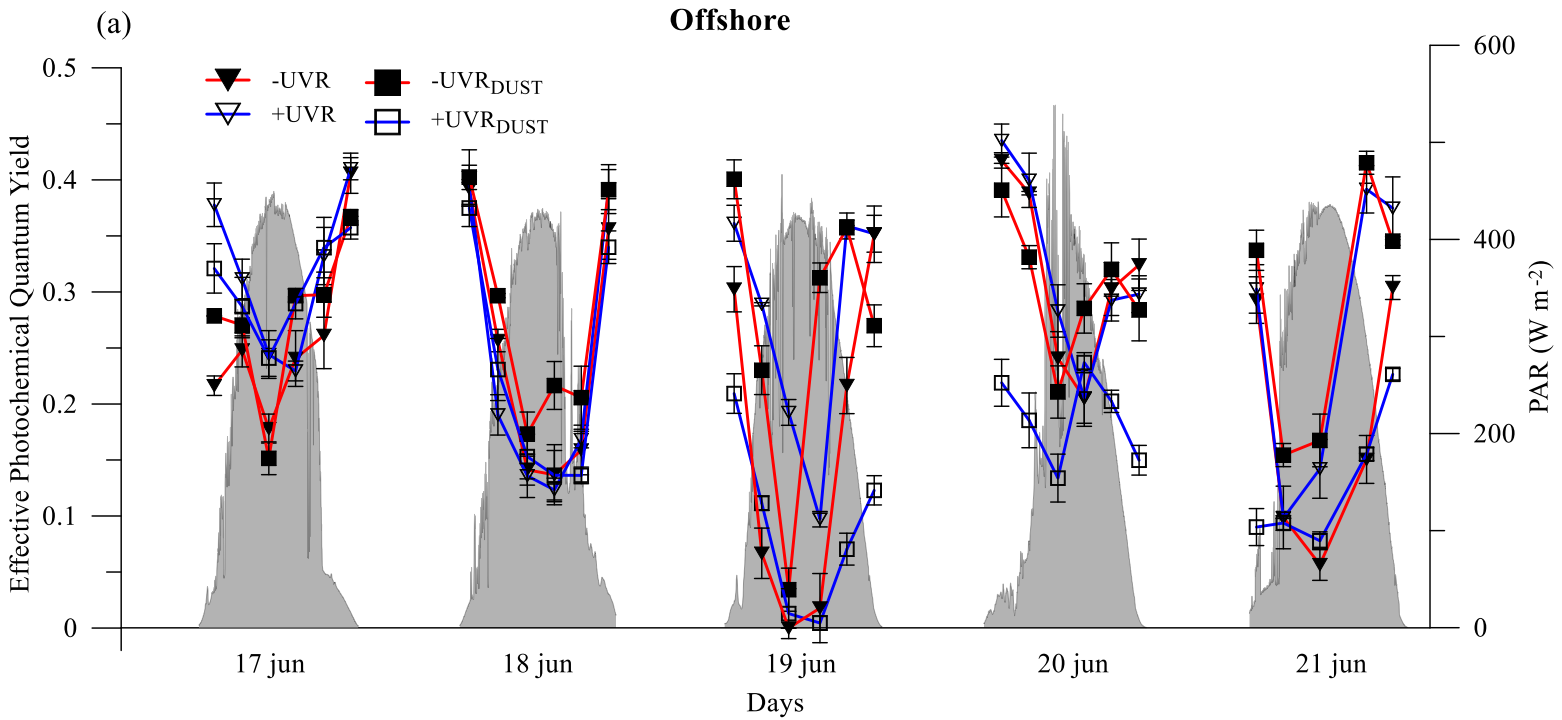

Figure S2-part A. Effective photochemical quantum Yield (a) over the experiment in Offshore area. Shaded area represents PAR radiation.

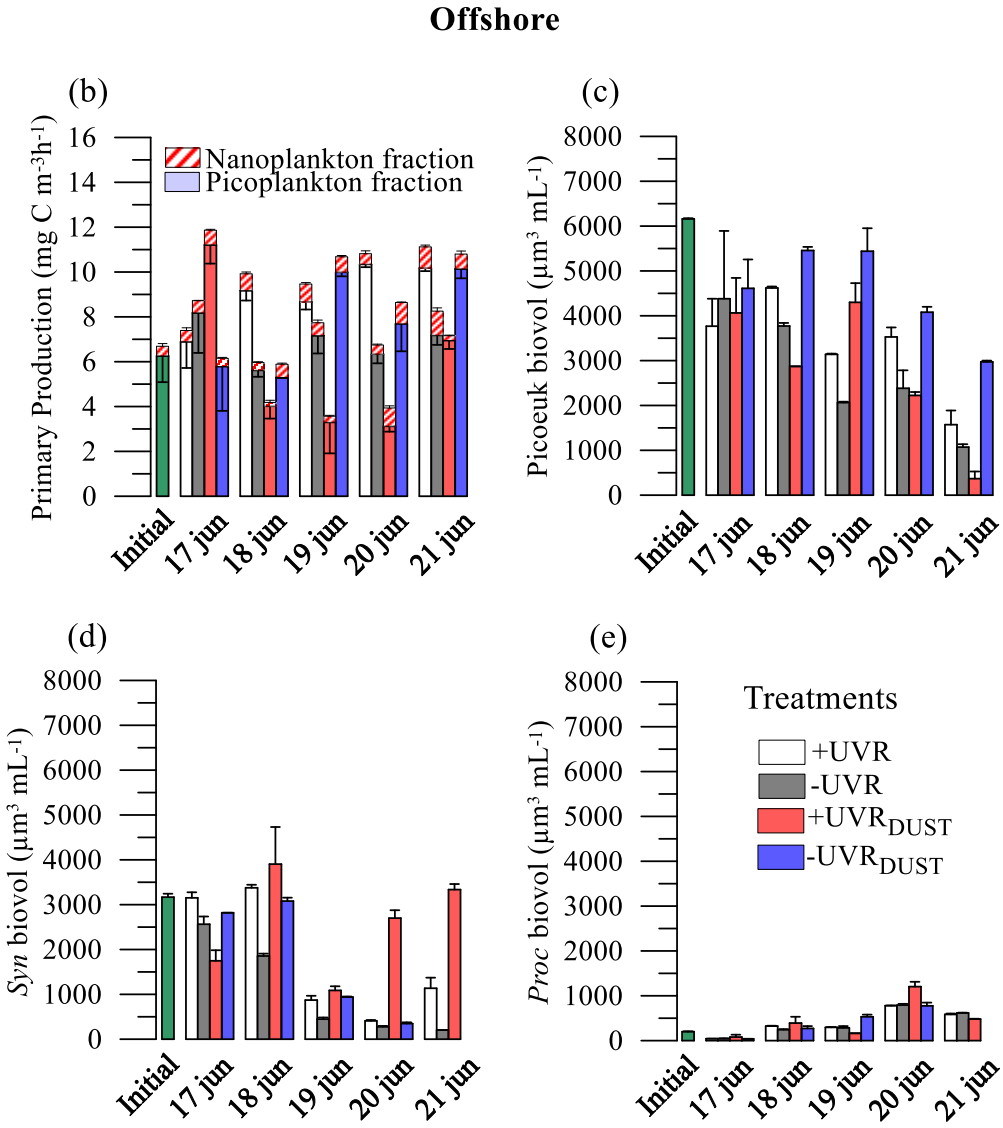

Figure S2-part B. Pico- and nanoplanktonic primary production (b), and Picoeukaryotes (Picoeuk, c), Synechococcus (Syn, d) and Prochlorococcus biovolume (Proc, e) over the experiment in Offshore area. Green bar shows initial concentration.

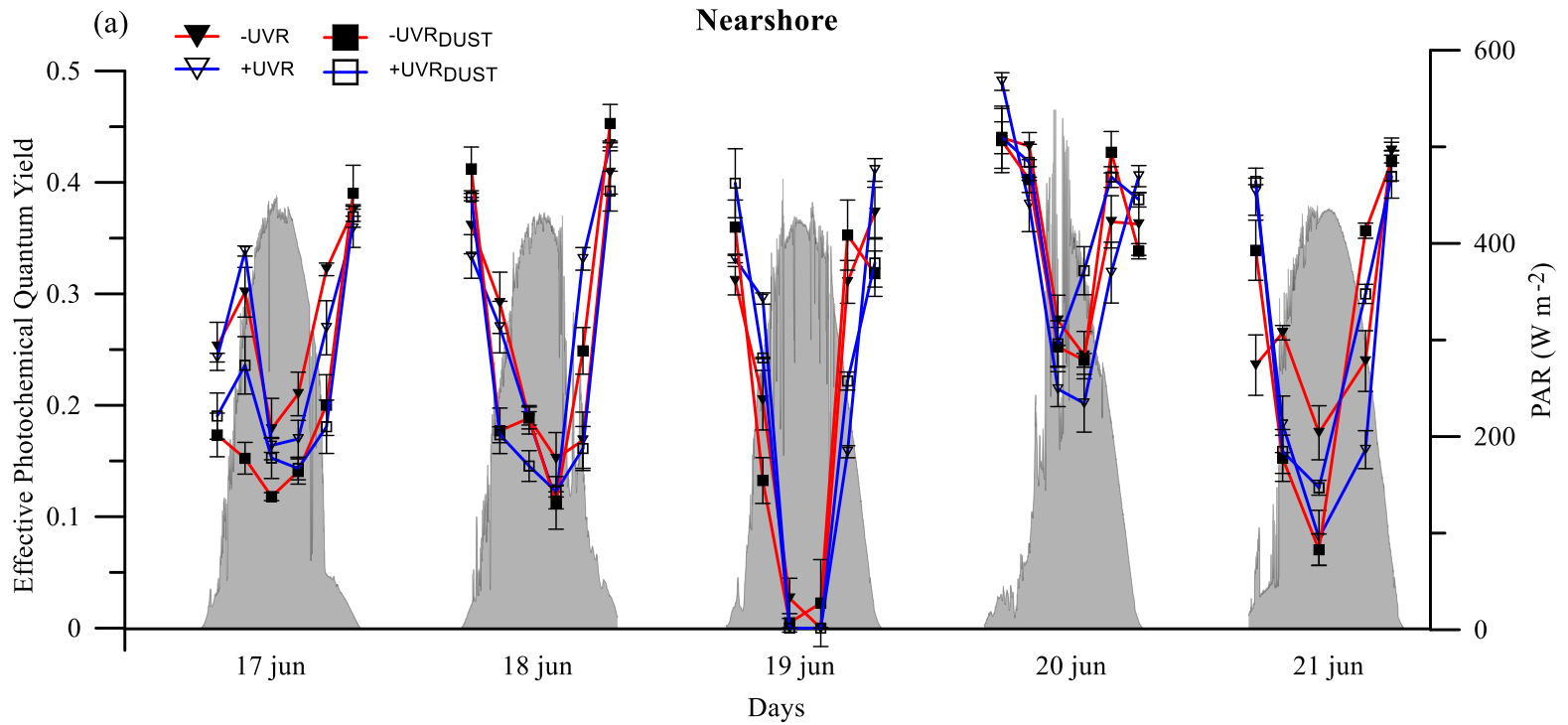

Figure S3-part A. Effective photochemical quantum Yield (a) over the experiment in Nearshore area. Shaded area represents PAR radiation.

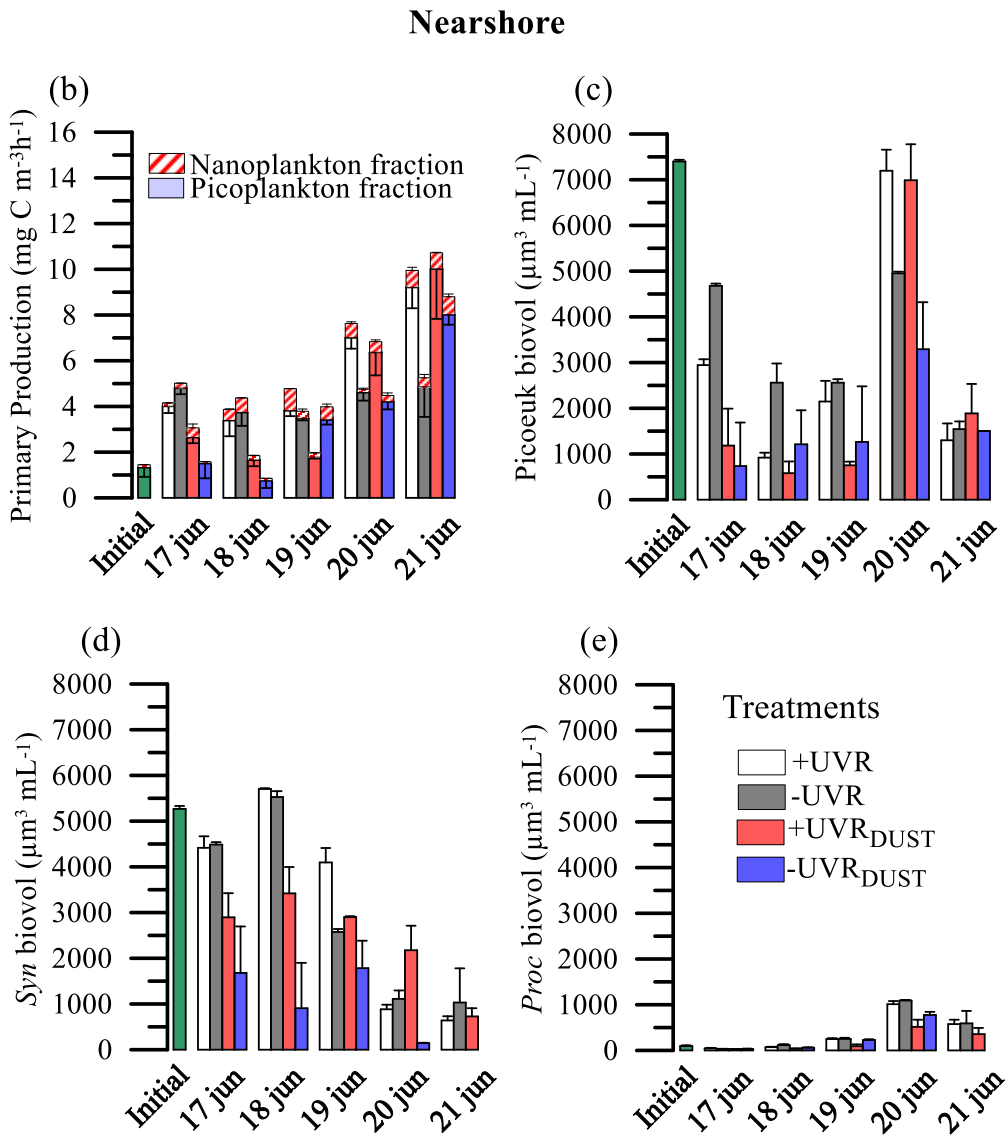

Figure S3-part B. Pico- and nanoplanktonic primary production (b), and Picoeukaryotes (Picoeuk, c), Synechococcus (Syn, d) and Prochlorococcus biovolume (Proc, e) over the experiment in Nearshore area. Green bar shows initial concentration.

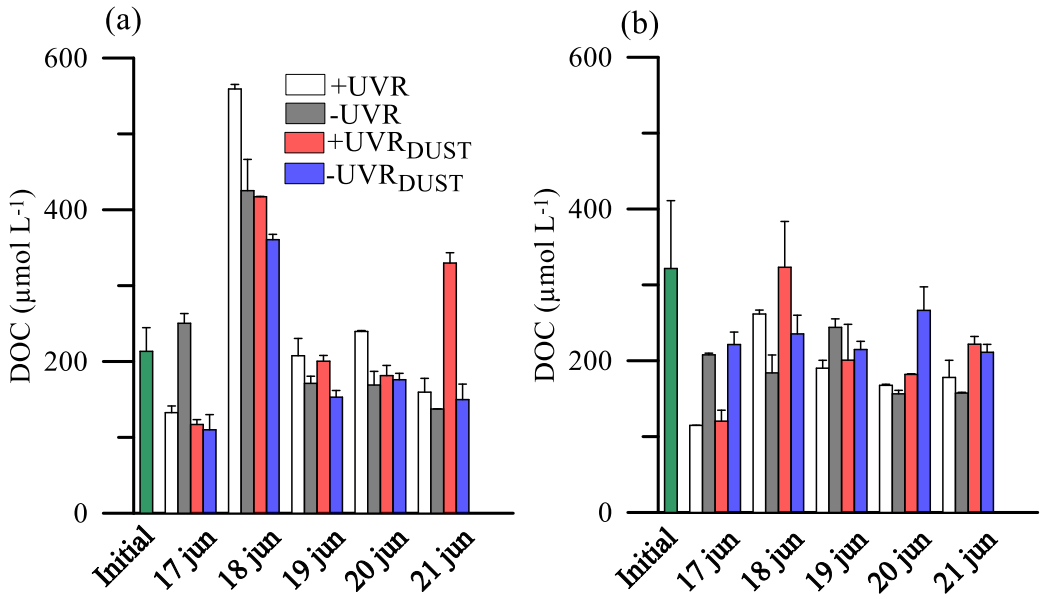

Figure S4. Dissolved Organic Carbon (DOC) concentrations over the experimental period for Offshore (a) and Nearshore (b) area. Green bar shows initial concentration. Each bar represents the mean of three replicates while the vertical lines indicate the standard deviation.

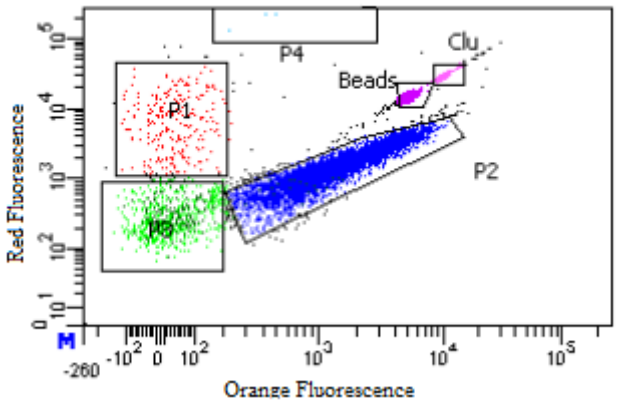

Figure S5. Autotrophic picoplankton from Alboran Sea analysed by Flow Cytometry. The populations were distinguished and enumerated based on fluorescence (colour and intensity) signals depicted in bivariate plots. Chlorophyll fluorescence (red fluorescence) vs. phycoerythrin fluorescence (orange fluorescence) allowed us to distinguish the populations of picoeukaryotes (P1), Synechococcus (P2) and Prochlorococcus (P3).

Table S1. Mean (±SD) of the Synechococcus (Syn), Prochlorococcus (Proc), picoeukaryotes (Picoeuk) and total APP abundances in the Alboran Sea. The stations sampled, its position (latitude and longitude), Total dissolved Nitrogen (TDN) and Phosphorous (TDP), Temperature (Temp), salinity and vertical light extinction coefficient at 320 nm (k_d 320) and PAR (k_d PAR) in each station are shown. Results for each station are mean of samples at 3 and 15 m depth.

Station	Position	*Syn.* (cell mL^{-1})	*Proc.* (cell mL^{-1})	Picoeuk. (cell mL^{-1})	APP (cell mL^{-1})	TDN (µM)	TDP (µM)	Temp. (ºC)	Salinity (PSU)	k_d 320 (m^{-1})	k_d PAR (m^{-1})
1	36º37' N, 4º24' W	11845	536	4412	16794	92 (10)	0.10 (0.01)	17.78 (1.14)	36.8 (0.04)	0.25	0.15
2	36º21' N, 4º22' W	22268	135	1731	24135	171 (62)	0.65 (0.18)	22.19 (0.95)	36.7 (0.04)	0.27	0.11
3	35º59' N, 4º19' W	7129	1121	3674	11924	95 (26)	0.54 (0.01)	16.84 (0.77)	37.0 (0.07)	0.31	0.09
4	36º32' N, 3º48' W	26119	643	2901	29663	101 (19)	0.52 (0.06)	21.58 (1.37)	36.6 (0.01)	0.24	0.13
5	36º21' N, 3º46' W	16852	907	3044	20803	117 (31)	0.45 (0.05)	20.15 (1.66)	36.5 (0.01)	0.33	0.16
6	36º09' N, 3º42' W	21984	24511	3523	50018	194 (8)	0.56 (0.04)	18.05 (0.60)	36.6 (0.01)	0.29	0.12
7	36º32' N, 3º10' W	6684	1130	4288	12102	100 (48)	0.43 (0.00)	20.45 (1.20)	36.6 (0.05)	0.30	0.11
8	36º25 N, 2º45' W	21476	436	2250	24162	121 (19)	0.22 (0.05)	22.06 (0.76)	36.9 (0.10)	0.23	0.10
9	36º39' N, 2º25' W	26454	222	175	26851	217 (2)	0.33 (0.26)	23.5 (0.05)		0.18	0.10
10	36º27' N, 2º13' W	34095	281	302	34678	100 (35)	0.43 (0.06)	23.18 (0.41)		0.21	0.11
11	36º08' N, 1º50' W	29044	491	354	29889	146 (34)	0.40 (0.01)	23.64 (0.03)		0.14	0.08
12	36º40' N, 2º09' W	32953	337	260	33550	144 (51)	0.32 (0.09)	23.65 (0.30)	37.7 (0.04)	0.27	0.15
13	36º26' N, 1º55' W	19418	485	278	20181	137 (20)	0.48 (0.06)	23.75 (0.66)	37.2 (0.10)	0.19	0.09
14	36º16' N, 1º43' W	28102	485	226	28814	123 (14)	0.51 (0.01)	23.69 (0.04)	37.2 (0.08)	0.19	0.10

CHAPTER 3

Scientific expedition to Larga Lake

CHAPTER 3 - Climate-driven shifts in algal-bacterial interaction of high-mountain lakes in two years spanning a decade

J. M. González-Olalla, J. M. Medina-Sánchez, I. L. Lozano, M. Villar-Argáiz, and P. Carrillo

Published in Scientific Reports; 8: 10278; 2018; https://doi.org/10.1038/s41598-018-28543-2

Abstract

Algal-bacterial interactions include mutualism, commensalism, and predation. However, how multiple environmental conditions that regulate the strength and prevalence of a given interaction remains unclear. Here, we test the hypothesis that the prevailing algal-bacterial interaction shifted in two years (2005 *versus* 2015), due to increased temperature (T) and Saharan dust depositions in high-mountain lakes of Sierra Nevada (S Spain). Our results support the starting hypothesis that the nature of the prevailing algal-bacterial interaction shifted from a bacterivory control exerted by algae to commensalism, coinciding with a higher air and water T as well as the lower ratio sestonic nitrogen (N): phosphorous (P), related to greater aerosol inputs. Projected global change conditions in Mediterranean region could decline the functional diversity and alter the role of mixotrophy as a carbon (C) by-pass in the microbial food web, reducing the biomass-transfer efficiency up the web by increasing the number of trophic links.

1. Introduction

Algae and bacteria numerically dominate the ocean and freshwater communities (Sarmento & Gasol, 2012), comprising the majority fraction of particulate organic carbon (Simon *et al*., 1992). Hence, the interactions between algae and bacteria

are crucial in aquatic environments as they control nutrient cycles and biomass production in the trophic web (Seymour *et al*., 2017). These relationships encompass commensalism (Carrillo *et al*., 2006), predation (Unrein *et al*., 2014) and mutualism (Amin *et al*., 2015), forming a continuum of the interaction modes (Ramanan *et al*., 2016). In fact, several studies have reported the commensalistic interaction between the two metabolic groups (Medina-Sánchez *et al*., 2002; Cho *et al*., 2015), where bacteria derive C for growth from the excreted organic carbon (EOC) provided by algae (Aota & Nakajima, 2001; Sarmento & Gasol, 2012). Thus, bacteria can consume up to 50% of the C fixed by phytoplankton (Fuhrman & Azam, 1982). In predation (i.e. bacterivory), bacteria supply C and nutrients (N, P or Fe) to mixotrophic algae (Lindehoff *et al*., 2011; Hartmann *et al*., 2012). Mutualism is established when bacteria, by decomposing organic matter, supply mineral nutrients (Thompson *et al*., 2012) or vitamins (Cruz-López & Maske, 2016) for algal growth (Seymour *et al*., 2017) while the algae supply C for bacterial growth. Furthermore, a complex mutualistic interaction develops when a dual control acts simultaneously through the bacterial dependence on EOC (i.e. a resource-based control), together with a predatory control by mixotrophic algae (Medina-Sánchez *et al*., 2004; Cabrerizo *et al*., 2017).

The nature and strength of these interspecific interactions can change depending on environmental conditions (Ramanan *et al*., 2016). Thus, nutrient input can alter the interaction in several ways. For example, moderated nutrient amendments can shift an algal–bacterial interaction from commensalism to competition depending on bacterial N:P ratio (Gurung *et al*., 1999; Villar-Argaiz *et al*., 2002) , whereas high P enrichment (>30 $\mu g\ P\ L^{-1}$) favours the development of strict autotrophic against mixotrophic algae, thereby reinforcing commensalistic interaction (Cabrerizo *et al*., 2017). In addition, the strength of algal-bacterial interaction is regulated by T, due to a stimulatory effect on phytoplankton (Paver & Kent,

2017), which increase EOC, supporting bacterial carbon demand and reinforcing the commensalistic relationship (Durán *et al*., 2016). These findings contrast with the stronger effect of T on heterotrophic than autotrophic processes predicted by metabolic theory (Yvon-Durocher *et al*., 2010) (although a recent study (Chen & Laws, 2017) has questioned this theory), implying that, at the organism level, there is a shift toward heterotrophic metabolism of mixotrophic algae through increased bacterivory (Wilken *et al*., 2013). Therefore, the predominance of strict autotrophs or mixotrophs might encourage commensalistic *or* bacterivory interaction under warming, with the consequent effect on the regulation of the microbial food web.

Furthermore, warming can strength stratification in lakes, and therefore the exposure of microorganisms to ultraviolet radiation (UVR) in the upper layers of the water column (Gao *et al*., 2012). It has widely been reported that UVR has a negative impact on several targets and processes (e.g. photosynthesis, and nutrient uptake, primary production (PP) and heterotrophic bacterial production (HBP)) (Häder *et al*., 2015). Nevertheless, it has also been demonstrated that planktonic organisms have a great capacity to acclimatize to high UVR in oligotrophic ecosystems by increasing the percentage EOC (Korbee *et al.,* 2012), stimulating the growth of UVR-resistant bacteria (Xenopoulos & Schindler, 2003) or increasing the consumption of bacteria by mixotrophic algae (Medina-Sánchez *et al*., 2004; Carrillo *et al*., 2017).

The joint effect of nutrient enrichment, T, and UVR on algal-bacterial interaction and microbial food web has been reported from experiments in single lakes (Medina-Sánchez *et al*., 2013; Gu & Wyatt, 2016; Su *et al*., 2017). However, little attention has been placed on the way in which these environmental factors alter the algal–bacterial relationship across systems over the long term. In this context, our study was conducted in high-mountain lakes distributed in an area of

86,200 ha in Sierra Nevada National Park, within the Mediterranean region. The effects of global change are accentuated in this region (Belkin, 2009), and even more so in high-elevation areas compared to the global average (Wang, 2014), due to their greater ecological sensitivity to such change (Pepin, 2015). Particularly, the Mediterranean region is exposed to the increasingly nutrient-rich aerosol inputs from the Saharan Desert (De la Paz *et al*., 2013), and Sierra Nevada is specifically receptive to Saharan dust due to its location and altitude (Morales-Baquero *et al*., 2006). In addition, the high elevation implies that the lakes are exposed to high-intensity UVR during the ice-free period, which may prolong over time because of rising T. These characteristics, together with their oligotrophic state and simple trophic web structure, make these lakes particularly sensitive indicators of the past and current global conditions and also serve as models to predict future changes because they register environmental change more directly (Battarbee *et al*., 2002), being considered sentinels of global change (Weckstrom *et al*., 2016).

For these reasons, our objective was to assess whether the regulation of the algal-bacterial interaction has changed in 2015 respect to 2005, after a period in which Saharan dust transport to the Mediterranean basin and air T have increased, while chronic UVR levels remain high. Our hypothesis is that greater dust deposition to Sierra Nevada lakes and higher T have shifted the algal metabolism towards stricter autotrophy and higher PP, and therefore, we expect a reinforcement of the commensalistic interaction between algae and bacteria to the detriment of the predatory interaction.

2. Material and Methods

a. Remote Sensing

The remote-sensing data for the Sierra Nevada area were gathered from 1980 to 2015. Daily data of the area-average aerosol index, air T, and surface UVR fluxes

in this region were downloaded from Giovanni v. 4.18.3 (Acker & Leptoukh, 2007). Aerosol index data were taken from the Total Ozone Mapping Spectrometer (TOMS) Nimbus-7 (March 21, 1979 – May 5, 1993), TOMS Earth Probe (July 22, 1996 – June 28, 2005) and the Ozone Monitoring Instrument (OMI) (June 29, 2005 – December 31, 2015) satellites (data from 1993 to 1996 are not available), while T and surface UVR-flux data came from the MERRA and MERRA-2 model, respectively. Aerosol index intensity was calculated as the mean value of aerosol index for each entire year, whereas the frequency of high load aerosol index events was calculated as the number of days per year with aerosol index >1.

b. Study Area

Our study was conducted in 14 lakes in 2005 and 13 in 2015, which 10 lakes were common between the two years. Some of the lakes could not be sampled in 2015 due to the severe hydric stress to which are subjected, affected by the Mediterranean climate. All lakes are located above the tree line in the Sierra Nevada Mountains (36.8559–37.8159 N, 2.8319–3.8409 W), in the southern Iberian Peninsula (Fig. S6 in Supplementary information). Sampling was conducted during the ice-free period (mid-July to mid-August) of each year.

These lakes are oligo- and mesotrophic (Chl *a* range from 0.25 to 12.66 μg L^{-1}). The external inputs of mineral nutrient occur mainly during thaws, and are associated with sporadic events of Saharan dust deposition (Talbot *et al*., 1986; Villar-Argaiz *et al*., 2001) containing high P levels, with a mean molar total N:total P ratio in total dust deposition ranging from 10 to 50 (Morales-Baquero *et al*., 2006). The lakes are characterized by their small size (<3 ha), high transparency, shallow water column (<10 m maximum depth) and by the simplicity of the pelagic fishless community, with a low abundance of

heterotrophic nanoflagellates and ciliates, and the presence or dominance of mixotrophic protists in the trophic web (Carrillo *et al*., 2006).

c. Field Sampling

From each lake, an integrated sample representative of the mixing layer of the water column was collected using 10 L-Niskin Bottle and used for biological and chemical analyses. The samples were then filtered through a 45-µm pore-size mesh to remove zooplankton, and subsamples for each variable analysed were taken in triplicate (see below).

Morphometric and physical measurements were also performed for characterizing each lake (see below).

d. Physical parameters

d.1 Temperature and light measurement

Vertical profiles of radiation and T of water column were determined at noon using a submersible radiometer BIC (Biospherical Instruments Inc., CA, USA) that registered measurements of downwelling irradiance at wavelengths representative of the different regions of the solar spectrum (305, 320, and 380 nm and full PAR [400–700 nm]). The k_d were determined from the slope of the linear regression of the natural logarithm of downwelling irradiance *vs*. depth for each wavelength.

I_m for PAR and UVR was calculated as in next equation:

$$Im\ (\lambda) = \frac{I_0(\lambda)[1 - \exp(-k_d(\lambda)z)]}{k_d(\lambda)z}$$

where I_0 is the mean incident surface irradiance; k_d is the mean attenuation coefficient for UVR at 305, 320, 380 nm and PAR; and z is the maximum depth for each lake.

e. Chemical parameters

The concentrations of total P and total dissolved P were determined in 25-ml aliquots after digestion with a mixture of potassium persulphate and boric acid at 120 °C for 30 min (APHA, 1992). Total N and total dissolved N samples were also digested with persulfate and measured as nitrate following the ultraviolet spectrophotometric screening method (APHA, 1992). For determination of total dissolved N and total dissolved P, the water samples were previously filtered at low pressure (<100 mmHg) using glass-fibre filters (0.7 µm pore-size, Whatman GF/F). To determine sestonic C, N, and P, water samples (0.5 L for C/N and 0.5 L for P) were filtered through precombusted (1 h at 550 °C) glass-fibre filters of 1-µm pore size (Whatman GF/B) at low pressure (<100 mm Hg). The filters were immediately frozen at −20 °C, and the C and N analyses were performed using a Perkin-Elmer 2400 elemental analyser. The sestonic P was determined with the same method as that described for total P.

For dissolved organic carbon determination, samples were filtered through pre-combusted (2 h at500 °C) glass fibre filters (Whatman GF/F) and acidified with HCl 1 N. The analyses were carried out in a total organic carbon analyzer (TOC-VCSH/CSN Shimadzu).

f. Biological parameters

f.1 Chlorophyll-a Concentration

Chl-*a* concentrations were determined by fluorometric techniques (Jeffrey & Humphrey, 1975). The samples were filtered onto a Whatman GF/F filter (0.7 µm pore size) and the photosynthetic pigments extracted in 5 ml of absolute methanol at 4 °C in darkness.

Samples were measured at an excitation wavelength of 460 nm and emission at 670 nm, with a fluorometer LS55 Luminescence Spectrometer (Perkin-Elmer, Boston, MA, USA). Previously, a calibration curve was made with pure

chlorophyll spinach extract to transform fluorescence values in chlorophyll concentration.

f.2 Primary Production

Following the ^{14}C method proposed by Steeman-Nielsen (Steemann Nielsen, 1992), 140-ml samples from each lake were collected for PP measurements. Four 35-mL Teflon flasks for each treatment (three clear and one dark as control) were added with 9.25 MBq of $NaH^{14}CO_3$ (specific activity: 310.8 MBq mmol-1, DHI Water and Environment, Germany). The flasks were incubated for 4 h around noon, and the laboratory procedure was based on Carrillo *et al*. (2002). Thus, 4-ml aliquots were taken before filtration to measure the TPP produced, and 35-ml aliquots were filtered, retaining the organic carbon particles in Nuclepore filters of 1-µm pore size to determine the PP_P. From the filtrates (<1 µm), 4 ml were used for measuring the EOC.

Filters and filtrates were placed in 5- and 20-mL scintillation vials, respectively, and acidified with 100 µL of 1 N HCl in order to remove $DI^{14}C$. Vials were then kept open during 24 h in an aeration hood following the recommendations of Lignell (1992). Then, the vials were filled with scintillation cocktail (Ecoscint A) and counted using a scintillation counter (Beckman LS 6000TA) equipped with autocalibration.

The sum of EOC and PP_P corresponds with the TPP. The % EOC was calculated as in following equation:

$$\%\mathrm{EOC} = \frac{\mathrm{EOC}}{\mathrm{TPP}} \times 100$$

f.3 Abundance/biomass of Planktonic Organisms

Abundance and biomass of algae, heterotrophic nanoflagellates, ciliates, and nanoplankton were counted at 400x and 1000x magnification under an inverted microscope (Carl Zeiss AX10, LCC, USA).

For the quantification of autotrophic picoplankton and bacteria (Zubkov & Burkill, 2006), several 1.5 mL aliquots from each sample were fixed with paraformaldehyde (1% final concentration) and immediately stored at −180 °C until further processing. Autotrophic picoplankton abundance was quantified based on Chl *a* auto-fluorescence, whereas total picoplankton abundance was quantified after other 1.5-mL fixed aliquots were stained with SYBR Green I DNA (Sigma-Aldrich) 1:5000 final dilution of initial stock. Absolute cell-abundance values were determined using a Becton Dickinson FACScan flow cytometer (Oxford, UK) and Yellow-green-l µm beads (Fluoresbrite Microparticles, Polysciences, Warrington, PA, USA).

f.4 Herotrophic Bacterial Production

HBP was determined as incorporation of 3H-thymidine (specific activity = 52 Ci $mmol^{-1}$, Amersham Pharmacia) into the bacterial DNA. Briefly, 3H-thymidine was added to sets of six (four replicates plus two blanks per lake) sterile microcentrifuge tubes filled with 1.5 mL of sample to a final (saturating) concentration of 25 nM. The vials were then incubated at *in situ* T in darkness for 1 h. After incubation, the incorporation of 3H-thymidine was stopped by adding trichloroacetic acid (TCA, 5% final concentration). Likewise, blanks were TCA-killed before the radiotracer was added. After the cold 5% TCA extraction, the precipitate was collected by centrifugation at 16,000 g for 10 min, rinsed (and centrifuged) twice with 5% TCA, and measured in a scintillation counter equipped with autocalibration (Beckman LS 6000 TA). The conversion factor 1.5×10^{18} cell mol^{-1} was used to estimate the number of bacteria produced per

mole of incorporated ^{3}H-thymidine (Bell *et al.*, 1983). The factor 20 fg C cell^{-1} was applied to convert bacterial production into C (Lee & Fuhrman, 1987).

f.5 Bacterivory

BV was determined from the amount of bacteria traced with ^{3}H-thymidine that were captured by algae following the method proposed by Medina-Sánchez (2004). For determining BV, sets of four Teflon bottles (three replicates and one blank per lake) were filled with 25 ml of water samples each, radiotraced with ^{3}H-thymidine to a final concentration of 25 nM, and incubated for 1 h in full sunlight. After incubation, the bacterivory was stopped by adding neutralized formaldehyde (0.75% w/v final concentration). Likewise, blanks were formaldehyde-killed before the incubation with the radiotracer. Aliquots of 1.5 ml were obtained from each replicate for determining total activity in the sample. The remaining sample volume (23.5 ml) was filtered through 1 µm pore-size cellulose nitrate filter (Sartorius). Aliquots of 1.5 ml were taken from the filtrate to determine the residual activity, while the activity registered on the filter served to determine BV. The filters were dissolved using acetone 100% and then subjected to centrifugation at 16,000 g for 10 min at 4 °C. Supernatant acetone was removed, and the pellet was re-suspended with 5% TCA (1.5 ml). The subsequent procedure was similar to HBP. %BV was calculated as in equation:

$$\%\mathrm{BV} = \frac{\mathrm{Bacterivory}}{\mathrm{HBP}} \times 100$$

where bacterivory was determined from the bacterial incorporation rate by fraction >1 µm retained on the filter. Bacterivory values were converted to cell number and bacterial C captured using the same conversion factors as for HBP determination.

g. Statistical analysis

Paired *t*-test for dependent samples analysis was carried out with the 10 lakes that were sampled both years (2005 and 2015) to determine significant differences in Chl-*a*, PP_P, HBP, %BV, sestonic N:P ratio, dissolved organic carbon and T between 2005 and 2015. The homogeneity of the variances was verified by Levene's and/or the Brown and Forsythe test.

SMR were carried out with all the lakes sampled each year (14 and 13 lakes in 2005 and 2015, respectively) to quantify the influence of biotic and abiotic factors (I_{m305}, I_{m320}, I_{m380}, I_{mPAR}, total dissolved P, total P, total dissolved N, total N, T, dissolved organic carbon, EOC, TPP, Chl *a*, I_m:total dissolved P, I_m: total P, I_m: total dissolved N, I_m:T, bacterial abundance) on PP_P, HBP and %BV in 2005 and 2015. Linearity and multiorthogonality among independent variables were verified by previous correlation analysis and controlled by specifying 0.6 as the minimum acceptable tolerance. Because some factors co-vary with those included by SMR, single regression analyses were performed to assess strength of: i) the C-based control (EOC or dissolved organic carbon) on HBP; ii) the abiotic control (T, UVR, I_{m305}:T, I_{mPAR}:T, I_{m305}:Total P, I_{m305}: total dissolved P) on PP_P and %BV; iii) the predatory control (%BV or bacterial abundance) on HBP, to evaluate changes in the algal-bacterial interaction. The normal distribution of residues in all regressions was checked by Kolmogorov-Smirnov tests (Statsoft 1997).

3. Results

a. Remote sensing data

Environmental factors associated with global change have steadily varied over the last 35 years from the south-eastern Iberian Peninsula. While UVR striking the Sierra Nevada Mountains remained high during the summer period (300.25–306.47 W m^{-2}; Supplementary Fig. S7), Saharan dust input and air T followed a positive trend during the 10 years covered by our metabolic measurements

(Fig. 12). The UV aerosol index has increased progressively from the 1980s on, both in intensity and frequency (Fig. 12), accompanied by dust inputs during the winter of recent years, which is highly unusual in this region (Fig. 13). Specifically, during the last decade the aerosol index intensity has increased from 0.39 in 2005 to 0.44 in 2015, and the frequency of high-intensity events (aerosol index >1) has increased from 22 in 2005 to 49 in 2015. Also, the mean air T in summer has risen from 15.42 °C in 2005 to 16.45 °C in 2015.

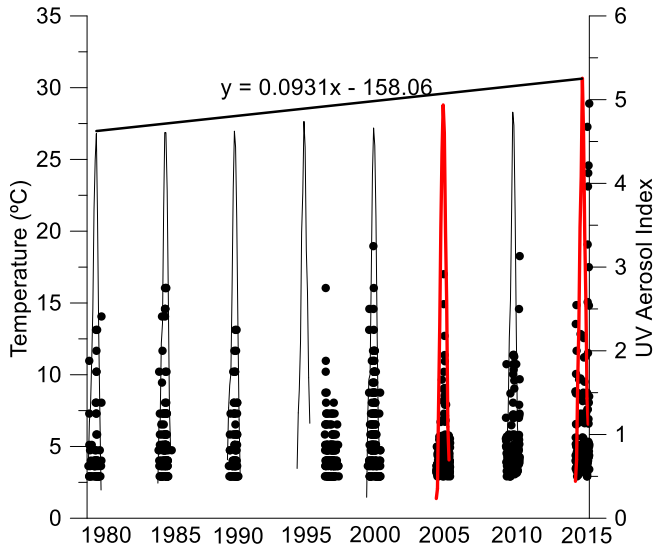

Figure 12. Environmental conditions (air Temperature (represented as lines) and UV aerosol index (represented as points)) for Sierra Nevada region (37°1', −3°23', 37°4', −3°17') for 1980 to 2015 period. Diagonal line represents the temperature trend during the ice-free period and the red lines the temperature of the two years studied.

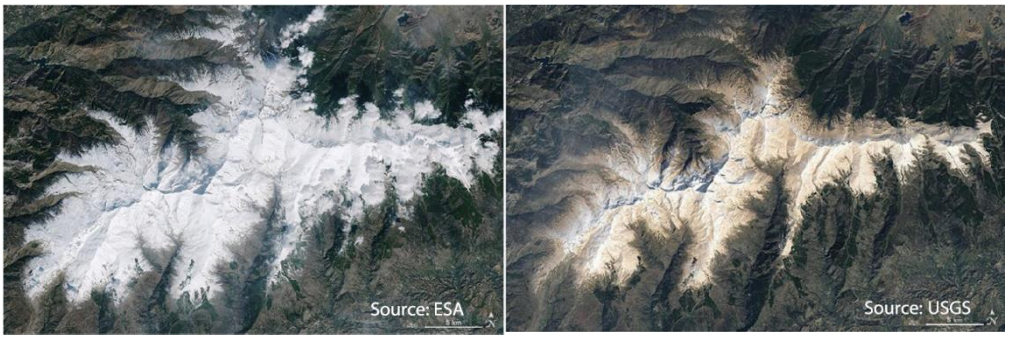

Figure 13. Aerial photography captured by the Sentinel 2-A (Left; courtesy of European Space Agency, ESA) and Landsat 8 (Right; courtesy of the U.S. Geological Survey) satellites corresponding to February 18 and February 27, 2017, after an intrusion of atmospheric dust over the Sierra Nevada National Park.

b. Abiotic and Biotic changes in the Lakes in 2005 and 2015

Diffuse attenuation coefficient for downward radiation (*kd*) showed low values of UVR (305 nm) and photosynthetically active radiation (PAR) throughout the water column, with the lakes Gabata, Larga, Caldera, and Yeguas exhibiting greater transparency to UVR ($kd\ UVR_{305} = 0.31–0.92\ m^{-1}$), while the lakes Chico de la Virgen, Grande de Rio Seco, and Alta de Río Seco reached the highest values ($kd\ UVR_{305} = 4.04–7.5\ m^{-1}$). The mean water-column T for the 10 lakes sampled in both years ranged between 15.5 °C in 2005 and 16.1 °C in 2015, and 60% of the lakes analysed had higher T in 2015, although without significant differences between the two years (*t*-test $p > 0.05$).

The trophic status of the lakes sampled in 2005 (Durán *et al*., 2016) and 2015 spanned oligo- to mesotrophy, as indicated by the total dissolved P, with values ranging from 0.049 to 0.483 µM of P in the lakes Larga and Aguas Verdes, respectively (Table 6). No significant differences appeared in total dissolved P concentration between the two years (*t*-test $p > 0.05$). However, the mean value of the seston N:P ratio for the 10 lakes sampled both years was 48.9, with 50.0% of the lakes showing values higher than 30 in 2005, whereas mean N:P ratio decreased to 18.75 with only 11.1% of the lakes showing higher values than 30 in

2015 (*t*-test $p > 0.05$). The mean concentrations of chlorophyll *a* (Chl *a*) and dissolved organic carbon did not significantly differ (*t*-test $p > 0.05$) between years (3.84 µg Chl *a* L^{-1} and 95.0 µM in 2005; 5.41 µg Chl *a* L^{-1} and 53.25 µM in 2015; Table 6).

Regarding the functional variables, particulate primary production (PP_P) registered a mean value of 1.71 µg C L^{-1} in 2005, significantly increasing in 2015 (10.85 µg C L^{-1}; *t*-test, $p = 0.049$; Table 6 and Fig. 14). However, HBP mean values slightly decreased from 0.13 µg C L^{-1} h^{-1} in 2005 to 0.11 µg C L^{-1} h^{-1} in 2015, without significant differences between the two years (*t*-test $p > 0.05$; Table 6 and Fig. 14). The mean bacterivory rate (BV) was 18.48 ng C L^{-1} h^{-1} in 2005 and 9.71 ng C L^{-1} h^{-1} in 2015 (Table 6). The BV rates normalized by HBP (%BV) significantly decreased from 31.45% (2005) to 9.08% (2015 (*t*-test $p = 0.032$, Fig. 14).

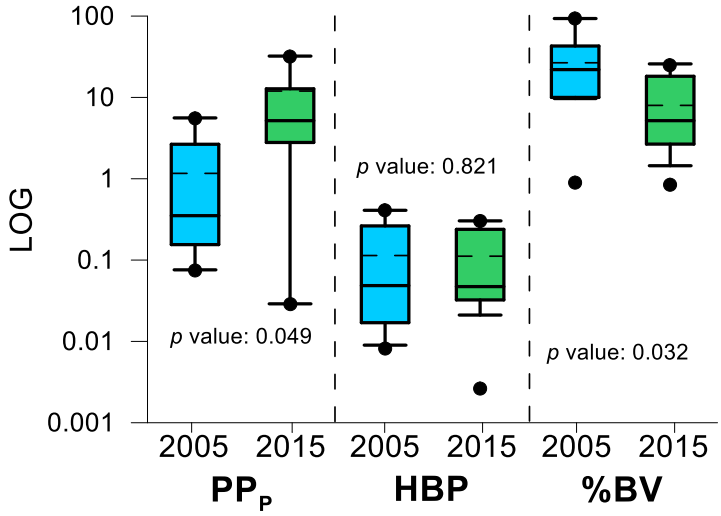

Figure 14. Box-Plot of particulate primary production (PPP), heterotrophic bacterial production (HBP) and % bacterivory (%BV) in Lakes of Sierra Nevada. Full lines and discontinuous lines inside the box represent the median and mean value, respectively. The boxes represent the upper and lower quartiles, while vertical lines indicate the 10th and 90th percentiles, and the points the 5th and 95th percentiles. 2005 and 2015 data were significantly different (paired t-test for dependent samples analysis) for PPP and %BV with p value showed in the graph.

Table 6. Characterization of high-mountain lakes of Sierra Nevada for 2005 and 2015. Units are given in brackets. TDP: Total dissolved phosphorous, TDN: Total dissolved nitrogen, DOC: Dissolved organic carbon, BA: Bacterial abundance.

	LAKES	$k_{d\ UVR\ 305}$ (m^{-1})	$k_{d\ PAR}$ (m^{-1})	T^a (ºC)	TDP (µM)	TDN (µM)	DOC (µM)	Seston N:P	HBP (µg C L^{-1} h^{-1})	PP_P (µg C L^{-1} h^{-1})	EOC (µg C L^{-1} h^{-1})	Bacterivory (µg C L^{-1} h^{-1})	Chl *a* (µg L^{-1})	BA (cell ml^{-1} x10^5)
2005	Caballo	5.75	0.64	15	0.43	30.40	77	50.26	0.025	0.300	1.090	0.005	0.66	5.90
	Yeguas 1	0.61	0.2	15.50	0.10	7.10	89	227.11	0.008	2.651	0.530	0.005	7.77	2.40
	Yeguas 2	2.03	0.66	15.39	0.14	25.00	na	45.21	0.018	1.824	1.280	0.008	11.99	4.30
	Grande de la Virgen	1.19	0.45	11.80	0.13	9.10	65	32.55	0.021	0.943	1.860	0.019	0.54	15.70
	Chico de la Virgen	7.12	0.94	20.30	0.30	21.40	45	19.25	0.409	14.341	8.280	0.039	10.04	33.10
	Aguas Verdes	7.11	1.05	16.20	0.48	34.50	123	19.93	0.228	1.123	1.940	0.031	2.03	7.30
	Alta de Río Seco	4.07	2.66	15.50	0.33	23.20	115	13.39	0.052	0.155	1.480	0.009	0.43	2.40
	Grande de Río Seco	4.35	1.82	17.10	0.30	21.40	98	12.91	0.045	0.100	0.440	0.014	1.39	2.30
	Gabata	0.92	0.38	12.20	0.10	7.20	76	41.82	0.067	5.595	2.870	0.017	3.6	7.70
	Larga	0.37	0.2	16.10	0.12	8.30	85	60.67	0.009	0.189	0.240	0.004	0.25	3.50
	Caldera	0.38	0.18	15.73	0.19	13.80	87	36.42	0.017	0.352	3.280	0.002	1.86	6.50
	Caldereta	2.02	0.66	17.64	0.25	18	103	14.50	0.200	4.381	3.380	0.064	4.94	1
	Borreguil	3.74	0.82	14.50	0.28	19.60	140	18.48	0.263	0.189	1.230	0.002	0.69	1.40
	Hondera	3.49	1.6	16.40	0.26	18.70	150	26.43	0.378	5.595	2.760	0.072	11.85	8.50
2015	Yeguas 1	0.49	1.18	12.77	0.14	16.64	33.33	13.24	0.052	2.792	0.005	0.009	3.16	6.39
	Grande de la Virgen	1.24	0.35	11.46	0.16	19.50	29.46	na	0.021	0.192	0.753	0.001	1.68	1.40
	Chico de la Virgen	7.50	1.05	20.40	0.10	11.79	77.71	0.71	0.032	4.091	1.693	0.001	3.04	4.93
	Tajos Coloraos	1.63	0.42	17.76	0.07	16.29	31.98	38.75	0.035	0.060	0	0.012	2.03	2.43
	Borreguil	1.96	0.38	17.37	0.09	19.57	60.88	26.19	0.114	3.586	5.226	0.011	4.25	10.88
	Hondera	3.16	1.05	17.03	0.09	21.21	43.21	30.32	0.301	32.143	8.233	0.057	5.12	17.31
	Vacares	0.92	0.21	17.29	0.13	55.43	144.88	35.13	0.049	10.754	8.412	0.011	3.72	9.88
	Caldera	0.45	0.19	18.64	0.06	18.21	37.42	11.10	0.042	12.750	1.964	0.001	5.46	7.29
	Grande de Río Seco	4.66	0.57	18.68	0.18	17.43	81.15	18.39	0.239	28.404	3.966	0.006	6.46	40.62
	Alta de Río Seco	4.04	0.66	17.60	0.28	24.36	87.42	21.90	0.303	12.573	6.845	0.003	10.14	22.54
	Larga	0.68	0.27	19.51	0.05	9.29	56.13	22.95	0.032	5.171	2.008	0.008	2.15	1.05
	Gabata	0.31	0.36	8.08	0.20	26.57	25.79	23.95	0.003	0.030	0.052	0.0002	12.66	7.65
	Mosca	0.42	0.24	8.61	0.13	34.43	31.50	18.53	0.021	0.342	0.488	0.005	1.72	2.46

c. Factors controlling the algal-bacterial interaction in 2005

The observed variability of PP_P of lakes during 2005 was explained by sestonic P (61.3% of variance; Table 7), according to the characteristic P limitation of the lakes (mean seston N:P ratio = 44.13). By contrast, water T, UV mean irradiance at 305 nm wavelength received throughout the water column (Im_{305}), and the ratios between Im_{305} and T (Im_{305}:T) or Im_{305} and total P (I_{m305}:total P), failed to explain the PP_P during 2005 (Fig. 15a,b).

HBP was explained by Chl *a* (44% of variance), I_{m305} (32.9%) and total dissolved P (19.2%; Table 7). The single regression assessing the C control on HBP showed a significant positive relation between EOC *vs*. HBP (Fig. 16c; $r^2 = 0.44$; β-slope = 0.662; $p < 0.05$), and dissolved organic carbon *vs*. HPB ($r^2 = 0.76$; β-slope = 0.873; $p < 0.05$); this appears to indicate that the C-control of HBP is exerted mainly by allochthonous C.

Table 7. Multiple stepwise regression for primary production (PPP), bacterivory (%BV) and bacterial production (HBP) in 2005 and 2015 (independent variables included in the table are only those which are statistically significant).

Dependent variable	**Independent variable**	**n**	**Beta**	**Multiple R^2**	**R^2 exchange**	***p***
PP_P 2005	Sestonic P	14	0.783	0.613	0.613	0.003
PP_P 2015	T	13	0.869	0.755	0.755	<0.001
HBP 2005	Chl *a*	14	0.899	0.440	0.440	0.013
	I_{m305}		0.693	0.961	0.329	<0.001
	TDP		0.798	0.632	0.192	0.045
HBP 2015	TPP	13	0.580	0.706	0.706	<0.001
	TP		0.513	0.902	0.196	0.001
%BV 2005	Sestonic N:P	14	0.780	0.608	0.608	0.003
%BV 2015	Sestonic N:P	13	0.515	0.405	0.405	0.002
	Chl *a*		-0.561	0.795	0.389	<0.001
	I_{m320}/TP		0.362	0.906	0.112	0.015

The %BV was explained by seston N:P (60.8%, $p < 0.05$, Table 7), suggesting that bacterivory was predominant in lakes with P impoverished seston. The single regression assessing the abiotic control (UVR, total dissolved P, and water T) on the %BV showed a positive relation between I_{m305}: total dissolved P *vs*. %BV ($r^2 = 0.39$; $p < 0.05$) but negative between I_{mPAR}:T *vs*. %BV ($r^2 = 0.38$; $p < 0.05$; Fig. 15c,d).

The high BV rates found for this year were reflected in a negative exponential relation ($r^2 = 0.34$; $p < 0.05$) between HBP and %BV, suggesting a bacterivory control of algae on bacteria (Fig. 16a). Moreover, the lack of positive relationship between bacterial abundance and HBP ($p > 0.05$; Fig. 16b) is consistent with a top-down control.

d. Factors controlling the algal-bacterial interaction in 2015

In 2015, water T explained the PP_P variance (75.5%, Table 7) and their relation was direct. Also, in contrast to 2005, the single regression assessing the abiotic control showed an exponential negative relation between I_{m305}:T or I_{m305}: total P and PP_P (Fig. 15e,f), according to a negative relation of I_{m305}, but positive of P (Fig. S8) or T on PP_P (Table 7).

Total primary production (TPP) and total P explained 70.6% and 19.6% of HBP variance, respectively (Table 7). The high relation between TPP and HBP is consistent with a significant direct C control between EOC and HBP, but not dissolved organic carbon (Fig. 16c,d). These findings support the contention that EOC rather than dissolved organic carbon controlled bacterial growth (bottom-up control; Fig. 16c,d), suggesting a reinforcement of the algal-bacterial commensalism in 2015.

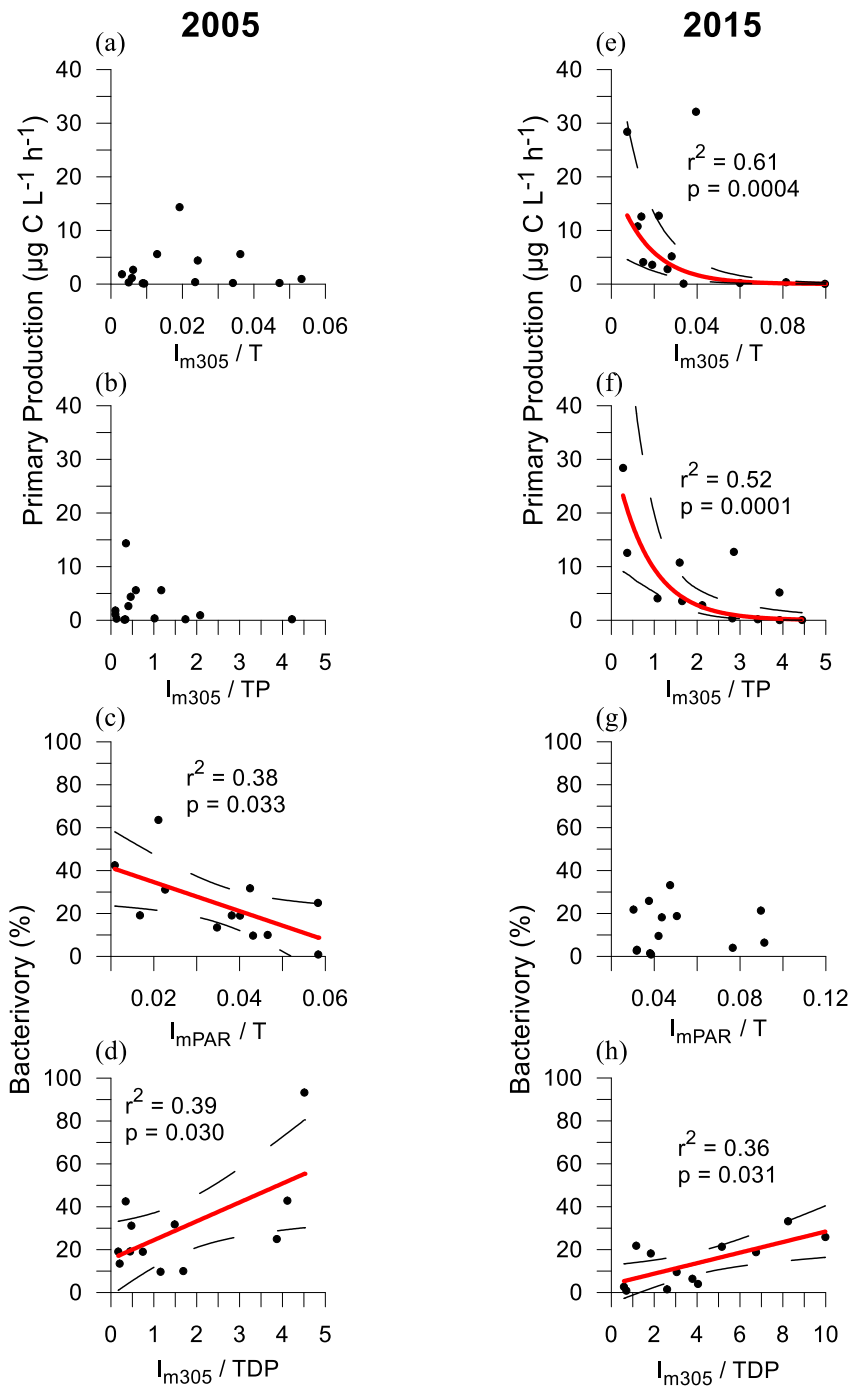

Figure 15. Response of PPP and BV rate to abiotic factors (Im305:T, Im305:Total P (TP), ImPAR:T and Im305:Total dissolved P (TDP)) in Sierra Nevada Lakes in 2005 (left panel) and 2015 (right panel). Regression line, correlation coefficient (r2) and p value are represented only for years with a significant relationship.

Sestonic N:P ratio and I_{m320}: total P were positively related to %BV, explaining 40.5% and 11.2% of %BV variance, respectively (Table 7, see also Fig. 15h), and Chl *a* was negatively related to %BV, explaining 38.9% of %BV variance (Table 7). These findings indicate that greater P availability among lakes simultaneously stimulated the Chl *a* concentration and weakened bacterivory.

The low %BV values found in 2015 (Fig. 14) together to the absence of bacterivory control between HBP and %BV (Fig. 16a) and a significant positive relationship ($r^2 = 0.63$; $p < 0.05$) between bacterial abundance and HBP (Fig. 16b), consistently suggest a weak consumption of bacteria by the algae.

4. Discussion

The main finding of our study was a shift in the nature of the interaction between algae and bacteria in high-mountain lakes of Sierra Nevada in 2005 and 2015, with a consistent and greater predominance of autotrophic metabolism in 2015 supported by an increase in the PP_P, and with the reinforcement of commensalistic algal-bacterial interaction against the weakening of bacterivory control (Fig. 17). This supports our hypothesis and highlights that temperature increase and a dustier world (Mahowald *et al*., 2007) like observed in 2015, can alter the functioning of high mountain lakes where BV rates strongly regulate the dynamics and structure of the microbial community.

The BV rate was altered in the two years of our analysis. In 2005, the predatory control by bacterivores rose to some 30%, this becoming a characteristic feature of the high-mountain lakes of Sierra Nevada. This feature is supported by predominance of mixotrophic organisms in Sierra Nevada lakes (Medina-Sánchez *et al*., 2004; Carrillo *et al*., 2006).

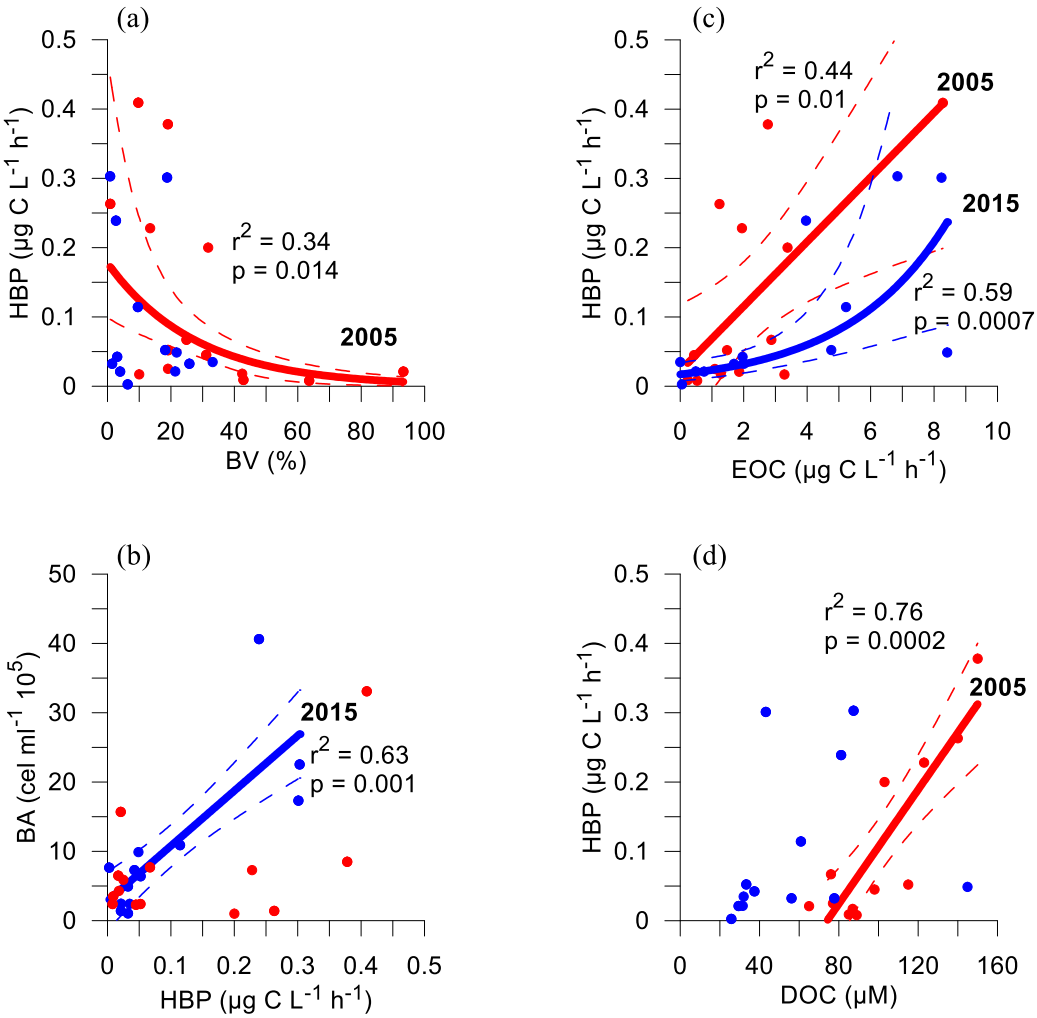

Figure 16. Relationship between Bacterial Production (HBP) and % bacterivory (%BV) (a), bacterial abundance (BA) (b), Excreted Organic Carbon (EOC) (c), and Dissolved Organic Carbon (DOC) (d). Data for 2005 and 2015 are represented in red and blue, respectively. Regression line, correlation coefficient (r^2) and p value are represented only for years with a significant relationship.

Field studies have revealed that mixotrophic algae are often numerically dominant in freshwater systems and can exert greater grazing impact on the bacterial community than can heterotrophic phagotrophs (Domaizon *et al.*, 2003; Carrillo *et al.*, 2017). Concretely, in 2005 the bacterivory of mixotrophs could constitute an advantageous nutritional mode against strict metabolisms under the typically

low P concentration of Sierra Nevada Lakes (see Table 7) (Medina-Sánchez *et al*., 2013; Cabrerizo *et al*., 2017) as has also been observed in other lakes with low P values (Winder & Sommer, 2012; Princiotta *et al*., 2016). In addition, the fact that %BV was positively correlated to I_{m305}:Total dissolved P ratio supports the idea that mixotrophy is an adaptive strategy to low P levels and also high UVR levels (Modenutti, 2014; Carrillo *et al*., 2017). The great adaptation of mixotrophs to high light intensity could be related with its capacity to grow as photoheterotrophs (Wilken *et al*., 2014), reducing the costs of investment in photoprotective mechanisms for photosystem II. Several studies have demonstrated increased grazing rates by mixotrophs in the epilimnion under high irradiance levels (Medina-Sánchez *et al*., 2004; Ptacnik *et al*., 2016). The reported adaptation of mixotrophs to low nutrient conditions (Modenutti, 2014; Unrein *et al*., 2014) is supported by loss of mixotrophs after a strong P-pulse as has been demonstrated experimentally in Sierra Nevada lakes (Medina-Sánchez *et al*., 2013; Cabrerizo *et al*., 2017) , in Andean lakes (Carrillo *et al*., 2017), in tropical and temperate lakes (Pålsson & Granéli, 2004), and in the laboratory (Urabe *et al*., 1999) as well as through studies of gradients of increasing trophic state (Saad *et al*., 2016).

In fact, in 2015, the %BV fell as much as 12.85% (Fig. 14) as the dust input intensified (Fig. 12), the sestonic N:P ratio diminished (Table 6), and concomitantly mixotrophs represented only 19.3% of the algae community as opposed to 61% of strict autotrophs in the ensemble of lakes (Fig. S9). The %BV reduction implied a weakening in bacterivory control with respect to 2005 (Fig. 16a), which was corroborated by a bacterial abundance:HBP coupling in 2015 (Fig. 16b). In this sense, in a coastal upwelling, it has been reported that when bacterial mortality by predation is low, all HBP can be converted into BA, and conversely, the absence of a bacterial abundance:HBP coupling is indicative of a strong bacterivory control (Teira *et al*., 2015).

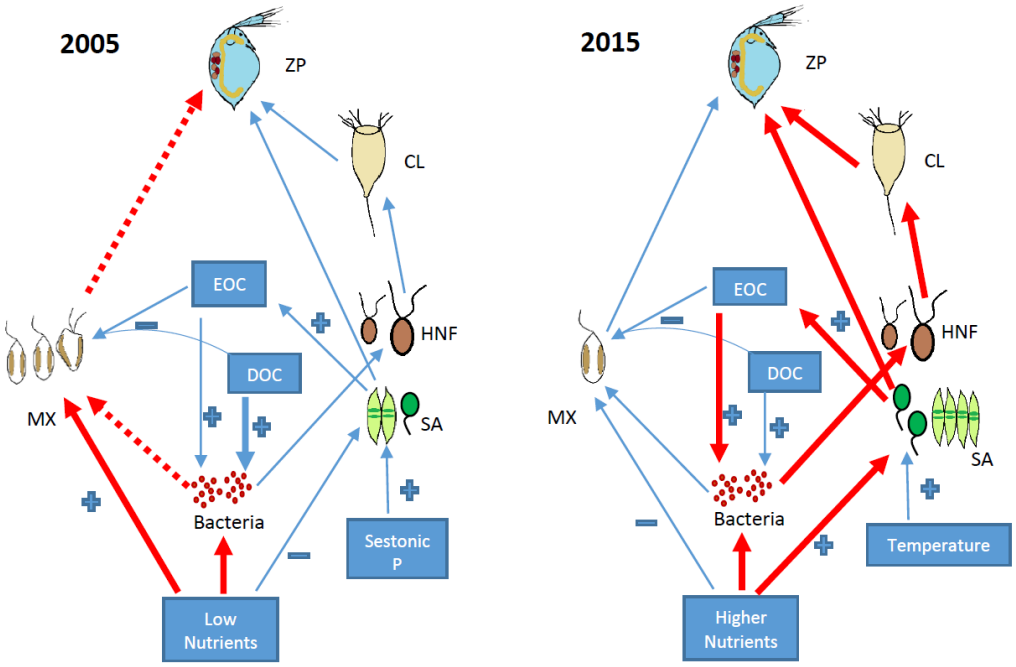

Figure 17. Scheme of the functional regulation of the trophic web in high mountain lakes in 2005 and 2015. Red and blue lines represent the type of interaction that is reinforced and diminished, respectively. Red dashed lines represent the C-bypass. ZP: zooplankton, CL: ciliates, HNF: heterotrophic nanoflagellates, SA: strict autotrophs, MX: mixotrophs, EOC: Excreted Organic Carbon, DOC: Dissolved Organic Carbon.

Contrary to 2005, in 2015 the predominant algal-bacterial interaction was commensalism, led by higher PP_P (and Chl *a*) (Fig. 14). The PP_P was triggered mainly by water T (Table 7) concomitantly with an increasing trend in aerosol dust intensity and air T on Sierra Nevada from 1980 to 2015 (Fig. 12). It is known that P, Fe, and other limiting nutrients contained in aerosol dust affect the phytoplankton physiology (Jickells & Moore, 2015) and enhance PP_P of lakes (Cabrerizo *et al*., 2017) and coast (Giovagnetti *et al*., 2013). The greater aerosol dust inputs to Sierra Nevada during the recent years of our study translated into a lower mean N:P ratio in 2015 and a lower percentage of lakes with a N:P ratio higher than 30 (see Results and Table 6), indicating P incorporation into seston,

as also observed in previous studies (Villar-Argáiz *et al*., 2002). The positive effect of nutrient-rich dust input in autotrophy could be enhanced by a stimulatory effect of T on phytoplankton photosynthetic yield (Takahashi *et al*., 2013) and an attenuation of UVR inhibition on autotrophs (Sobrino & Neale, 2007). Furthermore, rising T favoured the dominance of strictly autotrophic phytoplankton taxa, such as Chlorophyta (Rasconi *et al*., 2017).

Supporting the advantage of strict autotrophy after greater aerosol inputs and higher water T, we observed an EOC increase proposed as a protective mechanism to prevent the photosystem damage under high light irradiance (Carrillo *et al*., 2002; Carrillo *et al*., 2008). Furthermore, the EOC increase determined a reinforcement of commensalistic algal-bacterial interaction, since EOC was the main C source regulating HBP in 2015 whereas dissolved organic carbon was the source in 2005 (Fig. 16c,d and Fig. 17). In agreement with our results, an experiment in marine waters (Fouilland *et al*., 2014) showed that the direct C coupling between bacteria and phytoplankton exudates was greatest when the nutrient concentration was higher and grazing was lower, coinciding with a predominance of small autotrophic cells as the main components of the phytoplankton community.

6. Conclusions

The high UVR-adaptation of the algae inhabiting high-mountain lakes together with the rising water T and greater nutrient inputs linked to dust deposition that occurred in 2015 shifted the predominant algal-bacterial interaction from bacterivory to commensalism (Crane & Grover, 2010). While we cannot establish a consolidated trend from our study, it is true that the projections of the climatic change for the present century could be more similar to those conditions that occurred in 2015. Thus, the loss of a functional trait such as mixotrophy in high-mountain lakes could deteriorate the functional biodiversity (Delgado-Molina *et*

al., 2009; Carrillo *et al*., 2017) and biogeochemistry of these remote and fragile ecosystems, by altering processes such as C and nutrient cycles due to the disconnection between the microbial loop and higher trophic levels. Thus, the decrease in mixotrophs is expected to weaken the C bypass towards the grazing chain of the lakes (Ptacnik *et al*., 2016; Carrillo *et al*., 2017) , promoting the development of heterotrophic microbial food web and diminishing the energy-transfer efficiency due to a greater number of links (Fig. 17) (Medina-Sánchez *et al*., 2004; Ward & Follows, 2016).

References

Acker, J. G. & Leptoukh, G. (2007). Online analysis enhance NASA Earth science data. *EOS, Trans. AGU.* 88: 14–17

Amin, S. A. *et al*. (2015). Interaction and signalling between a cosmopolitan phytoplankton and associated bacteria. *Nature.* 522: 7554

Aota, Y. & Nakajima, H. (2001). Mutualistic relationships between phytoplankton and bacteria caused by carbon excretion from phytoplankton. *Ecol. Res.* 16: 289–299

APHA. (1992). *Standard methods for the examination of water and wastewater* (American Public Health Association)

Battarbee, R. W. *et al*. (2002). Comparing palaeolimnological and instrumental evidence of climate change for remote mountain lakes over the last 200 years. *J. Paleolimnol.* 28: 161–179

Belkin, I. M. (2009). Rapid warming of large marine ecosystems. *Prog. Oceanogr.* 81: 207–213

Bell, T. B., Ahlgren, G. M. & Ahlgren, I. (1983). Estimating bacterioplankton production by measuring 3H-thymidine incorporation in a eutrophic Swedish lake. *Appl. environ. Microbiol.* 45: 1709–1721

Cabrerizo, M. J., Medina-Sánchez, J. M., Dorado-García, I., Villar-Argaiz, M. & Carrillo, P. (2017). Rising nutrient-pulse frequency and high UVR strengthen microbial interactions. *Sci. Rep.* 7: 43615

Carrillo, P., Delgado-Molina, J. A., Medina-Sánchez, J. M., Bullejos, F. J. & Villar-Argaiz, M. (2008). Phosphorus inputs unmask negative effects of ultraviolet radiation on algae in a high mountain lake. *Glob. Change Biol.* 14: 423–439

Carrillo, P., Medina-Sánchez, J. M. & Villar-Argaiz, M. (2002). The interaction of phytoplankton and bacteria in a high mountain lake: Importance of the spectral composition of solar radiation. *Limnol. Oceanogr.* 47(5): 1294–1306

Carrillo, P., Medina-Sánchez, J. M., Villar-Argaiz, M., Bullejos, F. J., Durán, C., Bastidas-Navarro, M., Souza, M. S., Balseiro, E. G. & Modenutti, B. E. (2017). Vulnerability of mixotrophic algae to nutrient pulses and UVR in an oligotrophic Southern and Northern Hemisphere lake. *Sci. Rep.* 7: 6333

Carrillo, P., Medina-Sánchez, J. M., Villar-Argaiz, M., Delgado-Molina, J. A. & Bullejos, F. J. (2006). Complex interactions in microbial food webs: Stoichiometric and functional approaches. *Limnetica.* 25: 189–204

Chen, B. & Laws, E. A. (2017). Is there a difference of temperature sensitivity between marine phytoplankton and heterotrophs? *Limnol. Oceanogr.* 62: 806–817

Cho, D.-H. *et al*. (2015). Enhancing microalgal biomass productivity by engineering a microalgal–bacterial community. *Bioresour. Technol.* 175: 578–585

Crane, K. W. & Grover, J. P. (2010). Coexistence of mixotrophs, autotrophs, and heterotrophs in planktonic microbial communities. *J. Theoret. Biol.* 262: 517–527

Cruz-López, R. & Maske, H. (2016). The vitamin B1 and B12 required by the marine dinoflagellate Lingulodinium polyedrum can be provided by its associated bacterial community in culture. *Front. Microbiol.* 7: 560

De la Paz, D. *et al*. (2013). Modelling Saharan dust transport into the Mediterranean basin with CMAQ. *Atmos. Environ.* 70: 337–350

Delgado-Molina, J. A., Carrillo, P., Medina-Sánchez, J. M., Villar-Argáiz, M. & Bullejos, F. J. (2009). Interactive effects of phosphorus loads and ambient ultraviolet radiation on the algal community in a high-mountain lake. *J. Plankton Res.* 31(6): 619–634

Domaizon, I., Viboud, S. & Fontvieille, D. (2003). Taxon-specific and seasonal variations in flagellates grazing on heterotrophic bacteria in the oligotrophic Lake Annecy - importance of mixotrophy. *FEMS Microbiol. Ecol.* 46: 317–329

Durán, C., Medina-Sánchez, J. M., Herrera, G. & Carrillo, P. (2016). Changes in the phytoplankton-bacteria coupling triggered by joint action of UVR, nutrients, and warming in Mediterranean high-mountain lakes. *Limnol. Oceanogr.* 61: 413–429

Fouilland, E. *et al*. (2014). Bacterial carbon dependence on freshly produced phytoplankton exudates under different nutrient availability and grazing pressure conditions in coastal marine waters. *FEMS Microbiol. Ecol.* 87: 757–769

Fuhrman, J. A. & Azam, F. (1982). Thymidine incorporation as a measure of heterotrophic bacterioplankton production in marine surface waters: evaluation and field results. *Mar. Biol.* 66: 109–120

Gao, K., Helbling, E. W., Häder, D.-P. & Hutchins, D. A. (2012). Responses of marine primary producers to interactions between ocean acidification, solar radiation, and warming. *Mar. Ecol. Prog. Ser.* 470: 167–189

Giovagnetti, V., Brunet, C., Conversano, F., Tramontano, F., Obernosterer, I., Ridame, C. & Guieu, C. (2013). Assessing the role of dust deposition on phytoplankton ecophysiology and succession in a low-nutrient lowchlorophyll ecosystem: A mesocosm experiment in the Mediterranean Sea. *Biogeosciences.* 10: 2973–2991

Gu, L. Y. & Wyatt, K. H. (2016). Light availability regulates the response of algae and heterotrophic bacteria to elevated nutrient levels and warming in a northern boreal peatland. *Freshwater Biol.* 61: 1442–1453

Gurung, T. B., Nakanishi, M. & Urabe, J. (1999). Regulation of the relationship between phytoplankton Scenedesmus acutus and heterotrophic bacteria by the balance of light and nutrients. *Aquat. Microb. Ecol.* 17: 27–35

Häder, D.-P., Williamson, C. E., Wängberg, S. Å., Rautio, M., Rose, K. C., Gao, K., Helbling, E. W., Sinha, R. P. & Worrest, R. (2015). Effects of UV radiation on aquatic ecosystems and interactions with other environmental factors. *Photochem. Photobiol. Sci.* 14: 108–126

Hartmann, M., Grob, C., Tarran, G. E., Martin, A. P., Burkill, P. H., Scanlan, D. J. & Zubkov, M. V. (2012). Mixotrophic basis of Atlantic oligotrophic ecosystems. *Proc. Natl. Acad. Sci. USA.* 109: 5756–5760

Jeffrey, S. W. & Humphrey, G. F. (1975). New spectrophotometric equations for determining chlorophylls a, b, c1 and c2 in higher plants, algae and natural phytoplankton. *Biochem. Physiol. Pflanz.* 167: 191–194

Jickells, T. D. & Moore, C. M. (2015). The importance of atmospheric deposition for ocean productivity. *Ann. Rev. Ecol. Evol. Syst.* 46: 481–501

Korbee, N., Carrillo, P., Mata, M. T., Rosillo, S., Medina-Sánchez, J. M. & Figueroa, F. L. (2012). Effects of ultraviolet radiation and nutrients on the structure–function of phytoplankton in a high mountain lake. *Photochem. Photobiol. Sci.* 11: 1087–1098

Lee, S. & Fuhrman, J. A. (1987). Relationships between biovolume and biomass of naturally derived marine bacterioplankton. *Appl. Environ. Microb.* 53: 1298–1303

Lignell, R. (1992). Problems in filtration fractionation of 14C primary productivity samples. *Limnol. Oceanogr.* 37: 172–178

Lindehoff, E., Granéli, E. & Glibert, P. M. (2011). Nitrogen uptake kinetics of Prymnesium parvum (Haptophyte). *Harmful Algae* 12: 70–76

Mahowald, N. M., Ballantine, J. A., Feddema, J. & Ramankutty, N. (2007). Global trends in visibility: implications for dust sources. *Atmos. Chem. Phys.* 7(12): 3309–3339

Medina-Sánchez, J. M., Delgado-Molina, J. A., Bratbak, G., Bullejos, F. J. & Carrillo, P. (2013). Maximum in the middle: Nonlinear response of microbial plankton to ultraviolet radiation and phosphorus. *PLoS One.* 8: e60223

Medina-Sánchez, J. M., Villar-Argaiz, M. & Carrillo, P. (2002). Modulation of the bacterial response to spectral solar radiation by algae and limiting nutrients. *Freshwater Biol.* 47: 2191–2204

Medina-Sánchez, J. M., Villar-Argaiz, M. & Carrillo, P. (2004). Neither with nor without you: A complex algal control on bacterioplankton in a high mountain lake. *Limnol. Oceanogr.* 49: 1722–1733

Modenutti, B. (2014). Mixotrophy in Argentina freshwaters. *Advanc. Limnol.* 65: 359–374

Morales-Baquero, R., Pulido-Villena, E. & Reche, I. (2006). Atmospheric inputs of phosphorus and nitrogen to the southwest Mediterranean region: Biogeochemical responses of high mountain lakes. *Limnol. Oceanogr.* 51: 830–837

Pålsson, C. & Granéli, W. (2004). Nutrient limitation of autotrophic and mixotrophic phytoplankton in a temperate and tropical humic lake gradient. *J Plankton Res.* 26(9): 1005–14

Paver, S. F. & Kent, A. D. (2017). Direct and context-dependent effects of light, temperature, and phytoplankton shape bacterial community composition. *Ecosphere.* 8(9): e01948

Pepin, N. *et al*. (2015). Elevation-dependent warming in mountain regions of the world. *Nat. Clim. Change.* 5: 424e430

Princiotta, S. D., Smith, B. & Sanders, R. W. (2016). Temperature-dependent phagotrophy and phototrophy in a mixotrophic chrysophyte. *J. Phycol.* 52: 432–440

Ptacnik, R. *et al*. (2016). A light-induced shortcut in the planktonic microbial loop. *Sci. Rep.* 6: 29286

Ramanan, R., Byung-Hyuk, K., Dae-Hyun, C., Hee-Mock, O. & Hee-Sik, K. (2016). Algae bacteria interactions: Evolution, ecology and emerging applications. *Biotechnol. Adv.* 34: 14–29

Rasconi, S., Winter, K. & Kainz, M. J. (2017). Temperature increase and fluctuation induc phytoplankton biodiversity loss – Evidence from a multi-seasonal mesocosm experiment. *Ecol. Evol.* 00: 1–11

Saad, J. F., Unrein, F., Tribelli, P. M., López, N. & Izaguirre, I. (2016). Influence of lake trophic conditions on the dominant mixotrophic algal assemblages. *J. Plankton Res.* 00(00), 1–12

Sarmento, H. & Gasol, J. M. (2012). Use of phytoplankton-derived dissolved organic carbon by different types of bacterioplankton. *Environ. Microbiol.* 14(9): 2348–60

Seymour, J. R., Amin, S. A., Raina, J. B. & Stocker, R. (2017). Zooming in on the phycosphere: the ecological interface for phytoplankton–bacteria relationships. *Nat. Microbiol.* 2: 17065

Simon, M., Byung, C. C. & Azam, F. (1992). Significance of bacterial biomass in lakes and the ocean: comparison to phytoplankton biomass and biogeochemical implications. *Mar. Ecol. Prog. Ser.* 86: 103–110

Sobrino, C. & Neale, P. J. (2007). Short-term and long-term effects of temperature on photosynthesis in the diatom Thalassiosira pseudonana under UVR exposures. *J. Phycol.* 43: 426–436

Steemann Nielsen, E. (1952). The use of radio-active carbon (C14) for measuring organic production in the sea. *J. Cons. Perm. Int. Explor. Mer.* 18: 117–140

Su, X., Steinman, A. D., Xue, Q., Zhao, Y., Tang, X. & Xie, L. (2017). Temporal patterns of phyto- and bacterioplankton and their relationships with environmental factors in Lake Taihu, China. *Chemosphere.* 184: 299e308

Takahashi, S., Yoshioka-Nishimura, M., Nanba, D. & Badger, M. R. (2013). Thermal acclimation of the symbiotic alga Symbiodinium spp. alleviates photobleaching under heat stress. *Plant Physiol.* 161: 477–485

Talbot, R. W., Harriss, R. C., Browell, E. V., Gregory, G. L., Sebacher, D. I. & Beck, S. M. (1986). Distribution and geochemistry of aerosols in the tropical North Atlantic Troposphere: Relationship to Saharan Dust. *J. Geophys. Res.-Atmos.* 91: 5173–5182

Teira, E., Hernando-Morales, V., Fernández, A., Martínez-García, S., Álvarez-Salgado, X. A., Bode, A. & Varela, M. M. (2015). Local differences in phytoplankton−bacterioplankton coupling in the coastal upwelling off Galicia (NW Spain). *Mar. Ecol. Prog. Ser.* 528: 53–69

Thompson, A. W., Foster, R. A., Krupke, A., Carter, B. J., Musat, N., Vaulot, D., Kuypers, M. M. & Zehr, J. P. (2012). Unicellular cyanobacterium symbiotic with a single-celled eukaryotic alga. *Science.* 337: 1546–1550

Unrein, F., Gasol, J. M., Not, F., Forn, I. & Massana, R. (2014). Mixotrophic haptophytes are key bacteral grazers in oligotrophic coastal waters. *ISME J.* 8: 164–176

Urabe, J., Gudur, T. B. & Yoshida, T. (1999). Effects of phosphorus supply on phagotrophy by the mixotrophic alga *Uroglena Americana* (Chrysophyceae). *Aquat. Microb. Ecol.* 18: 77–83

Villar-Argaiz, M., Medina-Sánchez, J. M. & Carrillo, P. (2001). Inter- and intra-annual variability in the phytoplankton community of a high mountain lake: the influence of external (atmospheric) and internal (recycled) sources of P. *Freshwat. Biol* 46: 1017–1024

Villar-Argaiz, M., Medina-Sánchez, J. M. & Carrillo, P. (2002). Microbial plankton response to contrasting climatic conditions: insights from community structure, productivity and fraction stoichiometry. *Aquat. Microb. Ecol.* 29: 253–266

Wang, Q., Fan, X. & Wang, M. (2014). Recent warming amplification over high elevation regions across the globe. *Clim. Dynam.* 43: 87–101

Ward, B. A. & Follows, M. J. (2016). Marine mixotrophy increases trophic transfer efficiency, mean organism size, and vertical carbon flux. *PNAS.* 113(11): 2958–63

Weckström, K., Weckström, J., Huber, K., Kamenik, C., Schmidt, R., Salvenmoser, W., Rieradevall, M., Weisse, T., Psenner, R. & Kurmayer, R. (2016). Impacts of climate warming on Alpine lake biota over the past decade. *Arct. Antarct. Alp. Res.* 48(2): 361–376

Wilken, S., Huisman, J., Naus-Wiezer, S. & Van Donk, E. (2013). Mixotrophic organisms become more heterotrophic with rising temperature. *Ecol Lett.* 16(2): 225–33

Wilken, S., Schuurmans, M. J. & Matthijs, H. C. P. (2014). Do mixotrophs grow as photoheterotrophs? Photophysiological acclimation of the chrysophyte *Ochromonas danica* after feeding. *New Phytol.* 204: 882–889

Winder, M. & Sommer, U. (2012). Phytoplankton response to a changing climate. *Hydrobiologia.* 698: 6–16

Xenopoulos, M. A. & Schindler, D. W. (2003). Differential responses to UVR by bacterioplankton and phytoplankton from the surface and the base of the mixed layer. *Freshwater Biol.* 48: 108–122

Yvon-Durocher, G., Jones, J. I., Trimmer, M., Woodward, G. & Montoya, J. M. (2010). Warming alters the metabolic balance of ecosystems. *Phil. Trans. R. Soc. B.* 365: 2117–2126

Zubkov, M. V. & Burkill, P. H. (2006). Syringe pumped high speed flowcytometry of oceanic phytoplankton. *Cytom A.* 69A: 1010–1019

Supplementary Information

This supplementary material contains the Figures from S6 to S9

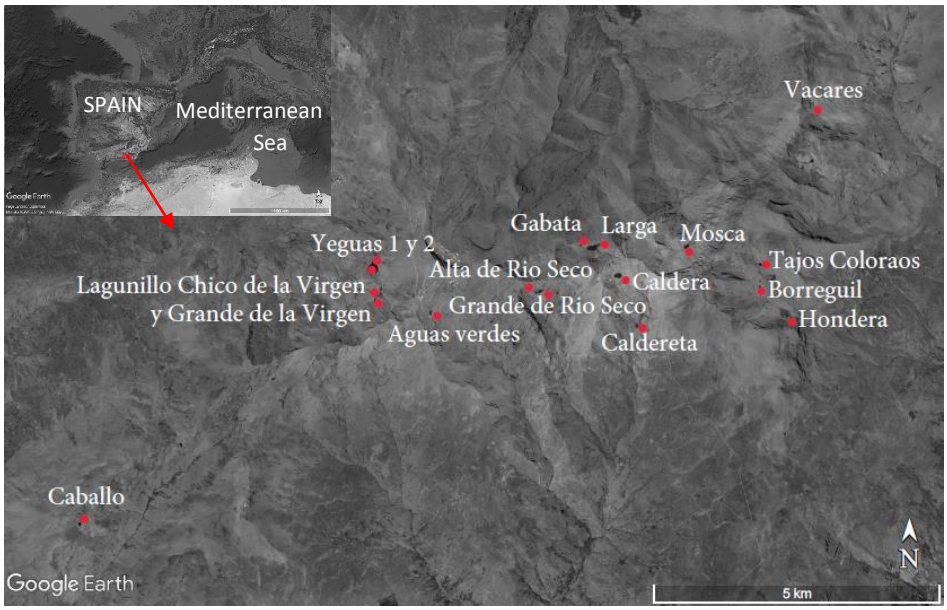

Figure S6. Location map of 17 Lakes of Sierra Nevada (southern Spain).

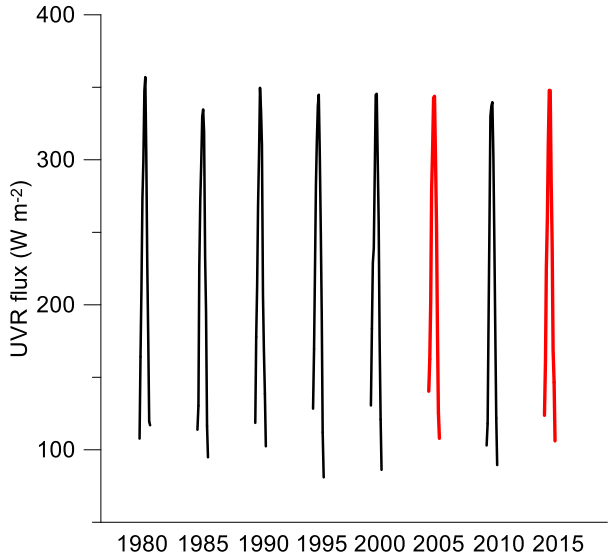

Figure S7. UVR flux incising on Sierra Nevada region (37°1', -3°23', 37°4', -3°17') for the period 1980 to 2015.

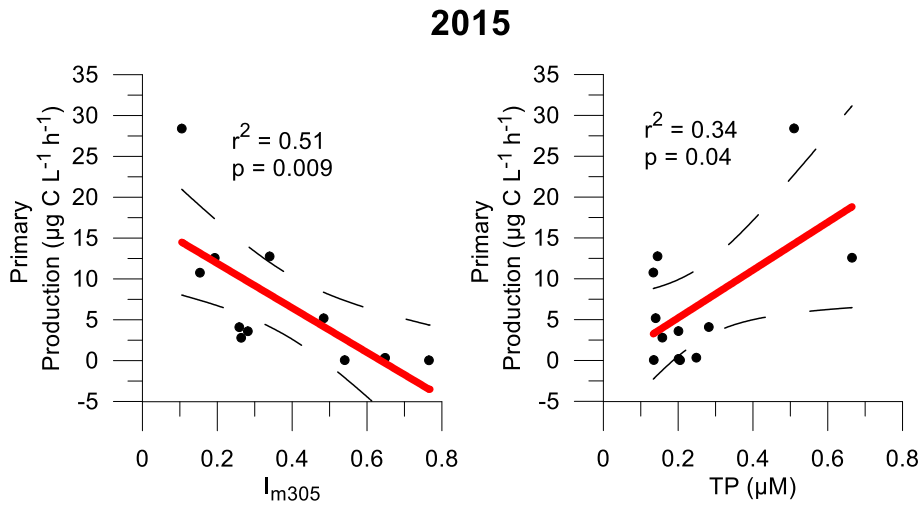

Figure S8. Response of PP_P to abiotic factors (I_{m305} and TP) in Sierra Nevada Lakes in 2015. Regression line, correlation coefficient (r^2) and p value are represented.

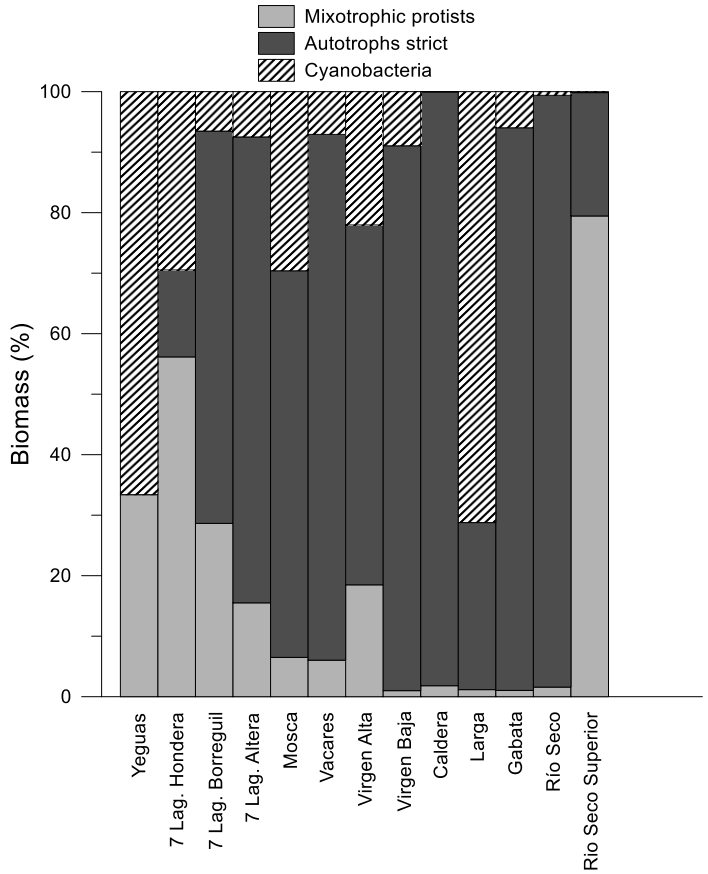

Figure S9. Biomass composition of Sierra Nevada lakes in July 2015.

CHAPTER 4

Mosca Lake

CHAPTER 4 - Testing the Metabolic Theory of Ecology on protists under fluctuating temperature and nutrient enrichment

J. M. González-Olalla, J. M. Medina-Sánchez and P. Carrillo

Abstract

The Metabolic Theory of Ecology (MTE) predicts that the temperature increases exert a common effect on organisms, stimulating metabolic rates and growth, this being stronger for a heterotrophic than for an autotrophic metabolism. However, no available studies within the framework of MTE have focused on organisms' response to fluctuating temperature or to this factor in interaction with others, such as nutrient availability. In this paper, we assess how nutrients alter the impact of increased temperature (+5ºC relative to control, *C*) or fluctuating temperature (±2.5ºC relative to increased temperature) on protist metabolism and species composition of a simplified community composed of a strict autotrophic species (*Monoraphidium minutum*) and a mixotrophic species (*Chromulina* sp.). Our hypothesis is that increased and fluctuating temperature will have a greater positive effect on heterotrophic metabolism and the mixotrophic species abundance, while interaction with nutrients will boost photosynthetic activity and the abundance of strict autotrophic species. Our results indicate that increased and fluctuating temperature stimulated all the metabolic rates, in agreement with the MTE. This stimulus was greater for the primary production (PP) rate under the increased-temperature treatment (in contrast to the MTE) and for the respiration (R) rate under fluctuating temperature (in agreement with the MTE). Only the fluctuating-temperature treatment stimulated *Chromulina* sp. and decreased *M. minutum* abundance. When nutrients were added, the interaction with increased or fluctuating temperature stimulated the PP and autotrophic species abundance against the heterotrophic metabolism and mixotrophic species abundance.

Remarkably, the responses observed demonstrated lower susceptibility of protists to global change and extreme events when nutrient concentrations increased. Our results indicate that a straight application of the MTE to protists does not hold under high nutrient conditions.

1. Introduction

Temperature is one of the vital factors that affect metabolism, growth rate, the spatial and temporal distribution, and the size structure of protist community (Sato *et al.*, 2015). At the end of the century, temperatures are predicted to rise by 1-5ºC (IPCC, 2013), this perhaps followed by an increase in the diel temperature variation (Zhang *et al.*, 2016), as well as frequency and intensity of daily temperature extremes (Bindoff *et al.*, 2013). Water temperature will follow this trend (Magnuson *et al.*, 1997), leading to alterations in the thermal regime of many aquatic habitats (Webb & Nobilis, 2007).

According to the Metabolic Theory of Ecology (MTE), a temperature increase is predicted to exert a common effect on all organisms, stimulating the metabolic rates (aerobic respiration, oxygenic photosynthesis, consumption, and growth; Brown *et al.*, 2004). This stimulus will be of greater magnitude for the heterotrophic than for the autotrophic metabolism, since photosynthesis is less temperature dependent than is respiration (Allen *et al.*, 2005; Rose & Caron, 2007). Therefore, heterotrophic organisms are expected to be favoured against strict autotrophs by this temperature trend (Yang *et al.*, 2016). Moreover, an increase in mean temperature will lead to a predominance of heterotrophic nutrition in mixotrophic organisms (Wilken *et al.*, 2013), i.e. those able to combine the autotrophic and heterotrophic metabolism within the same cell (Mitra *et al.*, 2014). The stimulatory effect at the metabolic level will be transferred to the level of organisms (Gillooly *et al.*, 2002), populations (Savage *et al.*, 2004), communities (Padfield *et al.*, 2017), and ecosystems (Anderson *et*

al., 2006; O'Connor & Bernhardt, 2018)**.** The warming impact associated with climate change on aquatic environments has previously been studied through a change in mean temperature (Parmesan & Yohe, 2003; Chen *et al.*, 2011). However, more attention has recently been paid to the effects of temperature fluctuations on metabolic processes (Zhang *et al.*, 2019) since different experiments show that fluctuating temperatures can exacerbate the effects of warming on species and communities (Paaijmans *et al.*, 2013; Gerhard *et al.*, 2019). Thus, if rising temperatures are accompanied by fluctuation and extreme temperature events, the result may be depressed quantum yield of photosystem II, net photosynthesis (Davison, 1991; Ojeda-Pérez *et al.*, 2017), and growth rate (Gerhard *et al.*, 2019).

These protist responses to temperature fluctuation are accompanied by shifts in the distribution and relative abundance of species, profoundly disrupting community structure and functioning (Vasseur & McCann, 2007) and thus leading to a less diverse community (Thomas *et al.*, 2012; Rasconi *et al.*, 2017). Thus, diel temperature fluctuations negatively affect the growth of autotrophs such as chlorophyta and diatoms (Zhang *et al.*, 2019), but no information is available concerning the effect on mixotrophic species.

Environmental fluctuation and its interaction with other global-change drivers have also been scarcely studied (Jentsch *et al.*, 2007; Smith, 2011). It is known that protist response to increased and/or fluctuating temperature is regulated by nutrient availability (Cross *et al.*, 2015; Marañón *et al.*, 2018; Verbeek *et al.*, 2018) and MTE models generally do not account for the effects of factors other than size and temperature on metabolic rate, such as resource availability (Allen & Gillooly, 2009). In a fluctuating environment, the effect size of temperature fluctuation may strongly vary depending on the nutritional context (Koussoroplis *et al.*, 2017; Gerhard *et al.*, 2019). Thus, nutrient limitation could lead to a lower

thermal tolerance of protists (Thomas *et al.*, 2017), and increased and/or fluctuating temperature may exacerbate the uncoupling of protist metabolism (respiration and photosynthesis) (Barton *et al.*, 2018). On the other hand, Marañón *et al.* (2018) reported that the stimulatory effect of rising temperatures on protists (higher metabolic rates) will result if nutrient availability is high, whereas under nutrient limitation, temperature would have a minor influence on protist metabolism (Marañón *et al.*, 2018) and growth rate (Calvo-Díaz *et al.*, 2014).

The impact of temperature and nutrient interaction on protist metabolism may in turn affect the abundance of phototrophs and mixotrophs. The two factors can interact positively on strict autotrophs (Pålsson & Granéli, 2004), accelerating their growth rate (Wojewodzic *et al.*, 2011), but negatively on mixotrophs. However, no studies are available concerning how daily fluctuating temperature combined with nutrient availability might affect metabolism of protists and the abundance of phototrophs and mixotrophs. This is a crucial topic in aquatic ecosystems because the relative proportion of mixotrophs can affect the C and nutrient fluxes in the grazing chain (Ptacnik *et al.*, 2016) as well as energy-transfer efficiency (Medina-Sánchez *et al.*, 2004; Ward & Follows, 2016).

Given the above scenario, we designed an experimental study within MTE framework, using two protists species: *Monoraphidium minutum* and *Chromulina* sp., genera being typical of Sierra Nevada high-mountain lakes (southern Spain). The first organism is a strict autotrophic species, whereas the second has been previously demonstrated to be able to prey on bacteria and thus grow as a mixotroph (Medina-Sánchez *et al.*, 2004; González-Olalla *et al.*, 2019). In this study, we test the following i) whether metabolic rates of protist species are stimulated by higher temperatures and diminished by temperature fluctuation; ii) whether these responses favour the heterotrophic metabolism and mixotroph development; iii) and whether nutrient enrichment influences the temperature-

driven responses, favouring autotrophy. To address these issues, we experimentally measured changes in structural variables (abundance and growth rate) and metabolic rates (primary production [PP], bacterivory [BV] and respiration [R]) of a simplified community composed of the two protists species under different temperature regimes and nutrient conditions.

2. Material and Methods

a. Species and culture conditions

The protist species used in this experiment were *Monoraphidium minutum* (kindly provided by professor Pedro M. Sánchez-Castillo, University of Granada*)* and *Chromulina* sp. (CCAC, Culture collection of Algae at the University of Cologne, Germany). Both were cultured separately in diluted SF medium (Synthetic Freshwater Medium; CCAC, Germany; SFM/16), which had a P concentration of 25 µg P L^{-1}. Prior to the experiment, the maximum growth rate was determined and non-axenic cultures were maintained at this phase by applying a corresponding dilution rate for at least 5 generations. The maximum growth rate was calculated from the cell counts using the equation explained in the section on biological parameters.

During the growing and acclimation period at 19ºC, both species were exposed to ~100 µmol photon m^{-2} s^{-1} of photosynthetically active radiation (PAR, 400-700 nm) under a 12:12 h photoperiod (Fig. 18).

b. Experimental set-up

For the experiment, a two-species assemblage consisted of a strict autotroph *M. minutum,* and a mixotrophic species *Chromulina* sp., mixing 1.5×10^5 cell mL^{-1} for each species (showing *Chromulina* sp. a biomass content 4-fold higher than *M. minutum*; 41.17 vs. 10.53 pg C $cell^{-1}$). However, similar abundance of the species in the assemblage was used for two reasons: i) to ensure that metabolic

responses would not be biased by different initial cell concentrations; ii) the cell concentration for both species would be in the exponential growth phase, so that the results would not be swayed by species growing at different stages. Then, 18 quartz flasks of 500 mL each were filled and placed in an aquarium system with adjustable temperature by refrigeration (Teco® S. R. L. tank TK 2000, EU) and with radiation from light-emitting diode lamps (nano LED light v.2.0, BLAU aquaristic) for PAR. The inability of *M. minutum* and the ability of *Chromulina* sp. to prey on bacteria was previously tested in the laboratory.

For an assessment of the combined impact of T and nutrient supply, a 3×2 full factorial experimental design (in triplicate) was implemented with: a) three temperature treatments: *control* at 19ºC (hereafter "*C*" treatment), *increased temperature* at 24ºC (hereafter "*iT*" treatment) and *fluctuating temperature* at 24±2.5ºC (hereafter "*fluT*" treatment); and b) two nutrient treatments, ambient (SFM/16) vs. nutrient enrichment (SFM/16 + N and P; hereafter "NUT"; see Fig. 18). Therefore, six treatments were used: *C*, C_{NUT}, *iT*, iT_{NUT}, *fluT*, and $fluT_{NUT}$. The 5ºC temperature increase lies within the range predicted by IPCC for the late 21st century climate (IPCC, 2013, Scenario RCP8.5). The NP enrichment, performed by adding 168.58 ug L^{-1} of K_2HPO_4 and 1.316 mg L^{-1} of $NaNO_3$, was intended to recreate a realistic input of P (30 µg P L^{-1}, adjusted to Redfield ratio [molar N:P=16:1] to avoid N limitation) from Saharan dust deposited onto lake surfaces in the southern Iberian Peninsula (Villar-Argaiz *et al.*, 2002; Morales-Baquero *et al.*, 2006; Carrillo *et al.*, 2008), where both species of organisms are typically found.

The water temperature in all the aquariums was controlled by a computerized system, and flasks were exposed to irradiance of 100 µmol photon m^2 s^{-1} of PAR under a photoperiod of 12 h light:12 h dark for 9 days. For the *fluT* treatments, each period shift of 2.5ºC of amplitude lasted 12 h, the lowest and the highest

temperature coinciding with the end of the dark period and at the middle of light period, respectively. The design of *fluT* treatments were not meant to mimic temperature variation in natural environment, but to contrast stable vs. fluctuating conditions on protists and thereby test their acclimation ability. Nevertheless, the fluctuation range used in this experiment (±2.5ºC) is not unusual given that the temperature regime registered in other freshwater environments can exceed 5ºC (Jacobs *et al.*, 2008; Woolway *et al.*, 2016).

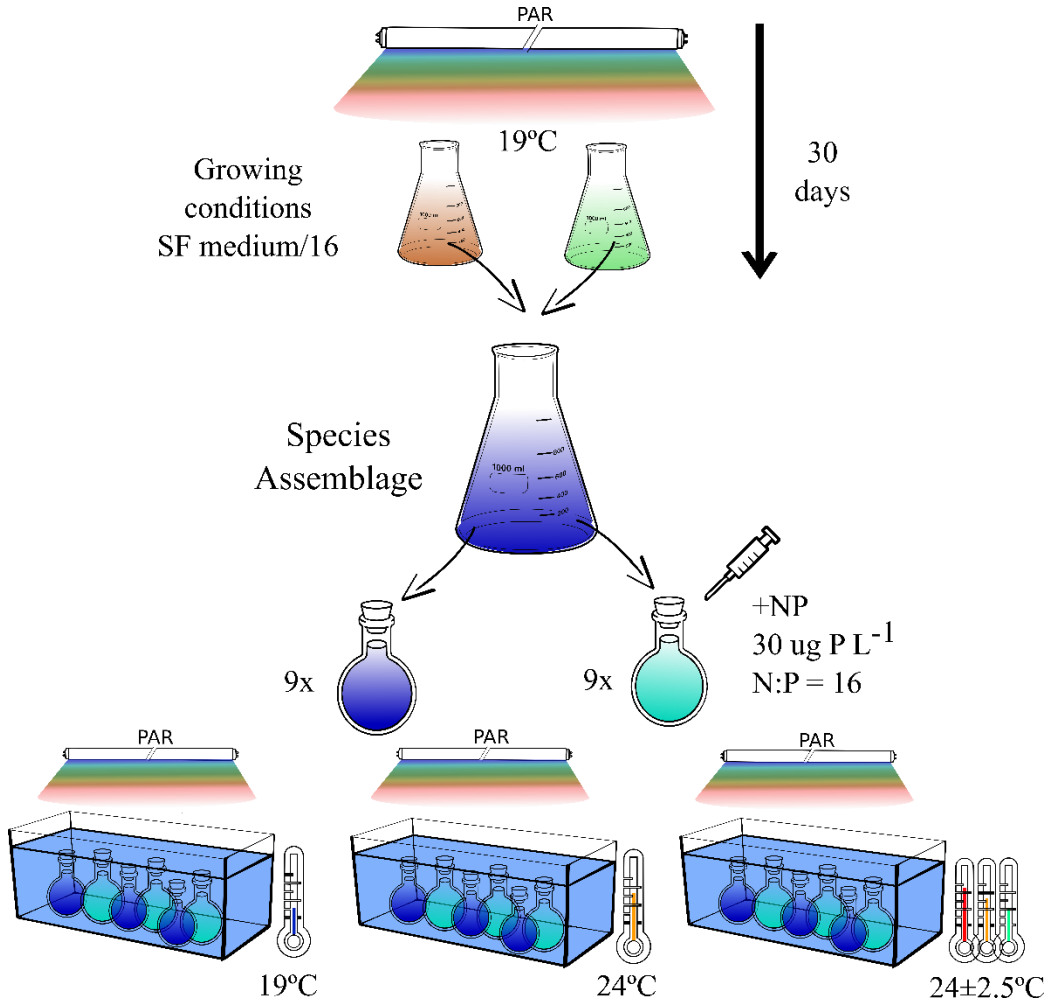

Figure 18. Graphic scheme of the experimental design for a mix culture of Monoraphidium minutum and Chromulina sp. The design included two nutrient treatments (ambient [25 µg P L^{-1}] and nutrient enrichment [25 µg P L^{-1} + NP]) and three temperature treatments (control, C [19°C], increased temperature, iT [24°C] and fluctuating temperature, fluT [24±2.5ºC]). Six treatments were set up (C, C_{NUT}, iT, iT_{NUT}, fluT, and $fluT_{NUT}$).

c. Biological parameters

c.1 Cell abundance

A volume of 5 mL per replicate was taken daily to estimate protist cell abundance. Samples of orgnanisms were fixed with lugol's solution at 2.5% and 10 µL were pipetted into a Neubauer's chamber (American Optical, Buffalo, NY, USA) and counted at 400x using an inverted microscope (Carl Zeiss AX10, LCC, USA).
The growth rate (GR) by periods was calculated from the cell counts ussing the following equation:

$$\mu = \frac{\text{Ln } C_2 - \text{Ln } C_1}{t_2 - t_1}$$

where C is cell abundance (cell mL^{-1}) at time (t) 1 and 2 within the exponential growth phase. For our experiment, we considered three periods coinciding with days of metabolic measurements: day 0-2, day 2-5 and day 5-8.

c.2 Chlorophyll a concentration

For Chl *a* determination, 10 mL for each replicate were filtered onto a Whatman GF/F filter (0.7 µm pore size; Whatman®, Sanford, ME, USA). Then, the photosynthetic pigments were extracted from the filter for 24 h at 4°C in darkness using 5 ml of acetone 90% (v/v). Samples were measured with a fluorometer LS 55 Luminiscence Spectrometer (Perkin-Elmer, Boston, MA, USA) at an excitation wavelength of 460 nm and emission at 670 nm. The fluorescence values were transformed into chlorophyll concentration from a calibration curve made with spinach-chlorophyll extract.

c.3 Primary production (PP)

10-mL of each experimental replicate were taken daily and placed in 4 quartz flasks (three clear and one dark as control) with 9.25 MBq of $NaH^{14}CO_3$ (specific activity: 310.8 MBq mmol-1, DHI Water and Environment, Germany) following the ^{14}C method proposed by (Nielsen, 1952). The quartz flasks were incubated for 1 h during the central hours of light exposure, and then killed by adding neutralized formaldehyde (0.5% w/v final concentration). Samples were stored at 4ºC until processed. One mL of sample was used to determine total ^{14}C activity and another 1 mL to determine the total organic carbon produced (TOC). The PP was determined by filtering 8-mL aliquots at low pressure (<100mmHg) through Nucleopore filters of 1-µm pore size. Filters were put into 6-mL scintillation vials, respectively, and acidified with 100 µL of 1N HCl in order to remove $DI^{14}C$ that was not fixed. After the vials were kept open for 24 h in an aeration hood (Lignell, 1992), they were filled with scintillation cocktail (Ecoscint A) and organisms were counted using a scintillation counter (Beckman LS 6000TA). The PP rates were measured throughout the experiment (day 0, 2, 5, and 8).

c.4 Bacterivory (BV)

For daily measurements of BV, we followed the ^{3}H-thymidine method described by Medina-Sánchez *et al.* (2004). For this, 15-mL samples were collocated into 25-mL quartz flasks, and ^{3}H-thymidine was added to independent sets of four samples (three replicates and one blank per treatment) to a final concentration of 25 nM, and incubated for 1 h under light. After incubation, the bacterivory was stopped by adding neutralized formaldehyde (0.75% w/v final concentration). Blanks were formaldehyde-killed before the incubation, and radiotraced at the end of the incubation. The samples were preserved at 4ºC until processed in the laboratory. Aliquots of 1.5 ml were taken from each replicate to determine the total activity in the sample. The remaining sample volume (13.5 mL) was filtered

through a cellulose nitrate filter of 1.2 µm pore size (Sartorius, Goettingen, Germany). The filters were dissolved using 100% acetone and centrifuged at 16,000 *g* for 10 min at 4ºC. Acetone was removed without removing the pellet, which was finally fixed and suspended with 1.5 ml of TCA (5% final concentration). After the cold 5% TCA extraction (at 0ºC for 20 min), the precipitate was collected by centrifugation at 16,000 g for 10 min, rinsed (and centrifuged) twice with 5% TCA, and measured in a scintillation counter equipped with autocalibration (Beckman LS 6000 TA). The activity registered on the filter served to measure the BV rate from the amount of growing bacteria traced with [methyl-^{3}H]-thymidine that were captured by mixotrophic protists (Medina-Sánchez *et al.*, 2004). The conversion factor 1.5×10^{18} cell mol^{-1} was used to estimate the number of bacteria depredated per mole of incorporated ^{3}H-thymidine (Bell *et al*., 1983). The factor 20 fg C cell^{-1} was applied to convert bacterial predation into C (Lee & Fuhrman, 1987). BV rates were measured over the experiment (day 0, 2, 5, and 8).

c.5 Respiration rate

One set of 18 samples (3 replicates per treatment) were used to fill 40-mL transparent Teflon bottles equipped with O_2 sensor-spot optodes (SP-PSt3-NAU-D5-YOP; PreSens GmbH, Germany; more details in Medina-Sánchez *et al.* (2017). The bottles were gently filled without bubbles, sealed to avoid gas exchanges and incubated in dark for 12 h after the light-exposure period, at each experimental temperature. Measurements were made during the first hours and at the end of incubation period using an oxygen transmitter (OXY-4 mini, Presens GmbH, Germany) connected to Oxyview 6.02 software to register data. This system was previously calibrated at 19ºC and 24ºC using two-point calibration (0% and 100% oxygen saturation) together with temperature and atmospheric-pressure data. Respiration rates (in µg C mg C^{-1} h^{-1}) were calculated as the slope

of the linear portion of the curve representing O_2 consumption vs. time. For the calculation of the *fluT* treatments, since the O_2 concentration is temperature-dependent, we used only the O_2values measured when temperature was the same (24ºC) over the cycle. Oxygen values were converted to C units assuming a respiratory quotient of 1 (del Giorgio & Cole, 1998). Meanwhile, R rates were measured throughout the experiment (day 0, 2, 5, and 8).

d. Calculation and statistical analysis

To assess the magnitude and direction of single and interactive effects of the study factors on the abundance for each species (*M. minutum* and *Chromulina* sp.) and the metabolic variables (PP, BV, and R rates), the effect size of temperature (*iT* or *fluT*), nutrients (Nut), and T(*iT* or *fluT*)×Nut interaction were calculated as follows:

$$\text{Effect size of nutrient enrichment (\%)} = \frac{C - C_{\text{NUT}}}{C} \times 100$$

$$\text{Effect size of } i\text{T (\%)} = \frac{C - iT}{\text{C}} \times 100$$

$$\text{Effect size of nutrients} \times i\text{T (\%)} = \frac{C - iT_{\text{NUT}}}{C} \times 100$$

$$\text{Effect size of } flu\text{T (\%)} = \frac{C - fluT}{C} \times 100$$

$$\text{Effect size of nutrients} \times flu\text{T (\%)} = \frac{C - fluT_{\text{NUT}}}{C} \times 100$$

Positive values indicate inhibition while negative values indicate stimulation. The error propagation was used to calculate the error of the effect size.

In addition, to determine the sensitivity of species to *iT* and *fluT* under ambient or nutrient-enriched conditions, we made a comparative analysis of the magnitude

of size effect of these temperature regimes for abundance of each species and metabolic variables (PP, BV and R rate) between ambient and nutrient-enriched treatments. For this, we firstly calculated the effect size of iT_{NUT} and $fluT_{NUT}$ under nutrient-enriched conditions as follows:

$$\text{Effect size of } iT_{NUT} \text{ under nutrient enrichment (\%)} = \frac{X_{C_{NUT}} - X_{iT_{NUT}}}{X_{C_{NUT}}} \times 100$$

$$\text{Effect size of } fluT_{NUT} \text{ under nutrient enrichment (\%)} = \frac{X_{C_{NUT}} - X_{fluT_{NUT}}}{X_{C_{NUT}}} \times 100$$

Where X is the variable response (*Chromulina* sp. and *M. minutum* abundance, PP, BV, R rate).

Then, from the effect size for each variable response, we calculated the difference of the *iT* and *fluT* effect for each day between the ambient or nutrient-enriched treatments, as follows:

Δ effect size = Effect size NUT treatment – Effect size ambient treatment

A two-way repeated measures analysis of variance (two-way RM-ANOVA) was used to test the effect of Nutrient, T and their interaction over time on all response variables (GR, PP, BV, and R rates). The sphericity assumption was verified by Mauchly's test. The Geisser-Greenhouse corrected degrees of freedom were used when Mauchly's test showed violation of sphericity. For Chl *a*, a 2-way ANOVA was applied for each day of measurement (day 0 and day 8), verifying the homogeneity of variances by Levene's test. Finally, differences among treatments were assessed by the *post hoc* test Fisher's least significant differences (LSDs) when significant interactive effects were found. All analyses were performed with the STATISTICA v7.0 software (Statsoft Inc., 2005).

3. Results

a. Metabolic variables

The analysis of effect size depicts a clearer pattern than that of the responses as absolute values of the metabolic and structural variables over the experiments shown in supplementary information (Figs. S10 and S11; Table S2 and S3). Thus, higher temperatures exerted a predominantly stimulatory effect on all the metabolic variables (PP, BV, and R rate; Fig. 19a).

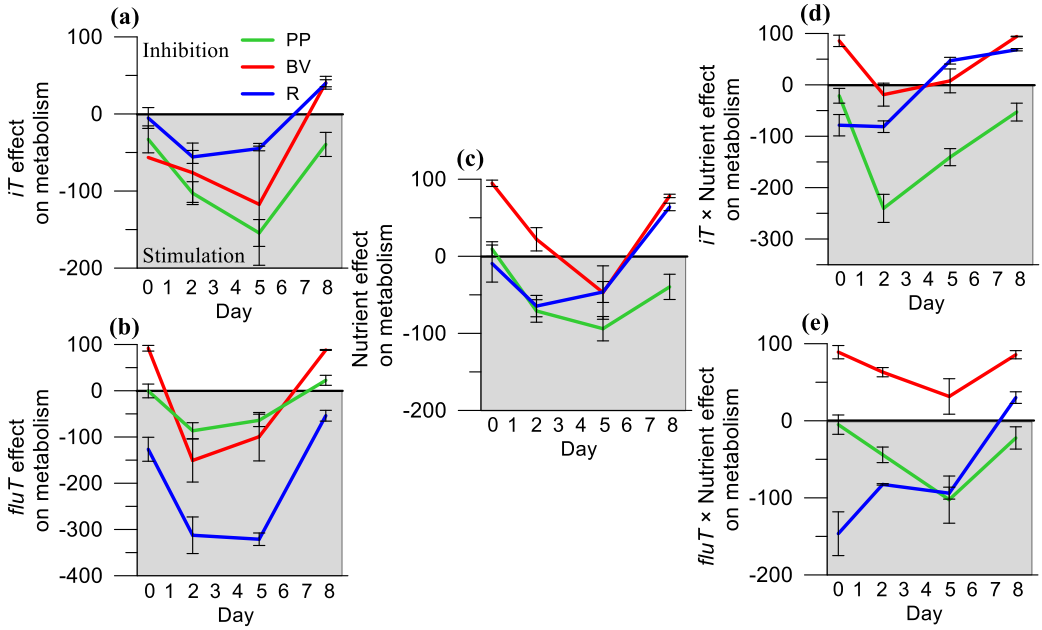

Figure 19. Effect size of increased temperature, iT (a), fluctuating temperature, fluT (b), nutrient (c), iT × nutrient (d), and fluT × nutrient (e) relative to control treatment [C] on metabolism (Primary Production, PP; Bacterivory, BV; and Respiration rate, R). Data are expressed as mean values ± SD (n = 3). Positive values indicates an inhibitory effect and negative values a stimulatory effect of stress factors.

Fluctuating temperature had a strong stimulatory effect only on the R rate throughout the experiment, whereas PP and BV rate were only mildly stimulated in the middle of the experiment but not at the end (Fig. 19b). The nutrient effect (Fig. 19c) and its interaction with increased (Fig. 19d) and fluctuating temperature (Fig. 19e) exerted a common effect for all the metabolic variables, stimulating the

PP, inhibiting the BV (particularly accentuated in *fluT*$_{NUT}$ treatment), and shifting the R rate from stimulation to inhibition throughout the experiment.

A comparison of the effect size of *iT* and *fluT* between ambient and enriched conditions is represented in Figure 20. The effect size of *iT* on PP proved greater under ambient than under enriched conditions, whereas no clear effect on BV and R rate were detected (Fig. 20a). The effect size of *fluT* was higher under ambient conditions for all the metabolic variables (PP, BV, and R rate; Fig. 20b).

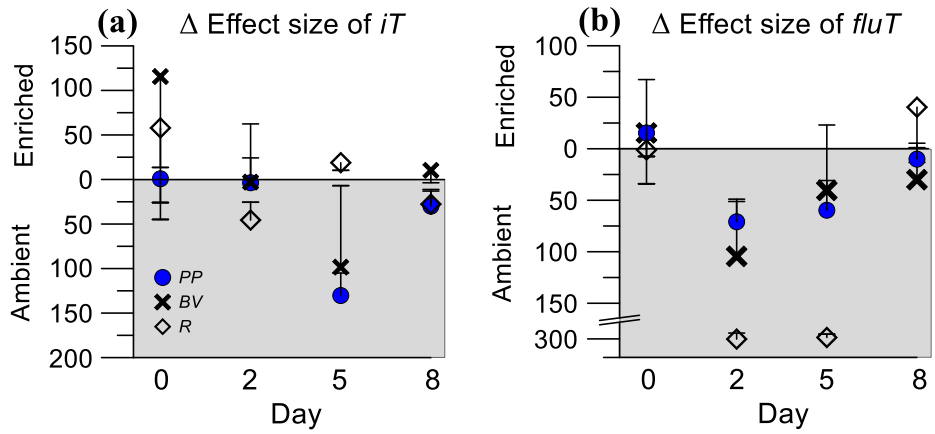

Figure 20. Difference of effect size between ambient and nutrient conditions for increased, iT (a), and fluctuating temperature, fluT (b), on PP rate, BV rate and R rate. Data are expressed as mean values ± SD (n = 3). Shaded areas indicate a greater effect size under ambient nutrient conditions, whereas white areas show a greater effect size under nutrient enriched conditions. Error bars are represented towards the reference (0 value).

The PP:R ratio revealed that the autotrophic metabolism (PP) increased under nutrient enrichment for all the temperatures (Fig. 21; Table S2). Furthermore, *iT* treatments (*iT* and *iT*$_{NUT}$) showed the highest values for each nutrient condition (3.0 ± 0.1 and 6.3 ± 0.2, respectively; $p<0.05$ *post-hoc* Fisher's LSD; Table S2; Fig. 21). The *fluT* treatments (*fluT* and *fluT*$_{NUT}$) led to the lowest values of PP:R ratio ($p<0.05$ *post-hoc* Fisher's LSD; Table S2), being under *fluT*-treatment when exhibited values lower than 1 throughout the experiment (Fig. 21).

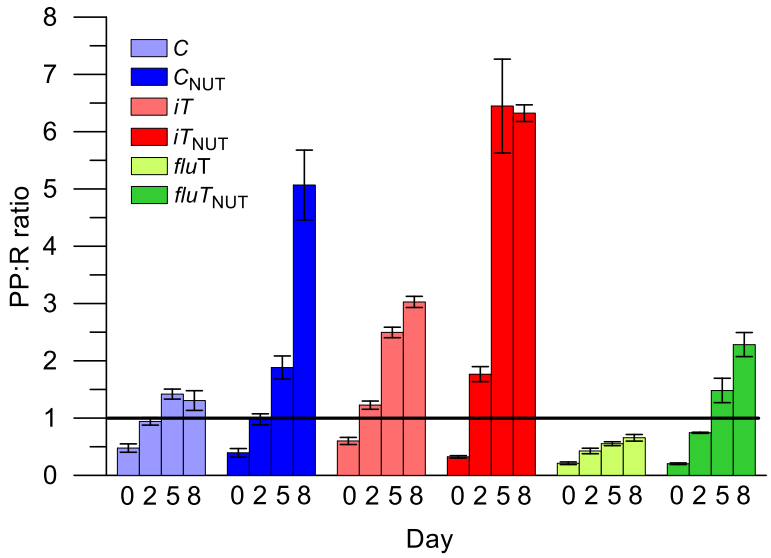

Figure 21. Ratio primary production (PP): respiration (R) over the experiment under different temperatures (control at 19°C, [C], increased temperature at 24°C, [iT] and fluctuating temperature at 24±2.5ºC, [fluT]) and nutrient treatments (ambient and nutrient enrichment [$_{NUT}$]). Data are expressed as mean values ± SD (n = 3).

b. Structural variables

Chlorophyll a (Chl *a*) was significantly affected by nutrients ($p<0.05$, *post-hoc* Fisher's LSD; Table S4, Fig. S11), showing a greater value (1.2 *vs* 0.9 mg Chl *a* L^{-1}) at the end of the experiment (day 8). Increased (*iT* and iT_{NUT}) and fluctuating temperature (*fluT* and $fluT_{NUT}$) also increased the Chl *a* content with respect to *C* and C_{NUT} at the beginning (day 0) for both nutrient conditions, but only under nutrient-enriched conditions at the end of the experiment ($p<0.05$ *post-hoc* Fisher's LSD; Table S4; Fig. S11).

These results agree with a positive effect of nutrient enrichment on total protist abundance ($p<0.05$ *post-hoc* Fisher's LSD; Table S4) for all the treatments at the end of the experiment (8-10 × 10^5 cell mL^{-1} in enriched treatments vs. 3-6 × 10^5 cell mL^{-1} in ambient nutrient treatments; Fig. S12), exhibiting the highest cell abundance under the iT_{NUT} treatment and the lowest in the *fluT* treatment (3±0.15 × 10^5 cell mL^{-1}; Fig. S12). The analysis of the effect size of the nutrients and

temperature on the abundance of each species indicated that *iT* did not exert a clear effect on either species, the inhibitory and stimulatory effects alternating (Fig. 22a). The *fluT* had a strong stimulatory effect on *Chromulina* sp. over the last days of experiment, but inhibitory on *M. minutum* (Fig. 22b). Contrarily, C_{NUT} exerted a stimulatory effect on *M. minutum* but inhibitory in *Chromulina* sp. (Fig. 22c). The nutrient effect on both species was intensified in iT_{NUT} (Fig. 22d) and the $fluT_{NUT}$ and C_{NUT} effect proved similar. Remarkably, *Chromulina* sp. became stimulated at the end of the experiment (-39.3±20.3; Fig. 22e).

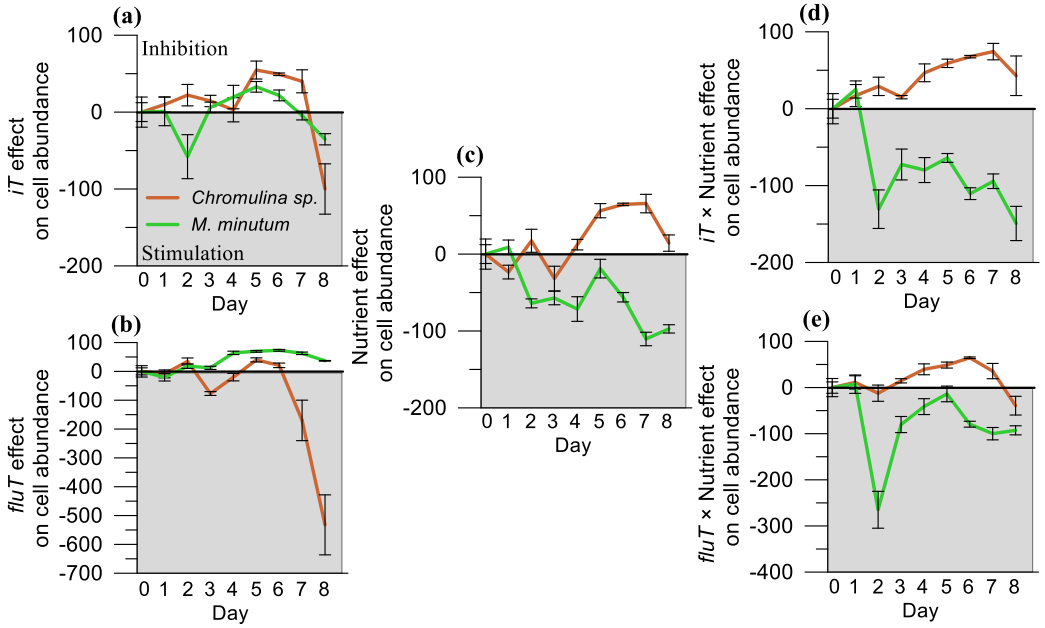

Figure 22. Effect size of increased temperature, iT (a), fluctuating temperature, fluT (b), nutrient (c), iT × nutrient (d) and fluT × nutrient (e) relative to control treatment [C] on cell abundance of Chromulina sp. and Monoraphidium minutum (M. minutum). Data are expressed as mean values ± SD (n = 3). Positive values indicate an inhibitory effect and negative values a stimulatory effect of stress factors.

The comparison of effect size of *iT* between ambient and enriched conditions for each species (Fig. 23a) revealed that the effect on *Chromulina* sp. was higher under ambient conditions from day 5 to the end of the experiment, whereas no significant differences were found for *M. minutum* over the experiment. For the

fluT effect (Fig. 23b), both species exhibited a stronger response under ambient conditions from the middle to the end of the experiment.

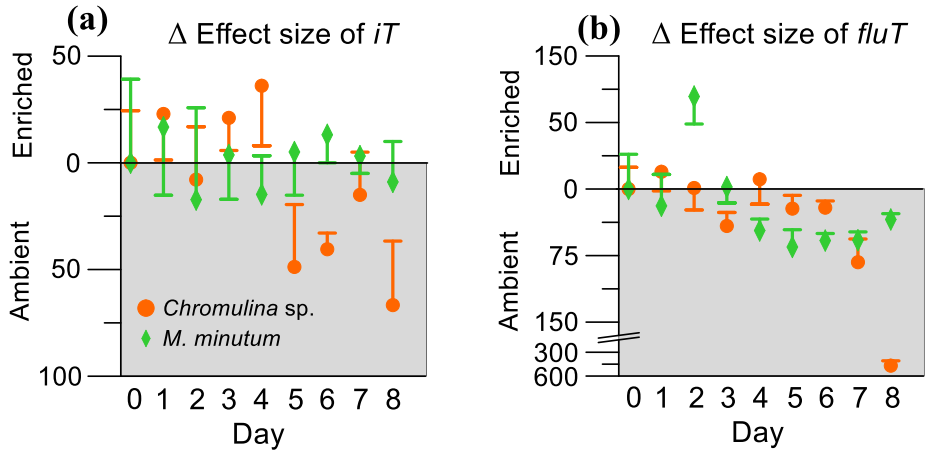

Figure 23. Difference of effect size between ambient and nutrient conditions for increased (a) and fluctuating temperature (b) on Chromulina and M. minutum abundance. Data are expressed as mean values ± SD (n = 3). Shaded areas indicates a greater effect size under ambient nutrient conditions, whereas white areas show a greater effect size under nutrient-enriched conditions. Error bars are represented towards the reference (0 value).

The analysis of GR by periods (Fig. 24) revealed two main results: i) differences appeared between species, with *M. minutum* showing positive values (excepting in the *fluT* treatment for period 0-2; $fluT_{NUT}$ treatment in period 2-5, and the *C* treatment in period 5-8), and *Chromulina* sp. exhibiting negative values (except for the $fluT_{NUT}$ treatment in period 0-2 and *fluT* treatment in period 5-8; Fig. 24); and ii) a greater difference appeared in GR values of the two species due to increased or fluctuating temperature under ambient nutrient than in nutrient-enrichment conditions. Thus, under ambient nutrient conditions, the growth rate for the *iT* and *fluT* treatments followed a different curve with respect to the *C* treatment, reflecting a positive effect in both species (Fig. 24a) during the last GR period (day 5-8; $p<0.05$ *post hoc* Fisher's LSD, Table S5). Specifically, the GR of *Chromulina* sp. in the *fluT*-treatment became significantly positive (0.07±0.04 d^{-1}; $p<0.05$ *post-hoc* Fisher's LSD; Table S5; Fig. 24a). However, under nutrient-

enrichment conditions, no clear differences were found among temperatures for each species, especially during the last period (p>0.05 *post-hoc* Fisher's LSD; Fig. 24b).

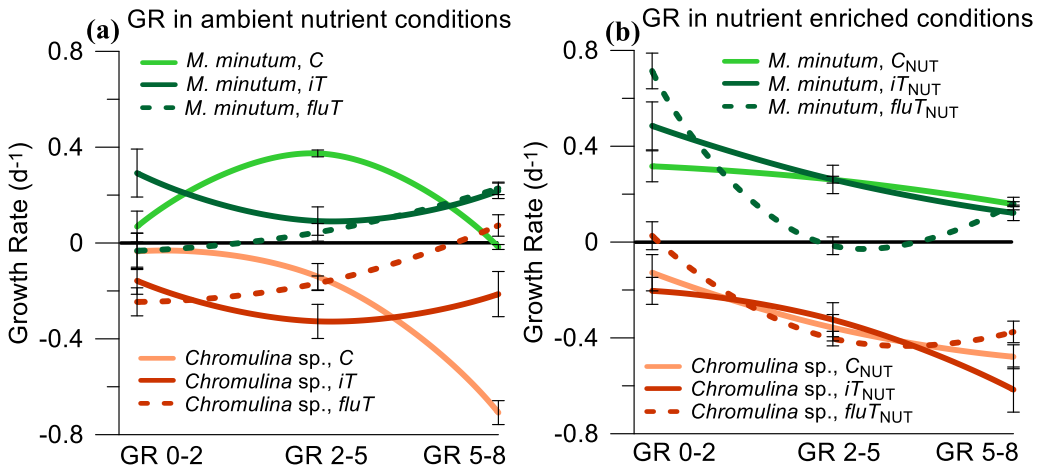

Figure 24. Growth Rate by periods for each species: Monoraphidium minutum (M. minutum) and Chromulina sp. under ambient (a) and nutrient enriched, $_{NUT}$ (b) conditions, and control temperature, C (clear line), increased temperature, iT (dark line) and fluctuation, fluT (dashed line) treatment. Data are expressed as mean values ± SD (n = 3).

4. Discussion

The main findings of our study were that fluctuating temperature enhanced the heterotrophic metabolism and the mixotroph abundance in a simplified protist community to a higher magnitude than did the increased temperature. By contrast, the combination of increased or fluctuating temperature and nutrients augmented primary production and favoured the growth of autotrophic species, challenging the MTE.

a. Protists' responses to increased or fluctuating temperature under ambient-nutrient conditions

According to the MTE (Brown *et al.*, 2004), increased temperature stimulated all the metabolic rates (PP, R, and BV). However, contrary to MTE, the stimulation was stronger for autotrophic metabolism (PP) than for heterotrophic metabolism (i.e. R and BV), making the PP:R ratio greatest at higher temperatures under ambient-nutrient conditions.

The finding that primary production depends more on temperature than respiration is contrary to previous patterns observed in plankton communities and theoretical models (Yvon-Durocher *et al.*, 2010; Barton *et al.*, 2018). However, another metabolic-balance model predicted an increase of PP:R ratio by warming (Iwata *et al.*, 2016). Recently, Padfield *et al.* (2016) proposed that a lesser increase of respiration than primary production at higher temperatures could be interpreted as an acclimation mechanism of protists to facilitate growth and maintain cell fitness.

Regarding species abundance, the strict autotrophic species (*M. minutum*) exhibited greater abundance with respect to *Chromulina* sp. in all the treatments, according to the MTE postulate of a higher growth rate of smaller cells (*M. minutum* biovolume = 62.8 μm^3; *Chromulina* sp. biovolume = 268 μm^3). However, it was surprising that the mixotrophic species (*Chromulina* sp.) abundance was not boosted as would be expected from the stimulation of its heterotrophic nutrition when temperatures rise (Wilken *et al.*, 2013).

For the first time, this study tests whether the MTE is supported under fluctuating temperature. Noticeably, *fluT* enhanced the heterotrophic metabolism (R rate of the protist community) and the relative abundance of the mixotroph at a higher magnitude than did increased temperature. Therefore, our results uphold the MTE. The stimulation of the heterotrophic metabolism by fluctuating temperature

led to a PP:R ratio lower than 1. This change in the balance between photosynthesis and respiration allows protist species to acclimate to short-term temperature variations (Staehr & Birkeland, 2006).

As also reported by Gerhard (2019), fluctuating temperature led to the lowest total community abundance. This seems to be a response related to a stress situation where metabolic energy is diverted, increasing the costs of repair and maintenance (Barton *et al.*, 2018). Thus, greater temperature variation may drive respiration to outpace resource intake, inducing a net loss of energy and lower growth, in a way similar to the responses by ectothermic invertebrates (Vasseur *et al.*, 2014).

The conditions of fluctuating temperature are what presumably led the mixotroph *Chromulina* sp. to register the highest stimulation, in agreement with the notion of greater individual flexibility in fluctuating environments (Shade *et al.*, 2012). Furthermore, the similarity of cell abundance between the two species under fluctuation (*fluT*) in comparison with other treatments, agrees with the idea that environmental fluctuations may induce species coexistence (Descamps-Julien & Gonzalez, 2005).

b. Protists' responses to increased or fluctuating temperature under nutrient-enriched conditions

Noticeably, the combination of increased or fluctuating temperatures and nutrients inhibited the heterotrophic metabolism (BV and R) and stimulated the autotrophic metabolism (PP and PP:R ratio), challenging the MTE. This outcome can be explained by the role of nutrient enrichment diminishing respiration due to temperature stress in the plant cell (Waraich *et al.*, 2012) or due to UVR stress in phytoplankton (Cabrerizo *et al.*, 2016). This finding could be also related to the well-established reduction of bacterivory activity as the nutrient concentrations increase (e.g. Modenutti, 2014; Saad *et al.*, 2016). Remarkably, González-Olalla *et al.* (2018) reported that nutrient input and higher mean temperature led to less

bacterivory and more PP in high-mountain lakes. These metabolic results are in line with the predominance of the strict autotroph *M. minutum* against the mixotroph *Chromulina* sp. in the *fluT*$_{NUT}$ and *iT*$_{NUT}$ treatments of our experiment. In general, chlorophytes (e.g. *M. minutum*) are benefited in comparison to other taxa when nutrient loads increase, since these organisms demand high nutrient availability (Reynolds, 1988; Deng *et al.*, 2014), whereas chrysophytes (e.g. *Chromulina* sp.) are generally more competitive under lower nutrient conditions (Doyle *et al.*, 2005; Jeppesen *et al.*, 2005; Saad *et al.*, 2016) due to their ability to prey on bacteria. Noticeably, recent studies (Rigosi *et al.*, 2014; Verbeek *et al.*, 2018) have reported a positive effect of temperature increase and nutrients on strict autotrosphs growth, and Yu *et al.* (2018) have demonstrated that the joint action of both factors augmented the proportion of chlorophytes vs. chrysophytes, in agreement with our results.

c. Nutrient enrichment reduces the sensitivity of protists to increased and fluctuating temperatures.

The results of the present study contribute to the controversy about whether the temperature sensitivity of protists depends on nutrient conditions. Marañón *et al.* (2018) observed that protist sensitivity to warming (from 8 to 20ºC) became more acute under high nutrient conditions and that nutrient limitation decreased the temperature dependence of metabolic rates. Likewise, Gerhard *et al.* (2019) found that protist growth under a nutrient supply with balanced N:P ratios was more sensitive to temperature fluctuation than when the N:P ratio was unbalanced. By contrast, numerous studies in ecosystems demonstrate that greater susceptibility to extreme temperatures under nutrient limitation could be a general physiological restriction (Thomas *et al.*, 2017; Bestion *et al.*, 2018). Thus, some algae belonging to order of Laminariales have less tolerance to temperature stress under limiting nutrient conditions (Gerard, 1997), while protists subject to warming and nutrient

limitation are also more vulnerable to environmental change (Bestion *et al.*, 2018). Our results imply greater susceptibility of protist metabolism and abundance to global change and extreme events when nutrient concentrations are lower. This is supported by a greater effect size of higher temperatures on PP and *Chromulina* sp. abundance, and of fluctuating temperature on all the metabolic variables and cell abundance, under ambient nutrient conditions. This means that the effect of temperature (especially temperature fluctuation) on metabolism and species abundance is considerably higher when the nutrient concentration is low.

5. Conclusions

Our experiment has demonstrated: i) that extreme temperature events associated with fluctuation can stimulate the heterotrophic metabolism and favour the predominance of mixotrophic species; and ii) the need to consider nutrient availability when scientists investigate the temperature effect on protists, since nutrient enrichment can diminish the magnitude of or counteract the impact of temperature.

Finally, our study demonstrates that the Metabolic Theory of Ecology does not hold for protist metabolism and abundance under nutrient enriched conditions. These results shed light on the application of MTE in a changing world.

References

Allen, A. P. (2005). Linking the global carbon cycle to individual metabolism. Funct. Ecol. 19(2): 202–213

Allen, A. P & Gillooly, J. F. (2009). Towards an integration of ecological stoichiometry and the metabolic theory of ecology to better understand nutrient cycling. Ecol. Lett. 12: 369–384

Anderson, K. J., Allen, A. P., Gillooly, J. F. & Brown, J. H. (2006). Temperature-dependence of biomass accumulation rates during secondary succession. Ecol. Lett. 9: 673–682

Barton, S., Jenkins, J., Buckling, A., Schaum, C. E., Smirnoff, N. & Yvon-Durocher, G. (2018). Universal metabolic constraints on the thermal tolerance of marine phytoplankton. bioRxiv: 358002

Bell, T. B., Ahlgren, G. M. & Ahlgren, I. (1983). Estimating bacterioplankton production by measuring 3H-thymidine incorporation in a eutrophic Swedish lake. *Appl. environ. Microbiol.* 45: 1709–1721

Bestion, E., García-Carreras, B., Schaum, C. E., Pawar. S. & Yvon-Durocher, G. (2018). Metabolic traits predict the effects of warming on phytoplankton competition. Ecol. Lett. 21: 655–664

Bindoff, N. L. et al. (2013). Detection and attribution of climate change: From global to regional BT - Climate Change 2013: The Physical Science Basis. Contribution of Working Group I to the Fifth Assessment Report of the Intergovernmental Panel on Climate Change. In: Stocker TF, Qin D, Plattner G-K, Tignor M, Allen SK, Doschung J, Nauels A, Xia Y, Bex V, Midgley PM, eds. Cambridge, UK: Cambridge University Press, 867–952

Brown, J. H., Gilooly, J. F., Allen, A. P., Savage, V. M. & West, G. B. (2004). Toward a metabolich theory of ecology. Ecology. 85: 1771–1789

Cabrerizo, M. J., Medina-Sánchez, J. M., González-Olalla., J. M., Villar-Argaiz, M. & Carrillo, P. (2016). Saharan dust inputs and high UVR levels jointly alter the metabolic balance of marine oligotrophic ecosystems. Sci. Rep. (6):1–11

Calvo-Díaz, A., Franco-Vidal, L. & Morán, XAG. (2014). Annual cycles of bacterioplankton biomass and production suggest a general switch between temperature and resource control in temperate coastal ecosystems. J. Plankton Res. 36: 859–865

Carrillo, P., Delgado-Molina, J. A., Medina-Sánchez, J. M., Bullejos, F. G & Villar-Argaiz, M. (2008). Phosphorus inputs unmask negative effects of ultraviolet radiation on algae in a high mountain lake. Glob. Change Biol. 14: 423–439

Chen, I-C., Hill, J. K., Ohlemüller, R., Roy, D. B. & Thomas, C. D. (2011). Rapid Range Shifts of Species Associated with High Levels of Climate Warming. Science. 333: 1024 LP – 1026

Cross, W. F., Hood, J. M., Benstead, J. P., Huryn, A. D. & Nelson, D. (2015). Interactions between temperature and nutrients across levels of ecological organization. Glob. Change Biol. 21: 1025–1040

Davison, I. R. (1991). Environmental effects on algal photosynthesis: Temperature. J. Phycol. 27: 2–8

Del Giorgio, P. A. & Cole, J. J. (1998). Bacterial Growth Efficiency in Natural Aquatic Systems. Annu. Rev. Ecol. Syst. 29: 503–541

Deng, J., Qin, B., Paerl, H. W., Zhang, Y., Wu, P., Ma, J. & Chen, Y. (2014). Effects of nutrients, temperature and their interactions on spring phytoplankton community succession in Lake Taihu, China. PLoS ONE. 9: 1–19

Descamps-Julien, B. & Gonzalez, A. (2005). Stable coexistence in a fluctuating environment: An experimental demonstration. Ecology. 86: 2815–2824

Doyle, S. A., Saros, J. E., Williamson, C. E. (2005). Interactive effects of temperature and nutrient limitation on the response of alpine phytoplankton growth to ultraviolet radiation. Limnol. Oceanogr. 50: 1362–1367

Gerard, V. A. (1997). The role of nitrogen nutrition in high-temperature tolerance of the kelp, Laminaria saccharina (Chromophyta). J. Phycol. 33: 800–810

Gerhard, M., Koussoroplis, A. M., Hillebrand, H. & Striebel, M. (2019). Phytoplankton community responses to temperature fluctuations under different nutrient concentrations and stoichiometry. Ecology

Gillooly, J. F., Charnov, E. L., West, G. B., Savage, V. M. & Brown, J. H. (2002). Effects of size and temperature on developmental time. Nature. 417: 70–73

González-Olalla, J. M., Medina-Sánchez, J. M. & Carrillo, P. (2019). Mixotrophic trade-off under warming and UVR in a marine and a freshwater alga. J. Phycol. 55(5): 1028-1040.

González-Olalla, J. M., Medina-Sánchez, J. M., Lozano, I. L., Villar-Argaiz, M. & Carrillo, P. (2018). Climate-driven shifts in algal-bacterial interaction of high-mountain lakes in two years spanning a decade. *Sci. Rep.* 8: 1–12.

IPCC. (2013). IPCC, 2013: Climate Change 2013 the Physical Science Basis: Working Group I Contribution to the Fifth Assessment Report of the Intergovernmental Panel on Climate Change (TF Stocker, D Qin, G-K Plattner, M Tignor, SK Allen, J

Doschung, A Nauels, Y Xia, V Bex, and PM Midgley, Eds.). Cambridge, UK: Cambridge University Press

Iwata, T., Mochizuki, N., Suzuki, T., Kohzu, A., Kojima, H., Fukui, M. & Urabe, J. (2016). Roles of Terrestrial Carbon Subsidies to Aquatic Community Metabolism in Mountain Lake Ecosystems. In: Kudo G, ed. Structure and Function of Mountain Ecosystems in Japan. Springer Japan, 115–144.

Jacobs, A. F. G., Heusinkveld, B. G., Kraai, A. & Paaijmans, K. P. (2008). Diurnal temperature fluctuations in an artificial small shallow water body. *Int. J. Biometeorol.* 52: 271–280.

Jentsch, A., Kreyling, J. & Beierkuhnlein, C. (2007). A new generation of climate-change experiments: events, not trends. Front. Ecol. Environ. 5: 365–374

Jeppesen, E. et al. (2005). Lake responses to reduced nutrient loading - An analysis of contemporary long-term data from 35 case studies. Freshw. Biol. 50: 1747–1771

Koussoroplis, A-M. , Pincebourde, S., Wacker, A. (2017). Understanding and predicting physiological performance of organisms in fluctuating and multifactorial environments. Ecol. Monogr. 87: 178–197

Lee, S. & Fuhrman, J. A. (1987). Relationships between biovolume and biomass of naturally derived marine bacterioplankton. *Appl. Environ. Microb.* 53: 1298–1303

Lignell, R. (1992). Problems in filtration fractionation of 14C primary productivity samples. Limnol. Oceanogr. 37: 172–178

Magnuson, J. J., Webster, K. E., Assel, R. A., Bowser, C. J., Dillon, P. J., Eaton, J. G., Evans, H. E, Fee, E. J., Hall, R. I., Mortsch, L. R. et al. (1997). Potential effects of climate changes on aquatic systems: Laurentian great lakes and Precambrian shield region. Hydrol. Process. 11: 825–871

Marañón, E., Lorenzo, M. P., Cermeño, P., Mouriño-Carballido, B. (2018). Nutrient limitation suppresses the temperature dependence of phytoplankton metabolic rates. ISME J. 12: 1836–1845

Medina-Sánchez, J. M., Herrera, G., Durán, C., Villar-Argaiz, M. & Carrillo, P. (2017). Optode use to evaluate microbial planktonic respiration in oligotrophic ecosystems as an indicator of environmental stress. Aquat. Sci. 79: 529–541

Medina-Sánchez, J. M., Villar-Argaiz, M. & Carrillo, P. (2004). Neither with nor without you: A complex algal control on bacterioplankton in a high mountain lake. Limnol. Oceanogr. 49: 1722–1733

Mitra, A. et al. (2014). The role of mixotrophic protists in the biological carbon pump. Biogeosciences. 11: 995–1005

Modenutti, B. (2014). Mixotrophy in Argentina freshwaters. Adv. Limnol. 65: 359–374

Morales-Baquero, R., Carrillo, P., Barea-Arco, J., Pérez-Martínez, C. & Villar-Argaiz, M. (2006). Climate-driven changes on phytoplankton-zooplankton coupling and nutrient availability in high mountain lakes of Southern Europe. Freshw. Biol. 51: 989–998

Nielsen, E. S. (1952). The Use of Radio-active Carbon (C14) for Measuring Organic Production in the Sea. ICES J. Mar. Sci. 18: 117–140

O'Connor, M. I. & Bernhardt, J. R. (2018). The metabolic theory of ecology and the cost of parasitism. PLoS. Biol. 16: 2–7

Ojeda-Pérez, Z. Z., Jiménez-Bremont, J. F. & Delgado-Sánchez, P. (2017). Continuous high and low temperature induced a decrease of photosynthetic activity and changes in the diurnal fluctuations of organic acids in Opuntia streptacantha. *PLOS ONE* 12: e0186540.

Paaijmans, K. P., Heinig, R. L., Seliga, R. A., Blanford, J. I., Blanford, S., Murdock, C. C. & Thomas, M. B. (2013). Temperature variation makes ectotherms more sensitive to climate change. Glob. Change Biol. 19: 2373–2380

Padfield, D., Lowe, C., Buckling, A., Ffrench-Constant, R., Jennings, S., Shelley, F., Ólafsson, J. S. & Yvon-Durocher, G. (2017). Metabolic compensation constrains the temperature dependence of gross primary production. Ecol. Lett. 20: 1250–1260

Padfield, D., Yvon-Durocher, G., Buckling, A., Jennings, S. & Yvon-Durocher, G. (2016). Rapid evolution of metabolic traits explains thermal adaptation in phytoplankton. Ecol. Lett. 19: 133–142

Pålsson, C. & Granéli, W. (2004). Nutrient limitation of autotrophic and mixotrophic phytoplankton in a temperate and tropical humic lake gradient. J. Plankton Res. 26: 1005–1014

Parmesan, C. & Yohe, G. (2003). A globally coherent fingerprint of climate change impacts across natural systems. Nature. 421: 37–42

Ptacnik, R., Gomes, A., Royer, S. J., Berger, S. A., Calbet, A., Nejstgaard, J. C., Gasol, J. M., Isari, S., Moorthi, S. D., Ptacnikova, R. et al. (2016). A light-induced shortcut in the planktonic microbial loop. Sci. Rep. 6: 1–10

Rasconi, S., Winter, K. & Kainz, M. J. (2017). Temperature increase and fluctuation induce phytoplankton biodiversity loss – Evidence from a multi-seasonal mesocosm experiment. Ecol. Evol. 7: 2936–2946

Reynolds, C. (1988). Functional morphology and the adaptive strategies of freshwater phytoplankton (C SD, Ed.). Cambridge, UK: Cambridge University Press. pp. 388-433

Rigosi, A., Carey, C. C., Ibelings, B. W. & Brookes, J. D. (2014). The interaction between climate warming and eutrophication to promote cyanobacteria is dependent on trophic state and varies among taxa. Limnol. Oceanogr. 59: 99–114

Rose, J. M. & Caron, D. A. (2007). Does low temperature constrain the growth rates of heterotrophic protists? Evidence and implications for algal blooms in cold waters. Limnol. Oceanogr. 52: 886–895

Saad, J. F., Unrein, F., Tribelli, P. M., López, N. & Izaguirre, I. (2016). Influence of lake trophic conditions on the dominant mixotrophic algal assemblages. J. Plankton Res. 38: 1–12

Sato, M., Kodama, T., Hashihama, F. & Ken, F. (2015). The effects of diel cycles and temperature on size distributions of pico- and nanophytoplankton in the subtropical and tropical Pacific Ocean. Plankton Benthos Res. 10: 26–33

Savage, V. M., Gillooly, J. F., Brown, J. H., West, G. B. & Charnov, E. L. (2004). Effects of Body Size and Temperature on Population Growth. Amer. Naturalist. 163: 429–441

Shade, A. et al. (2012). Fundamentals of microbial community resistance and resilience. Front. Microbiol. 3: 417

Smith, M. D. (2011). An ecological perspective on extreme climatic events: a synthetic definition and framework to guide future research. J. Ecol. 99: 656–663

Staehr, P. A., Birkeland, M. J. (2006). Temperature acclimation of growth, photosynthesis and respiration in two mesophilic phytoplankton species. Phycologia. 45: 648–656

Thomas, M. K., Aranguren-Gassis, M., Kremer, C. T., Gould, M. R., Anderson, K., Klausmeier, C. A. & Litchman, E. (2017). Temperature–nutrient interactions exacerbate sensitivity to warming in phytoplankton. Glob. Change Biol. 23: 3269–3280

Thomas, M. K., Kremer, C. T., Klausmeier, C. A. & Litchman, E. (2012). A Global Pattern of Thermal Adaptation in Marine Phytoplankton. Science. 338: 1085 LP – 1088

Vasseur, D. A., DeLong, J. P, Gilbert, B., Greig, H. S., Harley, C. D. G., McCann, K. S., Savage, V., Tunney, T. D. & O'Connor, M. I. (2014). Increased temperature variation poses a greater risk to species than climate warming. Proc. R. Soc. B-Biol. Sci. 281: 1779

Vasseur, D. A., McCann, K. S. (2007). The Impact of Environmental Variability on Ecological Systems (DA Vasseur and KS McCann, Eds.). Dordrecht, The Netherlands: Springer Netherlands

Verbeek, L., Gall. A., Hillebrand, H. & Striebel, M. (2018). Warming and oligotrophication cause shifts in freshwater phytoplankton communities. Glob. Change Biol. 24: 4532–4543

Villar-Argaiz, M., Medina-Sánchez, J. M. & Carrillo P. (2002). Microbial plankton response to contrasting climatic conditions: Insights from community structure, productivity and fraction stoichiometry. Aquat. Microb. Ecol. 29: 253–266

Waraich, E. A., Ahmad, R., Halim, A. & Aziz, T. (2012). Alleviation of temperature stress by nutrient management in crop plants: A review. J. Soil Sci. Plant Nutr. 12: 221–244

Ward, B. A. & Follows, M. J. (2016). Marine mixotrophy increases trophic transfer efficiency, mean organism size, and vertical carbon flux. Proceedings of the National Academy of Sciences. 113: 2958–2963

Webb, B. W. & Nobilis, F. (2007). Long-term changes in river temperature and the influence of climatic and hydrological factors. Hydrol. Sci. J. 52: 74–85

Wilken, S., Huisman, J., Naus-Wiezer, S. & Van Donk, E. (2013). Mixotrophic organisms become more heterotrophic with rising temperature. Ecol. Lett. 16: 225–233

Wojewodzic, M. W., Kyle, M., Elser, J. J., Hessen, D. O. & Andersen, T. (2011). Joint effect of phosphorus limitation and temperature on alkaline phosphatase activity and somatic growth in Daphnia magna. Oecologia. 165: 837–846

Woolway, R. I. *et al.* 2016. Diel Surface Temperature Range Scales with Lake Size. *PLOS ONE* 11: e0152466.

Yang, Z., Zhang, L., Zhu, X., Wang, J., Montagnes, D. J. S. (2016). An evidence-based framework for predicting the impact of differing autotroph-heterotroph thermal sensitivities on consumer-prey dynamics. ISME J. 10: 1767–1778

Yu, C., Li, C., Wang, T., Zhang, M. & Xu, J. (2018). Combined effects of experimental warming and eutrophication on phytoplankton dynamics and nitrogen uptake. *Water (Switzerland)* 10 (8).

Yvon-Durocher, G., Jones, J. I., Trimmer, M., Woodward, G., Montoya, J.M. (2010). Warming alters the metabolic balance of ecosystems. *Philos. Trans. R. Soc. B-Biol. Sci.* 365: 2117–2126.

Zhang, M., Guan, Y., Qin, B. & Wang, X. (2019). Responses of phytoplankton species to diel temperature fluctuation patterns. Phycol. Res. 67: 184–191

Zhang, M., Qin, B., Yu, Y., Yang, Z., Shi, X. & Kong, F. (2016). Effects of temperature fluctuation on the development of cyanobacterial dominance in spring: implication of future climate change. Hydrobiologia. 763: 135–146

Supplementary Information

This supplementary material contains the Figures from S10 to S12 and Tables from S2 to S5.

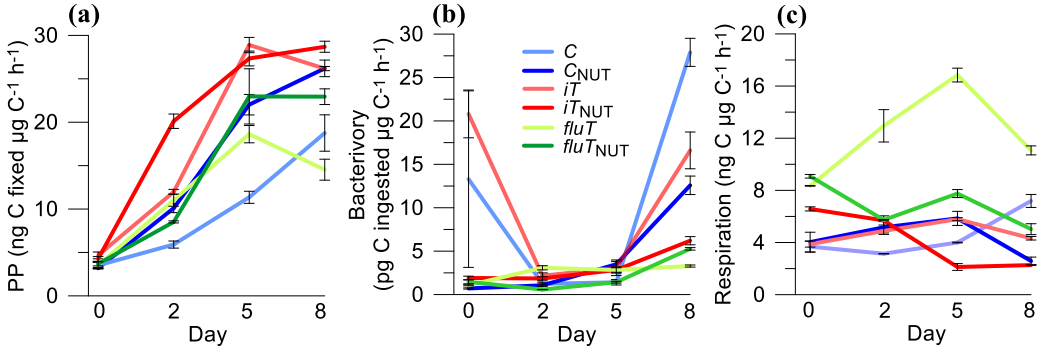

Fig. S10. Metabolic variables [Primary production, PP (a); Bacterivory (b); Respiration (c)] for the species assemblage of Monoraphidium minutum (M. minutum) and Chromulina sp. under different temperatures (control at 19°C, [C], increased temperature at 24°C, [iT] and fluctuating temperature at 24±2.5ºC, [fluT]) and nutrient treatments (ambient and nutrient enrichment [$_{NUT}$]). Data are expressed as mean values ± SD (n = 3).

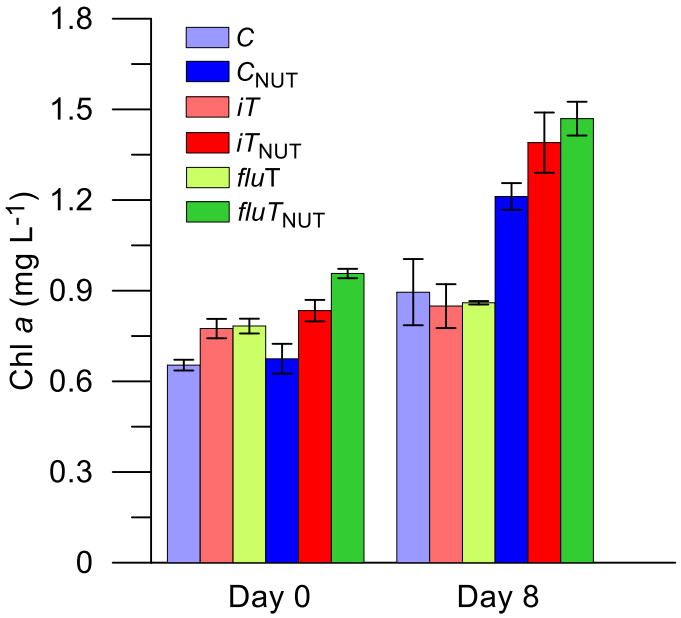

Figure S11. Chlorophyll a (Chl a) content at the beginning (day 0) and the end of the experiment (day 8) under different temperatures (control at 19°C, [C], increased temperature at 24°C, [iT] and fluctuating temperature at 24±2.5ºC, [fluT]) and nutrient treatments (ambient and nutrient enrichment [$_{NUT}$]). Data are expressed as mean values ± SD (n = 3).

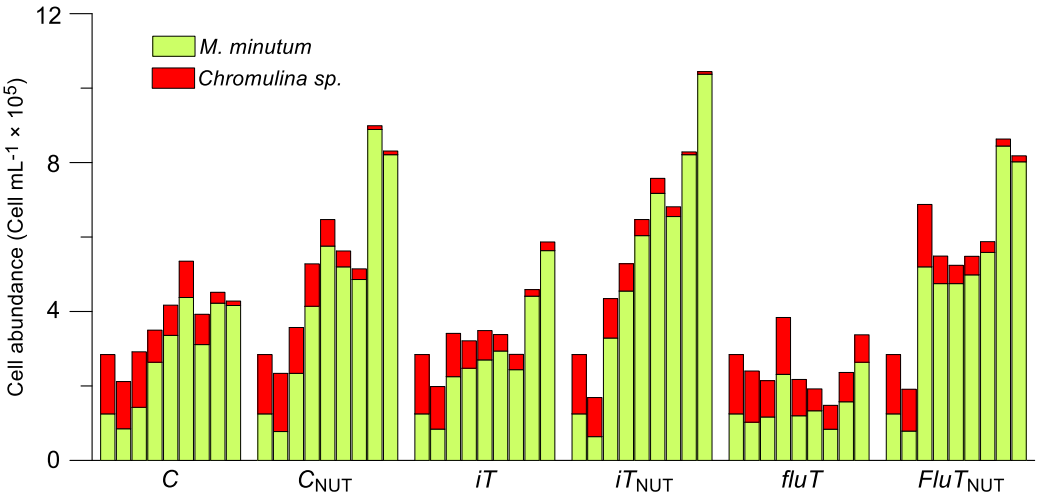

Figure S12. Total and specific cell abundance for Monoraphidium minutum (M. minutum) and Chromulina sp. over the experiment (from day 0 to day 8) under different temperatures (control at 19°C, [C], increased temperature at 24°C, [iT] and fluctuating temperature at 24±2.5ºC, [fluT]) and nutrient treatments (ambient and nutrient enrichment [$_{NUT}$]). Data are expressed as mean values ± SD (n = 3).

Table S2. Results of the two-way RM-ANOVA of temperatures (T) (control, increased and fluctuating temperature) and nutrients (Nut) (ambient and nutrient enriched conditions) on respiration rate (R), primary production rate (PP) and bacterivory rate (BV).

Treatment		R	PP	BV	Ratio PP:R
	df	p	p	p	p
Nutrients	1	**<0.0001**	**<0.0001**	**<0.0001**	**<0.0001**
Temperature	2	**<0.0001**	**<0.0001**	**<0.0001**	**<0.0001**
Nut×T	2	**<0.0001**	**<0.01**	**<0.01**	**<0.001**
Time	3	**<0.0001**	**<0.0001**	**<0.0001**	**<0.0001**
Time×Nut	3	**<0.0001**	**<0.0001**	**<0.0001**	**<0.0001**
Time×T	6	**<0.0001**	**<0.0001**	**<0.0001**	**<0.0001**
Time×Nut×T	6	**<0.0001**	**<0.0001**	**<0.0001**	**<0.0001**

Table S3. Results of the three-way RM-ANOVA of temperatures (T) (control, increased and fluctuating temperature) and nutrients (Nut) (ambient and nutrient enriched conditions) on cell abundance of Monoraphidium minutum and Chromulina sp.

Treatment		Abundance Assemblage	Abundance *M. minutum*	Abundance *Chromulina* sp.
	df		p	p
Temperature	2	**<0.01**	**<0.0001**	**<0.0001**
Nutrients	1	**<0.0001**	**<0.0001**	**<0.0001**
T×Nut	2	**<0.01**	**<0.0001**	**<0.0001**
Time	8	**<0.0001**	**<0.0001**	**<0.0001**
Time×T	16	**<0.0001**	**<0.0001**	**<0.0001**
Time×Nut	8	**<0.0001**	**<0.0001**	**<0.0001**
Time×T×Nut	16	**<0.0001**	**<0.0001**	**<0.0001**

Table S4. Results of the two-way ANOVA of temperatures (T) (control, increased and fluctuating temperature) and nutrients (Nut) (ambient and nutrient enriched conditions) on chlorophyll a content (Chl a) for the first day (day 0) and the end of the experiment (day 8).

Treatment		Chl *a* Day 0	Chl *a* Day 8
	df	p	p
Nutrients	1	**<0.0001**	**<0.0001**
Temperature	2	**<0.0001**	0.064
Nut×T	2	**<0.01**	**<0.05**

Table S5. Results of the three-way RM-ANOVA of temperatures (T) (control, increased and fluctuating temperature) and nutrients (Nut) (ambient and nutrient enriched conditions) on growth rate (GR) of Monoraphidium minutum and Chromulina sp.

Treatment		GR *M. minutum*	GR *Chromulina* sp.
	df	p	p
Nutrient	1	**<0.001**	**<0.01**
Temperature	2	0.1381	**<0.01**
Nut×T	2	0.1523	0.1631
Time	2	**<0.0001**	**<0.0001**
Time×Nut	2	**<0.0001**	**<0.0001**
Time×T	4	**<0.0001**	**<0.0001**
Time×Nut×T	4	**<0.0001**	**<0.0001**

CHAPTER 5

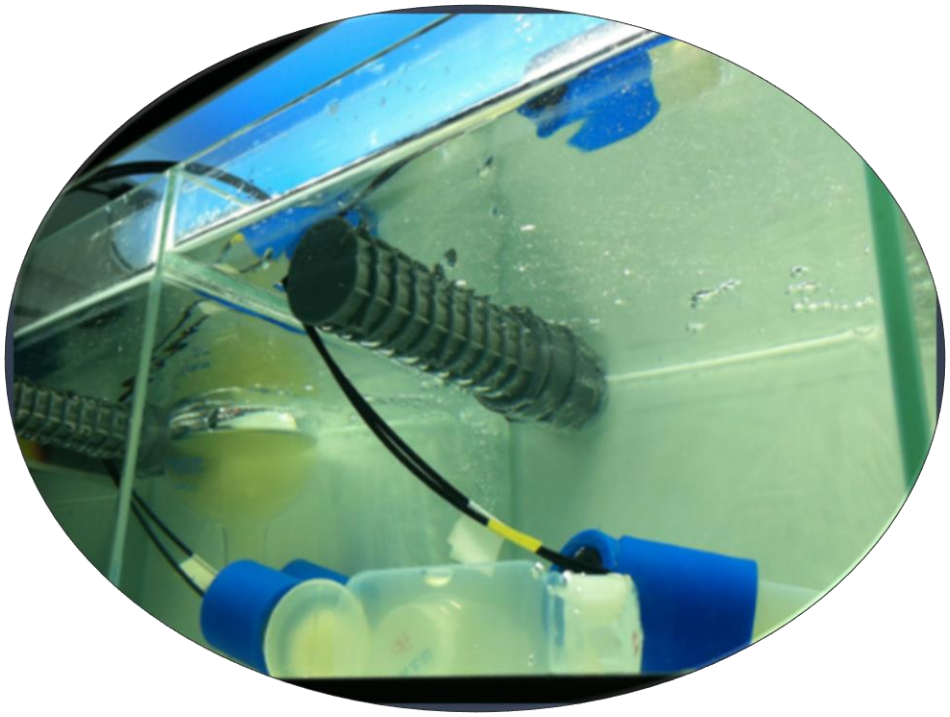

Automatic oxygen measurement in protists cultures
(Aqualab, University Institute of Water, UGR)

CHAPTER 5 – Mixotrophic trade-off under Warming and UVR in a marine and a freshwater alga

J. M. González-Olalla, J. M. Medina-Sánchez and P. Carrillo

Published in Journal of Phycology; 2019; 55(5): 1028-1040, https://doi.org/10.1111/jpy.12865

Abstract

Mixotrophic protists combine phagotrophy and phototrophy within a single cell. Greater phagotrophic activity could reinforce the bypass of carbon (C) flux through the bacteria-mixotroph link and thus lead to a more efficient transfer of C and other nutrients to the top of the trophic web. Determining how foreseeable changes in temperature and UVR affect mixotrophic trade-offs in favor of one or the other nutritional strategy, along the mixotrophic gradient, is key to understanding the fate of carbon and mineral nutrients in the aquatic ecosystem. Our two main hypotheses were: (i) that increased warming and UVR will divert metabolism toward phagotrophy, and (ii) that the magnitude of this shift will vary according to the organism's position along the mixotrophic gradient. To test these hypotheses, we used two protists (*Isochrysis galbana* and *Chromulina* sp.) located in different positions on the mixotrophic gradient, subjecting them to the action of temperature and of UVR and their interaction. Our results showed that the joint action of these two factors increased the primary production:bacterivory ratio and stoichiometric values (N:P ratio) close to Redfield's ratio. Therefore, temperature and UVR shifted the metabolism of both organisms toward greater phototrophy regardless of the original position of the organism on the mixotrophic gradient. Weaker phagotrophic activity could cause a less efficient transfer of C to the top of trophic webs.

1. Introduction

Mixotrophy, a metabolic trait long considered an exception, today is known to include most aquatic protists. This type of metabolism combines the acquisition of C or mineral nutrients through more than one trophic mode (Selosse *et al*., 2017). Mixotrophs are capable not only of photosynthesis but also of bacterial predation through phagotrophy. This dual ability is shared by most phylogenetic branches, clades, such as chrysophytes and haptophytes (Chan *et al*., 2018). All of these protists are widespread in natural communities (Unrein *et al*., 2007; Zubkov & Tarran 2008), especially in oligotrophic waters (Modenutti 2014), presumably due to their trophic advantage of acquiring limiting nutrients through bacterial predation (Raven *et al*., 2009; Tsai *et al*., 2016). From this perspective, the former paradigm of two protist groups (i.e., photoautotrophs and phagoheterotrophs) now includes mixotrophs as a new functional classification (Mitra *et al*., 2016).

Different numerical and experimental studies have demonstrated that mixotrophs exert a strong impact on aquatic ecosystems, boosting primary production and bacterial production, transferring C biomass to higher trophic levels, and stimulating the C-flux sink (e.g., Mitra *et al*., 2014; Ward & Follows, 2016). With the inclusion of mixotrophs in to trophic-web models, the prediction of how mixo-phytoplankton communities will respond to multiple environmental changes is currently a major scientific challenge (Reusch & Boyd, 2013; Cabrerizo *et al*., 2018). This requires quantifying how mixotrophic species with different positions in the gradient between photoautotrophy and heterotrophy respond to multiple stressors (Flynn *et al*., 2013).

A complex stressor, the climate change-associated temperature rise (IPCC, 2013), accentuates the stratification and shallowing of upper mixing layer in aquatic ecosystems. This stratification traps the organisms in surface waters, exposing them to intense radiation with high ultraviolet levels (UVR, 280–400 nm;

Villafañe *et al*., 2003; Carrillo *et al*., 2015). Also, the temperature increase reportedly affects phytoplankton, from raising the maximum quantum yield of photosystem II (PSII; Takahashi *et al*., 2013) to stunting growth (Halac *et al*., 2013; Cabrerizo *et al*., 2014). In addition, temperature can alter protist morphology (Mühling *et al*., 2003; Takabayashi *et al*., 2006), chlorophyll content (Verity, 1981) and the C:N:P composition (Yvon-Durocher *et al*., 2015). These latter authors have demonstrated that a higher sea-surface temperature is significantly and directly related to N:P and C:P ratios of marine algal assemblages, mainly because of the decline in P-rich ribosomes. Moreover, warming over an entire range from 13°C to 33°C (Wilken *et al*., 2012) and an increase of 5°C (Cabrerizo *et al*., 2018) exerts a stronger positive effect on phagotrophy than on phototrophy, although a temperature rise of 4°C can also aid both processes (Princiotta *et al*., 2016).

The shallowing of the upper mixing layer implies more intense UVR exposure for phytoplankton, which damages different cell components (i.e., DNA) and/or depresses photosynthesis and growth (Buma *et al*., 2003; Villafañe *et al*., 2003). However, in high-mountain lakes, mixotrophs have been shown to outcompete strict autotrophs under high UVR intensities (Carrillo *et al*., 2017), presumably because mixotrophs can tolerate the inhibition of C fixation or PSII, by taking up C through bacterivory (BV; Medina-Sánchez *et al*., 2004). Furthermore, it has been shown that UVR directly influences the elemental composition of phytoplankton by decreasing the sestonic C:P and N:P ratios (Rojo *et al*., 2012; Carrillo *et al*., 2015).

Today, it is increasingly evident that synergistic and antagonistic interactions among drivers must be taken into account in order to provide more realistic predictions of future ecosystem changes (Jackson *et al*., 2016; Villar-Argaiz *et al*., 2018). Several short-term experiments have indicated that a rise in

temperature promotes photochemical activity, improving the response to PAR and/or UVR (Sobrino & Neale, 2007; Halac *et al*., 2010; Villafañe *et al*., 2013). Likewise, temperature and UVR may alter metabolic activity of strict photoautotrophic protists, including shifts in their elemental composition, and altering the transfer of C and other limiting nutrients to higher trophic levels (Joint & Jordan, 2008; Montagnes *et al*., 2008). In addition, in a long-term experiment, the simultaneous action of warming and UVR has been found to reinforce the phagotrophic metabolism of *Isochrysis galbana* (Cabrerizo *et al*., 2018). However, in the current global warming scenario (see above), temperature could be understood as a press disturbance (i.e., chronic stress), whereas the UV radiation exposure would rather reflect a pulse disturbance (i.e., a combination of great intensity and short duration; see Harris *et al*., 2018). Therefore, it is key to evaluate the mixotrophic response to factors acting sequentially (Press vs. Pulse) on species and to quantify whether the magnitude of such a response depends on the organism's position in the mixotrophic gradient. Moreover, the stoichiometry modulating these responses might have a stronger explanatory role than previously thought.

We hypothesized: (i) that warming, UVR, and/or their interaction will shift the metabolism of mixotrophic protists toward greater phagotrophy; and (ii) that the magnitude of this shift will vary according to the organism's position along the mixotrophic gradient. Our hypotheses were tested with monospecific cultures of two characteristic species from marine and freshwater, and an a priori different position in the mixotrophic gradient. That is, *Isochrysis galbana* (Prymnesiophyceae) usually behaves proportionally more as a phototroph than a phagotroph (Anderson *et al*., 2018; Cabrerizo *et al*., 2018), whereas *Chromulina* sp. (Chrysophyceae) shows great versatility in its nutritional mode (Rottberger *et al*., 2013), although it usually acts as a phagotroph (Jones & Ilmavirta, 1988).

2. Material and Methods

a. Species and Culture mediums

Isochrysis galbana (Playa Unión, Argentina) was grown in F/2 medium (Guillard & Ryther, 1962), and *Chromulina* sp. (CCAC, Culture collection of Algae at the University of Cologne, Germany) was grown in SFM medium (Synthetic Freshwater Medium; CCAC, Germany) at 19°C.

b. Experimental set-up

The experiment was a split-plot design to study the effect on mixotrophic trade-off of a press (temperature) and a pulse factor (UVR), both being global-change drivers (see Introduction). The design included two temperature treatments (19°C and 22°C) applied at the plot level and four temperature × light treatments (19_{-UVR}, 19_{+UVR}, 22_{-UVR}, 22_{+UVR}) at the subplot level stemming from the combination of (i) two temperature levels, low and high temperature (19°C and 22°C, respectively) and (ii) two light levels, +UVR (>280 nm) versus -UVR (only photosynthetically active radiation, PAR; >400 nm; Fig. 25). The increase of 3°C of temperature is within the variation expected in global predictions for the late 21st century (IPCC, 2013, Scenario RCP8.5).

In the first part of the experiment (main plot, Fig. 25), both cultures were maintained in exponential growth for at least 11 generations (30 d) prior to any measurement. The cultures grew under a 12:12 h light:dark photoperiod, at the respective experimental temperature (19°C and 22°C) in 3 L flasks (one flask per species and temperature level). Both species were grown under mixotrophic conditions (nonaxenic culture) at 21.7 $W \cdot m^{-2}$(~100 μmol photons $\cdot m^{-2} \cdot s^{-1}$) of PAR (400–700 nm). Bacteria growing in each culture were those naturally associated with protist species culture (bacteria were not identified).

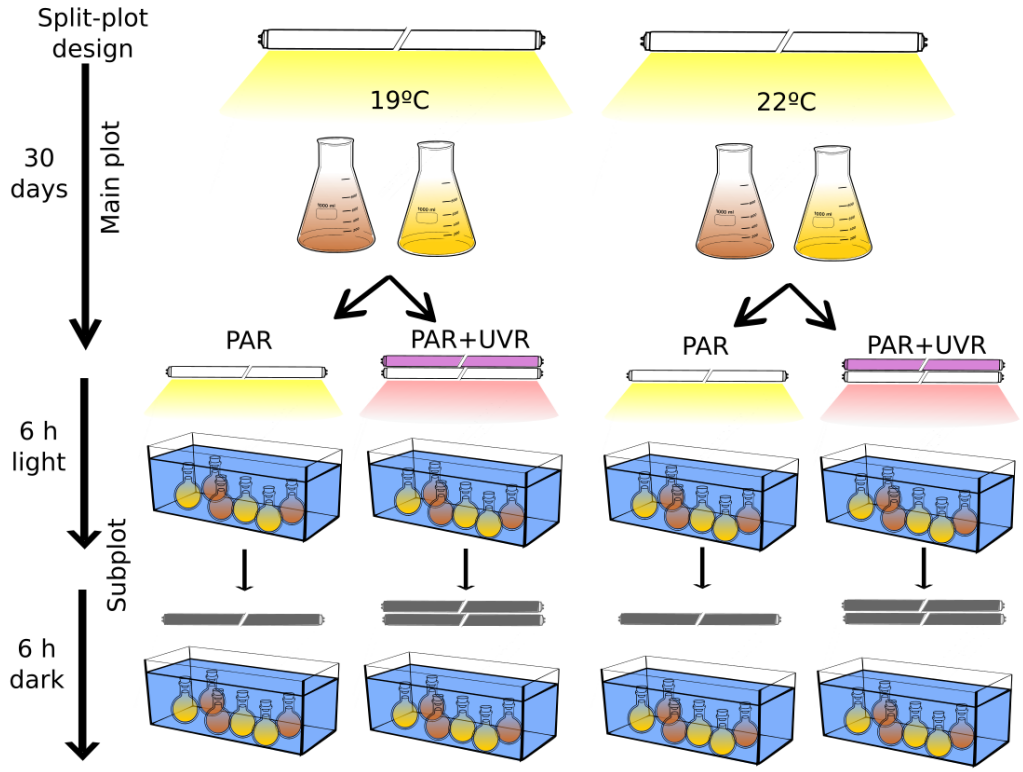

Figure 25. Graphic scheme of the experimental split-plot design for each species (Isochrysis galbana and Chromulina sp.).The design included two temperature (T) treatments (19°C and 22°C) applied at the main plot level and four T 9 light treatments at the subplot level (19_{-UVR}, 19_{+UVR}, 22_{-UVR}, 22_{+UVR}).

In the second part of the experiment (subplot, Fig. 25), aliquots from the cultures were transferred to 12 quartz flasks (250 mL, $n = 3$ per treatment) for each species. The flasks were placed in an aquarium system with adjustable temperature by refrigeration (Teco® S. R. L. tank TK 2000, EU) and radiation through light-emitting diode lamps (nano LED light v.2.0, BLAU aquaristic) for PAR, and Q-Panel tubes for UVR (Fig. 25). For 12 h, the cultures were subjected to a photoperiod of 6:6 h light:dark, with irradiance of 21.7 W · m^{-2}(100 µmol photons · m^2 · s^{-1}) of PAR and an additional 2.42 W · m^{-2} of UVR in the +UVR treatments.

From flasks, aliquots were taken to measure photosynthetic quantum yield (Φ_{PSII}), cell-specific Chl *a*, elemental C, N, and P (see below). Furthermore, 40-mL Teflon FEP narrow-mouth bottles (Nalgene) were filled in triplicate to measure respiration (R), PP, and BV.

c. Response variables

The response variables measured were the most relevant ones for stoichiometry as well as phototropic and phagotrophic metabolism of mixotrophs (see Introduction).

c.1 Stoichiometric variables

Elemental composition (C, N, and P) of each algal species was determined from 15 mL of each experimental unit by low-pressure filtration (<100 mmHg) through precombusted (1 h at 550°C) glass-fiber filters of 1 μm pore size (Whatman GF/B; Whatman®, Sanford, ME, USA). Filters (one for C and N determination and another for P) were immediately frozen at −20°C. The C and N analyses were performed using a Perkin-Elmer 2400 elemental analyzer. Elemental P was determined after the filters were digested with a mixture of potassium persulfate and boric acid at 120°C for 30 min and analyzed as soluble reactive P by applying the acid molybdate technique (APHA, 1992).

c.2 Chlorophyll *a* concentration

For the Chl *a* determination, 15 mL from each experimental unit was filtered through a Whatman GF/F filter (0.7 μm pore size), and the photosynthetic pigments were extracted during 24 h in darkness in 5 mL of acetone at 4°C to remove all the chlorophyll from the filters. The samples were measured at an excitation wavelength of 460 nm and emission at 670 nm, with a fluorometer LS 55 Luminescence Spectrometer (Perkin-Elmer, Boston, MA, USA). Previously, a

calibration curve was made with pure spinach chlorophyll extract to transform fluorescence values into chlorophyll concentration.

c.3 Photosynthetic activity

c.3.1 Chlorophyll fluorescence

An amount of 3 mL from each experimental unit was taken every 2 h throughout the experiment to measure in vivo the Chl *a* fluorescence using a portable pulse-amplitude-modulated fluorometer (Water-ED PAM, Walz, Germany). Because the time between sampling and fluorescence measurements was a few seconds, the intrinsic photochemical efficiency of PSII (Φ_{PSII}) in the light was determined (Maxwell & Johnson, 2000) as next equation:

$$\Phi_{PSII} = \frac{\Delta F}{F'm} = \frac{F'm - F't}{F'm}$$

where F'm is the instantaneous maximum fluorescence induced by a saturating light pulse (ca. 5,300 μmol photons · m^{-2} · s^{-1} in 0.8 s), and F't is the current steady-state fluorescence induced by an actinic light ~100 μmol photons · m^{-2} · s^{-1} in light-adapted cells. Each subsample was measured six times immediately after sampling, with each measurement lasting 10 s.

c.3.2 NonPhotochemical Quenching

Nonphotochemical quenching (NPQ) was used as a proxy of the dissipation of the excess energy as heat and was determined directly from the PAM fluorometer as following equation:

$$NPQ = \frac{Fm - F'm}{F'm}$$

where Fm is the maximal fluorescence of dark-adapted sample and F'm is the instantaneous maximum fluorescence induced by a saturating light pulse (c. 5,300 μmol photons · m^{-2} · s^{-1}in 0.8 s). This is the most important short-term

photoprotective mechanism activated by saturating radiation intensities. The software stored the Fm value that was then used with each sample to calculate the NPQ.

The Φ_{PSII} and NPQ areas were calculated for Φ_{PSII} and NPQ diel cycles (in triplicate for each treatment), following González-Olalla *et al*., (2017), as in next equation:

$$A = \int_{b}^{a} f(x)dx$$

where *a* and *b* are the initial and final measurement times, respectively, and *f*(*x*) is the curve describing the yield or NPQ over time for each treatment. The area under the curve was calculated using the software MATLAB® r2015a (Mathworks, Natick, MA, USA).

c.3.3 Primary Production

Following the ^{14}C method proposed by Nielsen, (1952) and modified by Carrillo *et al*., (2002), 40-mL Teflon flasks were filled from each experimental unit (three clear plus one dark as control) and added with 9.25 MBq of $NaH^{14}CO_3$ (specific activity: 310.8 MBq · $mmol^{-1}$; DHI Water and Environment, Germany). The flasks were incubated for 2 h during the central hours of light exposure, and then fixed with neutralized formaldehyde 0.5% w/v final concentration and stored at 4°C until processed. Then, 40-mL aliquots were filtered through Nuclepore filters of 1-µm pore size to determine the particulate PP. The filtrations were gently carried out at low pressure (<100 mmHg) to minimize cell breakage. The excreted organic carbon (EOC) was measured from 4-mL aliquots of the filtrate (<1 µm). The filters and filtrate were put into 5- and 20-mL scintillation vials, respectively, and acidified with 100 µL of 1 N HCl to remove $DI^{14}C$. Vials were then kept open for 24 h in an aeration hood following the recommendations of Lignell, (1992).

Then, the vials were filled with scintillation cocktail (Ecoscint A) and counted using a scintillation counter (Beckman LS 6000TA) equipped with autocalibration. Total Organic Carbon (TOC) was calculated as sum of PP and EOC, and the %EOC was calculated following the equation:

$$\%\mathrm{EOC} = \frac{\mathrm{EOC}}{\mathrm{TOC}} \times 100$$

c.4 Bacterivory Rate

The method of Medina-Sánchez *et al*., (2004) was used to measure the amount of growing bacteria traced with [methyl-^{3}H]-thymidine captured by mixotrophic protists. For determining BV, aliquots of 15 mL from each experimental unit were transferred to 40-mL Teflon flasks, added with [Methyl ^{3}H]-thymidine to a final concentration of 25 nM, and incubated during 1 h at each corresponding temperature × light treatment (three replicates and one blank per treatment). After incubation, the BV was stopped by adding neutralized formaldehyde (0.75% w/v final concentration). Likewise, blanks were formaldehyde-killed before the incubation. The samples were preserved at 4°C until processed in the laboratory. A volume of 1.5 mL was taken from each replicate for determining the total activity (i.e., total traced bacteria) in the sample. The remaining sample volume (13.5 mL) was filtered through a cellulose nitrate filter of 1.2 μm pore size (Sartorius). A volume of 1.5 mL was taken from the filtrate to determine the residual activity (i.e., traced bacteria not captured by protists), while the activity registered on the filter (i.e., traced bacteria captured by protists) served to measure the BV. The filters were dissolved using 100% acetone and centrifuged at 16,000 *g*for 10 min at 4°C. Supernatant acetone was eliminated without removing the pellet, which was finally fixed and re-suspended with 1.5 mL of TCA (5% final concentration). After TCA extraction (>20 min at <1°C), the precipitate was collected by centrifugation at 16,000*g* for 10 min at 4ºC, rinsed and centrifuged twice with 5% TCA, and measured in a scintillation counter equipped with

autocalibration (Beckman LS 6000 TA). The conversion factor 1.5×10^{18} cells · mol^{-1} was used to convert the incorporated ^{3}H-thymidine into the number of depredated bacteria (Bell *et al*., 1983). The factor 20 fg C · $cell^{-1}$ was applied to convert depredated bacteria into C units (Lee & Fuhrman, 1987).

c.5 Respiration Rate

From each experimental unit, 40-mL Teflon flasks equipped with sensor spots (SP-PSt3-NAU-D5-YOP), were filled without bubbles, sealed to avoid gas exchanges, and incubated at each experimental temperature for 6 h in dark after the corresponding light-exposure period (three replicates per treatment). Measurements were made continuously using an oxygen transmitter (OXY-4 mini, Presens GmbH, Germany) equipped with Oxyview 6.02 software to register the data. This system was previously calibrated using two-point calibration (0% and 100% oxygen saturation) controlling temperature and atmospheric-pressure measurements. Respiration rates (in μg C · mg C^{-1} · h^{-1}) were calculated as the slope of the regression fit of oxygen concentrations per C unit versus time. Oxygen values were converted to C units assuming a respiratory quotient of 1 (Del Giorgio & Cole, 1998).

d. Effect size and statistical analysis

The statistical significance of temperature as the main plot effect, and temperature × UVR interaction as the subplot effect, on each response variable (see above) was assessed by two-way split plot of repeated-measures analysis of variance (RM-ANOVA) after verifying the assumptions of homoscedasticity for each data group (using Levene's tests) and normality of residuals (by Shapiro–Wilk's test).

The effect size of temperature, UVR, and temperature × UVR interaction, as a measurement of the magnitude and direction of factor effect on the response variables (cell-specific Chl *a*, C-, N-, P cell quota, C:N and C:P ratio, specific-PP, Φ_{PSII} area, specific-BV, R, %EOC, and NPQ area) for each species was calculated as follows in equations:

$$\text{Effect size of temperature (\%)} = \frac{X_{19-UVR} - X_{22-UVR}}{X_{19-UVR}} \times 100$$

$$\text{Effect size of UVR(\%)} = \frac{X_{19-UVR} - X_{19+UVR}}{X_{19-UVR}} \times 100$$

$$\text{Effect size of temperature} \times \text{UVR(\%)} = \frac{X_{19-UVR} - X_{22+UVR}}{X_{19-UVR}} \times 100$$

where *X* is the response variable measured in the samples. Negative values indicate a stimulatory effect and positive values indicate an inhibitory effect of stress factors. Error propagation was used to calculate the variance of the effect size (as a percentage).

The differences between species for each response variable, (i) under identical experimental conditions and (ii) for the effect size of temperature, UVR, and temperature × UVR, were assessed by a *t*-test for independent samples after verifying the assumption of homoscedasticity (using Levene's test). All analyses were performed with the STATISTICA v7.0 software (Statsoft Inc., 2005).

3. Results

a. Chl *a* and stoichiometric responses

Overall, the cell-specific Chl *a*, C-, N-, and P cell quota values were lower in *I. galbana* than in *Chromulina* sp. (*t*-test $p < 0.05$; Table S6 in the Supplementary Information, Fig. 26, a–d).

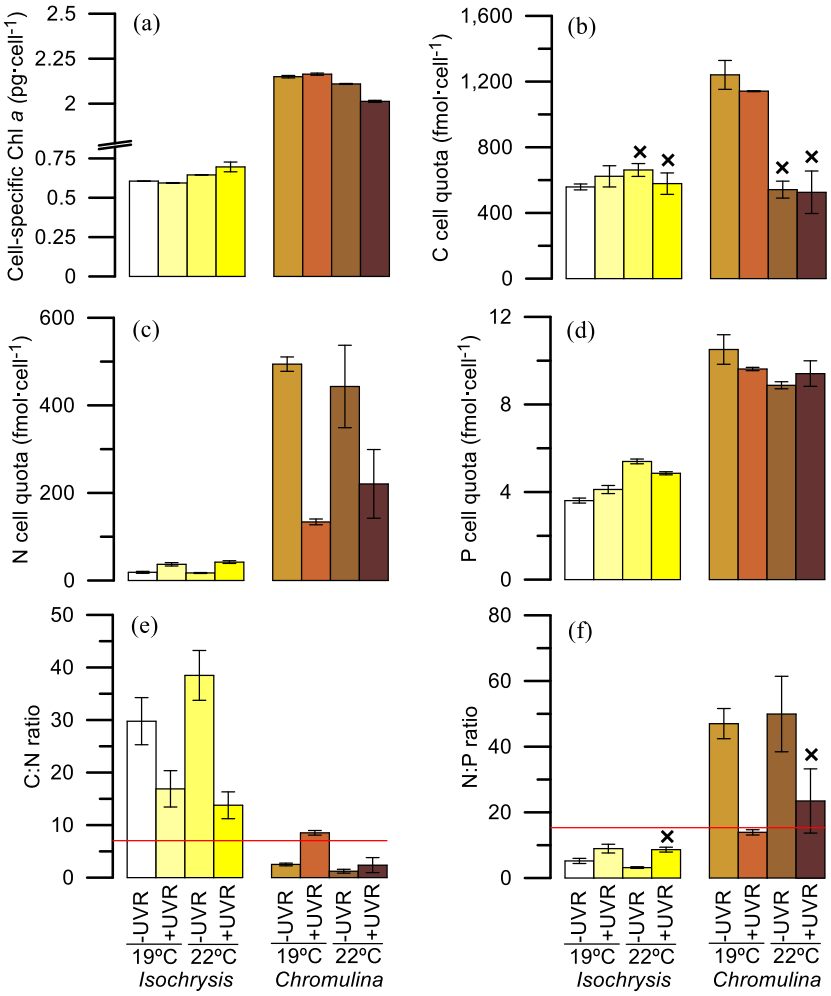

Figure 26. Chlorophyll a content and elemental composition of Isochrysis galbana and Chromulina sp. under temperature (T) (low T [19°C] and high T [22°C]) and light (full sunlight [+UVR] and photosynthetically active radiation [-UVR]) treatments. Cell-specific Chl a (a), C cell quota (b), N cell quota (c) and P cell quota (d), C:N ratio (e) and N:P ratio (f). Red line represents Redfield ratio. Cross symbols represent the experimental conditions that did not exhibit significant differences between species. Data are expressed as mean values ± SD (n = 3).

The C:N was higher and N:P lower than respective Redfield's ratios in *I. galbana*, whereas an opposite pattern was found in *Chromulina* sp. (except for the 19_{+UVR} treatment; Fig. 26e,f). temperature × UVR interaction was significant for all these variables, except for the C cell quota and N:P ratio in *I. galbana* (Subplot effect; Table S7 in the Supplementary Information).

The effect size of temperature, UVR, and temperature × UVR on cell-specific Chl *a* was weak (<15%), being that of temperature and temperature × UVR stimulatory in *Isochrysis galbana*but inhibitory in *Chromulina* sp. However, the effect size of UVR had an opposite pattern on both species ($p < 0.05$; Table S8 in the Supplementary Information; Fig. 27a).

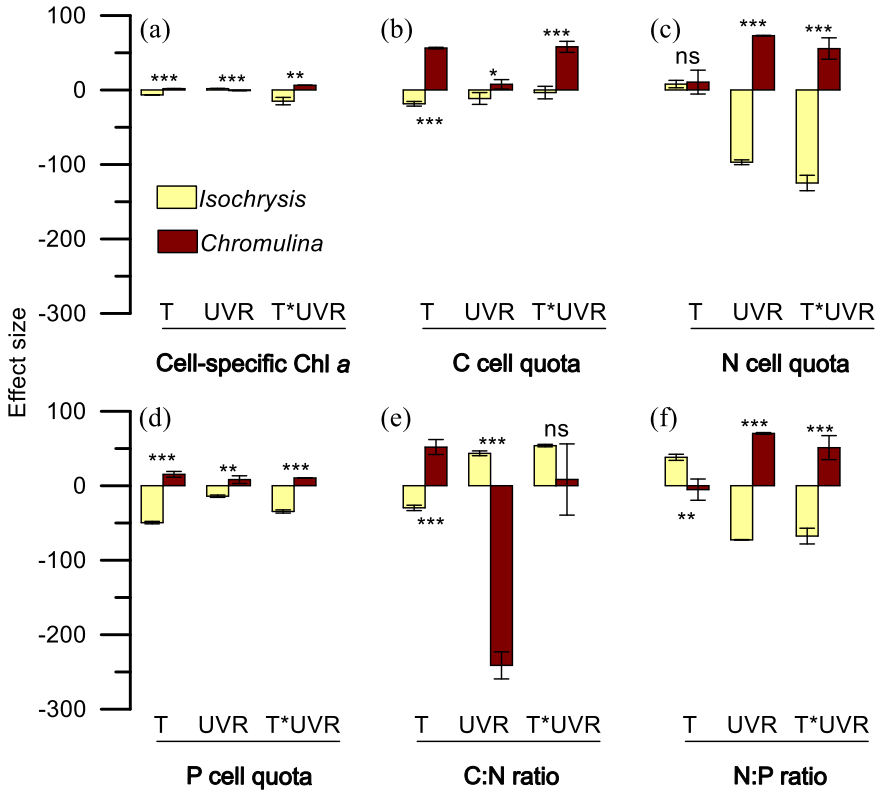

*Figure 27. Effect size of T, UVR, and T 9 UVR on cell-specific Chl a (a), C cell quota (b), N cell quota (c) and P cell quota (d), C:N ratio (e) and N:P ratio (f) of Isochrysis galbana and Chromulina sp. Data are expressed as mean values _ SD (n = 3). Asterisks show the significance value: ***P < 0.001; **P < 0.01; *P < 0.05; ns: not significant.*

Regarding elemental stoichiometric variables, the effect size of all factors was stimulatory in *I. galbana* (except those of temperature × UVR on C cell quota [no effect] and temperature on the N cell quota [inhibitory]), but inhibitory in *Chromulina* sp. (except that of temperature on the N cell quota [no effect]; $p < 0.05$, Table S8; Fig. 27b–d). The effect size of UVR and temperature × UVR on the N cell quota was found to be greater in both species (exceeding 50%, Fig. 27c). For C:P and N:P ratios, only the effect size of temperature in *I. galbana* and, notably, the effect size of UVR in *Chromulina* sp., proved stimulatory on C:N ratio, whereas the effect size of UVR and temperature × UVR was stimulatory on N:P ratio only in *I. galbana* (Fig. 27e, f).

b. Mixotrophic metabolism response to temperature and UVR

Isochrysis galbana and *Chromulina* sp. showed contrasting responses in the values of metabolic rates and in the magnitude and direction of the effect size of temperature, UVR, and temperature × UVR on most of these variables. Thus, the Φ_{PSII} area was higher in *I. galbana* than in *Chromulina* sp. (*t*-test $p < 0.05$; Table S6; Fig. 28a), whereas NPQ was lower in *I. galbana* than in *Chromulina* sp. (*t*-test $p < 0.05$; Table S6; Fig. S13a in the Supplementary Information). The specific-PP values in *I. galbana* were ca. 1/5 of those in *Chromulina* sp. ($p < 0.05$; Table S6; Fig. 28b). Accordingly, the %EOC values range 53.8%–72.2%, were higher in *I. galbana* than in *Chromulina* sp. ($p < 0.05$; Table S6; Fig. S13b). T × UVR interaction was significant for all these variables, but opposite effects between species were found (subplot effect; Table S9 in the Supplementary Information). The effect size of temperature and temperature × UVR on Φ_{PSII} area was inhibitory in *I. galbana* but stimulatory in *Chromulina* sp. ($p < 0.05$; Table S8; Fig. 29a), while the effect size of UVR was inhibitory in both species, with higher magnitude in *I. galbana* than in *Chromulina* sp. ($p < 0.05$; Table S8; Fig. 29a). Accordingly, the effect size of temperature, UVR, and

temperature × UVR on NPQ was stimulatory (even exceeding 100%), in *I. galbana* but inhibitory in *Chromulina* sp. ($p < 0.05$; Table S8; Fig. 29c). In contrast to Φ_{PSII} area, the effect size of temperature, UVR, and temperature × UVR was stimulatory on specific-PP in *I. galbana*, but inhibitory in *Chromulina*sp. (except for UVR; Fig. 29b). Notably, the effect size of temperature, UVR, and temperature × UVR on %EOC was inhibitory in both *I. galbana* and *Chromulina* sp., although their magnitudes were lower in *I. galbana* ($p < 0.05$ for UVR and temperature × UVR; Table S8; Fig. 29d).

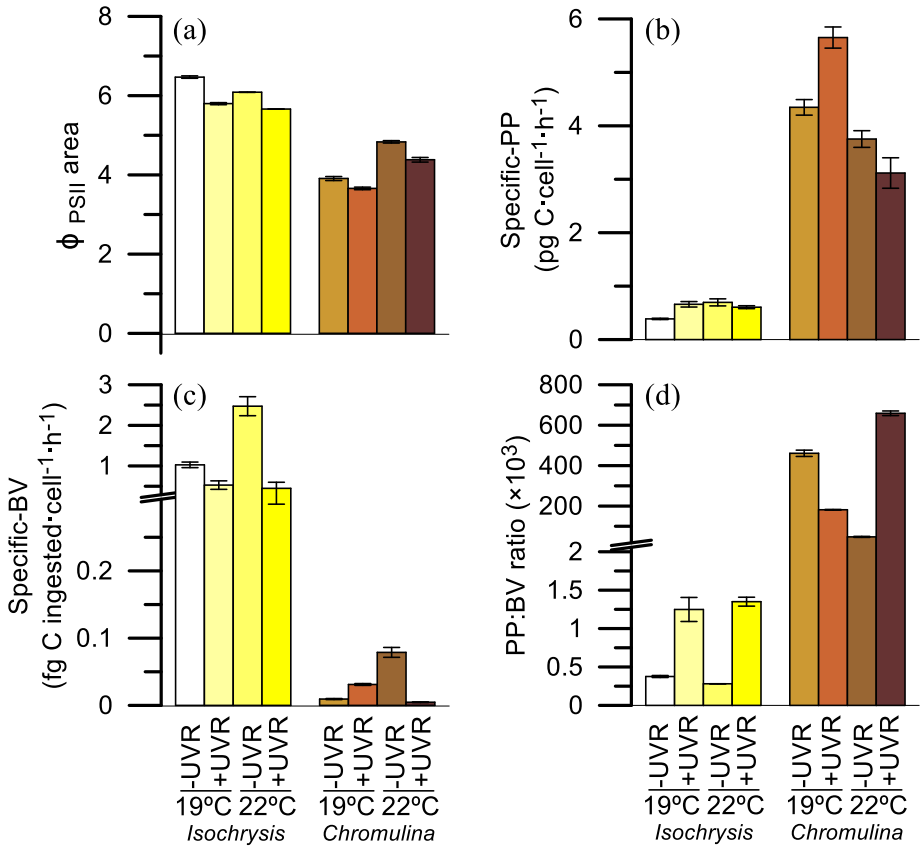

Figure 28. Metabolic variables of Isochrysis galbana and Chromulina sp. under Temperature (T) (low T [19°C] and high T [22°C]) and Light (full sunlight [+UVR] photosynthetically active radiation [-UVR]) treatments. Area under the curve for effective quantum yield (Φ_{PSII} area) (a), Specific primary production (specific-PP), (b), specific-bacterivory (specific-BV), (c) and PP:BV ratio (d). Data are expressed as mean values ± SD (n = 3).

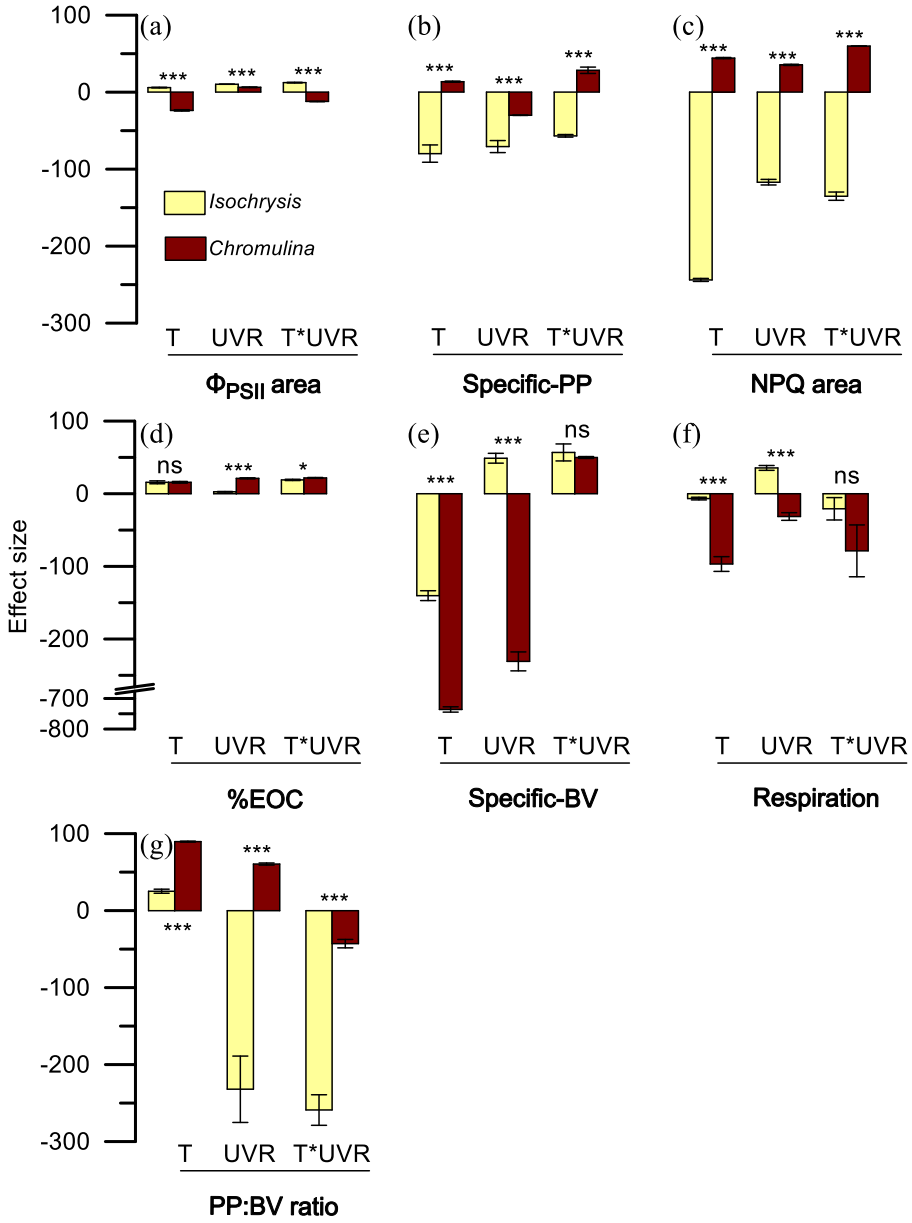

*Figure 29. Effect size of T, UVR, and T × UVR effect for the variables area under the curve for effective quantum yield (Φ_{PSII} area), (a) Specific primary production (specific-PP), (b) area under the curve for nonphotochemical quenching (NPQ area), (c) percentage of excreted organic carbon (%EOC), (d) specific-bacterivory (specific-BV), (e) respiration (R), (f) and PP:BV ratio (g) for Isochrysis galbana and Chromulina sp. Data are expressed as mean values ± SD (n = 3). Asterisks show the significance value: ***P < 0.001; *P < 0.05; ns: not significant.*

Regarding heterotrophic metabolism, the specific-BV was significantly higher in *Isochrysis galbana* than in *Chromulina* sp. (*t*-test $p < 0.05$; Table S6; Fig. 28c). The %BV in *I. galbana* and *Chromulina* sp. ranged from 1% to 35%, suggesting that mixotrophic protist activity was not limited by prey. Likewise, R rate was higher in *I. galbana* than in *Chromulina*sp. ($p < 0.05$; Table S6; Fig. S13c). There were significant T × UVR effects on both specific-BV and R rate in both species (subplot effect; Table S9). For specific-BV, the effect size of temperature was stimulatory, although the magnitude was lower in *I. galbana* (140%) than in *Chromulina* sp. (>700%). The effect size of UVR was opposite in the two species, being moderately (50%) inhibitory in *I. galbana* but strongly (>200%) stimulatory in *Chromulina* sp. ($p < 0.05$; Table S8; Fig. 29e). Finally, the effect size of temperature × UVR was (≈50%) inhibitory in both species, without significant differences between them ($p > 0.05$; Table S8; Fig. 29e). For R rate, the effect size of temperature and temperature × UVR was stimulatory for both species (Fig. 29f), the magnitude being greater in *Chromulina* sp. than in *I. galbana*, whereas the effect size of UVR was inhibitory in *I. galbana* but stimulatory in *Chromulina* sp. ($p < 0.05$; Table S8; Fig. 29f).

The PP:BV ratio was about two orders of magnitude higher in *Chromulina* sp. than in *Isochrysis galbana* ($p < 0.05$; Table S6; Fig. 28d). The effect size of temperature was inhibitory in both species, although of magnitude proved lower in *I. galbana* than in *Chromulina* sp. ($p < 0.05$; Table S8; Fig. 29g). The effect size of UVR was inhibitory in *Chromulina* sp. but strongly (>200%) stimulatory in *I. galbana* ($p < 0.05$; Table S8; Fig. 29g). Finally, the effect size of temperature × UVR was stimulatory in both species, particularly in *I. galbana* ($p < 0.05$; Table S8; Fig. 29g).

For each species and experimental condition, the difference between specific-BV and specific-PP (i.e., BV minus PP) from the results of the effect size (Fig. 29b,

e) is summarized in Figure 30. Our findings reveal that, while temperature exerted a common effect of stimulating the phagotrophic machinery with respect to photosynthesis in both species, UVR stimulated phagotrophy more in *Chromulina* sp. and the phototrophy more in *Isochrysis galbana*. Notably, the joint effect of temperature and UVR favored phototrophy machinery over phagotrophy in both cells.

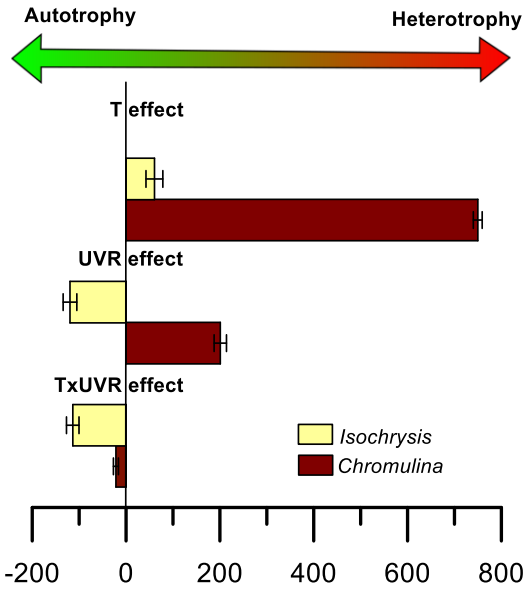

Figure 30. Comparative of machinery stimulation of specific primary production (specific-PP) or specific-bacterivory (specific-BV) in Isochrysis galbana and Chromulina sp. calculated as the difference between specific-BV and specific-PP from the results of the effect size of each factor (T, UVR and T × UVR).

4. Discussion

This study answered the key question concerning how the metabolic response to multiple stressors can differ in protists located in different positions along the mixotrophic gradient. We found two remarkable results: the first refered to the nutritional strategy of both species, while the second refered to the magnitude and direction of the effect of global-change factors on cell metabolism and the underlying mechanisms.

First, our results indicates that *Isochrysis galbana* has a proportionally greater dependence on photosynthesis than on phagotrophy, in agreement with Cabrerizo *et al*., (2017) and Anderson *et al*., (2018). However, *Chromulina* sp. acted more autotrophically than reported by Rottberger *et al*., (2013) and Jones and Ilmavirta, (1988). Therefore, our study revealed that *I. galbana* and *Chromulina* sp. were closer to autotrophy than to heterotrophy on the continuum of nutritional strategies established for mixotrophy by Mitra *et al*., (2016).

Despite that *Isochrysis galbana* exhibited a mostly autotrophic metabolism (high PP:BV values), this species displayed notable bacterivorous activity that corresponded to a higher respiratory rate and lower levels of NPQ than those shown by *Chromulina* sp.

The daily Φ_{PSII} differed between the two species, with *Chromulina* sp. showing the typical "U-shaped" curve during light-dark period, whereas *Isochrysis galbana* registered the strongest inhibition at the beginning of dark period (Fig. S14 in the Supplementary Information). Presumably, the low NPQ levels and excess light (exceeding the photosynthetic capacity of *I. galbana* and thus causing cumulative photodamage) gave rise to this atypical pattern of Φ_{PSII} (Aro *et al*., 1993; Ort, 2001). Surprisingly, *Chromulina* sp. showed greater predominance of autotrophic metabolism—that is, the highest PP:BV values, concomitant with high values of Chl *a* and N cell quota related to the great development of the photosynthetic apparatus (Kolber *et al*., 1988) and with higher NPQ values. The latter values could indicate a stronger photoprotective mechanism due to high photosynthetic activity (Halac *et al*., 2014; Cabrerizo *et al*., 2018). Stoichiometrically, both species suffered mineral limitation by N (*Isochrysis galbana*) and P (*Chromulina* sp.), related to their marine and freshwater origin.

Thus, according to these capacities, *Isochrysis galbana* and *Chromulina* sp. are type II constitutive mixotrophs (Mitra *et al*., 2016) or "phytoplankton" that feed on bacteria (Stoecker *et al*., 2017), although with low ingestion rates ($0.06 \cdot cell^{-1} \cdot h^{-1}$ for *I. galbana* and $0.002 \cdot cell^{-1} \cdot h^{-1}$ for *Chromulina* sp.).

Second, our complex experimental approach considered the temporal extent and action scales of press (over 1 month of warming 3°C) and pulse (6 h of UVR disturbance) as a realistic way to determine the metabolic trade-off of mixotrophs against these two global-change drivers. Thus, this study revealed that, regardless of their main nutritional strategy, the two species showed a similar metabolic trade-off in response to warming (Fig. 30). Warming favored the phagotrophic over the photosynthetic machinery in both species (Fig. 30) according to our hypothesis and the studies of Wilken *et al*., (2012) and Chan *et al*., (2018). For *Isochrysis galbana*, warming also stimulated specific-PP, apparently mediated by increasing metabolic pathways (i.e., RuBisCO; Helbling *et al*., 2011). The results also showed a notable mismatch between Φ_{PSII} and PP, as reported by Behrenfeld *et al*., (1998) and Gilbert *et al*., (2000). That Φ_{PSII} was inhibited (as also reported by Cabrerizo *et al*., 2018) and specific-PP stimulated by temperature was due probably to a change in coupling between electron transfer and C fixation (Moore *et al*., 2003; Wagner *et al*., 2006: Carrillo *et al*., 2015). The stimulation of both types of metabolism in *I. galbana* appears to be related to greater values for NPQ (Halac *et al*., 2014) and R (Smith *et al*., 2015). However, temperature as a single factor exerted a negative effect on specific-PP of *Chromulina* sp., in agreement with the results reported by Princiotta *et al*., (2016) for the chrysophyte *Dinobryon sociale* and by Sutton, (1972) for *Chromulina chionophila*. It is plausible that high temperature and the inhibition of NPQ to quench the excess of energy might provoke an accumulation of photodamage in *Chromulina* sp. Regarding cell stoichiometry, the absence of a significant effect of warming agrees with lack of response of C:N ratio of

phytoplankton community to temperature increase (Yvon-Durocher *et al*., 2017), although Yvon-Durocher *et al*., (2015) reported a higher N:P and C:P ratio under warming conditions for natural communities due to the decline of P-rich assembly machinery (ribosomes) relative to N-rich photosynthetic machinery.

The two species differed in their metabolic trade-off in response to UVR and it was similar for temperature × UVR (Fig. 30). Contrary to our hypothesis, UVR and temperature × UVR moved the cell metabolism of *Isochrysis galbana* toward autotrophy because of a stimulation of specific-PP and inhibition of specific-BV. The stimulation of specific-PP (also reported by Gao *et al*., 2007) was related to higher values of NPQ, consistent with their photoprotective function under UVR (Halac *et al*., 2014). The negative effect of UVR on specific-BV could be related to damage to the flagellar apparatus, leading to changes in cell morphology and motility (Sommaruga *et al*., 1996; Sommaruga & Buma, 2000). A positive effect of temperature × UVR on BV and a negative one on the electron-transport rate of *Isochrysis galbana* has been reported by Cabrerizo *et al*., (2018). By contrast, single UVR stimulated mainly phagotrophy in *Chromulina* sp., whereas temperature × UVR displaced the metabolism toward phototrophy. The phagotrophic ability of chrysophytes such as *Ochromonas* sp. and *Chromulina nevadensis* has been proposed as an adaptive strategy at high UVR levels in aquatic ecosystems (Carrillo *et al*., 2017; González-Olalla *et al*., 2018). This strategy could be based on the ability to circumvent the photoinhibition of PSII using only the PSI (Wilken *et al*., 2014) and deriving C from bacterial consumption. However, guided by specific-PP inhibition by temperature, the interaction temperature × UVR exerted a negative effect on the *Chromulina* sp., also inhibiting the specific-BV. In some species, phagotrophy is light-dependent, indicating that this species may need to synthesize some factor(s) during photosynthesis (Caron *et al*., 1993; Zhang & Watanabe, 2001). On this basis, *Chromulina* sp. could be considered an obligate phototroph.

In addition, cell stoichiometry was affected by UVR and temperature × UVR, both species exhibiting more balanced C:N ratios (close to 7.0) and N:P ratios (close to 16.0). Specifically, in *Isochrysis galbana* the C:N ratio rose and the N:P ratio fell, whereas in *Chromulina* sp. the nutrient ratio response was the opposite. These results contrast with others that have reported a fall in the C:N ratio in epilithic algae under UVR exposure (Tank *et al*., 2003) or no effect on marine phytoplankton (Carrillo *et al*., 2015). It bears noting that the stoichiometry after the action of the factors assayed became balanced, precluding its role as a first-order explanatory mechanism of the metabolic responses.

5. Conclusions

Warming and UVR induced shifts in the cell metabolism of both species from initial conditions, revealing a high metabolic trade-off (Fig. 30). This shift was consistently toward greater phagotrophy under a temperature increase, supporting our hypothesis. However, our study proved that temperature increase and UVR simultaneously affected the phototrophic and phagotrophic machinery in both mixotrophic protists, moving their metabolism toward greater autotrophy. The decrease in mixotrophy, driven by low phagotrophic activity, under temperature × UVR conditions could negatively affect the bypass of C flux through the bacteria-mixotroph link (Medina-Sánchez *et al*., 2004; Ptacnik *et al*., 2016), resulting in less efficient C flux and transfer inorganic nutrients in the aquatic food webs.

References

Anderson, R., Charvet, S. & Hansen, P. J. (2018). Mixotrophy in Chlorophytes and haptophytes—Effect of irradiance, macronutrient, micronutrient and vitamin limitation. *Front. Microbiol.* 9: 1704

APHA. (1992). Standard Methods for the Examination of Water and Wastewater. American Public Health Association, Washington, DC, USA

Aro, E. M., Virgin, I. & Andersson, B. (1993). Photoinhibition of photosystem II. Inactivation, protein damage and turnover. *Biochim. Biophys. Acta.* 1143: 113–34

Behrenfeld, M. J., Prasil, O., Kolber, Z. S., Babin, M. & Falkowski, P. G. (1998). Compensatory changes in Photosystem II electron turnover rates protect photosynthesis from photoinhibition. *Photosynth. Res.* 58: 259–68

Bell, T. B., Ahlgren, G. M. & Ahlgren, I. (1983). Estimating bacterioplankton production by measuring 3H-thymidine incorporation in a eutrophic Swedish lake. Appl. Environ. Microbiol. 45: 1709–21.

Buma, A. G. J., Boelen, P. & Jeffrey, W. (2003). UVR- induced DNA damage in aquatic organisms. In Helbling, E. W. & Zagarese, H. E. [Eds.] UV Effects in Aquatic Organisms and Ecosystems. Comprehensive Series in Photochemical and Photobiological Sciences. *The Royal Society of Chemistry, Cambridge.* pp. 291–327.

Cabrerizo, M. J., Carrillo, P., Villafañe, V. E. & Helbling, E. W. (2014). Current and predicted global change impacts of UVR, temperature and nutrient inputs on photosynthesis and respiration of key marine phytoplankton groups. *J. Exp. Mar. Biol. Ecol*. 461: 371–80

Cabrerizo, M. J., González-Olalla, J. M., Hinojosa-López, V. J., Peralta- Cornejo, F. J. & Carrillo, P. (2018). A shifting balance: responses of mixotrophic marine algae to cooling and warming under UVR. *New Phytol.* 221: 1317–27

Cabrerizo, M. J., Medina-Sánchez, J. M., Dorado-García, I., Villar-Argaiz, M. & Carrillo, P. (2017). Rising nutrient-pulse frequency and high UVR strengthen microbial interactions. *Sci. Rep.* 7: 43615

Caron, D. A., Sanders, R. W., Lim, E. L., Marras_e, C., Amaral, L. A., Whitney, S., Aoki, R. B. & Porte, K. G. (1993). Light-dependent phagotrophy in the freshwater mixotrophic chrysophytes Dinobryon cylinadricum. *Microb. Ecol.* 25: 93–111

Carrillo, P., Medina-Sánchez, J. M., Herrera, G., Durán, C., Segovia, M., Cortés, D., Salles, S., Korbee, N., Figueroa, F. L. & Mercado, J. M. (2015). Interactive effect of UVR and phosphorus on the coastal phytoplankton community of the western Mediterranean Sea: unravelling eco-physiological mechanisms. *PLoS ONE.* 10: e0142987

Carrillo, P., Medina-Sánchez, J. M. & Villar-Argaiz, M. (2002). The interaction of phytoplankton and bacteria in a high mountain lake: importance of the spectral composition of solar radiation. *Limnol. Oceanogr.* 47: 1294–306

Carrillo, P., Medina-Sánchez, J. M., Villar-Argaiz, M., Bullejos, F. J., Durán, C., Bastidas-Navarro, M., Souza, M. S., Balseiro, E. G. & Modenutti, B. E. (2017). Vulnerability of mixotrophic algae to nutrient pulses and UVR in an oligotrophic Southern and Northern Hemisphere lake. *Sci. Rep.* 7: 6333

Chan, Y. F., Chiang, K. P., Ku, Y. & Gong, G. C. (2018). Abiotic and biotic factors affecting the ingestion rates of mixotrophic nanoflagellates (Haptophyta). *Microb. Ecol.* 3: 607– 615

Del Giorgio, P. A. & Cole, J. J. (1998). Bacterial growth efficiency in natural aquatic systems. *Annu. Rev. Ecol. Syst.* 29: 503–41

Flynn, K. J., Stoecker, D. K., Mitra, A., Raven, J. A., Glibert, P. M., Hansen, P. J., Granéli, E. & Burkholder, J. M. (2013). Misuse of the phytoplankton–zooplankton dichotomy: the need to assign organisms as mixotrophs within plankton functional types. *J. Plankton Res*. 35: 3–11

Gao, K., Wu, Y., Li, G., Wu, H., Villafañe, V. E. & Helbling, E. W. (2007). Solar UV radiation drives CO2 fixation in marine phytoplankton: a double-edged sword. *Plant Physiol.* 144: 54–9

Gilbert, M., Domin, A., Becker, A. & Wilhelm, C. (2000). Estimation of primary productivity by chlorophyll a in vivo fluorescence in freshwater phytoplankton. *Photosynthetica*. 38: 111–26

González-Olalla, J. M., Medina-Sánchez, J. M., Cabrerizo, M. J., Villar-Argaiz, M., Sánchez-Castillo, P. M. & Carrillo, P. (2017). Contrasting effect of Saharan dust and UVR on autotrophic picoplankton in nearshore versus offshore waters of Mediterranean Sea. *J. Geophys. Res-Biogeo.* 122: 2085–103

González-Olalla, J. M., Medina-Sánchez, J. M., Lozano, I. L., Villar-Argaiz, M. & Carrillo, P. (2018). Climate-driven shifts in algal-bacterial interaction of high-mountain lakes in two years spanning a decade. *Sci. Rep.* 8: 10278

Guillard, R. R. L. & Ryther, J. H. (1962). Studies of marine planktonic diatoms. I. Cyclotella nana Husted, and Detonula confervacea (Cleve) Gran. *Can. J. Microbiol.* 8(2): 229–39

Halac, S. R., Guendulain-García, S. D., Villafañe, V. E., Helbling, E. W. & Banaszak, A. T. (2013). Responses of tropical plankton communities from the Mexican Caribbean to solar ultraviolet radiation exposure and increased temperature. *J. Exp. Mar. Biol. Ecol.* 445: 99–107

Halac, S. R., Villafañe, V. E., Gonçalves, R. J. & Helbling, E. W. (2014). Photochemical responses of three marine phytoplankton species exposed to ultraviolet radiation and increased temperature: role of photoprotective mechanisms. *J. Photoch. Photobio. B.* 141: 217–27

Halac, S. R., Villafañe, V. E. & Helbling, E. W. (2010). Temperature benefits the photosynthetic performance of the diatoms Chaetoceros gracilis and Thalassiosira weissflogii when exposed to UVR. *J. Photoch. Photobio. B.* 101: 196–205

Harris, R. M. B. *et al*. (2018). Biological responses to the press and pulse of climate trends and extreme events. *Nat. Clim. Change.* 8: 579–87

Helbling, E. W., Buma, A. G., Boelen, P., van der Strate, H. J., Fiorda Giordanino, M. V. & Villafañe, V. E. (2011). Increase in RuBisCO activity and gene expression due to elevated temperature partially counteracts ultraviolet radiation–induced photoinhibition in the marine diatom Thalassiosira weissflogii. *Limnol. Oceanogr.* 56: 1330–42

IPCC. (2013). Climate Change 2013: The Physical Science Basis. Contribution of Working Group I to the Fifth Assessment Report of the Intergovernmental Panel on Climate Change. In Stocker, T. F., Qin, D., Plattner, G. K., Tignor, M., Allen, S. K., Boschung, J., Nauels, A., Xia, Y., Bex, V. & Midgley, P. M. [Eds.] Cambridge University Press, Cambridge, UK and New York, NY, 1535 pp.

Jackson, M. C., Loewen, C. J. G., Vinebrooke, R. D. & Chimimba, C. T. (2016). Net effects of multiple stressors in freshwater ecosystems: a meta-analysis. *Glob. Change Biol.* 22: 180–9

Joint, I. & Jordan, M. B. (2008). Effect of short-term exposure to UVA and UVB on potential phytoplankton production in UK coastal waters. *J. Plankton Res.* 30: 199–210

Jones, R. & Ilmavirta, V. (1988). Flagellates in Freshwater Ecosystems. *Dev. Hydrob.* Springer Netherlands, Dordrecht, 288 pp

Kolber, Z., Zehr, J. & Falkowski, P. (1988). Effects of growth, irradiance and nitrogen limitation on photosynthetic energy conversion in photosystem II. *Plant Physiol.* 88: 923–9

Lee, S. & Fuhrman, J. A. (1987). Relationships between biovolume and biomass of naturally derived marine bacterioplankton. *Appl. Environ. Microbiol.* 53: 1298–303

Lignell, R. (1992). Problems in filtration fractionation of 14C primary productivity samples. *Limnol. Oceanogr.* 37: 172–8

Maxwell, K. & Johnson, G. N. (2000). Chlorophyll fluorescence—A practical guide. *J. Exp. Bot.* 51: 659–68

Medina-Sánchez, J. M., Villar-Argaiz, M. & Carrillo, P. (2004). Neither with nor without you: a complex algal control on bacterioplankton in a high mountain lake. *Limnol. Oceanogr.* 49: 1722–33

Mitra, A. *et al*. (2014). The role of mixotrophic protist in the biological carbon pump. *Biogeosciences*. 11: 995–1005

Mitra, A. *et al*. (2016). Defining planktonic protist functional groups on mechanisms for energy and nutrient acquisition: incorporation of diverse mixotrophic strategies. *Protist.* 167: 106–20

Modenutti, B. (2014). Mixotrophy in Argentina freshwaters. *Advanc. Limnol.* 65: 359–74

Montagnes, D. J. S., Morgan, G., Bissinger, J. E., Atkinson, D. & Weisse, T. (2008). Short-term temperature change may impact freshwater carbon flux: amicrobial perspective. *Glob. Change Biol.* 14: 2810–22

Moore, M. C., Suggett, D. J., Holligan, P. M., Sharples, J. & Abrahams, E. R. (2003). Physical controls on phytoplankton physiology at a shelf front: a fast repetition-rate fluorometer based field study. *Mar. Ecol. Prog. Ser.* 259: 29–45

Mühling, M., Harris, N., Belay, A. & Whitton, B. A. (2003). Reversal of helix orientation in the Cyanobacterium Arthrospira. *J. Phycol.* 39: 360–7

Ort, D. R. (2001). When there is too much light. *Plant Physiol.* 125: 29–32

Princiotta, S. D., Smith, B. T. & Sanders, R. W. (2016). Temperature-dependent phagotrophy and phototrophy in a mixotrophy Chrysophyte. *J. Phycol.* 52: 432–40

Ptacnik, R. *et al*. (2016). A light-induced shortcut in the planktonic microbial loop. *Sci. Rep.* 6: 29286

Raven, J. A., Beardall, J., Flynn, K. J. & Maberly, S. C. (2009). Phagotrophy in the origins of photosynthesis in eukaryotes and as a complementary mode of nutrition in phototrophs: relation to Darwin's insectivorous plants. *J. Exp. Bot.* 60: 3975–87

Reusch, T. B. H. & Boyd, P. W. (2013). Experimental evolution meets marine phytoplankton. *Evolution.* 67: 1849–59

Rojo, C., Herrera, G., Rodrigo, M. A., Ortíz-Llorente, M. J. & Carrillo, P. (2012). Mixotrophic phytoplankton is enhanced by UV radiation in a low altitude, P-limited Mediterranean lake. *Hydrobiologia.* 698: 97–110

Rottberger, J., Gruber, A., Boenigk, J. & Kroth, P. G. (2013). Influence of nutrients and light on autotrophic, mixotrophic and heterotrophic freshwater chrysophytes. *Aquat. Microb. Ecol.* 71: 179–91

Selosse, M. A., Charpin, M. & Not, F. (2017). Mixotrophy everywhere on land and in water: the grand écart hypothesis. *Ecol. Lett.* 20: 246–63

Smith, R. T., Bangert, K., Wilkinson, S. J. & Gilmour, D. J. (2015). Synergistic carbon metabolism in a fast growing mixotrophic freshwater microalgal species Micractinium inermum. *Biomass Bioenerg.* 82: 73–86

Sobrino, C. & Neale, P. J. (2007). Short-term and long-term effects of temperature on photosynthesis in the diatom Thalassiosira pseudonana under UVR exposures. *J. Phycol.* 43: 426–36

Sommaruga, R. & Buma, A. G. J. (2000). UV-induced cell damage is species-specific among aquatic phagotrophic protists. *J. Eukaryot. Microbiol.* 47: 450–5

Sommaruga, R., Oberleiter, A. & Psenner, R. (1996). Effect of UV radiation on the bacterivory of a heterotrophic nanoflagellate. *Appl. Environ. Microbiol.* 62: 4395–400

StatSoft Inc. (2005). Electronic Statistics Textbook. Tulsa, OK: Stat-Soft. [on-line] WEB: http://www.statsoft.com/textbook/stathome.html.

Steemann Nielsen, E. (1952). The use of radio-active carbon (C14) for measuring organic production in the sea. *J. Conseil.* 18: 117–40

Stoecker, D. K., Hansen, P. J., Caron, D. A. & Mitra, A. (2017). Mixotrophy in the marine plankton. *Annu. Rev. Mar.* Sci. 9: 311–35

Sutton, E. A. (1972). The physiology and life histories of selected Cryophytes of the Pacific Northwest. PhD thesis, Oregon State University, Corvalis, Oregon, USA, 107 pp.

Takabayashi, M., Lew, K., Johnson, A., Marchi, A. L., Dugdale, R. & Wilkerson, F. P. (2006). The effect of nutrient availability and temperature on chain length of the diatom, Skeletonema costatum. *J. Plankton Res.* 28: 831–40

Takahashi, S., Yoshioka-Nishimura, M., Nanba, D. & Badger, M. R. (2013). Thermal acclimation of the symbiotic alga Symbiodinium spp. alleviates photobleaching under heat stress. *Plant Physiol.* 161: 477–85

Tank, S. E., Schindler, D. W. & Arts, M. T. (2003). Direct and indirect effects of UV radiation on benthic communities: epilithic food quality and invertebrate growth in four montane lakes. *Oikos.* 103: 651–67

Tsai, S. F., Lin, F. W., Chan, Y. F. & Chiang, K. P. (2016). Vertical distribution of pigmented and non-pigmented nanoflagellates in the East China Sea. *Cont. Shelf Res.* 125: 107–13

Unrein, F., Massana, R., Alonso-Sáez, L. & Gasol, J. M. (2007). Significant year-round effect of small mixotrophic flagellates on bacterioplankton in an oligotrophic coastal system. *Limnol. Oceanogr.* 52: 456–69

Verity, P. G. (1981). Effects of temperature, irradiance, and daylength on the marine diatom Leptocylindrus danicus cleve. I. Photosynthesis and cellular composition. *J. Exp. Mar. Biol. Ecol.* 55: 79–91

Villafañe, V. E., Banaszak, A. T., Guendulain-García, S. D., Strauch, S. M., Halac, S. R. & Helbling, E. W. (2013). Influence of seasonal variables associated with climate change on photochemical diurnal cycles of marine phytoplankton from Patagonia (Argentina). *Limnol. Oceanogr.* 58: 203–14

Villafañe, V. E., Sundbäck, K., Figueroa, F. L. & Helbling, E. W. (2003). Photosynthesis in the aquatic environment as affected by UVR. In Helbling, E. W. & Zagarese, H. E. [Eds.] UV Effects in Aquatic Organisms and Ecosystems, Comprehensive Series in Photochemistry & Photobiology. The Royal Society of Chemistry, Cambridge, pp. 357–97

Villar-Argaiz, M., Medina-Sánchez, J. M., Biddanda, B. A. & Carrillo, P. (2018). Predominant non-additive effects of multiple stressors on autotroph C:N:P ratios propagate in freshwater and marine food webs. *Front. Microbiol.* 9: 69

Wagner, H., Jakob, T. & Wilhelm, C. (2006). Balancing the energy flow from captured light to biomass under fluctuating light conditions. *New Phytol.* 169: 95–108

Ward, B. A. & Follows, M. J. (2016). Marine mixotrophy increases trophic transfer efficiency, mean organism size, and vertical carbon flux. *Proc. Natl Acad. Sci. USA.* 113: 2958–63

Wilken, S., Huisman, J., Naus-Wiezer, S. & Van Donk, E. (2012). Mixotrophic organisms become more heterotrophic with rising temperature. *Ecol. Lett.* 16: 225–33

Wilken, S., Schuurmans, J. M. & Matthijs, H. C. P. (2014). Do mixotrophs grow as photoheterotrophs? Photophysiological acclimation of the chrysophytes Ochromonas danica after feeding. *New Phytol.* 204: 882–9

Yvon-Durocher, G., Dossena, M., Trimmer, M., Woodward, G. & Allen, A. P. (2015). Temperature and the biogeography of algal stoichiometry. *Glob. Ecol. Biogeogr.* 24: 562–70

Yvon-Durocher, G., Schaum, C. E. & Trimmer, M. (2017). The temperature dependence of phytoplankton stoichiometry: investigating the roles of species sorting and local adaptation. *Front. Microbiol.* 8: 2003

Zhang, X. & Watanabe, M. M. (2001). Grazing and growth of the mixotrophic Chrysomonad Poterioochromonas malhamensis (Chrysophyceae) feeding on algae. *J. Phycol.* 37: 738–43

Zubkov, M. V. & Tarran, G. A. (2008). High bacterivory by the smallest phytoplankton in the North Atlantic Ocean. *Nature.* 455: 224–6

Supplementary Information

This Supplementary material contains figures from S13 to S14 and tables from S6 to S9.

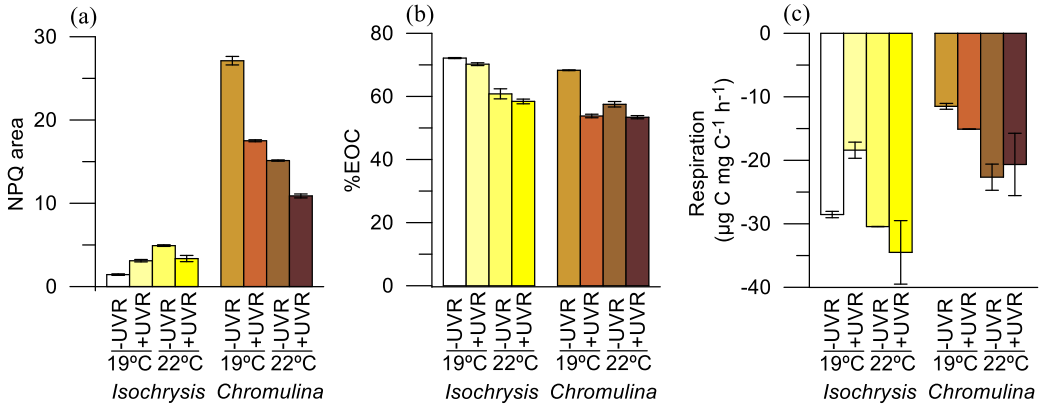

Figure S13. Metabolic and physiologic variables of Isochrysis galbana and Chromulina sp. under Temperature (T) (low T [19°C] and high T [22°C]) and Light (full sunlight [+UVR] photosynthetically active radiation [-UVR]) treatments. Respiration (R), (a), percentage of excreted organic carbon (%EOC), (b) and area under the curve for nonphotochemical quenching (NPQ area), (c) for Isochrysis galbana and Chromulina sp. Data are expressed as mean values ± SD (n = 3).

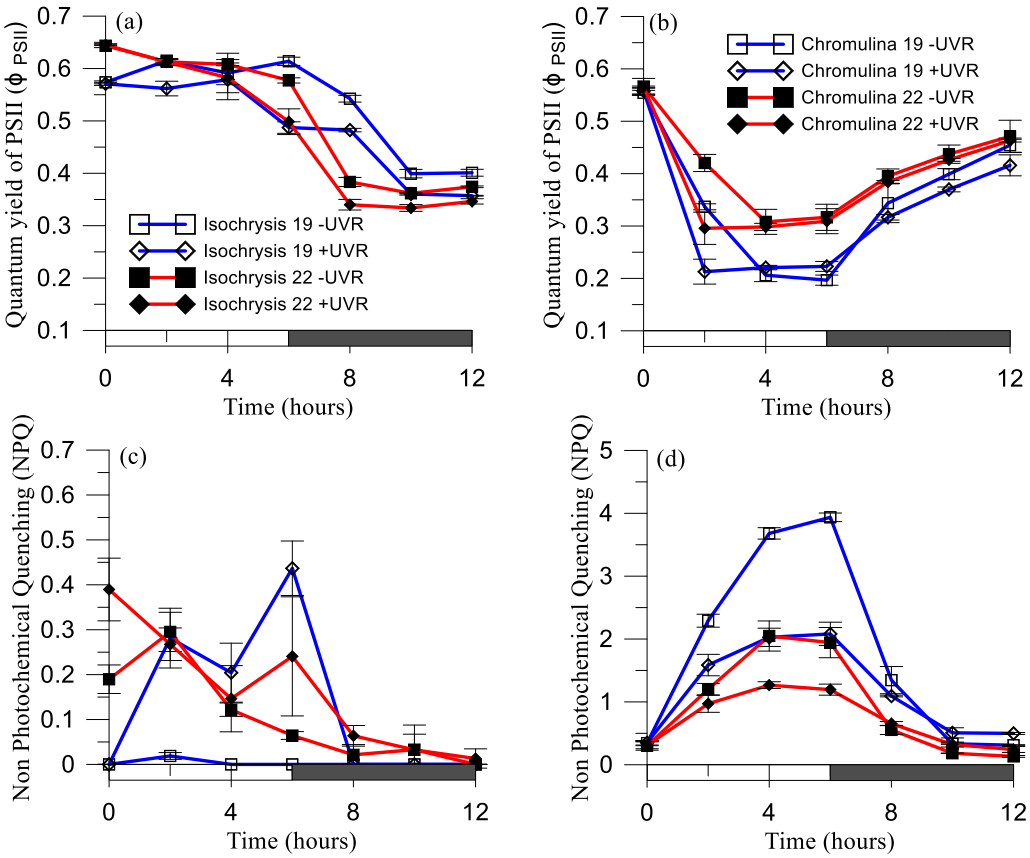

Figure S14. Photobiological variables of Isochrysis galbana and Chromulina sp. under Temperature (T) (low T [19°C] and high T [22°C]) and Light (full sunlight [+UVR] photosynthetically active radiation [-UVR]) treatments. Effective quantum yield (Φ_{PSII}) (a, b) and nonphotochemical quantum yield (NPQ), (c,d) values for I. galbana (left panel) and Chromulina sp. (right panel). Horizontal white and shaded areas on "X axis, time" represent the light and dark exposure period, respectively, throughout the experiment.

Table S6. Results of the t-test for independent samples to analyse the differences between species for each response variable [cell-specific Chl a, C cell quota, N cell quota and P cell quota, C:N and N:P ratios, area under the curve for photochemical quantum yield area (Φ_{PSII} area), specific primary production (sPP), specific-bacterivory (sBV), PP:BV ratio, area under the curve for non-photochemical quenching area (NPQ area), percentage of excreted organic carbon (%EOC), and respiration (R)], under identical experimental conditions.

Variable		Mean *Chromulina* sp.	Mean *I. galbana*	t-value	df	*p*		Mean *Chromulina* sp.	Mean *I. galbana*	t-value	df	*p*
Cell specific Chl *a* PAR		2.2	0.6	394.34	4	<0.001		2.1	0.6	950.99	4	<0.001
Cell specific Chl *a* UVR		2.2	0.6	428.12	4	<0.001		2.0	0.7	72.39	4	<0.001
C cell quota PAR		1240.7	558.3	13.15	4	<0.001		541.9	661.6	-2.50	4	0.066
C cell quota UVR		1141.5	622.9	9.87	4	<0.001		525.6	578.3	-0.57	4	0.597
N cell quota PAR		494.2	18.8	49.75	4	<0.001		443.2	17.2	7.84	4	<0.01
N cell quota UVR		133.8	36.9	22.21	4	<0.001		220.6	41.9	3.95	4	<0.05
P cell quota PAR		10.5	3.6	17.49	4	<0.001		8.9	5.4	31.25	4	<0.001
P cell quota UVR		9.6	4.1	47.29	4	<0.001		9.4	4.9	13.44	4	<0.001
C:N ratio PAR		2.5	29.8	-10.52	4	<0.001		1.2	38.5	-13.59	4	<0.001
C:N ratio UVR		8.5	16.9	-4.15	4	<0.05		2.4	13.8	-6.73	4	<0.01
N:P ratio PAR		47.0	5.2	15.60	4	<0.001		49.9	3.2	7.04	4	<0.01
N:P ratio UVR		13.9	8.9	5.57	4	<0.01		23.4	8.6	2.61	4	0.059
Φ_{PSII} area PAR	19ºC	3.9	6.5	-75.75	4	<0.001	22ºC	4.8	6.085	-73.08	4	<0.001
Φ_{PSII} area UVR		3.7	5.8	-88.85	4	<0.001		4.4	5.660	-38.48	4	<0.001
sPP PAR		4.3	0.4	46.58	4	<0.001		3.8	0.696	31.28	4	<0.001
sPP UVR		5.7	0.7	42.17	4	<0.001		3.1	0.606	15.27	4	<0.001
sBV PAR		0.0	1.0	-25.71	4	<0.001		0.1	2.472	-17.68	4	<0.001
sBV UVR		0.0	0.5	-8.24	4	<0.01		0.0	0.449	-5.14	4	<0.01
PP:BV ratio PAR		463413.3	376.9	34.45	4	<0.001		48283.3	281.361	17.99	4	<0.001
PP:BV ratio UVR		181702.4	1301.5	197.94	4	<0.001		580086.2	1548.294	127.41	4	<0.001
NPQ area PAR		27.1	1.4	85.32	4	<0.001		15.1	4.921	143.20	4	<0.001
NPQ area UVR		17.5	3.1	130.64	4	<0.001		10.9	3.365	29.83	4	<0.001
%EOC PAR		68.3	72.2	-34.53	4	<0.001		57.5	60.811	-3.16	4	<0.05
%EOC UVR		53.8	70.2	-39.53	4	<0.001		53.4	58.417	-9.67	4	<0.001
R PAR		-11.5	-28.5	43.73	4	<0.001		-22.7	-30.433	6.55	4	<0.01
R UVR		-15.1	-18.4	4.51	4	<0.05		-20.7	-34.506	3.43	4	<0.05

Table S7. Results of the two-way split-plot analysis of variance of Temperature (T) and UVR effects on cell-specific Chl a, C cell quota, N cell quota and P cell quota, C:N and N:P ratios. Numbers in bold indicate significant effect.

	Cell specific Chl *a*		C cell quota		N cell quota		P cell quota		C:N ratio		N:P ratio	
Isochrysis galbana												
Main plot effect	$F_{1,4}$	*p*	$F_{1,4}$	*p*	$F_{1,4}$	*p*	$F_{1,4}$	*p*	$F_{1,4}$	*p*	$F_{1,4}$	*p*
T	58.61	**0.002**	0.354	0.584	0.719	0.444	157.5	**<0.001**	0.809	0.419	2.98	0.159
Sub-plot effect												
UVR	5.03	0.088	0.127	0.739	904.7	**<0.001**	0.554	0.498	736.6	**<0.001**	481.8	**<0.001**
UVR×T	12.94	**0.023**	7.98	**0.047**	21.9	**0.009**	481.5	**<0.001**	73.01	**0.001**	16.28	**0.016**
Chromulina sp.												
Main plot effect												
T	483.9	**<0.001**	105.1	**<0.001**	0.127	0.740	9.172	**0.039**	44.10	**0.003**	0.97	0.381
Sub-plot effect												
UVR	1992	**<0.001**	3.827	0.122	2958	**<0.001**	0.716	0.445	134.9	**<0.001**	616.7	**<0.001**
UVR×T	3574	**<0.001**	1.977	0.232	165.5	**<0.001**	11.36	**0.028**	61.85	**0.001**	7.63	0.051

Table S8. Results of the t-test for independent samples to analyse the differences between species on the variables [cell-specific Chl a, C cell quota, N cell quota and P cell quota, C:N and N:P ratios, area under the curve for photochemical quantum yield area (Φ_{PSII} area), specific primary production (sPP), specific-bacterivory (sBV), PP:BV ratio, area under the curve for non-photochemical quenching area (NPQ area), percentage of excreted organic carbon (%EOC), and respiration (R)], for the effect size of T, UVR, and T×UVR.

Variable	Effect	Mean *Chromulina* sp.	Mean *I. galbana*	t-value	df	p	Variable	Effect	Mean *Chromulina* sp.	Mean *I. galbana*	t-value	df	p
Cell spec. Chl *a*	T	1.9	-6.5	76.23	4	<0.001	Φ_{PSII} area	T	-23.7	5.9	-54.95	4	<0.001
Cell spec. Chl *a*	UVR	-0.7	1.9	-19.85	4	<0.001	Φ_{PSII} area	UVR	6.4	10.4	-18.29	4	<0.001
Cell spec. Chl *a*	T×UVR	6.4	-14.9	7.5	4	<0.01	Φ_{PSII} area	T×UVR	-12.1	12.5	-108.71	4	<0.001
C cell quota	T	56.4	-18.4	39.43	4	<0.001	sPP	T	13.7	-79.8	14.44	4	<0.001
C cell quota	UVR	7.7	-11.4	3.26	4	<0.05	sPP	UVR	-30.1	-70.6	8.98	4	<0.001
C cell quota	T×UVR	57.9	-3.4	9.46	4	<0.001	sPP	T×UVR	28.4	-56.8	33.26	4	<0.001
N cell quota	T	10.7	7.9	0.28	4	0.792	sBV	T	-735.9	-140.3	-93.45	4	<0.001
N cell quota	UVR	72.9	-96.9	90.29	4	<0.001	sBV	UVR	-230.8	48.9	-32.97	4	<0.001
N cell quota	T×UVR	55.7	-124.8	17.63	4	<0.001	sBV	T×UVR	49.9	56.8	-1.02	4	0.364
P cell quota	T	15.4	-49.5	26.44	4	<0.001	PP:BV ratio	T	89.7	25.2	41.95	4	<0.001
P cell quota	UVR	8.3	-13.9	7.11	4	<0.01	PP:BV ratio	UVR	60.6	-232.0	11.73	4	<0.001
P cell quota	T×UVR	10.5	-34.5	35.28	4	<0.001	PP:BV ratio	T×UVR	-42.9	-259.0	18.24	4	<0.001
C:N ratio	T	51.9	-29.6	13.22	4	<0.001	NPQ area	T	44.2	-243.9	236.07	4	<0.001
C:N ratio	UVR	-241.1	43.6	-26.69	4	<0.001	NPQ area	UVR	35.4	-116.9	70.83	4	<0.001
C:N ratio	T×UVR	8.4	53.9	-1.65	4	0.175	NPQ area	T×UVR	59.9	-135.1	62.36	4	<0.001
N:P ratio	T	-5.3	38.3	-5.08	4	<0.01	%EOC	T	15.8	15.7	0.03	4	0.974
N:P ratio	UVR	70.3	-72.6	197.16	4	<0.001	%EOC	UVR	21.2	2.7	39.68	4	<0.001
N:P ratio	T×UVR	51.2	-67.6	10.67	4	<0.001	%EOC	T×UVR	21.8	19.0	4.54	4	<0.05
							R	T	-96.8	-6.7	-15.13	4	<0.001
							R	UVR	-31.4	35.5	-18.62	4	<0.001
							R	T×UVR	-78.6	-20.7	-2.58	4	0.061

Table S9. Results of the two-way split-plot analysis of variance of Temperature (T) and UVR effects on area under the curve for photochemical quantum yield area (Φ_{PSII} area), specific primary production (sPP), specific-bacterivory (sBV), PP:BV ratio, area under the curve for non-photochemical quenching area (NPQ area), percentage of excreted organic carbon (%EOC), and respiration (R). Numbers in bold indicate significant effect.

	Φ_{PSII} area		sPP		sBV		PP:BV ratio		NPQ area		%EOC		R	
Isochrysis galbana														
Main plot effect	$F_{1,4}$	*p*	$F_{1,4}$	*p*	$F_{1,4}$	*p*	$F_{1,4}$	*p*	$F_{1,4}$	*p*	$F_{1,4}$	*p*	$F_{1,4}$	*p*
T	260.6	**<0.001**	15.61	**0.017**	31.53	**0.005**	0.151	0.717	152.5	**<0.001**	276.1	**<0.001**	34.42	**0.004**
Sub-plot effect														
UVR	276192	**<0.001**	32.71	**0.005**	2244	**<0.001**	32.69	**0.005**	0.546	0.501	73.85	**0.001**	4.309	0.107
UVR×T	13851	**<0.001**	127.6	**<0.001**	819.9	**<0.001**	0.798	0.422	415.9	**<0.001**	0.77	0.429	23.69	**0.008**
Chromulina sp.														
Main plot effect														
T	562.2	**<0.001**	94.03	**<0.001**	83.74	**<0.001**	1.283	0.321	2073	**<0.001**	161.6	**<0.001**	17.22	**0.014**
Sub-plot effect														
UVR	1335	**<0.001**	71.31	**0.001**	175.2	**<0.001**	313.4	**<0.001**	3275	**<0.001**	2860	**<0.001**	0.900	0.396
UVR×T	112.4	**<0.001**	595.6	**<0.001**	585.2	**<0.001**	3315	**<0.001**	491.4	**<0.001**	892.2	**<0.001**	11.27	**0.028**

CHAPTER 6

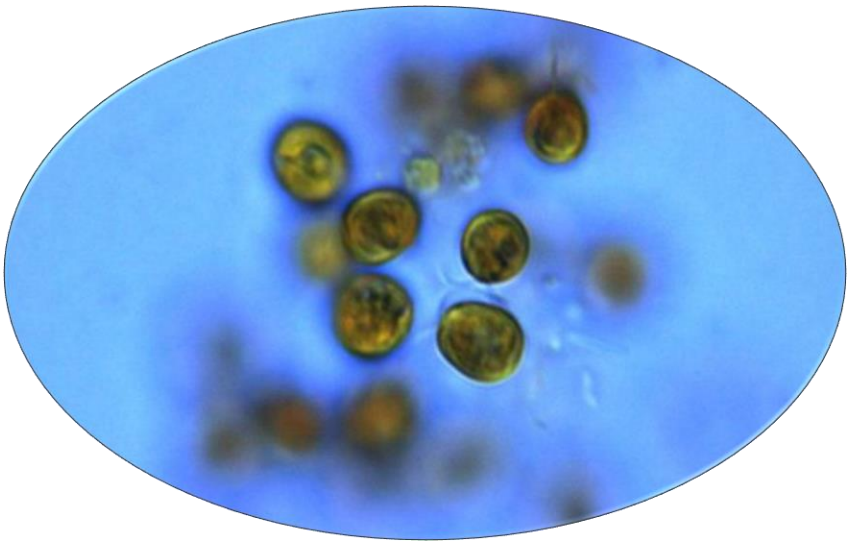

***Isochrysis galbana* cells**
(JRYoung SEM colln)

CHAPTER 6 - Regulation of phagotrophy in the mixotrophic haptophyte *Isochrysis galbana*

J. M. González-Olalla, P. Carrillo, J. M. Medina-Sánchez and M. Giordano

Abstract

Mixotrophy combines autotrophy and phagotrophy in the same cell. However, it is not known to what extent the relative proportion of phototrophy and phagotrophy influences metabolism, cell composition, and growth. Previous results suggest that phagotrophy in mixotrophs increases under low availability of resources (light and nutrients) in order to gain these resources from bacterial biomass. In this work, we assess, on the one hand, the role of phagotrophy in the cell metabolism, C, N, and S enzymatic activities and elemental and biochemical composition of *Isochrysis galbana*. On the other hand, we study how a predicted increase of phagotrophy under environmental conditions of low light and nutrients can affect the metabolism and growth of *I. galbana*. Our results for the first test revealed that consumption of bacteria stimulated β-carboxylases and glutamine synthetase activities and favored homeostasis of cell composition in *I. galbana*; in addition, the bacterivory increased the phosphorous and iron content, accelerating cell division, and improving the cell fitness. For the second test, under light or nutrient scarcity, *I. galbana* grew more slowly despite greater bacterial consumption, and the enzymatic activities were devoted to dissipation of reducing power excess. Contrary to recent studies, the phagotrophy under low nutrient and low irradiance does not always imply greater C flux, but it may be a mechanism to endure these adverse conditions.

1. Introduction

Mixotrophy is a mode of nutrition that combines phototrophy and heterotrophy in a single cell, where heterotrophy involves the utilization of either soluble

(osmotrophy) or particulate (phagotrophy) organic matter (Selosse *et al.*, 2017). In this paper, we use the term "mixotrophy" to refer to organisms that are phototrophs and phagotrophs simultaneously, with phagotrophy involving mostly bacterivory (Flynn *et al.*, 2013). Bacterivory (BV), in mixotrophic protists, can make use of elements such as carbon (C) nitrogen (N), phosphorus (P) and iron (Fe) acquired from the organic matter ingested, to supplement phototrophic metabolism (e.g. *Dinobryon divergens;* Rottberger *et al.*, 2013) or as a major nutritional source (e.g. *Ochromonas* sp.; Sanders *et al.*, 2001). BV also provides energy through the oxidation of organic matter (Raven, 1997; Stoecker *et al.*, 2017). Various studies have suggested that mixotrophs constitute a bypass in the energy flow in trophic webs (Medina-Sánchez *et al.*, 2004; Ptacnik *et al.*, 2016; Ward & Follows, 2016) and, in some cases, their contribution to nutrient fluxes can be greater than that of pure phototrophs (Mitra *et al.*, 2014; Stoecker *et al.*, 2017). The degree of phagotrophy in mixotrophs is to some extent genotypically fixed (Yelton *et al.*, 2016; McKie-Krisberg *et al.*, 2018), but it also results from acclimatory responses to environmental conditions (Flöder *et al.*, 2006; Unrein *et al.*, 2013; Selosse *et al.*, 2017). Even in the same organism, nutrition can range from full reliance on photosynthesis to prevailing heterotrophy with only a minor contribution of photosynthetic C fixation (Mitra *et al.*, 2016). In most cases, however, both phototrophic and phagotrophic machineries are maintained concomitantly. This may bring higher energetic costs, compared to exclusive autotrophs or heterotrophs (Raven, 1997; Ward *et al.*, 2011), although the persistence and diversity of mixotrophic organisms suggest that advantages surpass the physiological costs (Selosse *et al.*, 2017).

It has been proposed that the prevalence of mixotrophic organisms is often associated with light and/or nutrient limitation (Modenutti, 2014; McKie-Krisberg *et al.*, 2018), as observed for the flagellate chrysophyte *Ochromonas* sp. (Keller *et al.*, 1994), the cryptophyte *Geminigera cryophila* and the prasinophyte

Mantoniella antarctica (McKie-Krisberg *et al.*, 2015). However, a controversy exists over the environmental conditions that favors mixotrophy (Edwards, 2019), since some mixotrophs can also grow faster and become better competitors than strict autotrophs at high irradiance (see for example the dinophycean *Fragilidium subglobosum* in Hansen & Nielsen, 1997 and for *Ochromonas minima* in Fischer *et al.*, 2017a); this may be due to the occurrence of a synergy between nutrients from phagotrophy and photosynthetically fixed C from phototrophic machinery (Edwards, 2019). This contention is consistent with the high abundance of mixotrophs in oligotrophic and transparent waters in oceans (Unrein *et al.*, 2013). Also in haptophytes, phagotrophic activity can be modulated by irradiance although its effect is not clear. Thus, low light (5-25 µmol photons m^{-2} s^{-1}) conditions have been shown to bolster phagotrophy in *Chrysochromulina ericina* (Hansen & Nielsen, 1997) but weaken it in *Isochrysis galbana* (Anderson *et al.*, 2018).

The regulation of phagotrophy may help maintain (or constrain) composition homeostasis (Giordano, 2013; Moorthi *et al.*, 2017) and drive C partitioning among cellular pools (Montechiaro *et al.*, 2006; Palmucci *et al.*, 2011). However, the mechanisms by which phagotrophy influences cell composition remain unknown, and the phagotrophy-dependent processes involved in metabolism regulation and gene expression are not fully understood (McKie-Krisberg *et al.*, 2018). Lie *et al.*, (2018) showed that phagotrophic strains of *Ochromonas* sp. upregulated the genes involved in Calvin Cycle after prey depletion; on the other hand, in a more phototrophic strain of the same species, genes related to light harvesting and Calvin cycle were up-regulated when prey were available, suggesting, again, a synergic effect of phagotrophy and phototrophy. In *Prymnesium parvum*, changes in irradiance caused alterations in the expression of thousands of genes related to C and N metabolism. Thus, in the light, the expression of genes such as phosphoenolpyruvate carboxylase (PEPC) and

glutamine synthetase (GS) were higher than in the dark, suggesting that these enzymes were stimulated when photosynthesis was the main source of energy for the cell (Liu *et al.*, 2016). In the dark and/or in the presence of bacterial prey, when phagotrophy was the main source of C, the activities of pyruvate carboxylase (PYC; Lie *et al.*, 2017) and phosphoenolpyruvate carboxykinase (PEPCK) were stimulated in *Prymnesium parvum* (Liu *et al.*, 2016; Lie *et al.*, 2017). Thus, not surprisingly, it appears that different pathways for the assimilation and allocation of C and N are activated, depending on the prevalence of phototrophy or heterotrophy. However, the consequences of these metabolic differences in terms of nutrient utilization and C allocation remain unclear.

Based on the above information and on the gaps in knowledge that emerge from the literature, we formulated two objectives that were tested through two independent tests: In a first test, our objective was to know how phagotrophy affects the metabolism and composition of *I. galbana*. Our hypothesis is that phagotrophy improves the composition and stoichiometric balance in the cell by facilitating the concomitant maintenance of the photosynthetic machinery and enhancing cell growth. A second objective was to study the composition and metabolic regulation mechanisms in *I. galbana* when grows under conditions of light or nutrients scarcity. Our hypothesis is that low light and low nutrient increase phagotrophic activity but decrease the growth rate of *I. galbana* due to its predominantly phototrophic metabolism.

In marine as well as freshwater environments (Caron, 2016; Keeling & Del Campo, 2017), small (<20μm) mixotrophic flagellate protists appear to be important. So far, most studies have focused on dinoflagellates (Burkholder *et al.*, 2008; Jeong *et al.*, 2010) due to their important role in marine ecosystems (Hinder *et al.*, 2012). However, in the sea, small haptophytes (3-5 μm) can also exert strong predatory pressure on the bacterial population (Zubkov & Tarran, 2008) and a significant part of total BV is often attributable to them (Frias-Lopez *et al.*,

2009; Unrein *et al.*, 2013). *Isochrysis galbana* Parke, our experimental organism, is a well-characterized small marine haptophyte and widespread mixotrophic marine haptophyte (Guiry MD, 2017), which can strongly influence bacterial abundance (Cabrerizo *et al.*, 2019; González-Olalla *et al.*, 2019).

2. Material and Methods

a. Experimental setup

Isochrysis galbana was isolated from the southern Atlantic Ocean and maintained in the laboratory in xenic cultures: cells were grown semicontinuously in F/2 medium enriched with vitamins (Guillard & Ryther, 1962) in 0.5 L Erlenmeyer flasks in a Perani FT 700 (Climatic Technologies Industry, Milan, Italy) growth chamber, at 20ºC. The culture received 100 µmol photons m^2 s^{-1} of photosynthetically active radiation (PAR, 400-700 nm), in a 12:12 h light/dark cycle. The flasks were shaken manually twice per day. These conditions were considered as xenic treatment (hereafter named "*X*" treatment).

Three independent tests were carried out to corroborate our hypotheses (Table 8): 1) Comparison of xenic (*X* treatment) *vs* axenic treatment (hereafter named "*AX*" treatment). In the axenic treatment, cells were maintained in these same conditions, but in the absence of bacteria. Axenicity was established using a mix of antibiotics: ampicillin (25 µg mL^{-1}), gentamycin (5 µg mL^{-1}), kanamycin (10 µg mL^{-1}), neomycin (37.5 µg mL^{-1}), and streptomycin (5 µg mL^{-1}). The antibiotic concentrations were the lowest required to establish an axenic culture. After to achieve the axenic conditions, the culture was daily diluted at 20% adding fresh medium. This allowed to maintain the cells in exponential growth and to wash the antibiotics from the culture. The impact of the antibiotics on the algae was evaluated by determining the maximum quantum yield (Fv/Fm) and verifying that it was not lower than in the *X* treatment ($p>0.05$) (Table 8). The absence of bacteria in the cultures was checked after 48 hours since the addition of the

antibiotics and them every two days by adding 100 µL of culture to 60 x 15 mm sterile Petri dishes with F/2 medium, agar (1.5% w/w), peptone (0.5% w/w) and yeast extract (0.1% w/w). Cultures were retained and used for the experiments only when no bacterial growth was detected after 20 days.

Table 8. Scheme of experimental design.

First test			
Axenic cultura	Xenic culture		
Axenic treatment (AX)	Xenic treatment (X)	Low light xenic Treatment (X_{LL})	Low nutrient xenic treatment (X_{LN})
	Xenic cultures		
	Second and third test		

2) Comparison of xenic cultures grown at the high (100 µmol photons m^2 s^{-1}; *X* treatment) and low (25 µmol photons m^2 s^{-1}; low light xenic treatment, named "X_{LL}" treatment) irradiance. The low-light treatment differed from the high light one only for the irradiance; all other conditions were the same described above.
3) Comparison of xenic cultures grown in F/2 (*X* treatment) and in F/40 media (low nutrient xenic treatment, named "X_{LN}" treatment).

For the *X*, *AX* and X_{LL} treatments, the cell density was about 2×10^6 cell mL^{-1}; for the X_{LN} treatment the cell density was 1×10^6 cell mL^{-1}. All experiments were conducted in triplicate (i.e. three independent cultures per treatment were used for all measurements). Cells were allowed to acclimate to each growth regime for at least 5 generations.

b. Growth rate and cell size

Cell numbers of *I. galbana* and mean cell size were determined with an automatic cell counter (CASY TT, Innovatis AG, Reutlingen, Germany). The maximum

growth rate was calculated from the cell counts, in batch cultures, according to the following equation:

$$\mu = \frac{\mathrm{Ln}\ C_2 - \mathrm{Ln}\ C_1}{t_2 - t_1}$$

where C is cell abundance (cell mL^{-1}) at time (t) 1 and 2 within the exponential growth phase.

After determining the maximum growth rate, we maintained the cultures at this phase by applying a corresponding dilution rate. The net biomass production rate, expressed as C assimilated per day (fg C $cell^{-1}$ day^{-1}), was calculated by multiplying the growth rates by the C-cell quota.

c. Photosynthesis

c.1 Oxygen production and consumption

From each replicate, samples were transferred to transparent Teflon bottles provided of O_2 sensor-spot optodes (SP-PSt3-NAU-D5-YOP; PreSens GmbH, Germany; more details in Medina-Sánchez *et al.*, 2017). The bottles were gently filled, avoiding the formation of bubbles, sealed to avoid gas exchanges, and incubated at 20°C, under an irradiance of 100 µmol m^2 s^{-1}, except in the low-light treatment, where the irradiance was 25 µmol m^2 s^{-1}. Net O_2 production was measured over 6 h from the start of the light period using an OXY-4 mini oxygen meter (Presens GmbH, Regensburg, Germany) and analyzed with Oxyview 6.02 software (Presens GmbH, Regensburg, Germany). Values were corrected by temperature and atmospheric pressure.

The consumption of O_2 was measured on the same samples, subsequently incubated in the dark for 6 h. The rates of O_2 production and consumption (in mg O_2 L^{-1} h^{-1}) were calculated as the slope of the linear portion of the curve representing O_2 production/consumption vs. time.

For each culture, an additional set of Teflon bottles was filled with samples filtered through filters of 1 µm pore size (Whatman GF/B; Whatman®, Sanford, ME, USA). Bacterial respiration was not significantly different among xenic treatments ($p>0.05$). These samples were used to determine bacterial respiration in the light and in the dark; the resulting values were used to correct O_2 production and consumption by algae.

c.2 Chlorophyll fluorescence

The maximum quantum yield (Fv/Fm) of photosystem II (PS_{II}) was measured with an Aquapen AP100 fluorometer (Photon System Instruments, Drásov, Czech Republic). Chlorophyll was excited with blue light (455 nm). Samples were dark-adapted for 20 min before measurements to ensure that all the PS_{II} centers were open. The maximum fluorescence, Fm, was determined upon illumination with a saturating flash (Sun & Wang, 2018).

d. Bacterivory and Bacterial Production

BV was quantified as the amount of bacteria labeled with ^{3}H-thymidine that was incorporated by *I. galbana* cells (Cabrerizo *et al.*, 2019). Simultaneously, ^{3}H-thymidine uptake by bacteria was used to measure bacterial production (BP). For these measurements, a 10 mL aliquot was sampled from each flask and transferred to 40-mL Teflon bottles; subsequently, the cells were incubated for 1 h in the presence of 25 nM ^{3}H-thymidine, at the same irradiance used for growth. After incubation, BV was stopped by adding neutralized formaldehyde to the samples (2.5% w/v final concentration). Blanks were formaldehyde-killed before incubation and otherwise treated as the samples. The blanks provided a measure of the adsorption and passive uptake of ^{3}H-thymidine by *I. galbana* and bacteria higher than 1 µm that could be retained on the filter. The value obtained for these blanks was subtracted from that obtained for each treatment. Preliminary

experiments demonstrated that there was no significant difference between blanks and axenic cultures of *I. galbana* ($p>0.05$). Therefore, a significant ^{3}H-thymidine uptake by autotrophic cells could be excluded. After fixation with formaldehyde, the samples were preserved at 4ºC until processed. Total activity (i.e. total bacterial production) was measured in 1.5 mL sampled from each 10 mL sample, after cold trichloroacetic acid extraction (>20 min with TCA 5% f.c., on ice). The precipitate was collected by centrifugation at 16000 *g* for 10 min, at 4ºC. The remaining sample volume (8.5 mL) was filtered through 1-µm pore-size nitrocellulose filters (Nucleopore; Whatman®, Sanford, ME, USA). The filters were dissolved in 100% acetone and centrifuged at 16,000 *g* for 10 min, at 4ºC. Acetone was gently removed without disturbing the pellet, which was then subject to cold trichloroacetic acid extraction in 1.5 mL TCA (5% final concentration) and centrifuged at 16,000 *g* for 10 min. Finally, the pellet was washed twice with 5% TCA, and the ^{3}H radioactivity was measured in a scintillation counter (Beckman LS 6000 TA). The values measured on the filters represented the portion of BP incorporated by *I. galbana* through BV.

BV was estimated as the [^{3}H]-thymidine incorporation rate in the size fraction > 1 µm. A conversion factor of 1.5×10^{18} cell mol^{-1} was used to estimate the number of bacteria produced or grazed per mole of incorporated ^{3}H-thymidine (Bell *et al.*, 1983). A factor of 20 fg C cell^{-1} (Lee & Fuhrman, 1987), widely used in the literature (see Junger *et al.*, 2018 and Cabrerizo *et al.*, 2019) was used to convert BV and BP to carbon units (µg C L^{-1} h^{-1}). BV on a per cell basis (BV_{cell}; fg C cell^{-1} h^{-1}) was estimated by dividing BV (in carbon units) by the number of *I. galbana* cells in the sample. The percentage of BV was calculated using the following equation:

$$\%BV = \frac{BV}{\mathrm{BP}} \times 100$$

The contribution of BV to growth (%) was calculated as:

$$\%BV\ for\ growth = \frac{\text{BVcell}}{\text{Net biomass production}} \times 100$$

Where BV_{cell} and estimated net biomass production are expressed in fg C $cell^{-1}$ d^{-1}).

e. Cell composition

e.1 Elemental cell quotas

The C and N cell quotas were determined using an elemental combustion system (Costech 4010, Costech International S.p.A., Milan, Italy). About 2-5 mg of dry biomass for each replicate were dried at 80ºC in an oven until the weight stabilized. Sulfanilamide (C:N:S = 6:2:1) was used as standard (see Ratti *et al.*, 2011 for details).

The elemental cell quotas of P, S, and Fe were measured by Total Reflection X-ray Fluorescence spectrometry (TXRF, Fanesi *et al.*, 2014). Approximately 1 × 10^6 cells were harvested by centrifugation at 12,000 *g* for 5 min, and washed 3 times with an isosmotic ammonium formate solution to remove the salts in the growth medium. Then, the pellet was suspended in 1 mL of Milli-Q water. Gallium, used as internal standard, was added to all samples at a final concentration of 5 µg mL^{-1}. Finally, a 10-µL aliquot of cell suspension was deposited on a quartz sample carrier, dried on a hot plate, and measured in a Picofox S2 spectrometer (Bruker AXS microanalysis GmbH, Ettlingen, Germany). The interference by bacterial elements was checked by making the measurements on culture aliquots filter through 1 µm pore size filters (Whatman GF/B; Whatman®, Sanford, ME, USA); no detectable contamination by bacteria could be detected.

A *supplementary experiment*, carried out to prove the positive effect of bacterivory on P and Fe cell quota of *Isochrysis galbana*, is described in the Supplementary information section (Text S1).

e.2 Size of organic pools

The carbohydrate, lipid, and protein pools were determined by Fourier transform infrared spectroscopy (FTIR), using a Tensor 27 spectrometer (Bruker Optics GmbH, Ettlingen, Germany). Cells were harvested by centrifugation at 1,800 *g* for 15 min and concentrated to a final density of approximately 4×10^7 cells mL^{-1}. Next, they were washed with an iso-osmotic solution of ammonium formate to minimize interference by debris and IR absorbing medium constituents. Fifty µL aliquots of cell suspension were deposited on silicon windows (Crystran Ltd., Poole, UK). Blanks were prepared by depositing 50 µL of ammonium formate on the sample holders. Blanks and samples were dried in an oven, at 80°C for 3 h. The spectra of the samples and blanks were determined and analyzed according to Domenighini & Giordano (2009).

The pools were semi-quantified as described in Palmucci *et al.* (2011), using the absolute protein content as a reference.

e.3 Chlorophyll concentration

For chlorophyll determination, cells were concentrated by centrifugation (12,000 *g* for 10 min) to about 5×10^6 cells mL^{-1}. The supernatant was extracted and 1 mL of 90% acetone was added to the pellet; the extraction was allowed to continue for at least 3 h at 4°C, in the dark. The absorbance of the extract at 647 nm and 664 nm was determined spectrophotometrically with a Beckman DU 640 Spectrophotometer (Beckman Coulter); the amounts of Chl *a* and *b* were estimated using the equations in Jeffrey & Humphrey (1975).

e.4 Protein content

The protein content of *I. galbana* cells was determined spectrophotometrically with a Beckman DU 640 Spectrophotometer (Beckman Coulter), according to (Peterson, 1977).

f. Enzyme activities

For the determination of enzyme activities, cultures were harvested by centrifugation at 1,200 *g* for 10 min and resuspended in an extraction medium containing 50 mM HEPES (pH 7.5), 1 mM Na_2EDTA, 5 mM dithiothreitol (DTT), 2% (w/v) PVPP and 0.15% (w/v) of Triton (Giordano, 2001). The volume of the extraction medium was such that the final cell concentration was about 1×10^8 cell mL^{-1}. The cells were then lysed with a N_2 pressure bomb (Parr Instrument, Moline, Illinois, USA), on ice. The resulting crude extracts were kept on ice and used for the enzyme activity assays in the shortest time possible. As a means of ruling out that bacterial enzymes contributed to the measured activities, the same volume of xenic cultures used for the experiments was passed through 1-µm pore-size filters (Whatman GF/B; Whatman®, Sanford, ME, USA) and the filtrate was analyzed for enzyme activities; the activities measured in the filtrate were negligible.

Phosphoenolpyruvate carboxylase (PEPC), phosphoenolpyruvate carboxykinase (PEPCk) and pyruvate carboxylase (PYC) activities were assayed spectrophotometrically as described by Holdsworth & Bruck (1977) and Wurtele & Nikolau (1992). The β-carboxylation reactions were followed through the oxidation of NADH to NAD at 340 nm in a coupled reducing reaction; the assays were carried out at 25ºC, with a thermostated Beckman DU 640 Spectrophotometer (Beckman Coulter).

Nitrate reductase (NR) activity was determined colorimetrically following the procedure described by Giordano *et al.* (2005), determining the NO_2^- increase at

540 nm and interpolating the absorbance values of the samples in a standard curve prepared with $NaNO_2$ (2.5-100 nM).

Nitrite reductase (NiR) activity was assayed according to Ramírez *et al.* (1966) using reduced methyl viologen as an electron donor and determining the NO_2^- consumption at 540 nm and 30ºC colorimetrically.

Glutamine synthetase (GS) activity was determined from the formation of L-glutamate γ-monohydroxamate, as described in O'Neal & Joy (1973) and Oaks *et al.* (1980). The standard curve was constructed using 0 to 25 mM L -glutamate γ -monohydroxamate.

ATP sulfurylase (ATPS) activity was measured spectrophotometrically, at 25°C, following NADPH formation at 340 nm (Burnell, 1984). The reaction mixture contained 1 mM adenosine 5'-phosphosulfate (APS), 1 mM PPi, 5 mM $MgCl_2$, 5 mM glucose, 300 µM NADP, 5 units each of hexokinase and glucose-6-P dehydrogenase from baker's yeast (H8629 Sigma-Aldrich), 50 mM TRIS-HCl pH 8.0. The assay mix (Burnell, 1984) was added with 10 mM dithiothreitol.

g. Statistical analysis

All experimental treatments were conducted in triplicate (i.e. on three independent cultures per each treatment). Three one-way analysis of variance (ANOVA) were used to determine the effect of bacteria presence, low irradiance, or low nutrient availability on all measured variables. The level of significance was set at 95% in all cases. The ANOVA was run with the software Statistica v. 7.0 (Stat Soft, 2007). Error propagation was used to calculate the variance of the elemental and composition ratios.

3. Results

a. Influence of prey on *Isochrysis galbana* (*AX* vs. *X* treatment)

Our results confirm the predatory ability of *I. galbana*. In the presence of bacteria (*X*-treatment, around 1×10^6 bacteria mL^{-1}), the BV_{cell} was 0.33 fg C $cell^{-1}$ h^{-1} (Fig. 31), the % BV was 12.6% (Fig. S15, see Supplementary information) and its contribution to growth was 0.63 ± 0.15% (Table 9). In the *AX*-treatment, the growth rate and net O_2 consumption were lower than in the *X*-treatment (Table 9 and Fig. 31; $p<0.05$). Instead, cell volume, Fv/Fm and net O_2 production were significantly higher in *AX*-treatment (Table 9 and Fig. 31; $p<0.05$). The estimated net biomass production rate showed no significant differences in the presence and absence of bacteria (Table 9; $p>0.05$).

Table 9. Growth rate, cell volume, maximum quantum yield of PS_{II} (Fv/Fm) of Isochrysis galbana acclimated to axenic (AX), xenic (X), xenic low light (X_{LL}) and xenic low nutrient (X_{LN}) conditions. Data are expressed as mean values ± SD (n=3; three independent replicates). Asterisks indicate significant differences with respect to xenic treatment for each test (X vs AX; X vs X_{LL} and X vs X_{LN}).

Growth regime	*X*	*AX*	X_{LL}	X_{LN}
Growth rate (d^{-1})	0.24 (0.01)	0.18 (0.02)*	0.12 (0.01)*	0.16 (0.01)*
Mean cell volume (μm^3)	39.71 (6.37)	55.51 (7.04)*	41.28 (5.77)	36.97 (3.75)
Fv/Fm	0.59 (0.01)	0.62 (0.01)*	0.75 (0.03)*	0.64 (0.01)*
Net biomass production rate (fg C $cell^{-1}$ d^{-1})	1282 (68)	1409 (192)	735 (75)*	878 (77)*
BV for growth (%)	0.63 (0.15)	-	1.70 (0.82)	3.64 (0.59)*

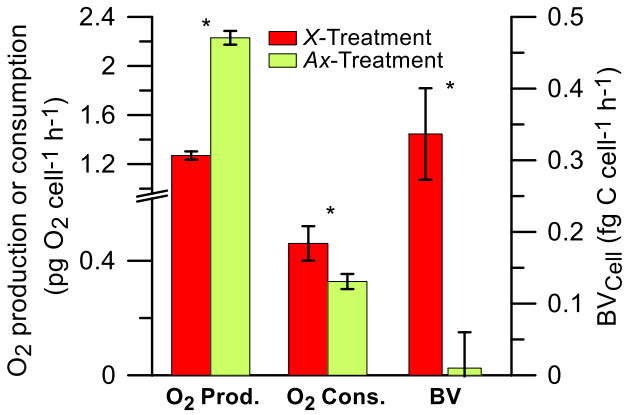

Figure 31. Metabolic variables of Isochrysis galbana under xenic (X) and axenic (AX) treatments. Net oxygen production (O_2 prod.,) oxygen consumption (O_2 cons.) and bacterivory (BV). Data are expressed as mean values ± SD (n=3). Asterisks indicate significant differences between treatments.

The cell quotas of C and N and the Chl *a* content were higher in axenic culture (Table 10 and 11; $p<0.05$), without significant differences in the C:Chl *a* ratio (Table 11; $p>0.05$). Despite the higher C and N content under axenic conditions, no significant difference was found in the C:N ratio of cells grown in each treatment (Table 10; $p>0.05$). P and Fe cell quotas were 50 and 90% lower, respectively, in the *AX*-treatment than in the *X*-treatment (Table 10; $p<0.05$). The N:P ratio was 3-fold higher in the axenic than in the xenic culture (16.75 vs. 5.59; Table 10; $p<0.05$). Also, when bacteria were added (either alive or dead) to an axenic culture at a concentration of 1×10^6 cell ml^{-1}, (Fig. S16, see supplementary information) results showed a positive effect of dead and live bacteria on the P-cell quota of *I. galbana*. However, for Fe-cell quota, only live bacteria showed higher significant values than in axenic treatment (Fig. S16).

In the *AX*-treatment, C was allocated mainly to lipids (Table 11). The carbohydrates and protein cell contents were lower than in *X*-treatment whereas the carbohydrate:protein ratio did not significantly differ between treatments (Table 11).

Table 10. Elemental composition of Isochrysis galbana acclimated to axenic (AX), xenic (X), xenic low light (X_{LL}) and xenic low nutrient (X_{LN}) conditions. Data are expressed as mean values ± SD (n=3; three independent replicates). Asterisks indicate significant differences with respect to xenic treatment for each test (X vs AX; X vs X_{LL} and X vs X_{LN}).

Growth regime	*X*	*AX*	X_{LL}	X_{LN}
C cell quota (fg cell^{-1})	5329 (63)	7687 (44)*	5912 (84)*	5350 (18)
N cell quota (fg cell^{-1})	769 (4)	1101 (8)*	772(14)	477 (5)*
C:N (molar ratio)	8.08 (0.13)	8.15 (0.11)	8.86 (0.26)*	13.15 (0.04)*
N:P (molar ratio)	5.59 (0.49)	16.75 (2.93)*	7.84 (1.02)*	18.05 (0.25)*
S cell quota (fg cell^{-1})	11.19 (2.01)	13.97 (7.43)	10.24 (2.77)	3.84 (2.21)*
P cell quota (fg cell^{-1})	304.6 (25.6)	145.5 (24.5)*	219.7 (25.3)*	58.2 (0.6)*
Fe cell quota (fg cell^{-1})	436.6 (34.0)	46.62 (10.72)*	352.3 (24.01)*	91.42 (13.60)*

PEPC (2-fold), NiR (4-fold), and ATPS activities (1.5-fold) proved higher in the *AX* than the *X*-treatment (Fig. 32a-c; $p<0.05$). On the contrary, PYC, PEPCK, NR, and GS exhibited lower activities in the *AX*-treatment (Fig. 32a, b; $p<0.05$).

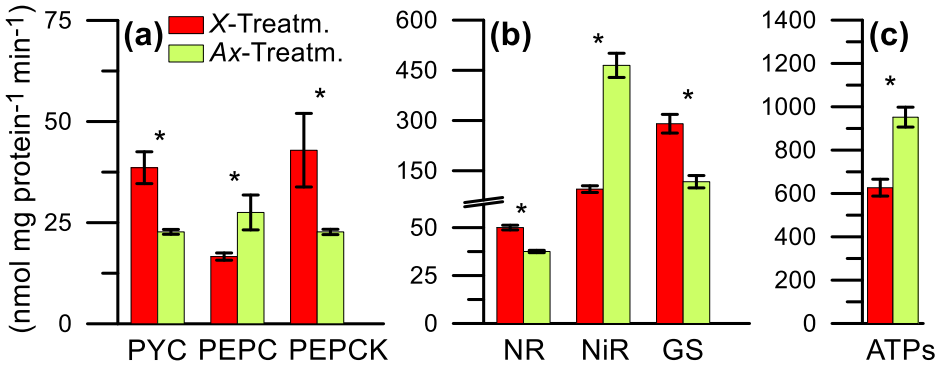

Figure 32. Enzymatic activities of C metabolism (a), N metabolism (b), and S metabolism (c) in Isochrysis galbana under xenic (X) and axenic (AX) treatments. Enzymatic activity of pyruvate carboxylase (PYC), phosphoenol pyruvate carboxylase (PEPC), and phosphoenol pyruvate carboxykinase (PEPCK) for C metabolism; nitrate reductase (NR), nitrite reductase (NiR), and glutamine synthetase (GS) for N metabolism; and ATP-sulfurylase (ATPS) for S metabolism are shown. Data are expressed as mean values ± SD (n=3). Asterisks indicate significant differences between treatments.

b. Influence of low irradiance on mixotrophy (X vs X_{LL} treatment)

The growth rate, the estimated net biomass production, the net O_2 production and consumption were lower when cells were subject to the low light (25 µmol m^{-2} s^{-1}, X_{LL}-treatment) than in the high-light (100 µmol m^{-2} s^{-1}, *X*-treatment) (Table 9 and Fig. 33; $p<0.05$). By contrast, Fv/Fm was higher in X_{LL} than in the *X*-treatment (Table 9; $p<0.05$). However, BV_{cell} (Fig. 33), %BV (Fig. S15), and the %BV for growth (Table 9) did not change as a function of irradiance ($p>0.05$).

The Chl *a* content, C cell quota and C:N and N:P ratios were higher with low light than in the *X*-treatment, but C:Chl *a* ratio and the P and Fe cell quotas showed the opposite response (Table 10, 11; $p<0.05$).

I. galbana cells acclimated to low light had smaller protein pools than their high light grown counterparts, while the size of the carbohydrates and lipid pools were unaffected (Table 11).The enzymatic activities of PEPC, NR, and ATPS were significantly higher (Fig. 34a-c; $p<0.05$) in the low light condition. However, PEPCK and GS activities were 50% and 25% lower, respectively, under X_{LL} compared to the *X*-treatment (Fig. 34a, b; $p<0.05$).

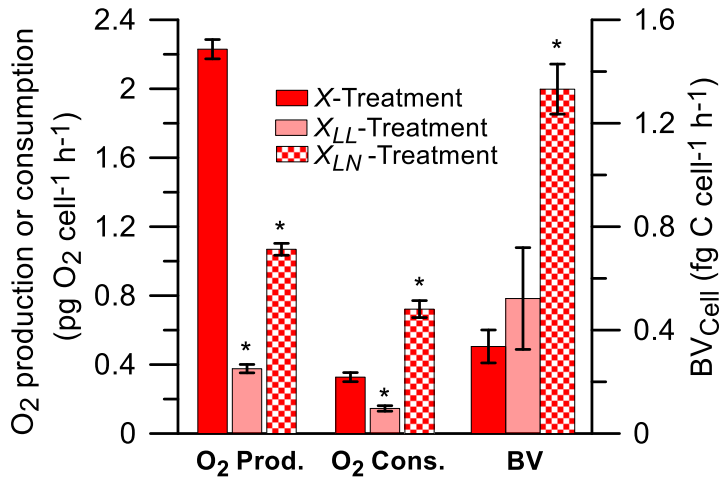

Figure 33. Metabolic variables of Isochrysis galbana under xenic (X), xenic low light (X_{LL}) and xenic low nutrient (X_{LN}) treatments. Net oxygen production (O_2 prod.,) oxygen consumption (O_2 cons.) and bacterivory (BV). Data are expressed as mean values ± SD (n=3). Asterisks indicate significant differences with respect to X treatment for each test (X vs X_{LL} and X vs X_{LN}).

Table 11. Organic composition of Isochrysis galbana acclimated to axenic (AX), xenic (X), xenic low light (X_{LL}) and xenic low nutrient (X_{LN}) conditions. Data are expressed as mean values ± SD (n=3; three independent replicates). Asterisks indicate significant differences with respect to xenic treatment for each test (X vs AX; X vs X_{LL} and X vs X_{LN}).

Growth regime	*X*	*AX*	X_{LL}	X_{LN}
Protein (pg cell^{-1})	2.57 (0.12)	2.06 (0.08)*	2.28 (0.01)*	1.26 (0.03)*
Semiquantitative Carbohydrates	1 (0.09)	0.82 (0.07)*	0.93 (0.33)	0.61 (0.02)*
Semiquantitative Lipid	1 (0.13)	1.11 (0.08)	1.40 (0.45)	0.66 (0.01)*
Carbohydrate : protein FTIR ratio	2.69 (0.23)	2.73 (0.23)	2.83 (0.99)	3.35 (0.08)*
Lipid : protein FTIR ratio	0.12 (0.02)	0.17 (0.01)*	0.19 (0.06)	0.16 (0.01)*
Carbohydrate : lipid FTIR ratio	22.19 (1.57)	16.32 (1.53)*	14.82 (3.29)*	20.59 (0.44)
Chl a (pg cell^{-1})	0.11 (0.03)	0.16 (0.01)*	0.21 (0.01)*	0.03 (0.01)*
C:Chl a ratio	48.08 (12.45)	48.40 (0.41)	28.71 (1.36)*	177 (66.77)*

c. Influence of nutrient availability on mixotrophy (X vs X_{LN} treatment)

Biomass and net O_2 production were lower in the X_{LN}-treatment than in the *X*-(high nutrient) treatment (Table 9 and Fig. 33; $p<0.05$) whereas Fv/Fm (Table 9) O_2 consumption (Fig. 33), bacterivory variables [BV_{cell} (Fig. 33) %BV (Fig. S15) and %BV for growth (Table 9)] were greater in the X_{LN}-treatment ($p<0.05$).

The Chl *a* content and the cell quotas of C, N, S, P, and Fe were lower in the X_{LN} than in the *X*-treatment (Table 10, 11; $p<0.05$) whereas the C: Chl *a*, C:N and N:P ratios were significantly higher in the X_{LN}-treatment (Table 10, 11; $p<0.05$). The protein, carbohydrate, and lipid pools were smaller in the X_{LN}-treatment (Table 11). PEPC, NR, and ATPS activity were higher in cells acclimated to growth in the X_{LN}-treatment (Fig. 34a-c; $p<0.05$), whereas PYC and GS activity were lower (Fig. 34a, b; $p<0.05$); PEPCK and NiR activities showed no significant changes as a function of nutrient availability (Fig. 34a, b; $p>0.05$).

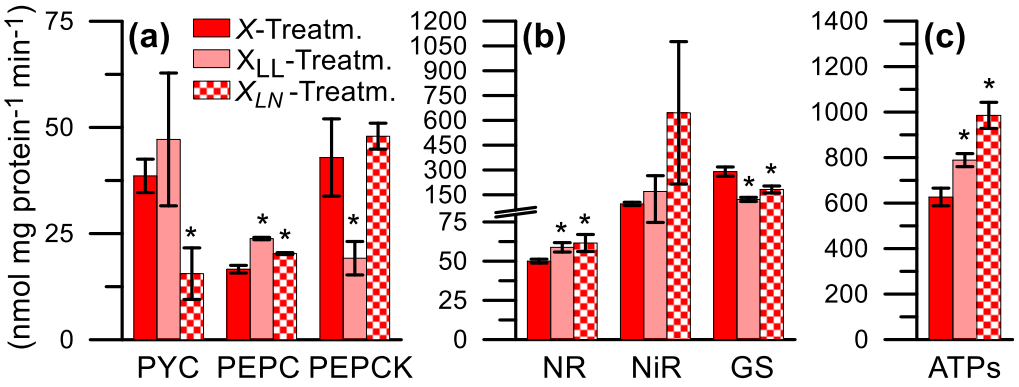

Figure 34. Enzymatic activities of C metabolism (a), N metabolism (b), and S metabolism (c) in Isochrysis galbana under xenic (X), xenic low light (X_{LL}) and xenic low nutrient (X_{LN}) treatments. Enzymatic activity of pyruvate carboxylase (PYC), phosphoenol pyruvate carboxylase (PEPC), and phosphoenol pyruvate carboxykinase (PEPCK) for C metabolism; nitrate reductase (NR), nitrite reductase (NiR), and glutamine synthetase (GS) for N metabolism; and ATP-sulfurylase (ATPS) for S metabolism are shown. Data are expressed as mean values ± SD (n=3). Asterisks indicate significant differences with respect to X treatment for each test (X vs X_{LL} and X vs X_{LN}).

4. Discussion

Our results support our first hypothesis that phagotrophy in mixotrophic protists helps to retain homeostasis of cellular composition (C:N and carbohydrate:protein ratios), facilitating the concomitant maintenance (at least to some extent) of the heterotrophic and photosynthetic machineries and stimulating the growth rate of *I. galbana*. It goes without saying that, at this stage, we have no evidence of the fact that this is results can be generalized for all strains of *I. galbana*. In fact, strains heterogeneity may be one of the reasons for the discrepancy existing in the literature.

For instance, in some past publications bacteria inhibited the growth of *I. galbana*, possibly via secretory compounds (Jia-Yicao *et al.*, 2019). In other papers (Sandhya & Vijayan, 2019), the authors reported that bacteria associated to *I. galbana* cultures enhanced the growth of the alga due to the release of growth stimulatory compounds. In our experiment, the ingestion of bacteria provided the

cell with nutrients, especially P and Fe. Furthermore, in the *supplementary experiment* (Fig. S16 in Supplementary information), we show that both live and dead bacteria increased the P-cell quota of *I. galbana*. Higher P content likely promoted RNA production, as proposed by the growth-rate hypothesis (Sterner & Elser, 2002; Giordano *et al.*, 2015); this would also fit with the observed higher growth rate (~ 25%) of *I. galbana* in the *X*-treatment. Notably, the higher growth rate in terms of production of new cells was accompanied by a lower C-cell quota and did not translate into a greater net biomass production (Table 9, 10). This may have ecological consequences and potential evolutionary repercussions, since the higher growth and division rate can, in different ways, affect gene expression (Nordholt *et al.*, 2017; Bertaux *et al.*, 2018) and fitness of the alga in terms of clonal populations. However, it cannot be ruled out that if a higher division rate leads to a greater cell fitness, this could support the evolutionary pressure towards the mixotrophy (Selosse *et al.*, 2017). Furthermore, when phagotrophy occurs, C fixation in the Calvin–Benson cycle, net oxygen production and content of biochemical structures involved in photosynthesis are downregulated (Wan *et al.*, 2011), as reflected by the values of PS_{II} quantum yield and by the cellular Chl *a* content in the *X*-treatment. This downsizing of the photosynthetic machinery and its functioning under bacteria presence is contrary to the observed higher growth rate. Our results support the idea that phagotrophy must be the responsible of the increase in growth rate, probably due to a synergistic activity of both machineries (Edwards, 2019).

The aforementioned changes operate through a simultaneous stimulation of the enzymatic activities of β-carboxylases such as PEPCK, PYC, and the key enzyme for N assimilation, GS. When C fixation by Rubisco decreases, the stimulation of β-carboxylases could be part of a compensatory mechanism (Descolas-Gros & Oriol, 1992). This agrees with Liu *et al.*, (2015), who proposed that phagotrophic conditions induce the activities of PEPCK and PYC. This raises the question of

the role that enzymes have in phagotrophy. This is not immediately obvious, as some β-carboxylases have an anaplerotic function, providing intermediary metabolites to the Krebs cycle (Norici & Giordano, 2002). This may be required under conditions in which the oxidation of ingested organic substrates is accelerated by bacterivory, as suggested by the higher respiration rate in our *X*-treatment. In addition, PEPCK and PYC provide the oxaloacetate needed for the gluconeogenesis from lipids (Jitrapakdee & Wallace, 1999; Norici *et al.*, 2011). This fits with the greater carbohydrate content (approx. 20%) and the lower cell lipid content in our *X*-treatment. The higher PEPCK and PYC activities in mixotrophic cells may be required to support an increased provision of PEP and pyruvate, which stem from the glyceraldehyde-3P generated both in the Calvin Cycle and in the oxidative pathways that use sugars and amino acids from bacterial biomass (Fig. 35).

Notably, the larger carbohydrate pool of phagotrophic cells did not result in a major change in the C:N ratio, since it was accompanied by a higher protein content (approx. 25%; Table 11). The higher protein content is consistent with the higher GS activity measured in this cells, which catalyzes the incorporation of NH_4^+ in glutamine and then in protein (Giordano & Raven, 2014) (see Fig. 35). The fact that no greater N content was detected in the *X*-treatment and that the C:N ratio was not lower suggests that the higher protein content of mixotrophic cells results from the conversion of low-mass N pools already present in the algal cells (e.g. amino acids, glutathione) to protein or from the remineralization of acquired bacterial compounds (De-Bashan *et al.*, 2008; Giordano & Raven, 2014) (with assimilation of C in stoichiometrically balanced amounts). Since C, N, and S metabolism compete for the reducing power in the cell (Ruan *et al.*, 2017), the stimulation of N assimilation may contribute to the lower ATPS activity (especially if light is not saturating, see Ruan *et al.*, 2017). Despite the lower ATPS activity in the presence of bacteria, the S cell quota did not differ

significantly between *AX*- and *X*-treatment so it is possible that *I. galbana* acquired reduced sulfur compounds (e.g. sulfolipids, cysteine or glutathione) from bacterial organic matter.

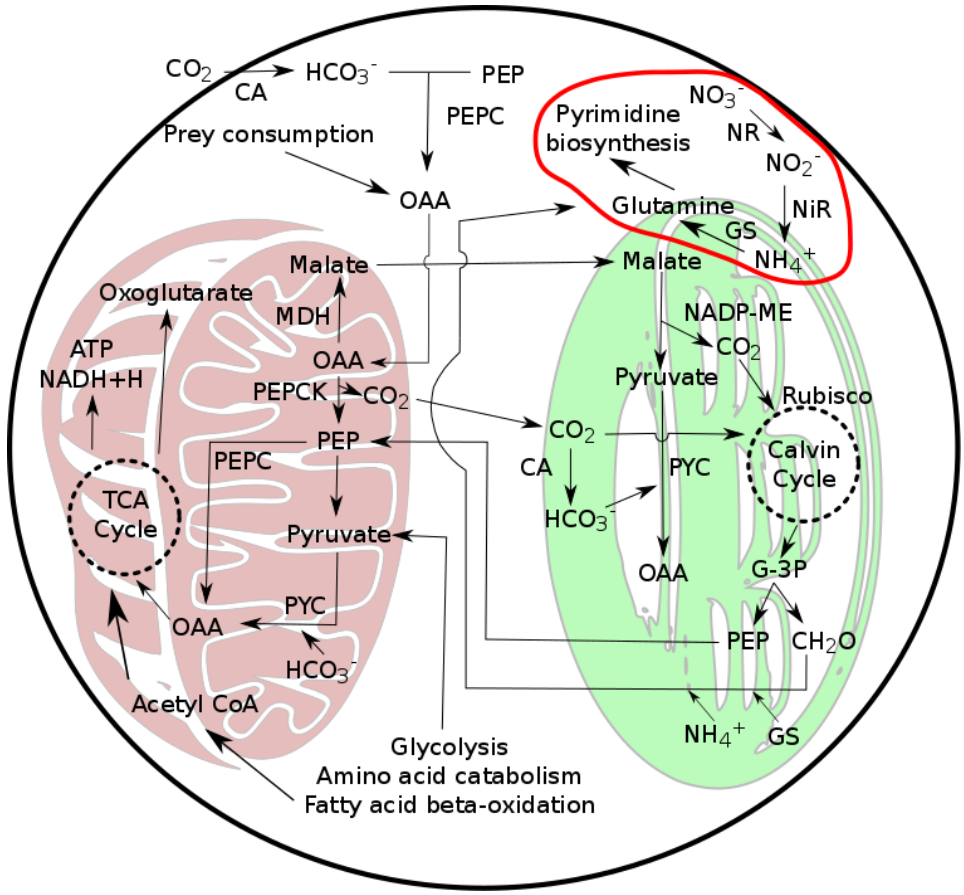

Figure 35. Model of single-cell C_4 photosynthesis for Isochrysis galbana. The red and green organelles represent the mitochondria and the chloroplast, respectively. Enzyme abbreviations: PEPC: phosphoenol pyruvate carboxylase; PEPCK: phosphoenol pyruvate carboxykinase; PYC: pyruvate carboxylase; CA: carbonic anhydrase; MDH: malate dehydrogenase; NADP-ME: NADP-dependent malic enzyme; NR: Nitrate reductase; NiR: nitrite reductase; GS: glutamine synthetase. A red line encircles the N metabolism in cell.

Our second hypothesis was that energy and nutrient limitations stimulate the phagotrophic metabolism and machinery in xenic cultures of *I. galbana*. However, the results show that, under low light, BV was not stimulated, the growth rate was 50% lower, the net O_2 production per cell plummeted (75% lower), and elemental stoichiometry was altered (higher C:N and N:P ratios). These data corroborate what was reported by Anderson *et al.* (2018), who showed that *I. galbana* is an obligate phototroph that requires medium to high light intensity to grow. Recently, Edwards (2019) have showed that mixotrophs needs sufficient light to grow under oligotrophic conditions, demonstrating that light play an important role in mixotrophs growth. In fact, under low light, *I. galbana* did not resort to phagotrophy enough to compensate fully for the lower photon availability, although the proportional contribution of BV to growth was higher (0.7% in *X*-treatment and 1.7% in the X_{LL}-treatment). The energy of the cell obtained from both mechanisms was invested to expand antennas, as suggested by the higher Chl *a* content and the lower C:Chl *a* ratio, a common response of phototrophic cells under low light (Arteaga *et al.*, 2016; Tanaka & Tanaka, 2019). FTIR data indicate that cells grown in low light had a lower carbohydrate-to-lipid ratio than did their counterparts grown at higher irradiance. Lipid synthesis demands more energy per unit of C than that of carbohydrates (Montechiaro *et al.*, 2006; Norici *et al.*, 2011) and this allocation patterns is rather atypical for a light-limited alga. Following our hypothesis, we expected that a greater BV under scarce light conditions could reinforce the enzymatic activities stimulated by phagotrophy in the first test. However, an unusual response under low light was observed, with higher NR and ATPS activity, reactions that are at the beginning of pathways that use large amounts of reducing power, mostly from photosynthesis (O'Leary *et al.*, 2011; Sanz-Luque *et al.*, 2015). The stimulation of both enzymes did not lead to a higher N and S content or to a decline in the C:N and N:P ratios, but rather the opposite (Table 10). We have no explanation

for this unexpected behavior of *I. galbana* growing under subsaturating irradiance in the presence of bacteria. These results show that *I. galbana* growing at low light did not invest its energy in growth or functional pools (e.g. nucleic acid or protein), but rather triggers energy-dispersive processes that act as sinks of reducing power, such as higher C allocation to lipids or nitrate and sulfate reduction. Thus, under our experimental conditions, phagotrophy does not appear to offset insufficient light and *I. galbana* shows unbalanced cellular activity.

With respect to growth in low-nutrient conditions, our results point towards a down-regulation of phototrophic metabolism (lower O_2 production) and an up-regulation of phagotrophy (higher BV) in *I. galbana*. This result shows an increase of bacterivorous activity under conditions of nutrient shortage, although the ratios remained balanced (F/40 medium), compared to other experiments where phagotrophy is increased in response to a nutrient limitation, usually P (e.g. Unrein *et al.*, 2007 and Fischer *et al.*, 2017b). However, the stimulation of phagotrophy does not translate into the acquisition of nutrients from the bacterial biomass that compensates for their short supply in the medium. Also, the X_{LN}-treatment determined a lower P and N cell quota, and a greater C:N, N:P and carbohydrate:protein ratio (Table 10,11).

Notably, low-nutrient conditions stimulated PEPC activity. As mentioned above, this enzyme is involved in a number of functions. Some of these functions may be related to the necessity of saving nutritional resources such as P, which appears to be especially critical in our X_{LN}-treatment. PEPC can also supply malate (via oxaloacetate) to the TCA cycle, replacing the ADP-dependent pyruvate kinase (PK) activity in low P environments (O'Leary *et al.*, 2011); this also agrees with the higher mitochondrial respiration (as O_2 consumption) measured in our X_{LN}-treatment.

Under low-nutrient conditions, the cell-protein content was lower, in agreement with other studies (McKew *et al.*, 2015; Abd El-Hady *et al.*, 2016). If the lower

cell-protein content is due to a lower rate of protein synthesis from exogenous N, this also explains why GS activity is lower (Hellebust & Ahmad, 1989; Alaoui *et al.*, 2001). In our X_{LN}-treatment, S was also low and this may elicit responses in cells (Ratti *et al.*, 2011). In fact, we detected appreciably higher ATPS activity (Prioretti & Giordano, 2016). ATPS is the first enzyme in the pathway of cysteine synthesis, a pathway that uses substantial amounts of reducing power. Under low nutrient availability, and similarly to X_{LL}-treatment, sulfate reduction may be used as a way of dissipating excess energy. Furthermore, cysteine is a precursor of glutathione, one of the main quenchers of excess reactive O_2 species in cells (Song *et al.*, 2013; Giordano & Prioretti, 2016). The protection from damages associated with excess reducing power and reactive O_2 species may be critical for nutrient-limited cells.

5. Conclusions

Our study reveals the mechanisms involved in metabolic and enzymatic regulation associated with phagotrophy in a cosmopolitan mixotrophic protist. The results show that at the cell level, metabolic and enzymatic regulation allowed to retain, at some extent, the homeostasis of the cellular composition and a higher rate of cell division, but not a higher rate of assimilation of C. This suggests that bacterivory is not always involved in C and nutrient fluxes in aquatic ecosystems. Moreover, in our second test under suboptimal conditions (low light and nutrient), *I. galbana* was critically affected due to its predominantly phototrophic metabolism. Bacterial consumption did not translate as greater growth while regulation of C, N and S enzymatic activities was devoted to dissipate the excess of reducing power caused by environmental stress. This led to an imbalance in the cell composition. This study proves that a physiological perspective is necessary to determine whether increased phagotrophic activity in low-nutrient or low-light environments could shape the biogeochemical cycles in aquatic ecosystems.

References

Abd El-Hady, H. H., Fathey, S. A., Ali, G. H. & Gabr, Y. G. (2016). Biochemical profile of phytoplankton and its nutritional aspects in some khors of Lake Nasser, Egypt. *Egypt J. Basic. Appl. Sci.* 3(2): 187–93

Alaoui, S. E. L., Díez, J., Humanes, L., Toribio, F., Partensky, F. & García-Fernández, J.M. (2001). In Vivo Regulation of Glutamine Synthetase Activity in the Marine Chlorophyll b -Containing Cyanobacterium Prochlorococcus sp . Strain PCC 9511 (Oxyphotobacteria)†. *Appl. Environ. Microbiol.* 67(5): 2202–7

Anderson, R., Charvet, S. & Hansen, P. J. (2018). Mixotrophy in Chlorophytes and Haptophytes—Effect of Irradiance, Macronutrient, Micronutrient and Vitamin Limitation. *Front. Microbiol.* 9(July): 1–13

Arteaga, L., Pahlow, M. & Oschlies, A. (2016). Modeled Chl:C ratio and derived estimates of phytoplankton carbon biomass and its contribution to total particulate organic carbon in the global surface ocean. *Global Biogeochem. Cycles.* 30(12): 1791–810

Bell, R. T. & Ahlgren, G. M. & Ahlgren, I. (1983). Estimating bacterioplankton production by measuring [3H]thymidine incorporation in a eutrophic Swedish lake. *Appl. Environ. Microbiol.* 45(6): 1709–21

Bertaux, F., Marguerat, S. & Shahrezaei, V. (2018). Division rate, cell size and proteome allocation: Impact on gene expression noise and implications for the dynamics of genetic circuits. *R. Soc. Open. Sci.* 5(3): 172234

Burkholder, J. M., Glibert, P. M. & Skelton, H. M. (2008). Mixotrophy, a major mode of nutrition for harmful algal species in eutrophic waters. *Harmful algae* 8: 77–93.

Burnell, J. N. (1984). Sulfate Assimilation in C4 Plants. *Plant. Physiol.* 75: 873–5

Cabrerizo, M. J., González-Olalla, J. M., Hinojosa-López, V. J., Peralta-Cornejo, F. J. & Carrillo P. (2019). A shifting balance: responses of mixotrophic marine algae to cooling and warming under UVR. *New Phytol.* 221(3): 1317–27

Caron, D. A. (2016). Mixotrophy stirs up our understanding of marine food webs. *Proc. Natl. Acad. Sci.* 113(11): 2806–8

De-Bashan, L. E., Magallon, P., Antoun, H. & Bashan, Y. (2008). Role of glutamate dehydrogenase and glutamine synthetase in Chlorella vulgaris during assimilation of ammonium when jointly immobilized with the microalgae-growth-promoting bacterium Azospirillum brasilense. *J. Phycol.* 44(5): 1188–96

Descolas-Gros, C. & Oriol, L. (1992). Variations in carboxylase activity in marine phytoplankton cultures. B-carboxylation in carbon flux studies. *Mar. Ecol. Prog. Ser.* 85: 163–9

Domenighini, A. & Giordano, M. (2009). Fourier transform infrared spectroscopy of microalgae as a novel tool for biodiversity studies, species identification, and the assessment of water quality. *J. Phycol.* 45(2): 522–31

Edwards, K. F. (2019). Mixotrophy in nanoflagellates across environmental gradients in the ocean. *Proc. Natl. Acad. Sci.* 116(13): 6211–20

Fanesi, A., Raven, J. A. & Giordano M. (2014). Growth rate affects the responses of the green alga Tetraselmis suecica to external perturbations. *Plant Cell Environ.* 37(2): 512–9

Fischer, R., Giebel, H. A., Hillebrand, H. & Ptacnik, R. (2017a). Importance of mixotrophic bacterivory can be predicted by light and loss rates. *Oikos.* 126(5): 713–22

Fischer, R., Giebel, H. A. & Ptacnik, R. (2017b). Identity of the limiting nutrient (N vs. P) affects the competitive success of mixotrophs. *Mar. Ecol.-Prog. Ser.* 563: 51–63

Flöder, S., Hansen, T. & Ptacnik, R. (2006). Energy-Dependent Bacterivory in Ochromonas minima-A Strategy Promoting the Use of Substitutable Resources and Survival at Insufficient Light Supply. *Protist.* 157(3): 291–302

Flynn, K. J., Stoecker, D. K., Mitra, A., Raven, J. A., Glibert, P. M., Hansen, P. J., Granèli, E. & Burkholder, J. M. (2013). Misuse of the phytoplankton-zooplankton dichotomy: The need to assign organisms as mixotrophs within plankton functional types. *J. Plankton. Res.* 35(1): 3–11

Frias-Lopez, J., Thompson, A., Waldbauer, J. & Chisholm, S. W. (2009). Use of stable isotope-labelled cells to identify active grazers of picocyanobacteria in ocean surface waters. *Environ. Microbiol.* 11(2): 512–25

Giordano, M. & Prioretti, L. (2016). Sulphur and algae: metabolism, ecology and evolution. "The Physiology of Microalgae'', Developments in Applied Phycology Series", Borowitzka M.A., Beardall J." RJA (eds.)., editor. Springer-Verlag, Berlin Heidelberg;. 185–09 p.

Giordano, M. & Raven, J. A. (2014). Nitrogen and sulfur assimilation in plants and algae. Aquat. Bot. 118: 45–61

Giordano, M. (2001). Interactions between C and N metabolism in Dunaliella salina cells cultured at elevated CO2 and high N concentrations. J. Plant Physiol. 158(5):

577–81

Giordano, M. (2013). Homeostasis: An underestimated focal point of ecology and evolution. *Plant. Sci.* 211: 92–101

Giordano, M., Chen, Y. B., Koblizek, M. & Falkowski, P. G. (2005). Regulation of nitrate reductase in Chlamydomonas reinhardtii by the redox state of the plastoquinone pool. *Eur. J. Phycol.* 40(4): 345–52

Giordano, M., Palmucci, M. & Raven, J. A. (2015). Growth rate hypothesis and efficiency of protein synthesis under different sulphate concentrations in two green algae. *Plant Cell Environ.* 38(11): 2313–7

González-Olalla, J. M., Medina-Sánchez, J. M. & Carrillo P. (2019). Mixotrophic trade-off under warming and UVR in a marine and a freshwater alga. *J. Phycol.* 55(5): 1028-1040.

Guillard, R. R. L.& Ryther, J. H. (1962). Studies of marine planktonic diatoms. I. Cyclotella nana Hustedt, and Detonula Confervacea (Cleve) . *Can. J. Microbiol.* 8(1140): 229–39

Guiry, M. D. (2017). AlgaeBase. World-wide electronic publication. Ireland: National University of Ireland.

Hansen, P. J. & Nielsen, T. G. (1997). Mixotrophic feeding of Fragilidium subglobosum (dinophyceae) on three species of Ceratium: Effects of prey concentration, prey species and light intensity. *Mar. Ecol. Prog. Ser.* 147(1–3): 187–96

Hellebust, J. A. & Ahmad, I. (1989). Biological Oceanography Regulation of Nitrogen Assimilation in Green Microalgae. *Biol. Oceanogr.* 5581: 241–55

Hinder, S. L., Hays, G. C., Edwards, M., Roberts, E. C., Walne, A. W. & Gravenor, M. B. (2012). Changes in marine dinoflagellate and diatom abundance under climate change. *Nat. Clim. Chang.* 2: 271–275.

Holdsworth, E. S. & Bruck, K. (1977). Concerned with p-Carboxylation in Marine Phytoplankter of Phosphoenolpyruvate contributed to the fixation of CO , by Phosphoenolpyru- to providing an anaplerotic sequence to the acid cycle (2-4). On the other in C , plants is approximately in C3 plants. Arch. Biochem. Biphysics. 182: 87–94

Jeffrey, S. W. & Humphrey, G. F. (1975). New spectrophotometric equations for determining chlorophylls a, b, c1 and c2 in higher plants, algae and natural phytoplankton. *Biochem. und. Physiol. der. Pflanz.* 167(2): 191–4

Jeong, H. J., Yoo, Y. Du., Kim, J. S., Seong, K. A., Kang, N. S. & Kim, T. H. (2010). Growth, feeding and ecological roles of the mixotrophic and heterotrophic dinoflagellates in marine planktonic food webs. *Ocean Sci.* 45: 65–91.

Jia-Yicao, J. Y., Kong, Z. Y., Zhang, Y. F., Ling, T., Xu, J. L., Liao, K., Zhou, C. X. & Yan, X. J. (2019). Bacterial community diversity and screening of growth-affecting bacteria from isochrysis galbana following antibiotic treatment. *Front.Microbiol.* 10: 1–11.

Jitrapakdee, S. & Wallace, J. C. (1999). Structure, function and regulation of pyruvate carboxylase. *Biochem. J.* 340(1): 1–16

Junger, P. C., Amado, A. M., Paranhos, R., Cabral, A. S., Jacques, S. M. S. & Farjalla, V. F. (2018). Salinity Drives the Virioplankton Abundance but Not Production in Tropical Coastal Lagoons. *Microb. Ecol.* 75: 52–63.

Kamjunke, N., Henrichs, T. & Gaedke, U. (2006). Phosphorus gain by bacterivory promotes the mixotrophic flagellate Dinobryon spp. during re-oligotrophication. *J. Plankton Res.* 29: 39–46.

Keeling, P. J. & Del Campo, J. (2017). Marine Protists Are Not Just Big Bacteria. *Curr. Biol.* 27(11): R541–9

Keller, M. D., Shapiro, L. P., Haugen, E. M., Cucci, T. L., Sherr, E. B. & Sherr, B. F. (1994). Phagotrophy of fluorescently labeled bacteria by an oceanic phytoplankter. *Microb. Ecol.* 28(1): 39–52

Lee, S. & Fuhrman, J. A. (1987). Relationships between biovolume and biomass of naturally derived marine bacterioplankton. *Appl. Environ. Microbiol.* 53(6): 1298–303.

Lie, A. A. Y., Liu, Z., Terrado, R., Tatters, A. O., Heidelberg, K. B. & Caron, D. A. (2018). A tale of two mixotrophic chrysophytes: Insights into the metabolisms of two Ochromonas species (Chrysophyceae) through a comparison of gene expression. *PLoS. One.* 13(2): 1–20

Lie, A. A. Y., Liu, Z., Terrado, R., Tatters, A. O., Heidelberg, K. B. & Caron, D. A. (2017). Effect of light and prey availability on gene expression of the mixotrophic chrysophyte, Ochromonas sp. *BMC Genomics.* 18(1): 1–16

Liu, Z., Campbell, V., Heidelberg, K. B. & Caron, D. A. (2016). Gene expression characterizes different nutritional strategies among three mixotrophic protists. *FEMS. Microbiol. Ecol.* 92(7): 1–11

Liu, Z., Jones, A. C., Campbell, V., Hambright, K. D., Heidelberg, K. B. & Caron, D.

A. (2015). Gene expression in the mixotrophic prymnesiophyte, Prymnesium parvum, responds to prey availability. *Front. Microbiol.* 6(MAR): 1–12

McKew, B. A., Metodieva, G., Raines, C. A., Metodiev, M. V. & Geider, R. J. (2015). Acclimation of Emiliania huxleyi (1516) to nutrient limitation involves precise modification of the proteome to scavenge alternative sources of N and P. *Environ. Microbiol.* 17(10): 4050–62

McKie-Krisberg, Z. M. , Gast, R. J. & Sanders, R. W. (2015). Physiological Responses of Three Species of Antarctic Mixotrophic Phytoflagellates to Changes in Light and Dissolved Nutrients. *Microb. Ecol.* 70(1): 21–9

McKie-Krisberg, Z. M., Sanders, R. W. & Gast, R. J. (2018). Evaluation of Mixotrophy-Associated Gene Expression in Two Species of Polar Marine Algae. *Front. Mar. Sci.* 5(August): 1–12

Medina-Sánchez, J. M., Herrera, G., Durán, C., Villar-Argaiz, M. & Carrillo, P. (2017). Optode use to evaluate microbial planktonic respiration in oligotrophic ecosystems as an indicator of environmental stress. *Aquat. Sci.* 79(3): 529–41

Medina-Sánchez, J. M., Villar-Argaiz, M. & Carrillo, P. (2004). Neither with nor without you: A complex algal control on bacterioplankton in a high mountain lake. *Limnol. Oceanogr.* 49(5): 1722–33

Mitra, A. et al. (2014). The role of mixotrophic protists in the biological carbon pump. *Biogeosciences.* 11(4): 995–1005

Mitra, A. et al. (2016). Defining Planktonic Protist Functional Groups on Mechanisms for Energy and Nutrient Acquisition: Incorporation of Diverse Mixotrophic Strategies. *Protist.* 167(2): 106–20

Modenutti, B. (2014). Mixotrophy in Argentina freshwaters. *Adv. Limnol.* 65: 359–74

Montechiaro, F., Hirschmugl, C. J., Raven, J. A. & Giordano, M. (2006). Homeostasis of cell composition during prolonged darkness. *Plant Cell Environ.* 29(12): 2198–204

Moorthi, S. D., Ptacnik, R., Sanders, R. W., Fischer, R., Busch, M. & Hillebrand, H. (2017). The functional role of planktonic mixotrophs in altering seston stoichiometry. *Aquat. Microb. Ecol.* 79(3): 235–45

Nordholt, N., Van Heerden, J., Kort, R. & Bruggeman, F. J. (2017). Effects of growth rate and promoter activity on single-cell protein expression. *Sci Rep.* 7(1): 6299

Norici, A. & Giordano, M. (2002). Anaplerosis in microalgae. Recent. Res. Dev. Plant.

Physiol. 3(January 2002): 153–64

Norici, A., Bazzoni, A. M., Pugnetti, A., Raven, J. A. & Giordano, M. (2011). Impact of irradiance on the C allocation in the coastal marine diatom Skeletonema marinoi Sarno and Zingone. *Plant Cell Environ.* 34(10): 1666–77

O'Leary, B., Park, J. & Plaxton, W. C. (2011). The remarkable diversity of plant PEPC (phosphoenolpyruvate carboxylase): recent insights into the physiological functions and post-translational controls of non-photosynthetic PEPCs. *Biochem. J.* 436(1): 15–34

O'Neal, D. & Joy, K. W. (1973). Glutamine synthetase of pea leaves. I. Purification, stabilization, and pH optima. *Arch. Biochem. Biophys.* 159(1): 113–22

Oaks, A., Stulen, I., Jones, K., Winspear, M. J., Misra, S. & Boesel, I. L. (1980). Enzymes of Nitrogen Assimilation in Maize Roots. *Planta.* 148: 477–84

Palmucci, M., Ratti, S. & Giordano, M. (2011). Ecological and evolutionary implications of carbon allocation in marine phytoplankton as a function of nitrogen availability: A fourier transform infrared spectroscopy approach. *J. Phycol.* 47(2): 313–23

Peterson, G. L. (1977). A simplification of the protein assay method of Lowry et al. which is more generally applicable. Anal. Biochem. 83(2): 346–56

Prioretti, L. & Giordano, M. (2016). Direct and indirect influence of sulfur availability on phytoplankton evolutionary trajectories. J. Phycol. 52(6): 1094–102

Ptacnik, R. et al. (2016). A light-induced shortcut in the planktonic microbial loop. *Sci. Rep.* 6: 1–10

Ramírez, J. M., Del Campo, F. F., Paneque, A. & Losada, M. (1966). Ferredoxin-nitrite reductase from spinach. *Biochim. Biophys. Acta - Enzymol. Biol. Oxid.* 118(1): 58–71

Ratti, S., Knoll, A. H. & Giordano, M. (2011). Did sulfate availability facilitate the evolutionary expansion of chlorophyll a+c phytoplankton in the oceans? *Geobiology*. 9(4): 301–12

Raven, J. A. (1997). Phagotrophy in phototrophs. *Limnol Oceanogr*. 42(1): 198–205

Rottberger, J., Gruber, A., Boenigk, J. & Kroth, P. G. (2013).Influence of nutrients and light on autotrophic, mixotrophic and heterotrophic freshwater chrysophytes. *Aquat. Microb. Ecol.* 71(2): 179–91

Ruan, Z., Raven, J. A. & Giordano, M. (2017). In Synechococcus sp. competition for

energy between assimilation and acquisition of C and those of N only occurs when growth is light limited. *J. Exp. Bot.* 68(14): 3829–39

Sanders, R. W., Caron, D. A., Davidson, J. M., Dennett M. R. & Moran, D. M. (2001). Nutrient acquisition and population growth of a mixotrophic alga in axenic and bacterized cultures. *Microb. Ecol.* 42(4): 513–23

Sandhya, S. V. & Vijayan, K. K. (2019). Symbiotic association among marine microalgae and bacterial flora: a study with special reference to commercially important Isochrysis galbana culture. *J. Appl. Phycol.* 31(4): 2259–2266.

Sanz-Luque, E., Chamizo-Ampudia, A., Llamas, A., Galvan, A. & Fernandez, E. (2015). Understanding nitrate assimilation and its regulation in microalgae. *Front. Plant. Sci.* 6: 899

Selosse, M. A., Charpin, M., & Not, F. (2017). Mixotrophy everywhere on land and in water: the grand écart hypothesis. *Ecol. Lett.* 20(2): 246–63

Song, P., Li, L. & Liu, J. (2013). Proteomic analysis in nitrogen-deprived Isochrysis galbana during lipid accumulation. *PLoS One.* 8(12): 1–13

Sterner, R. W. & Elser, J. J. (2002). Ecological Stoichiometry The Biology of Elements from Molecules to the Biosphere. First Edit. Princeton: Princeton University Press

Stoecker, D. K., Hansen, P. J., Caron, D. A. & Mitra, A. (2017). Mixotrophy in the Marine Plankton. *Ann. Rev. Mar. Sci.* 9(1): 311–35

Sun, D. & Wang, Q. (2018). Linear Relationships between Photosynthetic Rate and Photochemical Energy Expressed by PAR × Fv/Fm. *Am. J. Plant Sci.* 09(2): 125–138

Tanaka, A. & Tanaka, R. (2019). The biochemistry, physiology, and evolution of the chlorophyll cycle. In: Grimm B, editor. Metabolism, Structure and Function of Plant Tetrapyrroles: Introduction, Microbial and Eukaryotic Chlorophyll Synthesis and Catabolism. First. Cambridge (EEUU): Academic Press (Elsevier); p. 328

Unrein, F., Gasol, J. M., Not, F., Forn, I. & Massana, R. (2013). Mixotrophic haptophytes are key bacterial grazers in oligotrophic coastal waters. 8(1): 164–76

Unrein, F., Massana, R., Alonso-Sáez, L. & Gasol, J. M. (2007). Significant year-round effect of small mixotrophic flagellates on bacterioplankton in an oligotrophic coastal system. *Limnol. Oceanogr.* 52(1): 456–469.

Wan, M., Liu, P., Xia, J., Rosenberg, J. N., Oyler, G. A., Betenbaugh, M. J. et al. (2011). The effect of mixotrophy on microalgal growth, lipid content, and

expression levels of three pathway genes in Chlorella sorokiniana. *Appl. Microbiol. Biotechnol.* 91(3): 835–44

Ward, B. A. & Follows, M. J. (2016). Marine mixotrophy increases trophic transfer efficiency, mean organism size, and vertical carbon flux. *Proc. Natl. Acad. Sci.* 113(11): 2958–63

Ward, B. A., Dutkiewicz, S., Barton, A. D. & Follows, M. J. (2011). Biophysical Aspects of Resource Acquisition and Competition in Algal Mixotrophs. *Am. Nat.* 178(1): 98–112

Wurtele, E. S. & Nikolau, B. J. (1992). Differential Accumulation of Biotin Enzymes during Carrot Somatic Embryogenesis. Plant. Physiol. 99(4): 1699–703

Yelton, A. P., Acinas, S. G., Sunagawa, S., Bork, P., Pedrós-Alió, C. & Chisholm, S. W. (2016). Global genetic capacity for mixotrophy in marine picocyanobacteria. *ISME J.* 10(12): 2946–57

Zubkov, M. V. & Tarran, G. A. (2008). High bacterivory by the smallest phytoplankton in the North Atlantic Ocean. *Nature*. 455(7210): 224–6

Supplementary Information

This supplementary material contains the Figures S15 and S16, and Text S1.

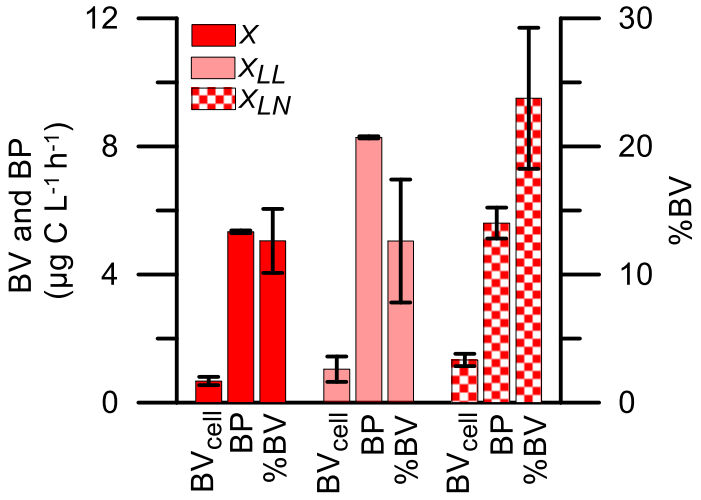

Figure S15. Bacterivory on a cell basis (BV_{cell}), bacterial production (BP) and percentage of bacterivory (%BV) in Isochrysis galbana under xenic (X), xenic low-light (X_{LL}) and xenic low-nutrient (X_{LN}) treatment. Data are expressed as mean values ± SD (n=3).

Text S1. Bacterivory effect on P and Fe-cell quota. A *supplementary experiment* to prove the positive effect of bacterivory on P and Fe cell quota was carried out with *Isochrysis galbana*. We start our experiment from twelve 150 mL-axenic cultures of *I. galbana* growing at the exponential phase (2×10^6 cell ml^{-1}) for one month at 20ºC and 100 µmol photons m^2 s^{-1} of Photosynthetically Active Radiation (PAR, 400-700 nm). The cultures were exposed to a 12:12 h light/dark daily cycle. After one month, growing conditions for *I. galbana* were modified and divided into four treatments: i) axenic; ii) axenic plus additional P and Fe; iii) axenic plus live bacteria and iv) axenic plus dead bacteria added to the culture. Cultures of *I. galbana* were incubated for 2 days before of the cell-quota (P and Fe) analysis. The addition of inorganic mineral P and Fe to the axenic treatment maintained the same ratio P:Fe (4:1) in the F/2 medium. Thus, the F/2 medium was enriched with additional 500 µg P L^{-1} and 240 µg Fe L^{-1}. The bacteria concentration ($\approx1\times10^6$ cell ml^{-1}) in the axenic plus dead bacteria treatment was the same as for the axenic plus live bacteria treatment. For that, the bacteria contained in 600 ml of a mixotrophic culture of *I. galbana* growing in our laboratory were filtered through 1 µm pore-size (Whatman GF/B) and bacteria were collected from the filtrate. To obtain heat-killed bacteria, we placed 300-mL of bacterial culture in a water bath at 70°C for at least 1h to be heat killed. Then, heat-killed and live bacteria were transferred into 50-ml sterile

Falcon tubes and concentrated using a centrifuge (Beckman Coulter, Inc., Brea, CA, USA) at 5000 r.p.m for 15 min. Supernatant was discarded and cells re-suspended using sterile F/2 medium. Aliquots of 5 mL each with live and dead bacteria were added to axenic cultures at the same concentration as in our mixotrophic culture. The effectiveness of the heat-killing process was verified, demonstrating that bacteria did not growth after incubation in Petri dishes with F/2 medium, agar (1,5% w/w), peptone (0,5% w/w), and yeast extract (0.1% w/w). For cell-quota analysis, 50 mL from each replicate were passed through a cellulose nitrate filter of 1.2 μm pore size (Sartorius). The filters were dissolved using 100% acetone and centrifuged at 16,000 g for 10 min at 4ºC. Then, the samples were left open in extraction chamber until the complete evaporation of the acetone. Finally, the sample was resuspended with 10 mL of Milli-Q water and stored cold until the analysis. Cation (P and Fe) analyses were performed by Inductively Coupled Plasma Optical Emission Spectroscopy (ICP-OES) using a Perkin Elmer Optima 8300. All samples were run in triplicate. The results showed a positive effect of inorganic nutrient addition as well as dead and live bacteria on the P-cell quota of *I. galbana*. However, for Fe-cell quota only inorganic nutrients and live bacteria showed higher significant values than in axenic treatment.

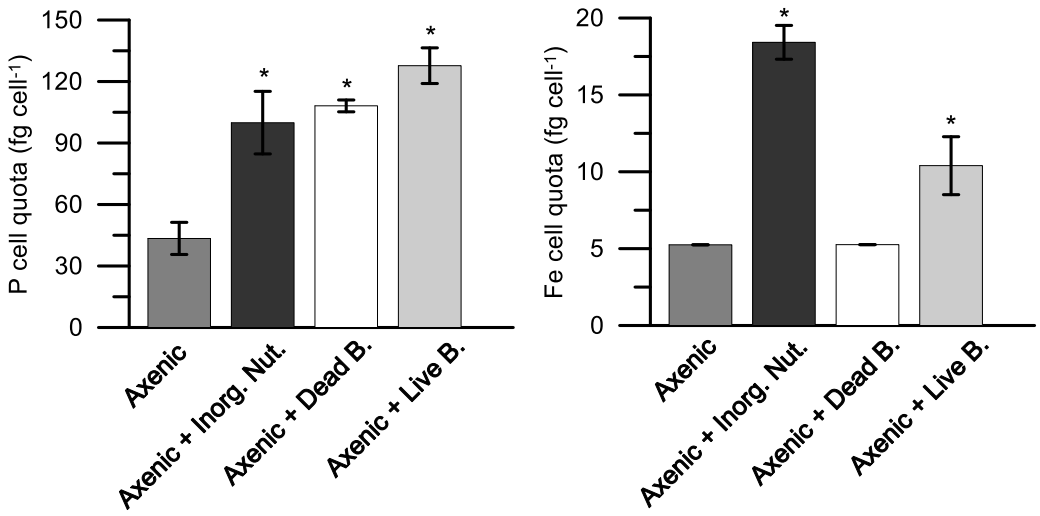

Figure S16. P and Fe-cell quota in axenic culture and amended axenic cultures of Isochrysis galbana cells with inorganic nutrients, dead and live bacteria.

CHAPTER 7

CHAPTER 7 - Synthesis

This Thesis offers an advance in the knowledge of how the interaction of factors related to global change (temperature, UVR exposure, and increased nutrient concentration or dust inputs) affects phytoplankton ecophysiology, and more specifically, mixotrophic protists. For this, phytoplankton responses are analysed along spatial and temporal scales, as well as at different levels of organization (from cell to ecosystem). In this thesis, the following questions are addressed:

- **How does the UVR × Dust interaction affect the phytoplankton community in the Alboran Sea?**

The joint action of UVR exposure and its interaction with Saharan dust revealed a contrasting sensitivity of autotrophic picoplankton from two areas (nearshore and offshore) located outside and inside, respectively, an oligotrophic oceanic gyre (Chapter 2). Thus, the nearshore area, having lower mean irradiance values of UVR and PAR, showed a greater sensitivity to UVR than did the offshore area. However, the joint action of Saharan dust inputs and UVR reduced or inverted the UVR damage on the photosynthetic quantum yield (Φ_{PSII}) and picoplanktonic primary production (PP_P) in the nearshore area but accentuated it offshore. This contrasting effect between areas was partially explained by an increase in nonphotochemical quenching (NPQ), acting as a photorepair mechanism to dissipate the excess energy absorbed by PSII. The physiological state of the community was driven fundamentally by picoeukaryotes, although *Synechococcus* was the most abundant group due to its high acclimation capacity under UVR × Dust conditions. This dual sensitivity of nearshore vs. offshore picoplankton to dust inputs and UVR fluxes may show a potential future response of the microbial food web under global-change conditions. The observed response to UVR and dust interaction over the 5 days of the

experiment raised the question as to whether phytoplankton communities exposed to high intensities of these factors for longer periods (years) would have modified their metabolism and interaction with bacteria. Therefore, the next question was:

- **Has the global change modified phytoplankton metabolism and its relationship with bacteria over a greater temporal scale?**

To respond to this question (Chapter 3), an observational study was made during 2005 and 2015 in high-mountain lakes of Sierra Nevada for two main reasons: i) data was available from 13 lakes for the year 2005 to compare with recent data; and ii) the Mediterranean mountains region is exposed to high UVR fluxes, nutrient inputs from Sahara Desert and increased temperature. The results showed that the nature of prevailing algae-bacteria interaction shifted from a bacterivory control exerted by mixotrophic algae to an algae-bacteria commensalism. This coincided with higher air and water temperatures as well as a lower sestonic N:P ratio, related to greater dust inputs. The shift in the relationship between the two components of the trophic web was accompanied by greater primary production and lower bacterivory (mixotrophy) in the lakes. Future global-change conditions in Mediterranean region could alter the role of mixotrophy as a carbon by-pass in the microbial trophic web. Furthermore, the greater number of trophic links could reduce the biomass-transfer efficiency up the web. These findings raised the question of how temperature and nutrients could modulate the metabolism and mixotroph:autotroph ratio.

- **Do nutrients modify the phytoplankton response to rising or fluctuating temperatures?**

In the Chapter 4, an experimental study was conducted with two protist species typical of high-mountain lakes, i.e. *Monoraphidium minutum* (strict autotroph)

and *Chromulina* sp. (mixotroph). The fluctuating temperatures had a positive effect on heterotrophic metabolism, in agreement with the Metabolic Theory of Ecology (MTE), and stimulated the growth of mixotrophic species. By contrast, the increase in nutrients altered the temperature dependent-effects, increasing the PP:R ratio and abundance of the strict autotroph *M. minutum*, challenging the MTE under high nutrient concentrations. Therefore, future studies of temperature effects on metabolism and trophic web structure should consider nutrients as modulators of protist response. In fact, the role that mixotrophs can play in the trophic web has received growing attention over the last decade, and the effect that global-change factors can exert on its metabolism and composition will determine its ability to cope with future environmental conditions. For this reason, the question proposed for the Chapter 5 was:

- **Is the mixotrophic balance and the elemental or stoichiometric composition of mixotrophic species affected by Temperature × UVR interaction?**

Chapter 5 examines whether the response of mixotrophs to the T × UVR interaction varies depending on the ability of these organisms to take advantage of phototrophy or phagotrophic machinery (mixotrophic balance). For this, an experiment was performed with two mixotrophic protists located in different positions of the mixotrophic gradient (*Isochrysis galbana* and *Chromulina* sp.). The results show that the joint action of the two factors increased the primary production:bacterivory ratio while the stoichiometric values (N:P ratio) tended to Redfield's ratio. Therefore, T and UVR shifted the metabolism of both protists towards greater phototrophy regardless of original position of the organism on the mixotrophic gradient. This lower phagotrophic activity could reduce the C-transfer efficiency at the top of trophic webs under future environmental conditions. However, if this is true, the question arises:

- **Does the combination of phototrophy and phagotrophy give the mixotrophic cell an advantage that could explain its ubiquity?**

Different tests were designed to determine whether phagotrophy is an advantage to the cell and how the greater phagotrophic activity under light limitation or nutrient scarcity might affect the metabolism in the model mixotroph *I. galbana*, widely distributed in marine water. The results for the first test revealed that the consumption of bacteria in a xenic culture stimulated β-carboxylases and glutamine synthetase activities to higher levels than in an axenic culture. Furthermore, phagotrophy increased the P cell quota, accelerating cell division and improving cell fitness. For the second test, the predicted surge in phagotrophy under low light and low nutrients led *I. galbana* to grow more slowly despite greater bacterial consumption, and the enzymatic activities were devoted to the dissipation of excess reducing power. These results showed that higher phagotrophy under low nutrient and low irradiance in *I. galbana* does not imply greater C flux, but it may help the organism endure these adverse conditions.

CHAPTER 8

1. For mixotrophic cells, phagotrophy is an advantage in that it accelerates their growth rate. The underlying mechanism is that predation of bacteria stimulates the enzymatic activities of β-carboxylases (PEPCK, PYC) and a key enzyme for N assimilation (GS), in addition to increasing the cell-P content.

2. The most extreme future environmental conditions, i.e. higher temperatures, fluctuating temperatures, intensified UVR-exposure, and greater nutrient concentrations, will negatively affect mixotrophic protists but will benefit strict autotrophs. This conclusion emerges from the present study at different scales:

a) At metabolic level, Chromulina sp. and Isochrysis galbana, two mixotrophic species located at distinct positions of the mixotrophic gradient, responded to Temperature × UVR interaction, shifting their metabolism towards autotrophy and augmenting the primary production:bacterivory ratio.

b) At the species level, in agreement with the Metabolic Theory of Ecology (MTE), the fluctuation at higher temperature benefited the heterotrophic metabolism and mixotrophic species in a simplified community. By contrast, the combination of rising or fluctuating temperatures and increased nutrients augmented primary production and favoured autotrophic species growth, challenging the MTE.

c) At the ecosystem level in high-mountain lakes, the decadal increase of temperature and atmospheric P inputs altered the algae-bacteria interaction from a predatory control towards commensalism, and resulted in the loss of mixotrophy, a key metabolism in oligotrophic lakes.

d) At the ecosystem level in marine waters, the intensified UVR exposure and dust inputs changed the sensitivity of autotrophic picoplankton in nearshore versus offshore areas in the Alboran Sea. Saharan dust inputs reduced UVR damage on picoeukaryotes in the nearshore area but accentuated it offshore.

This result underlines the importance of the different previous light and nutrient history linked to spatial scale.

1. Para las células mixotróficas como *Isochrysis galbana*, la fagotrofia supone una ventaja ya que acelera su tasa de crecimiento. El mecanismo subyacente a esta respuesta es que la depredación de bacterias estimuló la actividad enzimática de las β-carboxilasas (PEPCK, PYC), una enzima clave para la asimilación del N (GS), además de incrementar el contenido de P celular.

2. Las futuras condiciones ambientales más extremas, caracterizadas por una más alta temperatura, fluctuación térmica, una más intensa exposición a UVR e incremento en la entrada de nutrientes, tendrán un efecto negativo sobre los protistas mixótrofos, pero beneficiarán a los autótrofos estrictos. Esta conclusión emerge de nuestro estudio a diferentes niveles:

a) A nivel metabólico, *Chromulina* sp. e *Isochrysis galbana*, dos especies mixotróficas ubicadas en diferentes posiciones del gradiente mixotrófico, respondieron a la interacción Temperatura × UVR desplazando su metabolismo hacia la autotrofia e incrementando el ratio producción primaria: bacterivoría.

b) A nivel de especie, de acuerdo con la Teoría Metabólica de la Ecología (MTE), la fluctuación a más alta temperatura favoreció el metabolismo heterotrófico y la especie mixótrofa de una comunidad protista simplificada. Por el contrario, la combinación de una temperatura más alta o fluctuante y de los nutrientes, incrementó la producción primaria y benefició el crecimiento de la especie autótrofa, retando a la MTE.

c) A nivel de ecosistema en lagunas de alta montaña, el incremento de temperatura y las entradas de polvo atmosférico enriquecido en P a lo largo de una década modificaron la interacción alga-bacteria, desde un control por bacterivoría hacia el comensalismo, provocando la pérdida de mixotrofia, un metabolismo clave en lagos oligotróficos.

d) A nivel de ecosistema en ambientes marinos, la exposición más intensa a UVR y las entradas de polvo modificaron la sensibilidad del picoplancton autótrofo en la zona de costa frente a la de mar abierto en el área de mar de Alborán. Las entradas de polvo sahariano redujeron el daño de UVR sobre los picoeucariotas en el área de costa, pero lo acentuaron en mar abierto. Este resultado subraya la importancia del diferente historial previo de luz y nutrientes vinculados a la escala espacial.

List of common acronyms

- APP = Autotrophic Picoplankton
- ATPs = ATP sulfurylase
- BV = Bacterivory
- C = Carbon
- DOC = Dissolved Organic Carbon
- EOC = Excreted Organic Carbon
- GR = Growth Rate
- GS = Glutamine synthetase
- HBP = Heterotrophic Bacterial Production
- N = Nitrogen
- NiR = Nitrite reductase
- NPP = Net Primary Production
- NPQ = Non-Photochemical Quenching
- NR = Nitrate reductase
- P = Phosphorous
- PAR = Photosynthetically Active Radiation
- PEPC = Phosphoenolpyruvate carboxylase
- PEPCK = Phosphoenolpyruvate carboxykinase
- POC = Particulate Organic Carbon
- PP = Primary Production
- PP_M = Nanoplanktonic Primary Production
- PP_P = Picoplanktonic Primary Production
- PYC = Pyruvate carboxylase
- R = Respiration
- T = Temperature
- TOC = Total Organic Carbon
- UVR = Ultraviolet Radiation
- Φ_{PSII} = Photosynthetic Quantum yield of photosystem II